C-H bond activation catalyzed by Ruthenium nanoparticles

Longhui Gao

▶ **To cite this version:**

Longhui Gao. C-H bond activation catalyzed by Ruthenium nanoparticles. Organic chemistry. Université Paris-Saclay, 2017. English. NNT : 2017SACLS348 . tel-02169205

HAL Id: tel-02169205
https://theses.hal.science/tel-02169205

Submitted on 1 Jul 2019

HAL is a multi-disciplinary open access archive for the deposit and dissemination of scientific research documents, whether they are published or not. The documents may come from teaching and research institutions in France or abroad, or from public or private research centers.

L'archive ouverte pluridisciplinaire **HAL**, est destinée au dépôt et à la diffusion de documents scientifiques de niveau recherche, publiés ou non, émanant des établissements d'enseignement et de recherche français ou étrangers, des laboratoires publics ou privés.

NNT : 2017SACLS348

C-H BOND ACTIVATION CATALYZED BY RUTHENIUM NANOPARTICLES

Thèse de doctorat de l'Université Paris-Saclay
préparée à l'Université Paris-Sud

École doctorale n°571 2MIB
Spécialité de doctorat: Chimie

Thèse présentée et soutenue à CEA Saclay, le 06/11/2017, par

M. Longhui Gao

Composition du Jury :

M. Damien Prim Professeur, Université Paris-Saclay (Université de Versailles Saint-Quentin)	Président
Mme. Montserrat Gomez Professeur, Université Paul Sabatier	Rapporteur
Mme. Françoise Colobert Professeur, CNRS, Université de Strasbourg	Rapporteur
M. Sébastien Roy Docteur, Sanofi	Examinateur
M. Jérôme Hannedouche Docteur, Université Paris-Saclay (Université Paris Sud)	Examinateur
M. Bernard Rousseau Docteur, CEA Saclay	Directeur de thèse
M. Grégory Pieters Docteur, CEA Saclay	Invité

Thèse de doctorat

Dedicated to my grandmother

Acknowledgments

I would like to thank Dr. Bernard Rousseau and Prof. Peiqiang Huang (Xiamen University) first of all, who offered me the opportunity to do my thesis in CEA Saclay. During these three years, Dr. Bernard Rousseau gave me a lot of useful advices in my works, which have led to the accomplishment of my thesis. Besides, he also gave me a lot of help in my daily life, such as renting and registration.

I would like to thank Dr. Grégory Pieters, who gave me a lot of help in both professional and personal life during these three years. He is always patient with me and is just like a good friend with a great sense of humor. He also gave me very useful advices during the preparation of my thesis.

I would like to thank Dr. Sophie Feuillastre, who helped me a lot during the preparation of my thesis and gave me many useful advices in organic chemistry.

I would like to thank Sébastien Garcia-Argote, who helped me a lot in the operation of tritium labeling and many things in the lab.

I would like to thank Dr. Serge Perato and Dr. Céline Taglang, who taught me the operations of deuterium labeling. Besides, their preliminary works on deuterium labeling inspired me a lot.

I would like to thank the members in analysis group: David Buisson, Céline Chollet and Elodie Marcon. They helped me a lot in the characterization of isotopically labeled molecules and the HPLC analyses.

I would like to thank Prof. Bruno Chaudret (INSA Toulouse), who provided us various well-characterized ruthenium nanoparticles in the exploration of new C-H functionalization reactions. He also gave me some useful advices in my works.

I would like to thank Dr. Gilles Clavier (ENS Cachan), who helped us to detect the photophysical properties of the synthesized compounds.

I would like to thank Dr. Bo Gao, who is a good friend of me and helped me a lot in my daily life. He was my “private translator”, and he was always in good mood and humorous.

I would like to thank Dr. Eric Doris and Dr. Edmond Gravel for their useful advices during these three years.

I would like to thank all the other members in the tritium lab: Florence Pillon for her kindly concern, Dr. Alaric Desmarchelier for his advices and helps, Anaëlle Doerflinger for her help in the lab, and

also Dr. Christophe Dugave, Dr. Emilie Nehlig, Dr. Dinh Vu Nguyen, Dr. Praveen Prakash, Dr. Arun Kumar Ramar, Dr. Gopi Elumalai, Dr. Marielle Tamigney, Victor Pfeifer, Alberto Palazzolo, Minh Duc Hoang, Olivia Carvalho, Leonid Lavnevich, Boris Solda, Mathilde Pauton, Paul Chassagne for their encouragements and kindness during these three years.

Also, I would like to thank Chantal Faux for her patience and responsibility during these three years.

In addition, I would like to thank Dr. Frédéric Taran for his responsibility, Dr. Davide Audisio, Dr. Jean-Christophe Cintrat, Dr. Karen Hinsinger and all the other members of SCBM for their kindness.

At the same time, I would like to thank my parents and my grandmother. Their unconditional supports and love offer me the endless power to overcome all the difficulties in my life.

I also thank all my Chinese friends in France, especially Zong, Haiyan, Yongpeng, Chenge, Bo, for their companionship. They brought a lot of joys and laughs to me during these three years.

Finally, I sincerely thank Xiudan, my dear wife, who is always at my side for all these three years. Her endless love makes me strong and offers me endless power. I also thank her for bringing Yiwei, my lovely daughter, into my life. The little girl is my angel, and all the other things become unimportant when I am with her.

Résumé de thèse

Les molécules marquées par des isotopes de l'hydrogène possèdent de nombreuses applications dans divers domaines tels que la chimie, la biologie ou en science des matériaux. Dans le domaine de la recherche de nouveaux médicaments, les études liées à la pharmacocinétique nécessitent un accès rapide à des molécules marquées afin de ne pas impacter les coûts et les délais de développement. Le développement de la métabolomique a aussi entrainé une augmentation du besoin en molécules marquées isotopiquement. En effet, les molécules deutérées peuvent être utilisées en tant qu'étalons internes pout la quantification rapide des métabolites présents dans des tissus ou des fluides biologiques. La première partie de cette thèse concerne le développement d'une méthode générale de marquage de motifs de type thioéther dans des molécules complexes à l'aide d'une nouvelle réaction d'échange isotopique (catalysée par des nanoparticules de Ruthénium).

Examples de molécules d'interet comportant des sous-structures de type thioether :

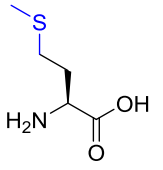

Methionine

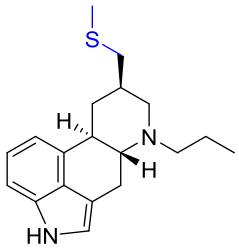

Pergolide
Antiparkinsonien

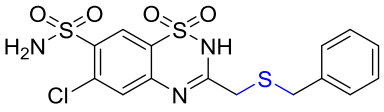

Benzthiazide
Diuretique

Méthode développée durant cette thèse :

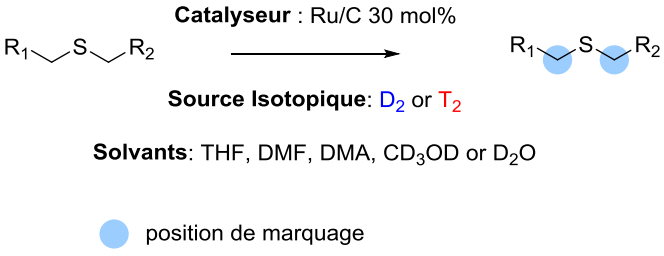

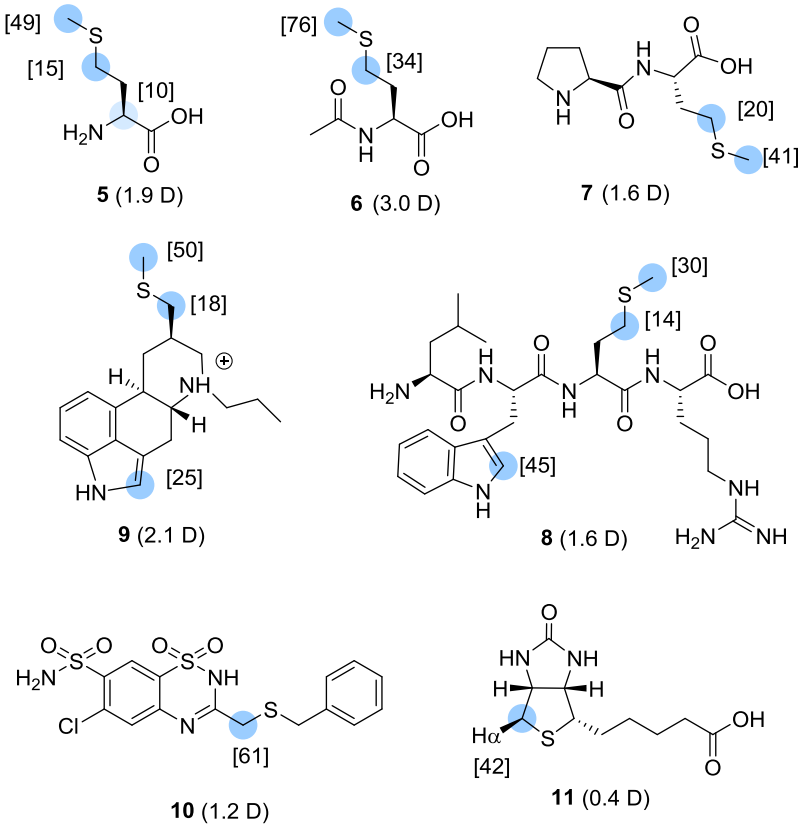

D'un point de vue fondamental cette transformation représente le premier exemple de C(sp^3)-H activation dirigée par un atome de soufre. En termes d'application, cette nouvelle réaction permet la synthèse rapide d'étalons internes pour la quantification LC-MS/MS et le marquage tritium de molécules complexes. La robustesse du système catalytique, et notamment sa capacité à maintenir sa réactivité dans différents solvants protiques deutérés ou aprotiques, a permis de marquer une large gamme de produits contenant un motif thioéther. Ainsi en fonction de la solubilité et de la stabilité des composés d'intérêt, différents milieux réactionnels (solvants : THF, MeOD, DMF, DMA, D_2O) ont été utilisés pour marquer des principes actifs et des peptides contenant des sous-structures de type thioethers avec un grande régioselectivité. Par la suite, il a été démontré que cette méthode permettait d'accéder rapidement à molécules deutérées pouvant être utilisé en tant que standards internes pour la quantification LC/MS. En effet, en réalisant plusieurs cycles de catalyse (3) plus de 4 atomes de deutérium ont pu être incorporés sur des molécules complexes. Cette réaction a aussi été optimisée dans le cadre du marquage tritium et le pergolide radiomarqué (activité spécifique : 15 Ci/mmol) a été obtenu en une étape dans des conditions douces ($P(T_2)$ = 0.9 bar).

La seconde partie de cette thèse relate le développement d'une nouvelle méthode d'homocouplage de phénylpyridines catalysée par un catalyseur de ruthénium hétérogène (Ru/C) et utilisant le chlorure de

fer (III) comme oxydant. Différents substrats comportant des substituants diverses ont été dimérisés avec de bons rendements (voir figure ci-dessous).

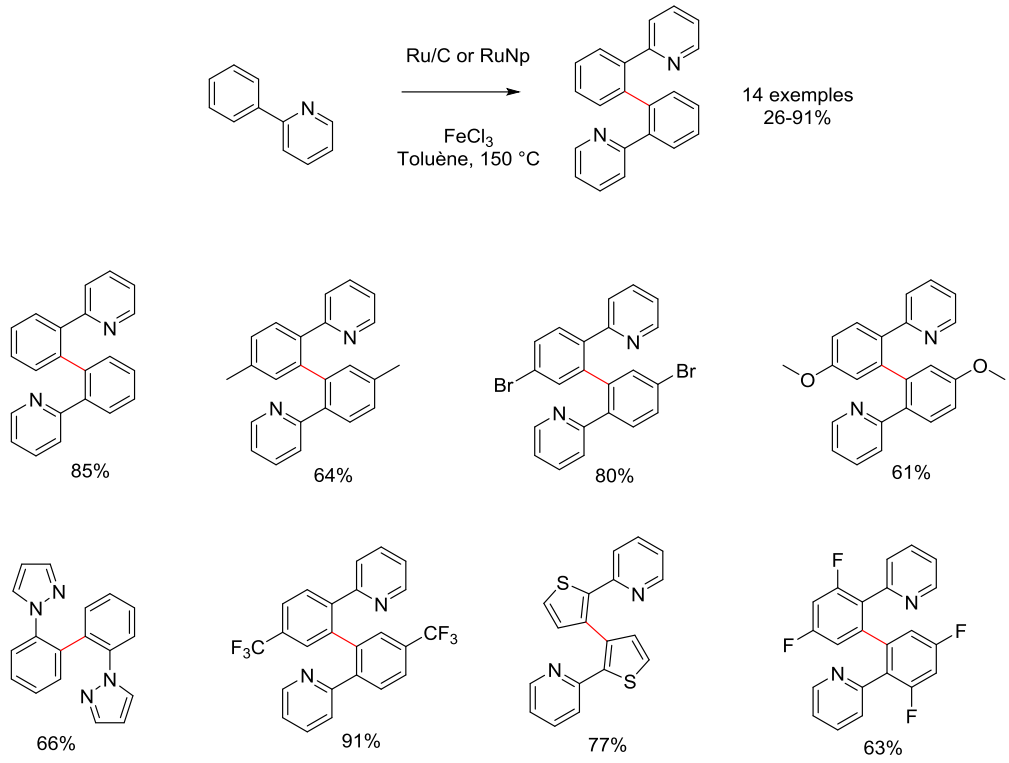

Des études de cinétique et de mécanistique ont été conduites afin de déterminer la nature de l'espèce catalytique active. Ces dimères ont ensuite été utilisés pour synthétiser de nouveaux complexes de bore dont les propriétés photophysiques ont été étudiées. Ces nouvelles espèces possèdent des rendements quantiques élevés et des brillances supérieures aux espèces monomériques. L'utilisation de ces nouveaux complexes de bores en tant qu'émetteurs dans des diodes électroluminescentes sera prochainement étudiée.

Dans une troisième partie, la mise au point d'une réaction palladocatalysée permettant d'obtenir des molécules polycycliques contenant un motif de type pyridine est développée (voir schéma ci-dessous).

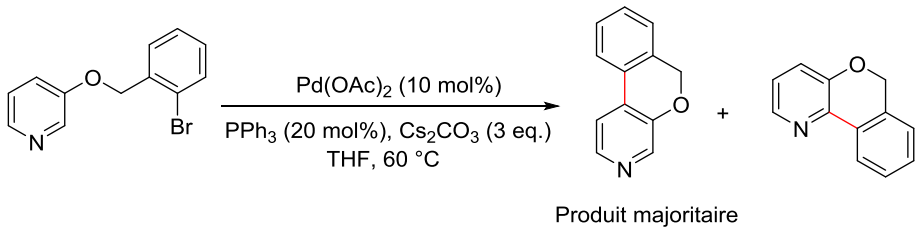

Les résultats préliminaires ont montré que la réaction développée permettait d'obtenir de manière sélective le produit résultant de de l'activation de la liaison C-H en para de l'atome d'azote de la pyridine. Le champ d'application de cette réaction a été étudié et un mécanisme réactionnel expliquant la regiosélectivité observée proposé.

Table of Contents

ABBREVIATION LIST

Ac: acetyl group

Ad: adamantyl group

ADME: absorption, distribution, metabolism, and excretion

AIBN: azobisisobutyronitrile

Ar: aromatic group

BArF: tetrakis[3,5-bis(trifluoromethyl)phenyl]borate

BINIQ: 2,2'-binaphthyl-1,1'-biisoquinoline

bMepi: 1,3-(6'-methyl-2'-pyridylimino)isoindolate

Bn: benzyl group

Bu: butyl group

CDA: cross-dehydrogenative arylation

CDC: cross-dehydrogenative coupling

CMD: concerted metalation-deprotonation

cod: 1,5-cyclooctadiene

cot: 1,3,5-cyclooctatriene

Cy: cyclohexyl group

CYP: cytochrome P450s

DCC: *N*,*N*'-dicyclohexyl-carbodiimide

DCE: dichloroethane

DDQ: 2,3-dichloro-5,6-dicyanobenzoquinone

DFT: Density Functional Theory

DIAD: diisopropyl azodicarboxylate

DMA: *N*,*N*-dimethylacetamide

DMAP: 4-dimethylaminopyridine

DME: dimethoxyethane

DMF: *N*,*N*-dimethylformamide

DMSO: dimethyl sulfoxide

dppb: 1,4-bis(diphenylphosphino)butane

Et: ethyl group

FTIR: Fourier transform infrared spectroscopy

hcp: hexagonal close packed

Hex: hexyl group

HIE: hydrogen isotope exchange

HPLC: high-performance liquid chromatography

HREM: high resolution electron microscopy

HRMS: high-resolution mass spectrometry

HSCIE: high-temperature solid-state catalytic isotope exchange

HTBZ: dihydrotetrabenazine

ICP-AES: inductively coupled plasma-atomic emission spectrometry

ICy: *N*,*N*-dicyclohexylimidazol-2-ylidene

IDC: intramolecular-dehydrogenative-coupling

IR: infrared

KIE: kinetic isotope effect

LAE: ligand acceleration effect

LC-MS: liquid chromatography-mass spectrometry

LSC: Liquid Scintillation Counter

Me: methyl group

Mes: 2,4,6-trimethylphenyl group

MOF: metal-organic framework

Ms: mesyl group

NBO: natural bond orbitals

NBS: *N*-bromosuccinimide

NHC: *N*-heterocyclic carbene

NMP: *N*-methyl-2-pyrrolidone

NMR: nuclear magnetic resonance

NOBIN: 2-amino-2'-hydroxy-1,1'-binaphthyl

OLED: organic light-emitting diodes

PET: positron emission tomography

Ph: phenyl group

Piv: pivaloyl group

PMB: 4-methoxybenzyl group

PPy: polypyrrole

Pr: propyl group

p-TSA: *p*-toluenesulfonic acid

PVP: polyvinylpyrrolidone

Py: pyridine

S_EAr: electrophilic aromatic substitution

SEM: scanning electron microscopy

SET: single electron transfer

SM: starting material

TBAA: tetrabutylammonium acetate

TBAB: tetrabutylammonium bromide

TBHP: *tert*-butylhydroperoxyde

TEM: transmission electron microscopy

TFA: trifluoroacetic acid

TFAA: trifluoroacetic anhydride

THF: tetrahydrofuran

Tf: trifluoromethanesulfonyl group

TM: target molecule

TOF: turnover frequency

TON: turnover number

TRIP: 2,4,6-triisopropylphenyl

Ts: *p*-toluenesulfonyl group

UHPLC: Ultra High Pressure Liquid Chromatography

UV-Vis: ultraviolet-visible

VMAT2: vesicular monoamine transporter 2

WAXS: wide-angle X-ray scattering

XPS: X-ray photoelectron spectroscopy

XRD: X-ray diffraction

XRF: X-ray fluorescence spectroscopy

ZPE: zero-point energy

Chapter 1 Deuterium and Tritium Labeling of Bioactive Thioethers

1 Introduction and background

1.1 Deuterium and applications of deuterated compounds

A slight difference might cause huge effect, just as the case of hydrogen isotopes (**Figure 1.1**). Deuterium is one of two natural isotopes of hydrogen, with the symbol D or ^{2}H, which also known as heavy hydrogen. As an isotope of hydrogen, deuterium differs from hydrogen simply by possessing a single neutron, and it is the extra neutron that may make a massive difference in the reactivity of deuterium versus its isotope protium.

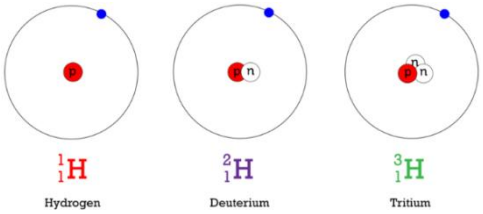

Figure 1.1 Hydrogen isotopes

Deuterium was discovered and named in 1931 by Harold C. Urey.[1] It has a natural abundance in Earth's oceans of about one atom over 6420 of hydrogen. The most common isotope (^{1}H) occupies more than 99.98% of all the naturally occurring hydrogen, while deuterium has a number of approximately 0.0156% (or on a mass basis 0.0312%). Notably, natural water from different sources or places has a slightly different abundance of deuterium.[2] For example, the deuterium content of surface water is about 5% lower than that of marine water, due to the repeated vaporization and condensation.

Multiple applications have been found for deuterated compounds in chemistry, biology and material science.[3] One of the most important applications in chemistry is due to the kinetic isotope effect (**Figure 1.2**). Since D is heavier than H, the vibrational frequency of a C-D bond is lower than the one

[1] a) H. C. Urey, F. G. Brickwedde, G. M. Murphy, *Phys. Rev.* **1932**, *39*, 164; b) H. C. Urey, F. G. Brickwedde, G. M. Murphy, *Phys. Rev.* **1932**, *40*, 1; c) F. G. Brickwedde, *Phys. Today* **1982**, *35*, 34.

[2] Y. Horibe, M. Kobayakawa, *Geochim. Cosmochim. Acta* **1960**, *20*, 273.

[3] a) J. Atzrodt, V. Derdau, T. Fey, J. Zimmermann, *Angew. Chem. Int. Ed.* **2007**, *46*, 7744; b) T. Junk, W. J. Catallo, *Chem. Soc. Rev.* **1997**, *26*, 401; c) Y. Sawama, Y. Monguchi, H. Sajiki, *Synlett* **2012**, *23*, 959.

of a C-H bond, which leads to a lower zero-point energy (ZPE) of the C-D bond. The lower ZPE of C-D bond results in higher activation energy for the C-D bond cleavage than that of C-H bond one: more energy is needed for a C-D bond to reach its transition state for bond cleavage. As a result, if the rate-determining step of a reaction involves the cleavage of a C-H/D bond, the deuterated analogues will have slower reaction rate than the unlabeled molecules. This effect is called the primary kinetic isotope effect (KIE). Normal KIE means that the reaction rate for a C-H bond cleavage is faster than the one for a C-D bond cleavage. There is also inverse KIE, which means that the reaction rate for a C-D bond cleavage is faster than the one for a C-H bond cleavage. The secondary isotope effect differs from the primary isotope effect by the fact that no C-D bond is formed or broken in the rate determining step.[4]

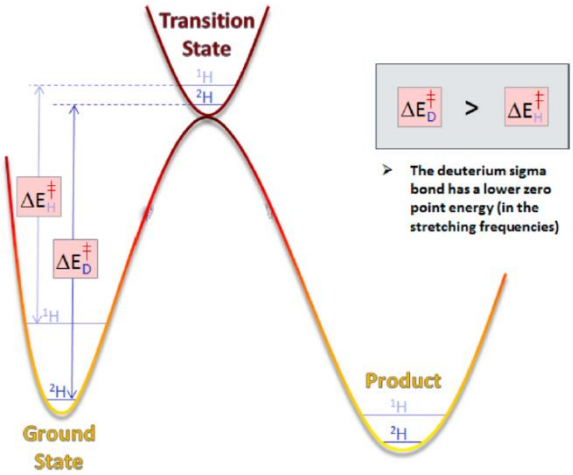

Figure 1.2 Origins of the deuterium kinetic isotope effect[5]

An important application of deuterated compounds is their use in mechanistic studies.[6] For example, deuterated toluenes were employed as substrates for aromatic hydroxylation catalyzed by the natural and G103L isoforms of the diiron enzyme toluene 4-monooxygenase to understand the reaction mechanism by C. E. Rogge and co-workers.[6d] By observing the magnitudes of isotope effects and patterns of deuterium retention of the hydroxylation, the authors concluded that an active site-directed opening of position-specific transient epoxide intermediates might contribute to the chemical mechanism and the regiospecificity of the reaction (**Figure 1.3**). Generally, by comparing the reaction rate of deuterated substrates with the hydrogenated ones, the researchers might know whether the rate

[4] C. L. Perrin, Y. Dong, *J. Am. Chem. Soc.* **2007**, *129*, 2759.

[5] T. G. Gant, *J. Med. Chem.* **2014**, *57*, 3595.

[6] a) T. Furuta, H. Takahashi, Y. Kasuya, *J. Am. Chem. Soc.* **1990**, *112*, 3633; b) C. H. Oh, H. H. Jung, K. S. Kim, N. Kim, *Angew. Chem. Int. Ed.* **2003**, *42*, 805; c) S. D. Nelson, W. F. Trager, *Drug Metab. Dispos.* **2003**, *31*, 1481; d) K. H. Mitchell, C. E. Rogge, T. Gierahn, B. G. Fox, *Proc. Natl. Acad. Sci. U.S.A.* **2003**, *100*, 3784; e) D. M. Marcus, M. J. Hayman, Y. M. Blau, D. R. Guenther, J. O. Ehresmann, P. W. Kletnieks, J. F. Haw, *Angew. Chem. Int. Ed.* **2006**, *45*, 1933; f) D. M. Marcus, K. A. McLachlan, M. A. Wildman, J. O. Ehresmann, P. W. Kletnieks, J. F. Haw, *Angew. Chem. Int. Ed.* **2006**, *45*, 3133; g) T. Zhang, Q. Peng, C. Quan, H. Nie, Y. Niu, Y. Xie, Z. Zhao, B. Z. Tang, Z. Shuai, *Chem. Sci.* **2016**, *7*, 5573.

determining step is the cleavage of the C-H/D bond or not;[7] by observing the final fate of the deuterium atom in substrate, one could suggest the possible reaction pathway.[8]

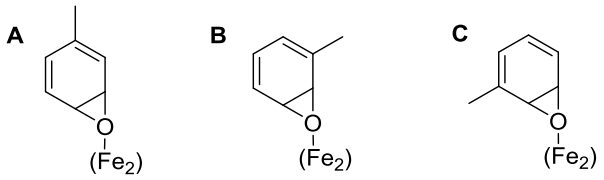

Figure 1.3 Binding modes of epoxide intermediates relative to the (Fe_2) center

Apart from mechanistic studies, isotopically labeled molecules have also found a major role in the quantitative liquid chromatography-mass spectrometry/mass spectrometry (LC-MS/MS) analysis as internal standards.[9] An internal standard is a compound that is very similar, but not identical to the target analyte. It should have the same effect of sample preparation as the target analyte, but the analytical method should be able to identify the analyte from the internal standard in some factors such as molecular mass. Deuterated compounds can act as internal standards due to several factors: they can be extracted from biological samples at the same content as their corresponding unlabeled analogues; they have the same retention times as the unlabeled analogues in chromatographic methods; the ionization behavior of deuterated compounds is the same as the unlabeled analogues in LC/MS analyses, but their molecular masses are different. Consequently, the quantitative determination of an analyte is possible when the mass difference is large enough between the analyte and its deuterated internal standard. In fact, in order to reduce the cross signal overlap between the analyte and the internal standard, the latter should be deuterated with a low content (less than 0.5%) of unlabeled material (D_0) and a representative mass peak (**Figure 1.4**).[9a] Thus, it should incorporate 3-5 deuterium atoms in order to be clearly identified from its natural isotope distribution.

[7] a) E. M. Simmons, J. F. Hartwig, *Angew. Chem. Int. Ed.* **2012**, *51*, 3066; b) H. Shi, P. Wang, S. Suzuki, M. E. Farmer, J.-Q. Yu, *J. Am. Chem. Soc.* **2016**, *138*, 14876.

[8] a) Z.-X. Wang, X.-Y. Bai, H.-C. Yao, B.-J. Li, *J. Am. Chem. Soc.* **2016**, *138*, 14872; b) L. Zhang, G. J. Lovinger, E. K. Edelstein, A. A. Szymaniak, M. P. Chierchia, J. P. Morken, *Science*, **2016**, *351*, 70.

[9] a) J. Atzrodt, V. Derdau, *J. Label. Compd. Radiopharm.* **2010**, *53*, 674; b) X. Diao, Z. Ma, H. Wang, D. Zhonga, Y. Zhang, J. Jin, Y. Fan, X. Chen, *J. Pharm. Biomed. Anal.* **2013**, *78-79*, 19; c) P. Bruheim, H. F. N. Kvitvang, S. G. Villas-Boas, *J. Chromatogr. A* **2013**, *1296*, 196; d) T. Yarita, Y. Aoyagi, T. Otake, *J. Chromatogr. A* **2015**, *1396*, 109; e) N. Bakaraki, D. S. Chormey, S. Bakirdere, G. O. Engin, *Anal. Methods* **2016**, *8*, 2660; f) H. B. Swan, E. S. M. Deschaseaux, G. B. Jones, B. D. Eyre, *Anal. Bioanal. Chem.* **2017**, *409*, 1929.

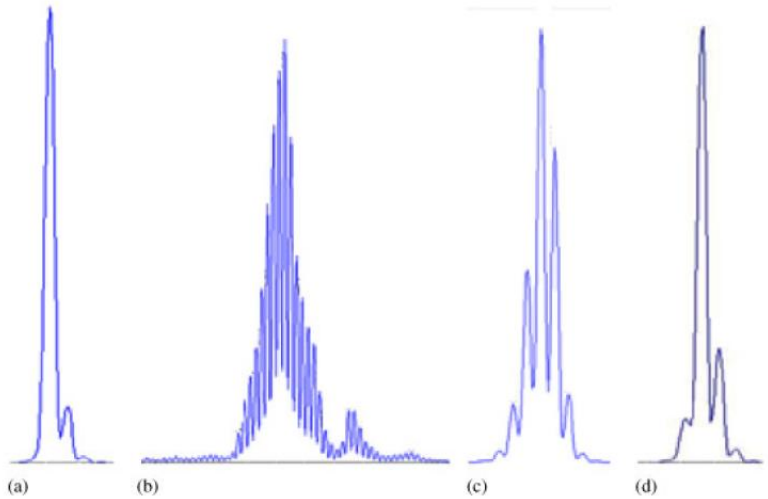

Figure 1.4 MS distribution patterns from different compounds: (a) natural isotope; (b) unselective H/D exchange; (c) moderately broad isotope cluster with a representative mass peak; (d) highly selective H/D exchange.

For example, 3-*n*-butylphthalide (**Figure 1.5**, compound **1.1.1a**) is a cardiovascular drug widely used in China for the treatment of cerebral ischemic stroke. It is of great importance to have a better understanding of the *in vivo* fate of **1.1.1a** and its four major metabolites (**Figure 1.5**, compounds **1.1.2a-1.1.5a**) for safety evaluation, good clinic practice and discovery of new antistroke drugs. In 2013, X. Chen *et al.* reported a method allowing the simultaneous quantitation of **1.1.1a** and its four major metabolites in human plasma by LC-MS/MS using the corresponding deuterated **1.1.1b-1.1.5b** as internal standards.[9b] Using this analytical method, they were able to quantify the five compounds with the lowest concentration of 3.00 ng/ml. Moreover, by following a single oral administration of 200 mg **1.1.1a** to healthy volunteers, the pharmacokinetic profiles of **1.1.1a-1.1.5a** were characterized successfully by this method.

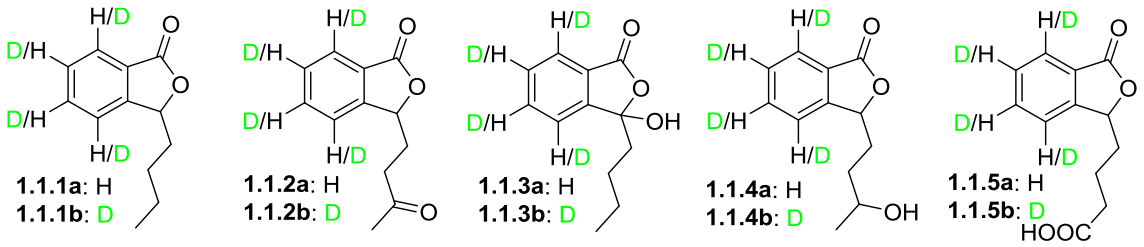

Figure 1.5 Structure of 3-*n*-butylphthalide and its four major metabolites

More recently, the first deuterated drug, deutetrabenazine (**Figure 1.6**), was approved by FDA.[10] Tetrabenazine is a vesicular monoamine transporter 2 (VMAT2) inhibitor, and it is used for the treatment of chorea associated with Huntington disease. It has been proved that its deuterated analogue, deutetrabenazine, has improved dosing and safety profiles, owing to the stronger bond energy of the C-D bond and thus better withstanding drug-metabolizing enzymes such as the cytochrome P450s (CYP), a class of monooxygenase for the oxidation of C-H bond. According to the *in vitro* experiments in human liver microsomes, deutetrabenazine is rapidly and extensively metabolized by carbonyl reductase to its major active metabolites, α-dihydrotetrabenazine (α-HTBZ, **Figure 1.6**) and β-dihydrotetrabenazine (β-HTBZ, **Figure 1.6**), which potently inhibit VMAT2 in the central nervous system. The active metabolites are subsequently metabolized majorly by cytochrome P450 2D6 (CYP2D6) through the oxidation of the methyl group. Since the cleavage of C-H bond is the rate-determining step in CYP catalyzed oxidation,[11] as a consequence, the deuterated analogues are more able to withstand the oxidation by CYP2D6 than the hydrogenated ones, owing to the stronger bond energy of C-D bonds than C-H bonds (primary KIE). As a result, the active metabolites of deutetrabenazine have a longer lifetime than the ones of tetrabenazine, hence improving the dosing and safety profiles.

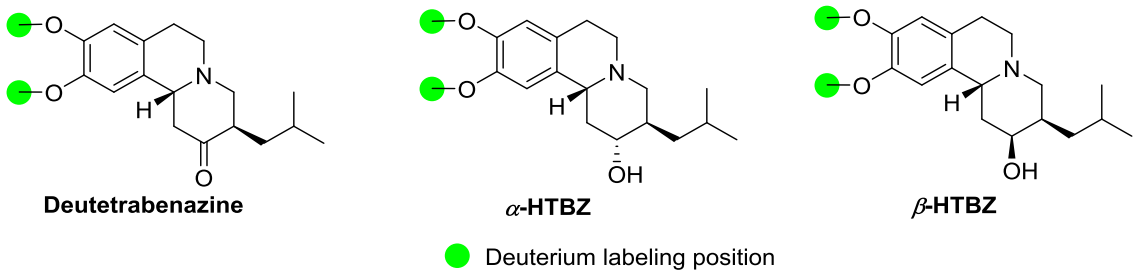

Figure 1.6 Deutetrabenazine and its major active metabolites

Indeed, the selective incorporation of deuterium into drugs can increase significantly their biological half-life, taking advantage of the primary kinetic isotope effect. Moreover, it has been reported that the formation of undesired or toxic metabolites could be reduced through selective deuteration of a drug, together with an enhancement of the formation of desired metabolites.[12] In fact, there are more and more deuterated drugs under preclinical and clinical investigations.[13]

[10] A. Mullard, *Nat. Rev. Drug Discov.* **2017**, *16*, 305.

[11] F. P. Guengerich, *Biol. Chem.* **2002**, *383*, 1553.

[12] S. L. Harbeson, R. D. Tung, *MedChem News* **2014**, *24*, 8.

[13] a) T. G. Gant, *J. Med. Chem.* **2014**, *57*, 3595; b) B. Halford, *Chem. Eng. News* **2016**, *94*, 32; c) A. Mullard, *Nat. Rev. Drug Discov.* **2016**, *15*, 219; d) R. D. Tung, *Future Med. Chem.* **2016**, *8*, 491.

In addition, isotopically labeled compounds also facilitate the rapid development of material science, especially the development of organic light-emitting diodes (OLEDs) and photovoltaics.[14] Generally, devices having deuterated molecules do not significantly change the physiochemical properties compared to the ones having hydrogenated compounds,[15] but different behaviors of devices having deuterated molecules might be observed due to the mass difference between hydrogen and deuterium. For example, it was reported that by using the devices made with deuterated compounds, the external quantum efficiency of electroluminescent devices could be increased significantly; besides, lower turn-on voltages and lower deterioration rates in the electroluminescence brightness were observed; a better highvoltage stability could happen.[14a] In another case, the isotopic effects of deuteration on optoelectronic properties of conducting polymers were studied by K. Xiao and co-workers.[14d] Different photovoltaic characteristics were found between the main-chain deuterated polymer (**Figure 1.7**, **1.1.6**-D_M) and side-chain deuterated polymer (**Figure 1.7**, **1.1.6**-D_S). For the former deuterated analogue, the short-circuit current was reduced due to the change of film crystallinity and morphology of the active layer resulted by the weak non-covalent intermolecular interactions of deuterated thiophene main-chain; for the latter deuterated analogue, the film morphology remained not changed, while the electronic coupling was decreased together with the formation of a charge transfer state and increased electron-phonon coupling, which has reduced significantly the open circuit voltage.

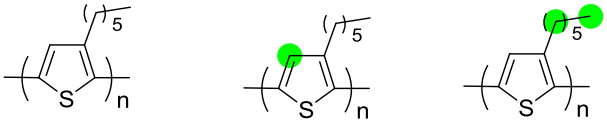

1.1.6 **1.1.6-D_M** **1.1.6-D_S**

Figure 1.7 Polymers studied by K. Xiao *et al.*

There are many other applications for deuterated molecules. For example, in metabolomics, deuterated molecules were used to provide accurate metabolite identification, absolute quantification and flux measurement.[16] As shown in **Figure 1.8**, metabolomic analysis by coupling H/D exchange and LC/MS was conducted by J. F. Banfield and co-workers.[16a] By comparing the mass spectrum of metabolites obtained from protonated solvents and the one obtained from deuterated solvents, the exchangeable hydrogens of the analytes could be figured out, which could help to identify the structure of the analytes. Through the analyses of the sample metabolites, the authors discovered that natural

[14] a) C. C. Tong, K. C. Hwang, *J. Phys. Chem. C* **2007**, *111*, 3490; b) T. D. Nguyen, G. Hukic-Markosian, F. Wang, L. Wojcik, X.-G. Li, E. Ehrenfreund, Z. V. Vardeny, *Nat. Mater.* **2010**, *9*, 345; c) T. A. Darwish, A. R. G. Smith, I. R. Gentle, P. L. Burn, E. Luks, G. Moraes, M. Gillon, P. J. Holden, M. James, *Tetrahedron Lett.* **2012**, *53*, 931; d) M. Shao, J. Keum, J. Chen, Y. He, W. Chen, J. F. Browning, J. Jakowshi, B. G. Sumpter, I. N. Ivanov, Y.-Z. Ma, C. M. Rouleau, S. C. Smith, D. B. Geohegan, K. Hong, K. Xiao, *Nat. Commun.* **2014**, *5*, 1; e) H. Tsuji, C. Mitsui, E. Nakamura, *Chem. Commun.* **2014**, *50*, 14870; f) A. Danos, R. W. MacQueen, Y. Y. Cheng, M. Dvořák, T. A. Darwish, D. R. McCamey, T. W. Schmidt, *J. Phys. Chem. Lett.* **2015**, *6*, 3061; g) A. T. Wagner, R. Zhou, K. S. Quinn, T. A. White, J. Wang, K. J. Brewer, *J. Phys. Chem. A* **2015**, *119*, 6781.

[15] T A Baillie, *Pharmacol. Rev.* **1981**, *33*, 81.

[16] a) C. R. Fischer, P. Wilmes, B. P. Bowen, T. R. Northen, J. F. Banfield, *Metabolomics*, **2012**, *8*, 566; b) A. Chokkathukalam, D.-H. Kim, M. P. Barrett, R. Breitling, D. J. Creek, *Bioanalysis* **2014**, *6*, 511.

acidophilic microbial communities contained *N*-methyl *lyso* phosphatidylethanolamines (PE) as abundant lipids.

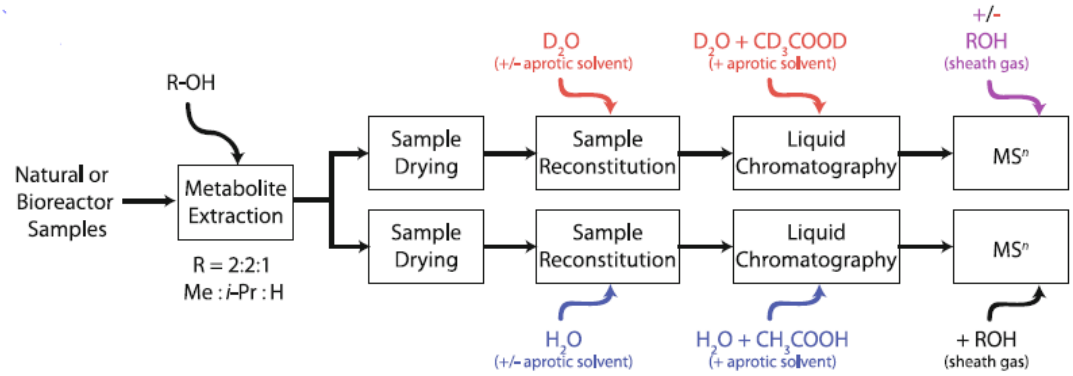

Figure 1.8 Sample handling workflow for deuterium exchange metabolomics studies[16a]

In pharmacokinetic and pharmacological absorption, distribution, metabolism, and excretion studies (ADME), deuterated molecules were used to slow down the metabolic rate and modulate pharmacokinetics.[17] In some special cases, deuteration was reported to protect amino acids against racemization,[18] enhance catalyst lifetime,[19] probe C-H activation process,[20] enable structure analysis of protein,[21] control the diastereoselectivity of ligand synthesis,[22] and facilitate the formation of desired product in total synthesis.[23] More importantly, various deuterated solvents are widely used in NMR analyses to understand the structure information of organic compounds.

1.2 Tritium and applications of tritiated compounds

Tritium is a radioactive isotope of hydrogen with a symbol of T or ^{3}H, which contains one proton and two neutrons. It was first produced from deuterium by Rutherford, M. L. Oliphant, and P. Harteck in 1934.[24] However, it was L. W. Alvarez and R. Cornog who isolated tritium for the first time and

[17] a) R. Sharma, T. J. Strelevitz, H. Gao, A. J. Clark, K. Schildknegt, R. S. Obach, S. L. Ripp, D. K. Spracklin, L. M. Tremaine, A. D. N. Vaz, *Drug Metab. Dispos.* **2012**, *40*, 625; b) J. Schofield, D. Brasseur, B. de Bruin, T. Vassal, S. Klieber, C. Arabeyre, M. Bourrié, F. Sadoun, G. Fabre, *J. Label. Compd. Radiopharm.* **2013**, *56*, 504; c) V. Uttamsingh, R. Gallegos, J. F. Liu, S. L. Harbeson, G. W. Bridson, C. Cheng, D. S. Wells, P. B. Graham, R. Zelle, R. Tung, *J. Pharmacol. Exp. Ther.* **2015**, *354*, 43; d) J. Jiang, X. Pang, L. Li, X. Dai, X. Diao, X. Chen, D. Zhong, Y. Wang, Y. Chen, *Drug Des. Dev. Ther.* **2016**, *10*, 2181.

[18] J. D. Lowenson, V. V. Shmanai, D. Shklyaruck, S. G. Clarke, M. S. Shchepinov, *Amino Acids* **2016**, *48*, 2189.

[19] N. Armenise, N. Tahiri, N. N. H. M. Eisink, M. Denis, M. Jäger, J. G. De Vries, M. D. Witte, A. J. Minnaard, *Chem. Commun.* **2016**, *52*, 2189.

[20] F. M. Chadwick, T. Krämer, T. Gutmann, N. H. Rees, A. L. Thompson, A. J. Edwards, G. Buntkowsky, S. A. Macgregor, A. S. Weller, *J. Am. Chem. Soc.* **2016**, *138*, 13369.

[21] A. Kita, Y. Morimoto, *Mol. Biotechnol.* **2016**, *58*, 130.

[22] R. A. Arthurs, C. J. Richards, *Org. Lett.* **2017**, *19*, 702.

[23] a) M. Miyashita, M. Sasaki, I. Hattori, M. Sakai, K. Tanino, *Science* **2004**, *305*, 495; b) K. W. Quasdorf, A. D. Huters, M. W. Lodewyk, D. J. Tantillo, N. K. Garg, *J. Am. Chem.Soc.* **2012**, *134*, 1396.

[24] a) M. L. Oliphant, P. Harteck, Rutherford, *Nature* **1934**, *133*, 413; b) M. L. E. Oliphant, P. Harteck, Lord Rutherford, *Proc. R. Soc. A* **1934**, *144*, 692.

discovered tritium's radioactivity.[25] According to the radionuclide safety data sheet (RSDS) developed by Radiation Safety Services (RSS), tritium has a physical half-life of 12.3 years, a high specific activity of 9650 Ci/g (28.8 Ci/mmol), and it emits beta particle with a range of 5 mm in air and average about 0.56 μm in water or tissue. [Specific activity is defined as the activity per quantity of atoms of a particular radionuclide. The unit of specific activity is Ci/g (Ci = Curie) or Bq/g (Bq = Becquerel), and 1 Ci/g = 3.7×10^{10} Bq/g.] The high specific activity together with insignificant penetrability through human skin makes tritium widely used as a radioactive tracer element in biological research, especially for the labeling of biomolecules such as peptides, proteins, oligonucleotides, and antibodies.[26]

Tritium gas is usually stored in the form of a solid metal tritide and the stored tritium will not be released until it is heated. For tritium labeling, the most convenient isotopic source is the tritium gas because it can be easily produced by heating the metal tritide, and it can be reabsorbed upon cooling down the metal tritide. Tritiated water is sometimes used as the isotopic source for tritiation. However, pure tritiated water is corrosive due to self-radiolysis. Hence, it is used in the dilute form, which mainly contains H_2O plus some HTO. Since tritium gas is easier and safer to handle, it has been mostly used for tritium labeling. For instance, recently, our group reported a method allowing the tritium labeling of DPA-714 (**Figure 1.9**), a fluorinated ligand of the translocator protein 18 kDa (TSPO), which could be used as a probe for positron emission tomography (PET) imaging, by using Pd/C as catalyst and T_2 gas as the tritium source.[26e] The tritiated molecule could help to better understand how it binds to the TSPO, and it also gave a combination of *in vitro* and *in vivo* studies performed with this tracer.

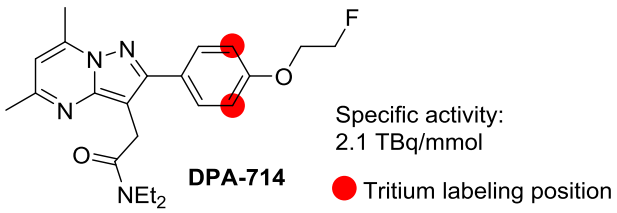

Figure 1.9 Structure of DPA-714

[25] a) L. W. Alvarez, R. Cornog, *Phys. Rev.* **1939**, *56*, 613; b) L. W. Alvarez, W. P. Trower, *Discovering Alvarez: Selected works of Luis W. Alvarez, with commentary by his students and colleagues*, University of Chicago Press, Chicago and London, 1987, 26-29.

[26] a) M. Saljoughian, P. G. Williams, *Curr. Pharm. Des.* **2000**, *6*, 1029; b) U. S. Larsen, H. B. Hansen, A.-M. Dahl, L. Sørensen, J. B. Kristensen, *J. Label. Compd. Radiopharm.* **2007**, *50*, 549; c) G. Tóth, J. R. Mallareddy, F. Tóth, A. W. Lipkowski, D. Tourwé, *ARKIVOC* **2012** (*v*), 163; d) G. Schwarzmann, C. Arenz, K. Sandhoff, *Biochim. Biophys. Acta* **2014**, *1841*, 1161; e) A. Damont, S. Garcia-Argote, D.-A. Buisson, B. Rousseau, F. Dollé, *J. Label. Compd. Radiopharm.* **2015**, *58*, 1.

In addition, tritiated molecules were applied to ADME studies.[27] Tritium labeled compounds are relatively simple and fast to synthesize compared with compounds labeled with other radioactive elements such as ^{14}C and ^{18}F, which are obtained mostly by multi-step synthesis. They can be obtained with high specific activity, which is useful for studying the highly potent compounds at a low dose. Tritium labeling facilitates the procurement of quantitative data of metabolites by avoiding the interference of complex biological matrices and metabolic changes to chemical structure. Through the analysis of radioactive metabolic profiles in excreta, it becomes possible to determine clearance mechanisms of drug candidates. In this context, the use of radioactive labeling is crucial in the safety assessment of novel pharmaceuticals. Therefore, the development of efficient late stage processes enabling the selective deuterium and tritium incorporation into complex molecules is of paramount importance.

For example, F. Lozac'h *et al.* used tritium labeled 2'-*O*-methyluridine to study its ADME properties in mice in order to understand the biological impact of this nucleoside in a siRNA sequence and to support preclinical safety studies and clinical development of siRNA therapeutics.[27h] The concentration of radiolabeled components were determined by Liquid Scintillation Counter (LSC). Metabolites were separated by Ultra High Pressure Liquid Chromatography (UHPLC) and subsequently identified using radiodetection and high-resolution mass spectrometry (HRMS). Through detecting the radioactivity by an intravenous administration of tritium labeled 2'-*O*-methyluridine after 48 hours, it was observed that tritiated 2'-*O*-methyluridine represented a minor component of the radioactivity (5.89%) in plasma; three metabolites (**Figure 1.10**) namely uridine (M_1), cytidine (M_2), and uracil (M_3) were the major circulating components representing 32.8%, 8.11%, and 23.6% of radioactivity area under the curve, respectively.

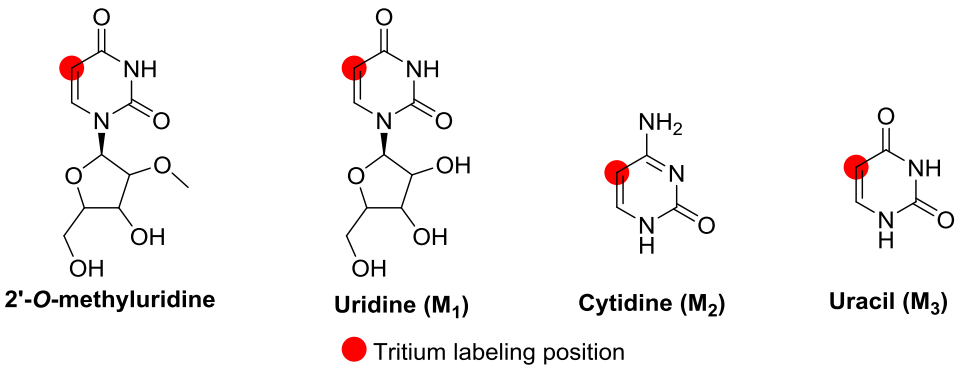

Figure 1.10 Tritium labeled 2'-O-methyluridine and its metabolites

[27] a) D. Dalvie, *Curr. Pharm. Des.* **2000**, *6*, 1009; b) F. P. Guengerich, *Chem. Res. Toxicol.* **2012**, *25*, 511; c) N. Penner, L. Xu, C. Prakash, *Chem. Res. Toxicol.* **2012**, *25*, 513; d) R. E. White, D. C. Evans, C. E. C. A. Hop, D. J. Moore, C. Prakash, S. Surapaneni, F. L. S. Tse, *Xenobiotica* **2013**, *43*, 219; e) R. S. Obach, A. N. Nedderman, D. A. Smith, *Xenobiotica* **2013**, *43*, 226; f) M. Pellegatti, *Expert. Opin. Drug Metab.* **2014**, *10*, 1615; g) A. Beattie, S. Madden, C. Lowrie, D. MacPherson, *Bioanalysis* **2015**, *7*, 507; h) F. Lozac'h, J. Christensen, T. Faller, E. van de Kerkhof, J. Krauser, M. Garnier, K. Litherland, A. Catoire, F. Natt, J. Hunziker, P. Swart, *Pharma Res Per* **2016**, *4*, e00209.

1.3 Synthesis of deuterium or tritium labeled compounds

There are two possible ways to achieve isotopically labeled molecules: (1) by a conventional multistep synthesis; (2) by direct hydrogen isotope exchange (HIE).

Starting from appropriate commercially available labeled precursors, more complex molecules could be synthesized in several steps. For example, in 2015, V. Uttamsingh and co-workers reported the synthesis of deuterated paroxetine hydrochloride salt **1.3.6** in 5 steps, with a total yield of 20% (**Scheme 1.1**).[28] Notably, deuterated sesamol **1.3.3** was synthesized separately in 3 steps, with a total yield of 53%. The advantage of this method was that it allowed the exclusive introduction of deuterium atoms with high isotopic enrichment (full deuterated starting material); however, it suffered the drawback of time and resources consuming and produced a lot of isotopically labeled wastes. Such drawback would be more underlined when dealing with tritium labeling.

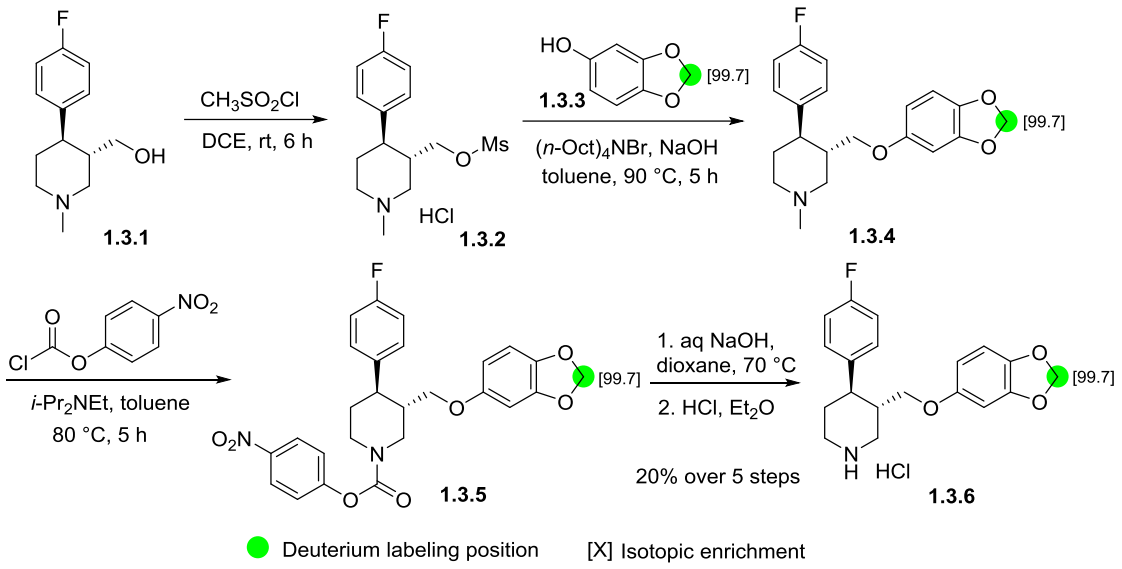

Scheme 1.1 Synthesis of deuterium labeled paroxetine hydrochloride salt

By contrast, the HIE process enables a direct isotopic labeling of the desired molecule in one single step, thus saving time and costs. Different types of catalysts have been applied in the HIE reactions. For metal catalysts, they could be divided into two types according to the active catalytic species: homogeneous catalysts and heterogeneous catalysts. Recently, our group developed a method allowing the regioselective and stereospecific deuteration of nitrogen containing compounds catalyzed by ruthenium nanoparticles,[29] and the deuteration of paroxetine has been achieved in one step with high

[28] V. Uttamsingh, R. Gallegos, J. F. Liu, S. L. Harbeson, G. W. Bridson, C. Cheng, D. S. Wells, P. B. Graham, R. Zelle, R. Tung, *J. Pharmacol. Exp. Ther.* **2015**, *354*, 43.

[29] G. Pieters, C. Taglang, E. Bonnefille, T. Gutmann, C. Puente, J.-C. Berthet, C. Dugave, B. Chaudret, B. Rousseau, *Angew. Chem. Int. Ed.* **2014**, *53*, 230.

deuterium incorporation and high yield (**Scheme 1.2**). Moreover, stereochemistry was retained over the deuteration process.

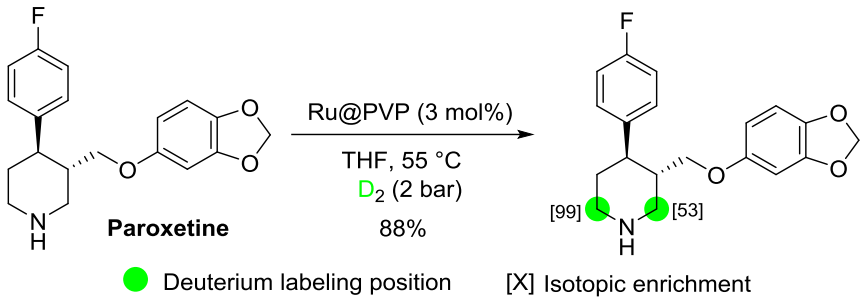

Scheme 1.2 H/D exchange of paroxetine catalyzed by RuNp@PVP

Obviously, the HIE process is preferred to obtain deuterated molecules. Achieving isotopically labeled molecules with high isotopic enrichment or high specific activity under mild reaction conditions is the main goal of HIE reactions. The main challenge of HIE process is the development of regio- and stereoselective procedures allowing the labeling of various functional group containing molecules.

A remarkable evolution was realized in the field of H/D exchange process since the pioneering work of J. L. Garnett half a century ago.[30] Using a homogeneous Pt-catalyst, Garnett succeeded to label a variety of aromatic compounds, despite the poor selectivity and low deuterium incorporation. Since then, rapid development has been achieved in the field of homogeneous catalytic H/D exchange reactions. Moreover, HIE reactions can be accomplished by either acid/base mediated H/D exchange or metal catalyzed H/D exchange. Remarkably, in the early 1980s, W. J. S. Lockley discovered that aromatic carboxylic acids and anilines could be labeled regioselectively using $RhCl_3$.[31] These distinguished works opened the door for a series of notable advances in regioselective H/D exchange reactions.

In the last 30 years, many research groups have made great contributions to the selective deuteration of various organic compounds.[32] One of the most remarkable advances may be the development and application of the Crabtree's catalyst $[(cod)Ir(PPh_3)(py)]PF_6$ (**Figure 1.11**),[33] which was first known as a hydrogenation catalyst in the beginning. Crabtree's catalyst is an air stable homogeneous catalyst developed by R. H. Crabtree in 1979, and it is now widely used for various catalytic reactions because

[30] a) J. L. Garnett, R. J. Hodges, *J. Am. Chem. Soc.* **1967**, *89*, 4546; b) M. R. Blake, J. L. Garnett, I. K. Gregor, W. Hannan, K. Hoa, M. A. Long, *J. Chem. Soc., Chem. Commun.* **1975**, 930.

[31] a) W. J. S. Lockley, *Tetrahedron Lett.* **1982**, *23*, 3819; b) W. J. S. Lockley, *J. Label. Compd. Radiopharm.* **1984**, *21*, 45; c) W. J. S. Lockley, *J. Label. Compd. Radiopharm.* **1985**, *22*, 623.

[32] For selected reviews, see *ref [2]*, *ref [8a]* and: a) R. Salter, *J. Label. Compd. Radiopharm.* **2010**, *53*, 645; b) W. J. S. Lockley, D. Hesk, *J. Label. Compd. Radiopharm.* **2010**, *53*, 704.

[33] a) R. H. Crabtree, H. Felkin, G. E. Morris, *J. Organomet. Chem.* **1977**, *141*, 205; b) R. Crabtree, *Acc. Chem. Res.* **1979**, *12*, 331.

of its robust catalytic activity and commercial availability.[34] Regarding the H/D exchange reaction mechanism catalyzed by Crabtree's catalyst, the key processes involve the coordination of substrate to the metal center, the activation of C-H bond adjacent to the functional group to form a five- or six-membered ring intermediate (**Figure 1.12**), ligand exchange and finally reductive elimination to yield the deuterated product.[35] It can be used either as a co-catalyst[36] or as an independent catalyst[35,37] in different deuteration reactions with high regioselectivity.

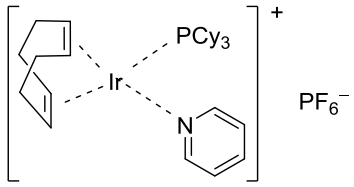

Figure 1.11 Structure of Crabtree's catalyst

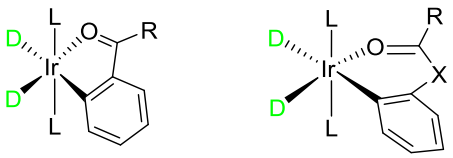

Figure 1.12 Key intermediates in H/D exchange reactions catalyzed by Crabtree's catalyst

The substrate scope of Crabtree's catalyst in H/D exchange is broad, ranging from aromatic esters, amides, ketones to heterocycles such as aryl substituted furan, thiophene, oxazole, thiazole, pyridine, pyrazole and so on.[37b] In some rare cases, Crabtree's catalyst is also used for C(sp^3)-H bond activation. For example, it has been applied to the selective H/T exchange of methapyrilene at C(sp^3)-H bond with high specific activity (**Figure 1.13**).[38]

[34] R. Salter, M. Chappelle, A. Morgan, T. Moenius, P. Ackermann, M. Studer, F. Spindler, *Synthesis and Applications of Isotopically Labelled Compounds*, John Wiley and Sons Ltd, Chichester, **2001**, 7, 63-67.

[35] a) A. Y. L. Shu, W. Chen, J. R. Heys, *J. Organomet. Chem.* **1996**, *524*, 87; b) J. S. Valsborg, L. Sørensen, C. Foged, *J. Label. Compd. Radiopharm.* **2001**, *44*, 209.

[36] S. C. Schou, *J. Label. Compd. Radiopharm.* **2009**, *52*, 376.

[37] a) D. Hesk, P.R. Das, B. Evans, *J. Label. Compd. Radiopharm.* **1995**, *36*, 497; b) G. J. Ellames, J. S. Gibson, J. M. Herbert, A. H. McNeill, *Tetrahedron* **2001**, *57*, 9487.

[38] a) N. Bushby, D. A. Killick, *J. Label. Compd. Radiopharm.* **2007**, *50*, 519; b) R. P. Yu, D. Hesk, N. Rivera, I. Pelczer, P. J. Chirik, *Nature* **2016**, *529*, 195.

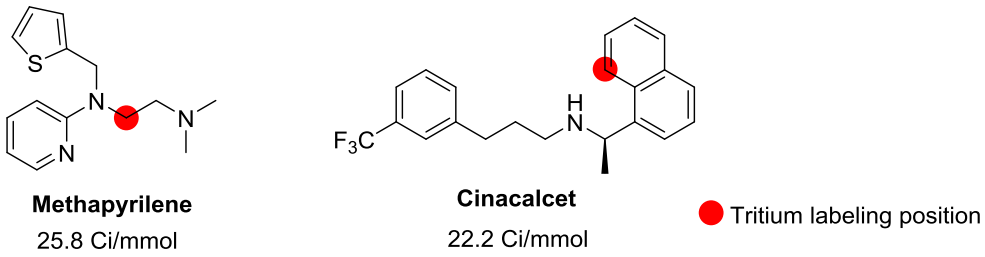

Figure 1.13 H/T exchange of bioactive compounds catalyzed by Crabtree's catalyst

However, despite the broad applications of the Crabtree's catalyst, a general drawback is its sensitivity to extraneous proton-bearing impurities.[39] Generally, dichloromethane is the only effective solvent used in the reaction. Besides, a significant loss of activity could happen when dealing with substrates with a functional group of alcohols or amines.[33] A general study of Crabtree's catalyst concerning the scope and limitations of deuteration has been done by J. M. Herbert and co-workers.[37b] They indicated that the Crabtree's catalyst was regularly required in stoichiometric amounts or even more, and often led to low isotope incorporation levels and undesirably lengthy reaction times. Moreover, the application of this catalyst to the tritium labeling leads to high amounts of (tritiated) wastes (labeled cyclooctane and/or cyclooctene from the ligand) because of the high catalyst loading.[40]

Numerous works have been recently dedicated to the development of new methods allowing selective and efficient labeling of biologically relevant compounds. Among them, several chemo- and regio-selective metal catalyzed H/D exchange procedures allowing the labeling of oxygen and nitrogen containing molecules have been described.[41] Compared to multistep syntheses, the H/D exchange process is a more steps and time saving way to achieve deuterated molecules. We review herein majorly the works published during the past ten years concerning the progress of metal-catalyzed HIE reactions through C-H activation processes.

1.4 H/D exchange reactions catalyzed by iridium complexes

Among all the metal catalysts used for the H/D exchange procedures, iridium complexes are the most wildly studied.[42] Many research groups have been working on iridium catalyzed H/D exchange reactions and great achievements have been obtained in this field.[32a] In recent years, numerous novel

[39] Y. Xu, D. M. P. Mingos, J. M. Brown, *Chem. Commun.* **2008**, 199.

[40] a) J. A. Brown, S. Irvine, A. R. Kennedy, W. J. Kerr, S. Anderssonb, G. N. Nilsson, *Chem. Commun.* **2008**, 1115; b) G. N. Nilsson, W. J. Kerr, *J. Label. Compd. Radiopharm.* **2010**, *53*, 662.

[41] For recent examples see *ref [35b]* and: a) L. V. A. Hale, N. K. Szymczak, *J. Am. Chem. Soc.* **2016**, *138*, 13489; b) B. Chatterjee, V. Krishnakumar, C. Gunanathan, *Org. Lett.* **2016**, *18*, 5892; c) B. Chatterjee and C. Gunanathan, *Org. Lett.* **2015**, *17*, 4794; d) W. J. Kerr, M. Reid, T. Tuttle, *ACS Catal.* **2015**, *5*, 402; e) W. J. Kerr, D. M. Lindsay, M. Reid, J. Atzrodt, V. Derdau, P. Rojahn, R. Weck, *Chem. Commun.* **2016**, *52*, 6669; f) L. Neubert, D. Michalik, S. Bähn, S. Imm, H. Neumann, J. Atzrodt, V. Derdau, W. Holla, M. Beller, *J. Am. Chem. Soc.* **2012**, *134*, 12239.

[42] A. R. Cochrane, S. Irvine, W. J. Kerr, M. Reid, S. Andersson, G. N. Nilsson, *J. Label. Compd. Radiopharm.* **2013**, *56*, 451.

methods based on HIE have been developed for the selective deuterium/tritium labeling of various organic compounds catalyzed by iridium complexes.[43]

1.4.1 Iridium catalyzed deuteration involving oxygen atom as directing groups

Oxygen is a common coordinating atom to many metals. It can coordinate in the form of different functional groups, such as alcohols, ketones, esters, carboxylic acids, amides or nitro group. Therefore, many works on H/D exchange have been achieved involving oxygen atom as directing groups catalyzed by iridium complexes.

Among the research groups working on iridium catalyzed H/D exchange reactions, W. J. Kerr's group has made huge contributions.[40a, 41d-e, 42, 43d-k] In 2008, Kerr reported[40a] the synthesis of a series of iridium complexes stabilized by bulky *N*-heterocyclic carbene (NHC) and their applications in the regioselective H/D exchange reactions (**Figure 1.14**). Excellent levels of labeling had been achieved over short reaction times and at low catalyst loadings. Moreover, these complexes were all air- and moisture-stable solids, which could be stored under air for more than 8 months without loss of catalytic activity.

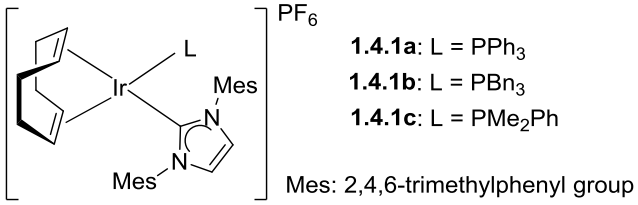

Figure 1.14 Structure of Kerr's catalysts

Since then, Kerr's group has been concentrating on the core structure of the iridium complex, by modifying the coordinating group or by changing the counterion, they have succeeded to deuterate/tritiate a variety of organic compounds. For example, through replacing PF_6 counterion with BArF (tetrakis[3,5-bis(trifluoromethyl)phenyl]borate), the catalytic activity could be improved at lower catalyst loadings, together with an improvement of solubility profile and applicable solvent

[43] For recent examples of iridium catalyzed H/D exchange reactions, see: a) V. M. Iluc, A. Fedorov, R. H. Grubbs, *Organometallics* **2012**, *31*, 39; b) M. C. Lehman, J. B. Gary, P. D. Boyle, M. S. Sanford, E. A. Ison, *ACS Catal.* **2013**, *3*, 2304; c) M. Parmentier, T. Hartung, A. Pfaltz, D. Muri, *Chem. Eur. J.* **2014**, *20*, 11496; d) J. A. Brown, A. R. Cochrane, S. Irvine, W. J. Kerr, B. Mondal, J. A. Parkinson, L. C. Paterson, M. Reid, T. Tuttle, S. Andersson, G. N. Nilsson, *Adv. Synth. Catal.* **2014**, *356*, 3551; e) A. R. Cochrane, C. Idziak, W. J. Kerr, B. Mondal, L. C. Paterson, T. Tuttle, S. Anderssonb, G. N. Nilsson, *Org. Biomol. Chem.* **2014**, *12*, 3598; f) A. R. Kennedy, W. J. Kerr, R. Moir, M. Reid, *Org. Biomol. Chem.* **2014**, *12*, 7927; g) W. J. Kerr, R. J. Mudd, L. C. Paterson, J. A. Brown, *Chem. Eur. J.* **2014**, *20*, 14604; h) J. Atzrodt, V. Derdau, W. J. Kerr, M. Reid, P. Rojahn, R. Weck, *Tetrahedron* **2015**, *71*, 1924; i) J. Devlin, W. J. Kerr, D. M. Lindsay, T. J. D. McCabe, M. Reid, T. Tuttle, *Molecules* **2015**, *20*, 11676; j) P. W. C. Cross, J. M. Herbert, W. J. Kerr, A. H. McNeill, L. C. Paterson, *Synlett* **2016**, *27*, 111; k) W. J. Kerr, R. J. Mudd, P. K. Owens, M. Reid, J. A. Brown, S. Campos, *J. Label. Compd. Radiopharm* **2016**, *59*, 601; l) A. Marek, M. H. F. Pedersen, S. B. Vogensen, R. P. Clausen, B. Frølund, T. Elbert, *J. Label. Compd. Radiopharm* **2016**, *59*, 476; m) I. Romanenko, S. Norsic, L. Veyre, R. Sayah, F. D'Agosto, J. Raynaud, C. Boisson, E. Lacôte, C. Thieuleux, *Adv. Synth. Catal.* **2016**, *358*, 2317; n) M. Hatano, T. Nishimura, H. Yorimitsu, *Org. Lett.* **2016**, *18*, 3674; o) S. Ibañez, M. Poyatos, E. Peris, *Dalton Trans.* **2016**, *45*, 14154; p) K. Jess, V. Derdau, R. Weck, J. Atzrodt, M. Freytag, P. G. Jones, M. Tamm, *Adv. Synth. Catal.* **2017**, *359*, 629; q) A. Burhop, R. Weck, J. Atzrodt, V. Derdau, *Eur. J. Org. Chem.* **2017**, 1418.

scope.[43f, k] Using the new catalyst **1.4.2**, they succeeded to label a drug molecule (niclosamide, **Scheme 1.3**) with an improved deuterium incorporation.

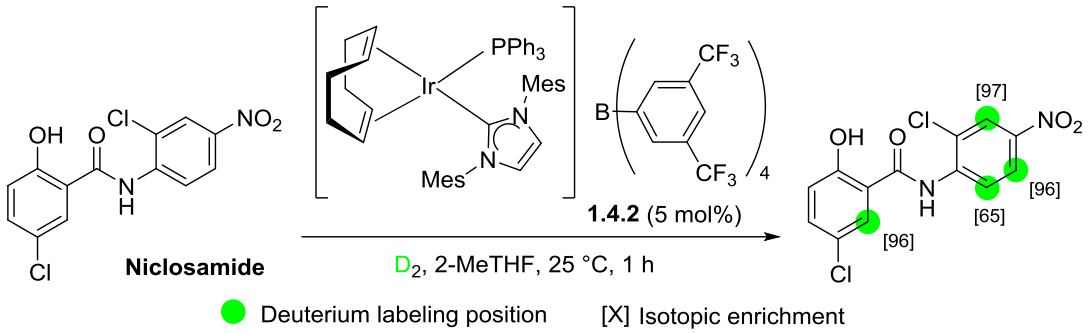

Scheme 1.3 Deuteration of niclosamide by iridium complex

Later, Kerr reported the first regioselective C-H deuteration of unsaturated organic compounds at the *β*-position with iridium catalyst **1.4.1a**.[43g] Under mild reaction conditions with low levels of catalyst loading, high levels of deuterium incorporation have been obtained with good selectivity over the potentially competing reduction process, across a series of *α*,*β*-unsaturated substrates (**Scheme 1.4**).

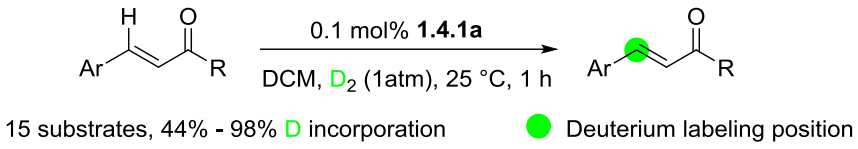

Scheme 1.4 Deuteration of *α*,*β*-unsaturated compounds with Kerr's catalyst

Besides, as an overview of Kerr's catalysts, they also examined their catalytic activities toward the labeling of benzoate ester derivatives comparing with Crabtree's catalyst.[43i] As a result, Kerr's catalyst **1.4.1a** showed more efficiency than Crabtree's catalyst in the deuteration of benzoate esters. Additionally, with a slightly raise of reaction temperature (from room temperature to 40 ℃), great improvements of deuterium incorporation were observed across all substrates examined. Thus, the application of Kerr's catalysts became wider by two ways: increasing the reaction temperature or switching the counterion.

Apart from Kerr's works, A. Marek and co-workers reported the labeling of unsaturated *γ*-hydroxybutyric acid (**1.4.3**, a potent ligand for high affinity *γ*-hydroxybutyric acid binding sites in the central nervous system) by comparison between H/D exchange reaction mediated by iridium complex and reduction by boro-deuterides (**Scheme 1.5**).[43l] Through changing the solvent, Crabtree's catalyst was able to control the selective deuteration of the substrate without over reduction. However, the

deuterium incorporation was low (< 10%). Kerr's catalyst was found to be more efficient than Crabtree's catalyst for the deuteration. However, over reduction always occurred together with high deuterium incorporation. By contrast, labeling through reduction by boro-deuterides gave α-deuterated alcohol with high yield. Using $LiB(OMe)_3D$ as reductant, the conversion of the reaction could reach 99% with 91% of yield, and it was even applicable to tritium labeling by using $LiB(OMe)_3T$.

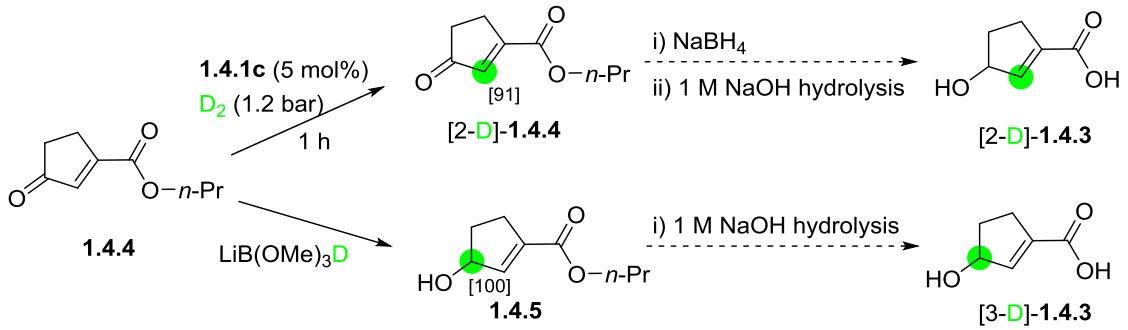

Scheme 1.5 The strategies of the deuterium labeling of **1.4.3**

Overall, Marek's group has provided an alternative way to the synthesis of deuterated γ-hydroxybutyric acid: the H/D exchange pathway using Kerr's catalysts **1.4.1a** and **1.4.1c**, even if the synthesis was accompanied by the formation of over reduced byproduct. Anyway, the different labeling sites of the molecule may help to better understand the *in vivo* activity of the molecule.

In 2016, C. Boisson and co-workers reported the synthesis of a polyethylene-supported iridium (III)-*N*-heterocyclic carbene catalyst (**Figure 1.15**) and its application for the H/D exchange reactions.[43m] According to the authors, the catalyst acted as a homogeneous catalyst at 100 ℃, but it could be easily recovered by filtration as a precipitate at room temperature due to the unique thermomorphic polyethylene properties.

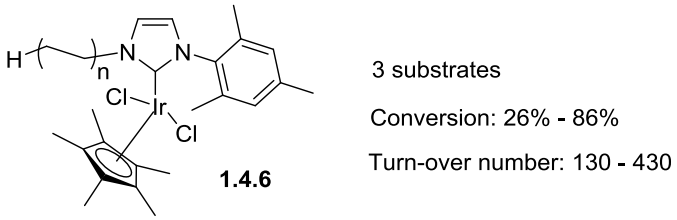

Figure 1.15 Polyethylene-supported iridium (III)-N-heterocyclic carbene catalyst

The advantages of the polyethylene-supported iridium catalyst were the low catalyst loading, short reaction time and its recyclable ability. When using 2 mol% of catalyst, the deuteration of

acetophenone was still efficient after the third cycle of the catalyst in just 5 min reaction time. However, the multistep synthesis of the catalyst and the narrow substrate scope (only 3 examples were given in the publication) have limited the application of the catalyst.

1.4.2 Iridium catalyzed deuteration involving nitrogen atom as directing group

Compared with oxygen, nitrogen atom displays stronger coordinating ability to transition metal catalysts because *N*-ligands are generally stronger Lewis bases than *O*-ligands, thus the coordination bond between transition metal and nitrogen is stronger than the one between transition metal and oxygen. Nitrogen can participate as coordinating atom in various functional groups, such as amines, sulfonamides and a series of *N*-heterocycles. Numerous works have been published recently based on the nitrogen directing groups.

Apart from the works of the deuteration involving oxygen atom, Kerr also applied his catalysts in the labeling of *N*-heterocycles[41e, 43h] and primary sulfonamides.[41d] For the labeling of *N*-heterocycles such as pyrimidine, imidazole, oxazole, oxazoline, isoxazole, thiazole, benzimidazole, benzoxazole and benzothiazole, catalyst **1.4.1a** proved to be the most efficient (**Scheme 1.6**, a);[43h] while for the labeling of unprotected tetrazoles, catalyst **1.4.2** worked best with the addition of Cs_2CO_3 as base since the reaction was a concerted metalation-deprotonation (CMD) pathway (**Scheme 1.6**, b).[41e] Moreover, through the optimization of reaction conditions, deuteration of complex molecules **1.4.7**-**1.4.9** and deuteration/tritiation of valsartan **1.4.10**, an angiotensin receptor blocker, were also achieved using the two catalysts separately (**Figure 1.16**).

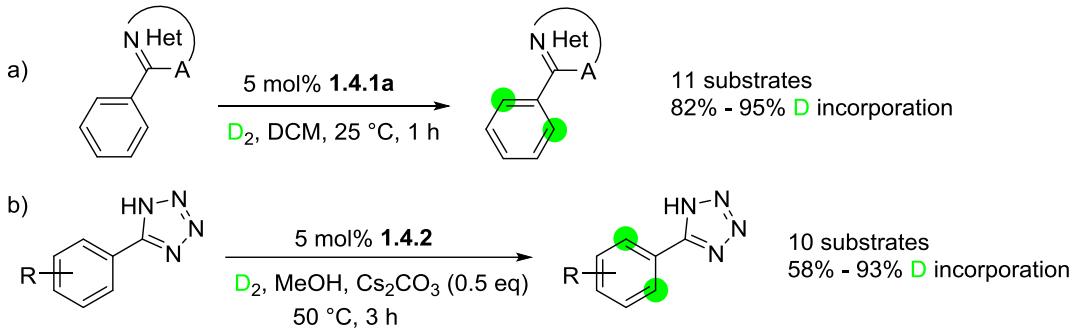

Scheme 1.6 Labeling of *N*-heterocycles by Kerr's catalyst

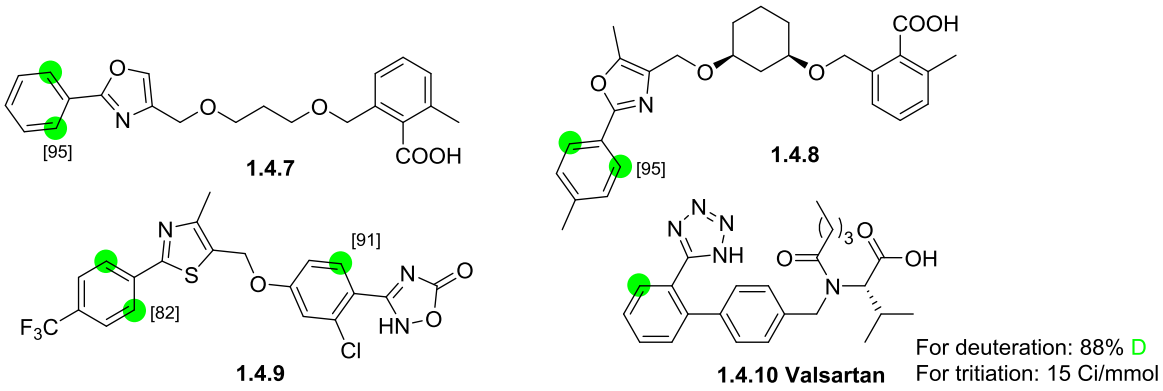

Figure 1.16 Labeling of complex molecules by Kerr's catalyst

In 2014, Kerr reported the first general method allowing the selective deuterium labeling of primary sulfonamides using a modified Kerr's catalyst **1.4.11** (**Scheme 1.7**).[41d] This catalyst had a sterically less hindered and more electron-rich chloride ligand, which could enhance the efficiency of the sulfonamide coordination and subsequent ortho-deuteration. A series of sulfonamides were selectively deuterated with various substituents on aryl rings, including two pharmaceuticals with good chemoselectivities (**Scheme 1.7**). However, a notable limitation of this method lies in the poor deuterium incorporation of some substrates due to their poor solubility in dichloromethane. A competition study was done to assess the chemoselectivity of the catalyst system, which revealed that the deuteration of primary sulfonamides could proceed smoothly with the presence of ketone, ester, nitro, and various amide directing groups; while the presence of *N*-heterocycles could change the chemoselectivity of the deuteration process to the labeling of these substrates.

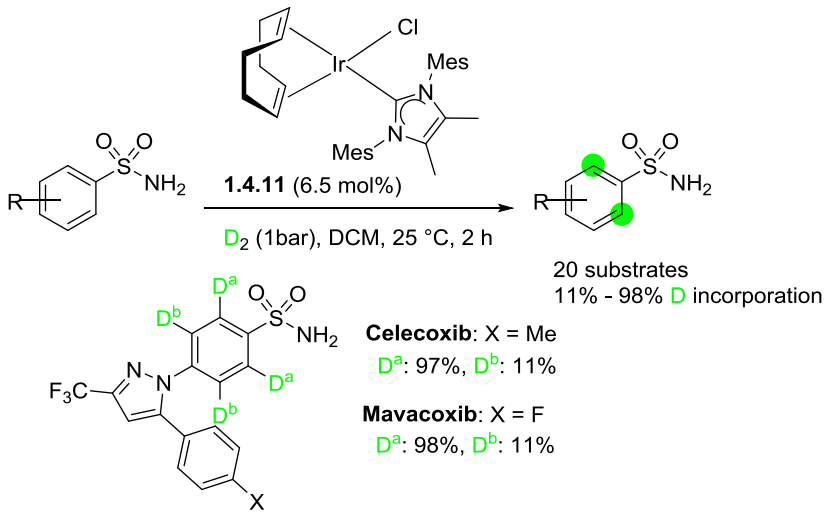

Scheme 1.7 Deuterium labeling of primary sulfonamides using a modified Kerr's catalyst

More recently, V. Derdau and co-workers reported the selective deuteration of secondary sulfonamides and the first selective aromatic deuteration of tertiary sulfonamides as well as sulfonylureas based on Kerr's catalyst **1.4.12** and the commercially available Burgess catalyst **1.4.13** (**Figure 1.17**).[43q] The Burgess catalyst **1.4.13**, which was developed as a catalyst for the asymmetric hydrogenation of olefins,[44] has never been applied in H/D exchange reactions before their publication.

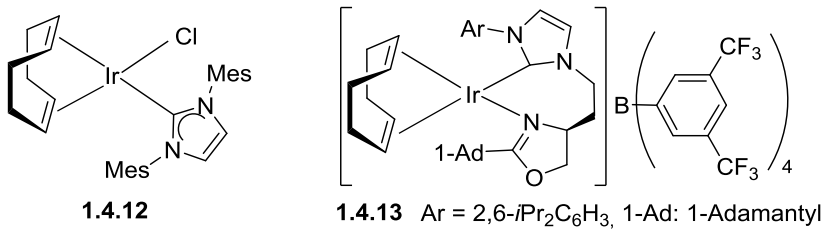

1.4.12 **1.4.13** Ar = 2,6-*i*Pr$_2$C$_6$H$_3$, 1-Ad: 1-Adamantyl

Figure 1.17 Structure of Kerr's catalyst **1.4.12** and Burgess catalyst **1.4.13**

By comparison of the catalytic activity of the two iridium complexes, the authors discovered that the Burgess catalyst **1.4.13** was more effective when conducting the deuteration reactions on tertiary sulfonamides, while the Kerr's catalyst **1.4.12** was more suitable for the labeling of secondary sulfonamides and ureas (**Scheme 1.8**). They also succeeded to adapt their method to the deuterium labeling of several drug molecules. Finally, the tritium labeling of glibenclamide was achieved after the optimization of reaction conditions (**Scheme 1.8**). Using 4 μmol of substrate, with 10 mol% of catalyst **1.4.12** and a reduced pressure of tritium gas (160-278 mbar), after heating at 100 ℃ in PhCl for 3 h, they succeeded to tritiate glibenclamide with a specific activity of 9 Ci/mmol.

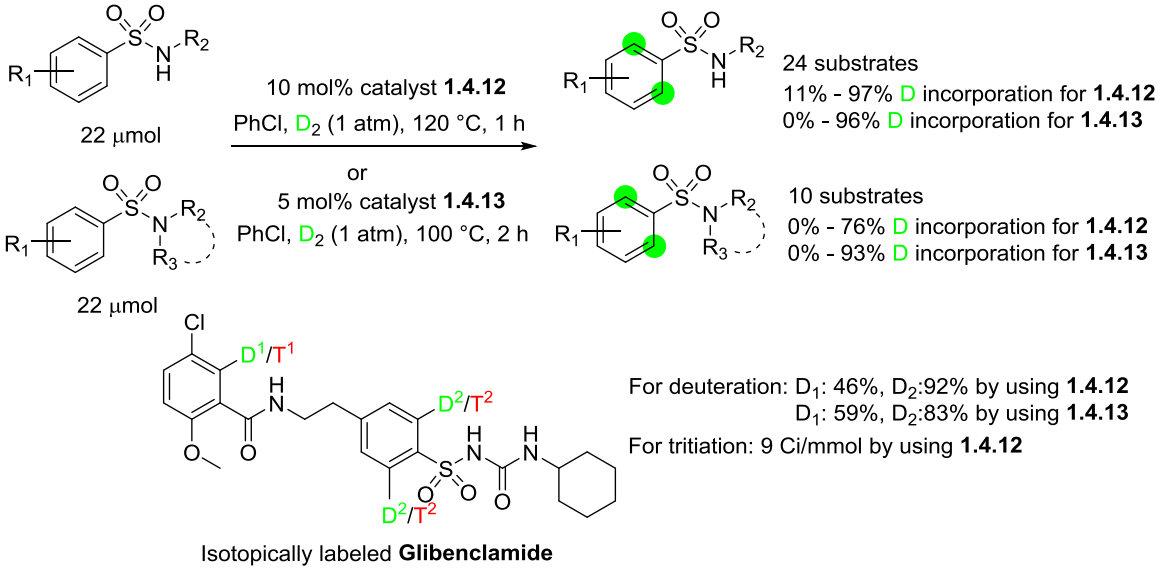

Scheme 1.8 Iridium complexes catalyzed isotopic labeling of sulfonamides

[44] M. C. Perry, X. Cui, M. T. Powell, D. R. Hou, J. H. Reibenspies, K. Burgess, *J. Am. Chem. Soc.* **2003**, *125*, 113.

1.4.3 Iridium catalyzed deuteration of various compounds with distinct functional groups

For the works described above, the catalysts could catalyze the H/D exchange of compounds with comparable functional groups. However, there are some more general catalysts that are able to catalyze H/D exchange of various compounds with different types of functional groups, such as Kerr's catalysts.[42, 43e, f, j, 45]

For catalysts containing an NHC and a chlorine ligands, after screening catalysts with different substituents on carbene ligand (**Figure 1.18**), Kerr discovered that catalyst **1.4.12** was able to deuterate various aryl ketones efficiently.[42] The catalyst could also deuterate amides with moderate deuterium incorporation, and *N*-heterocycles with high deuterium incorporation.

For catalysts containing an NHC and a phosphine ligands, Kerr showed that all the catalysts (**Figure 1.18**) were active toward the labeling of aryl ketones, aryl amides and *N*-heterocycles, despite a little difference of activities was observed among different substrates.[43e, f] One could choose different catalyst according to the functional groups of substrates. Kerr even succeeded to tritiate various molecules with different functional groups using catalysts **1.4.1a**-**1.4.1c** respectively. Replacing the phosphine ligand with pyridine (**Figure 1.18**, **1.4.1f**) also had similar catalytic activities towards various compounds with different functional groups.[43j]

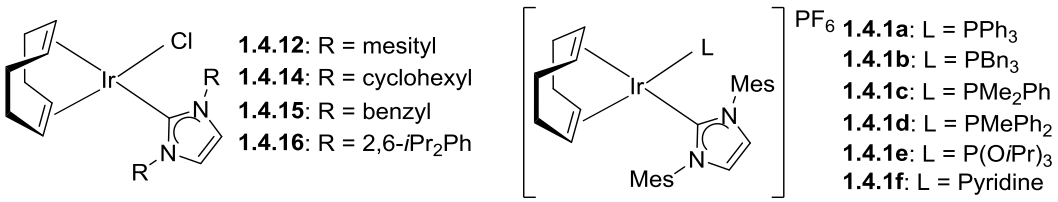

Figure 1.18 Chloro-carbene type and phosphine ligand type Kerr's catalysts

Despite the broad application of Kerr's catalysts, some other complexes based on iridium have also been designed for H/D exchange reactions. In 2014, D. Muri and co-workers selected a series of reported highly active iridium catalysts for asymmetric double bond reductions with different N, P-ligands to test their catalytic activities toward H/D exchange reactions.[43c] In this publication, through the scanning of the iridium catalysts with different ligands for the deuterium labeling of 2-phenylpyridine, the authors discovered that the catalysts containing electron-rich ligands (dicyclohexylphosphines or phosphinites) were excellent catalysts for efficient deuterium labeling of various compounds (**Scheme 1.9**). With these catalysts that contained electron-rich ligands, substrates with strong directing groups such as pyridines, ketones, and amides, as well as weak ligating units

[45] a) R. Simonsson, G. Stenhagen, C. Ericsson, C. S. Elmore, *J. Label. Compd. Radiopharm.* **2013**, *56*, 334; b) A. Modvig, T. L. Andersen, R. H. Taaning, A. T. Lindhardt, T. Skrydstrup, *J. Org. Chem.* **2014**, *79*, 5861.

such as nitro, sulfones, and sulfonamides, could be labeled efficiently using D_2 gas as the isotopic source.

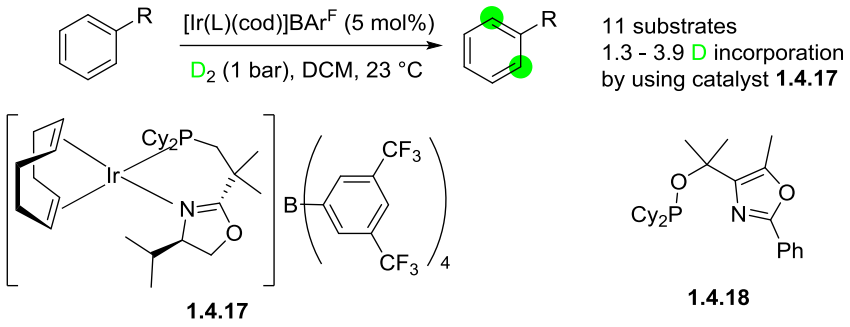

Scheme 1.9 H/D exchange catalyzed by iridium catalysts with N, P-ligands

Interestingly, by adding tris(pentafluorophenyl)borane to the reaction mixture, the authors were able to deuterate acetylbenzonitrile efficiently, which contains a strongly coordinating substituent, through the coordination of borane to nitrile group. Finally, they also developed an iridium catalyst that contained an achiral ligand (**Scheme 1.9**, **1.4.18**). After testing the reactivity of the new catalyst, they claimed that it was very efficient toward a variety of substrates in the H/D exchange process.

Later in 2016, E. Peris reported the synthesis of three iridium(III) complexes with pyrene-containing *N*-heterocyclic carbenes (**Figure 1.19**) and their catalytic activities toward H/D exchange reactions.[43o] Several substrates with different functional groups were tested with the three synthesized catalysts. Among them, the chloride complex **1.4.19** worked best for the deuteration of styrene and *trans*-stilbene with the addition of AgOTf as additive, while the carbonate complexes **1.4.20** and **1.4.21** deuterated THF efficiently without any additive; the latter was the best catalyst for the mono-deuteration of Benzo[*h*]quinoline. Besides, the catalysts were also tested for their catalytic activities for the C-C coupling of alcohols. Moderate to good yields were obtained for all catalysts, while complex **1.4.21** was the best catalyst for this transformation.

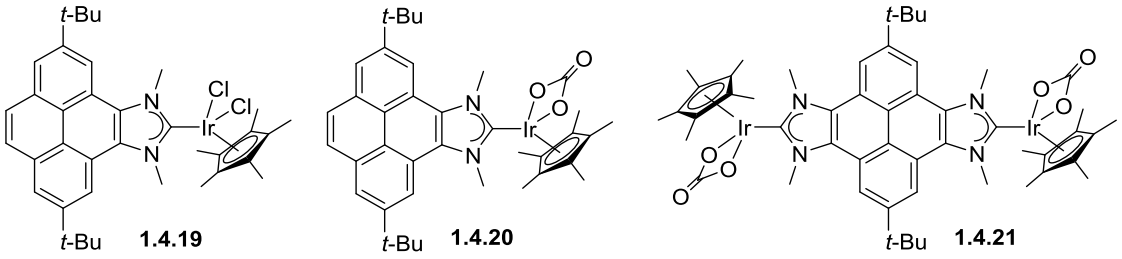

Figure 1.19 Iridium complexes synthesized by Peris

Recently, V. Derdau and co-workers reported the synthesis of iridium (I) complexes supported by phosphine-imidazolin-2-imine P, N ligands and its application in the H/D exchange reactions of aryl substrates.[43p] A total of 12 iridium complexes were synthesized, one of those displayed good activity toward the H/D exchange process (compound **1.4.22**, **Figure 1.20**). Various directing groups such as acetyl, *N*-heterocycles, amide, sulfone, ester and nitro group were tested with good deuterium incorporation. Moreover, through the optimization of the reaction conditions, substrates with the weakly coordinating methoxy group showed a sufficient degree of deuteration. A total of 23 substrates were deuterated using their method, which was highlighted by the deuteration of the structurally complex molecule Cabazitaxel (**Figure 1.20**).

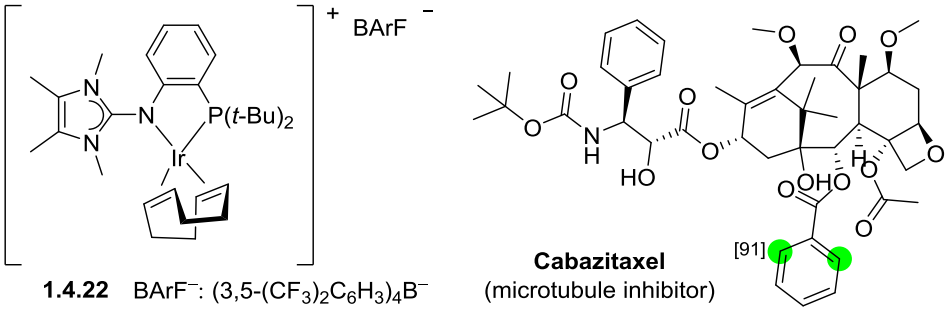

Figure 1.20 Iridium complex for H/D exchange reactions and example of substrate: Cabazitaxel

Overall, the reaction conditions of Derdau's method were mild (5 mol% of catalyst, 1 atm D_2 gas pressure and reacted for 1h in CH_2Cl_2 at ambient temperature), despite the fact that in order to achieve good deuterium incorporation for methoxy derivatives, higher temperature (50 ℃), longer reaction time (5 h) and higher catalyst loading (25 mol%) were necessary. The major limitation of Derdau's method was the multi-step synthesis of the iridium catalysts, and most of the catalysts had poor catalytic activity toward most substrates they used.

1.4.4 Iridium catalyzed deuteration of alkenes

In 2016, T. Nishimura reported a selective H/D exchange of vinyl and methylidene groups promoted by an iridium catalyst generated in situ from a hydroxoiridium complex and *N*-mesylbenzamide (**Scheme 1.10**).[43n] Various styrene derivatives were tested with good deuterium incorporations selectively at the vinyl group (**Scheme 1.10**, equation a). Moreover, the catalyst loading could be lowered down to 0.1 mol% with a prolonged reaction time (20 h) to achieve high level of deuterium incorporation, and the isotopic enrichment could also be improved by using a large excess of D_2O (200 eq.). Besides, the *in situ* generated iridium catalyst could also catalyze the deuteration of 1,1-disubstituted alkenes efficiently (**Scheme 1.10**, equation b), with a slightly increased amount of catalyst. The major disadvantage of this method was that it could not be applied to the H/D exchange

of terminal alkenes having allylic protons such as 1-octene because of fast isomerizations into inactive internal alkenes.

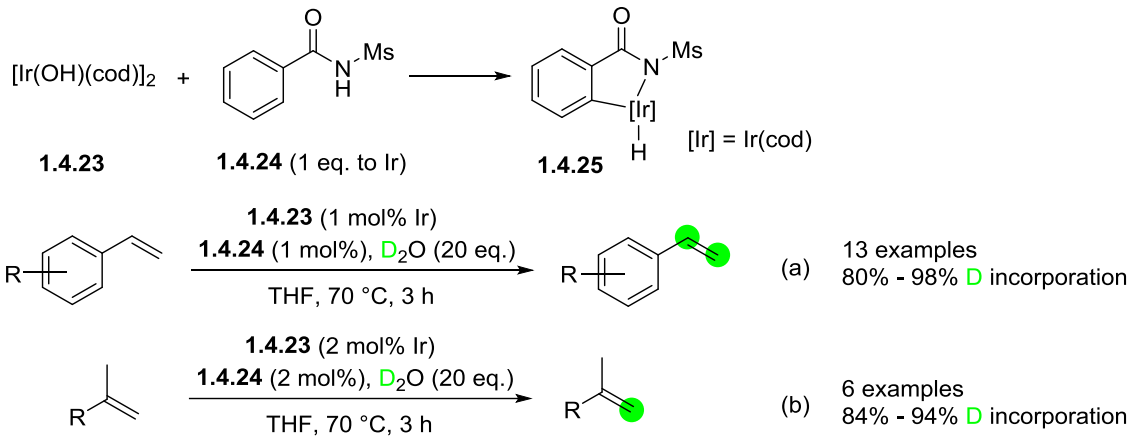

Scheme 1.10 In situ formation of iridium catalyst and its catalytic deuteration of alkenes

1.4.5 Iridium catalyzed deuteration of aromatic compounds

In 2012, R. H. Grubbs reported a PNP-pincer iridium dihydride complex (compound **1.4.26**, **Figure 1.21**) which catalyzed H/D exchange for aromatic substrates using D_2O or C_6D_6.[43a] Complete incorporation of deuterium into sterically accessible C_{Ar}-H bonds was observed at 80 ℃ after 3 days. According to the authors, steric factors played an important role in the deuteration process, since no deuterium incorporation was observed at *α*-position of methyl group in the arenes. Heteroarenes such as furan and thiophene were also deuterated efficiently under these conditions; however, substrates with strong coordinating atom such as pyridine were not able to be deuterated by this method, due to deactivation of the catalyst by pyridine's coordination to the metal center.

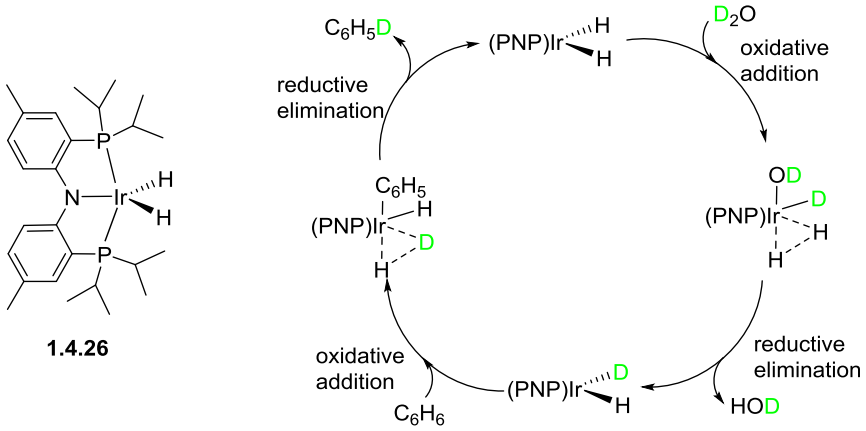

Figure 1.21 PNP-pincer iridium dihydride complex and its supposed catalytic mechanism

The authors also suggested a mechanism for their deuteration reactions (**Figure 1.21**). Both C_6D_6 and D_2O could be used as the isotopic source, while cyclohexane-D_{12} should be used as solvent with D_2O. Besides, the catalyst could also catalyze the H/D exchange of tertiary silanes. However, no example of functionalized arene was given, and the fact that the catalyst would be deactivated with the presence of a coordinating atom had limited the application of the method.

In 2013, E. A. Ison's group reported the Ir-complex catalyzed deuteration of benzene and the mechanistic studies.[43b] The authors tested a series of Ir-complexes (for example compound **1.4.27**) for the deuteration of benzene in three different solvent (CD_3OD, CD_3COOD and CF_3COOD), and they discovered that the deuteration process is dramatically influenced by the solvent used in the reactions. For acetic acid-d_4 and methanol- d_4, through the observation of primary isotope effects, the deuteration process was supposed to be an organometallic mechanism (**Figure 1.22**, mechanism **a**); whereas inverse isotope effects were observed in trifluoroacetic acid-d_1, thus an Ar-S_E mechanism was more reasonable (**Figure 1.22**, mechanism **b**).

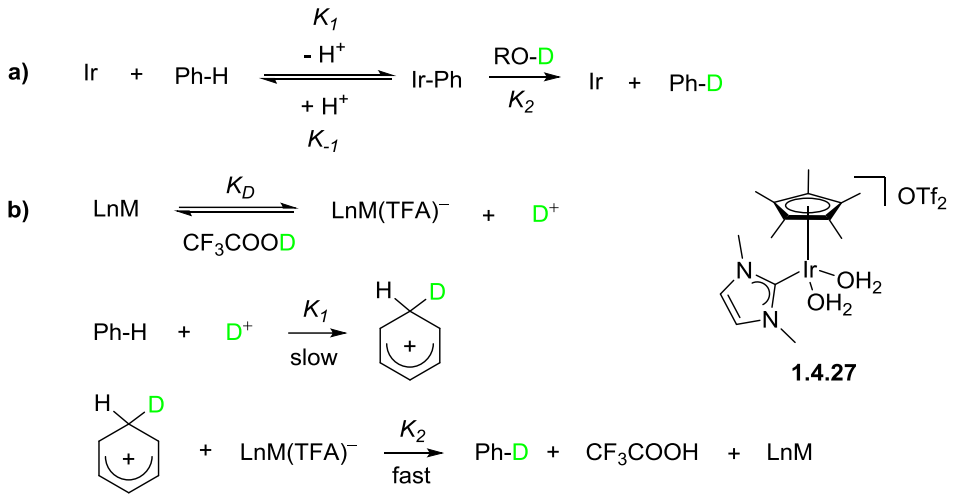

Figure 1.22 Proposed Mechanisms for H/D Exchange in different solvents

Besides, the authors demonstrated that the ancillary ligand of the catalyst also influences H/D exchange reactivity when using methanol-d_4 as solvent. The most active catalysts in methanol-d_4 contained strong donor ligands (PMe_3 and NHC), and hydride species had been identified in catalytic H/D exchange reactions in this solvent. However, a minimal impact of the ancillary ligand on H/D exchange reactivity was observed when conducting the reactions with acetic acid-d_4. In this solvent, C-H activation was proposed to proceed by an acetate-assisted σ bond metathesis mechanism. As a

conclusion, the authors claimed that the proper choice of solvent and ancillary ligand could result in the rational design of new C-H functionalization catalysts.

1.5 H/D exchange reactions catalyzed by ruthenium catalysts

Compared with iridium catalyzed H/D exchange reactions, ruthenium catalyzed H/D exchange reactions is another research hotspot. Thanks to the excellent coordinating ability of many functional groups (alcohol, amine, ester, amide, alkene, (hetero)arene…and so on) to the ruthenium atom, many catalysts based on ruthenium have been developed allowing the efficient and selective C-H deuteration of various organic compounds.[41f, 46]

1.5.1 Ruthenium catalyzed deuteration involving oxygen atom as directing groups

As mentioned above, oxygen is an excellent coordinating atom to many metals, including ruthenium complexes. Since it exists in various functional groups such as alcohols and carbonyl groups, many H/D exchange processes based on oxygen directing groups have been achieved catalyzed by ruthenium complexes.

Carbohydrates are important components of living organisms, and all of them contain certain number of hydroxyl groups which can act as directing groups. In 2010, H. Sajiki's group developed a method for the regioselective deuteration of primary and secondary alcohols as well as diols and triols catalyzed by Ru/C in D_2O under 1 bar of H_2 gas.[47] Based on this work, the same group reported a stereo- and regioselective deuterium labeling of various sugars catalyzed by Ru/C in D_2O under a hydrogen atmosphere.[48] The direct H/D exchange reaction could selectively proceed on carbons adjacent to the free hydroxyl groups. A series of pyranosides were deuterated with high isotopic enrichment and high isolated yield (**Scheme 1.11**). The products were transferred into the corresponding acetates in order to better analyze them by ^{1}H NMR. However, the deuteration of furanosides failed because they were easily hydrolyzed under heated aqueous conditions.

---

[46] For recent examples of ruthenium catalyzed H/D exchange reactions, see *ref [26]* and: a) B. Gröll, M. Schnürch, M. D. Mihovilovic, *J. Org. Chem.* **2012**, *77*, 4432; b) Y. Sawama, Y. Yabe, H. Iwata, Y. Fujiwara, Y. Monguchi, H. Sajiki, *Chem. Eur. J.* **2012**, *18*, 16436; c) E. Khaskin, D. Milstein, *ACS Catal.* **2013**, *3*, 448; d) M. Hirano, R. Fujimoto, K. Hatagami, N. Komine, S. Komiya, *ChemCatChem* **2013**, *5*, 1101; e) S. H. Lee, S. I. Gorelsky, G. I. Nikonov, *Organometallics* **2013**, *32*, 6599; f) M. Zhan, H. Jiang, X. Pang, T. Zhang, R. Xu, L. Zhao, Y. Liu, Y. Gong, Y. Chen, *Tetrahedron Lett.* **2014**, *55*, 5070; g) L. Piola, J. A. Fernández-Salas, S. Manzini, S. P. Nolan, *Org. Biomol. Chem.* **2014**, *12*, 8683 ; h) W. Bai, K.-H. Lee, S. K. S. Tse, K. W. Chan, Z. Lin, G. Jia, *Organometallics* **2015**, *34*, 3686; i) B. Chatterjee, C. Gunanathan, *Org. Lett.* **2015**, *17*, 4794; j) C. Taglang, L. M. Martínez-Prieto, I. del Rosal, L. Maron, R. Poteau, K. Philippot, B. Chaudret, S. Perato, A. S. Lone, C. Puente, C. Dugave, B. Rousseau, G. Pieters, *Angew. Chem. Int. Ed.* **2015**, *54*, 10474; k) E. Bresó-Femenia, C. Godard, C. Claver, B. Chaudret, S. Castillón, *Chem. Commun.* **2015**, *51*, 16342; l) L. Zhang, D. H. Nguyen, G. Raffa, S. Desset, S. Paul, F. Dumeignil, R. M. Gauvin, *Cat. Commun.* **2016**, *84*, 67; m) S. Bhatia, G. Spahlinger, N. Boukhumseen, Q. Boll, Z. Li, J. E. Jackson, *Eur. J. Org. Chem.* **2016**, 4230; n) B. Chatterjee, C. Gunanathan, *Chem. Commun.* **2016**, *52*, 4509; o) B. Chatterjee, V. Krishnakumar, C. Gunanathan, *Org. Lett.* **2016**, *18*, 5892; p) L. V. A. Hale, N. K. Szymczak, *J. Am. Chem. Soc.* **2016**, *138*, 13489.

[47] T. Maegawa, Y. Fujiwara, Y. Inagaki, Y. Monguchi, H. Sajiki, *Adv. Synth. Catal.* **2008**, *350*, 2215.

[48] Y. Fujiwara, H. Iwata, Y. Sawama, Y. Monguchi, H. Sajiki, *Chem. Commun.* **2010**, *46*, 4977.

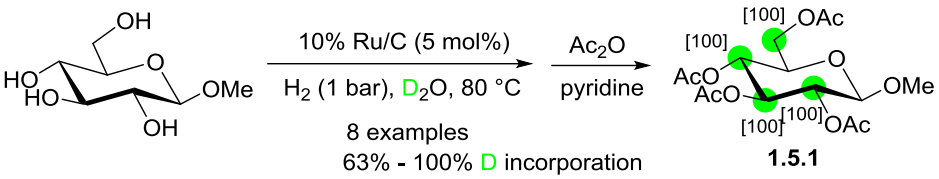

Scheme 1.11 Ru/C catalyzed deuteration of pyranosides

Later in 2012, Sajiki improved this method by adding an inorganic base, such as NaOH and LiOH, to the reaction mixture.[46b] By the addition of an inorganic base, the deuterium labeling of furanosides was realized (**Scheme 1.12**, compound **1.5.2**). Furthermore, through selective protection of the hydroxyl groups, the site selective deuteration of carbohydrates was achieved efficiently (**Scheme 1.12**, compounds **1.5.3** and **1.5.4**). The inorganic base (NaOH or LiOH) was added in order to avoid deprotection of the acetal moiety due to the Lewis acidity of the Ru/C or residual acidic constituent from the preparation process of Ru/C. The use of Ru/C as catalyst had certain advantages, such as its air stability, commercial availability and the convenient isolation of deuterated products by simple filtration. However, the use of D_2O under H_2 atmosphere made it difficult to determine the real deuterium source, due to the exchange between D_2O and H_2 to produce D_2.

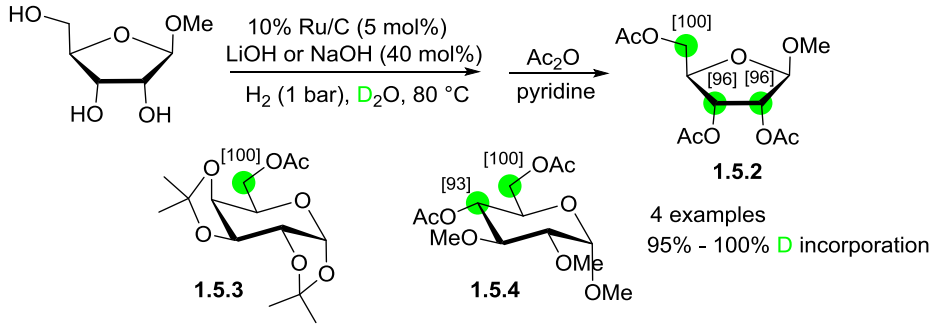

Scheme 1.12 Ru/C catalyzed deuteration of furanosides and protected pyranosides

Later in 2013, D. Milstein's group reported a ruthenium pincer catalyzed deuteration of primary and secondary alcohols.[46c] The air-stable homogeneous ruthenium catalyst (**1.5.5**, **Scheme 1.13**) could selectively deuterate alcohols with a low catalyst loading (0.2 mol%) by using D_2O as the deuterium source. NaOH was needed to promote the H/D exchange reaction. A number of functional groups were tolerated in their reaction conditions, such as amines, unactived double bonds and C-F bonds. However, the general need of high reaction temperature (120 ℃) and the loss of chirality when dealing with chiral alcohols had limited the application of the method. And the use of D_2O as the isotopic source also limited the possibility to transfer this method for tritium labeling.

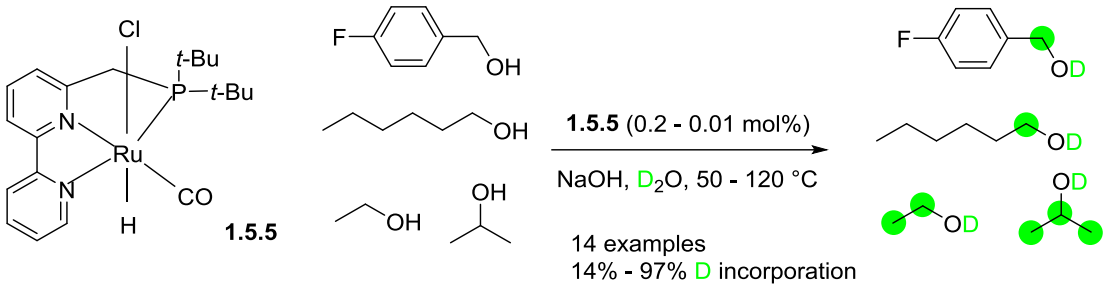

Scheme 1.13 Ruthenium pincer catalyst and its catalytic deuteration

A similar work was reported by G. Jia and co-workers in 2015.[46h] A series of ruthenium complexes were studied for their catalytic properties toward H/D exchange reactions of alcohols using D_2O as the isotopic source. According to the authors, ruthenium complexes with different auxiliary ligands were found to have different catalytic activities. Ruthenium η^6-cymene complexes such as (η^6-cymene)Ru {(*S*,*S*)-NHCHPhCHPhNTs} **1.5.6** catalyzed regioselective deuteration of alcohols at the β-carbon positions only; octahedral ruthenium complexes such as $RuCl_2(2\text{-}NH_2CH_2Py)(PPh_3)_2$ **1.5.7** catalyzed regioselective H/D exchange reactions at both the α- and β-carbon positions of alcohols (**Scheme 1.14**). Detailed mechanisms were proposed by the authors concerning the different catalytic activities. The H/D exchange reactions proceeded through reversible dehydrogenation/hydrogenation of alcohols involving hydride species and H/D exchange among D_2O and hydride species. The different regioselectivities of the H/D exchange reactions could be related to the relative ease of exchange reactions of ruthenium hydride intermediates with D_2O.

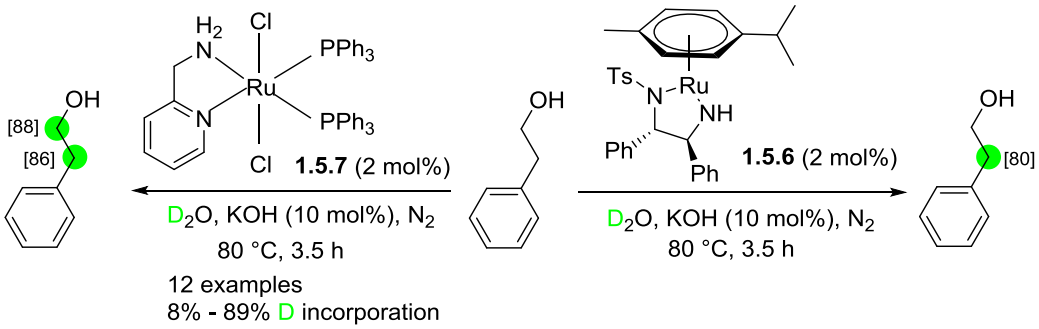

Scheme 1.14 H/D exchange reactions catalyzed by different ruthenium complexes

The authors also extended the substrate scope for the H/D exchange reactions catalyzed by **1.5.7**. A series of primary and secondary alcohols were tested under the reaction conditions. The results showed that secondary benzylic alcohols were the best candidates under the reaction conditions; primary alkyl alcohols were less effective at the β-carbon positions; secondary alkyl alcohols were less

reactive than primary alcohols. Although higher contents of deuterium could be achieved by increasing the reaction time, there was still a limitation which was the existence of a coordinating atom, such as nitrogen, strongly decreased the deuterium incorporation. This fact limited the application of the method for the labeling of many drug candidates which contained other coordinating moieties. More importantly, the use of D_2O as isotopic source limited the method for tritium labeling because pure tritiated water is corrosive and the most common tritium source is the tritium gas.

Soon after Jia's publication, a similar work concerning the selective *α*-deuteration of primary alcohols and *α*,*β*-deuteration of secondary alcohols catalyzed by a ruthenium pincer catalyst (Ru-MACHO, **Figure 1.23**)[49] was reported by C. Gunanathan.[46i] In Gunanathan's protocol, the isotopic source was also D_2O, but only 0.2 mol% of the catalyst was used, together with 0.5 mol% of *t*-BuOK as base.

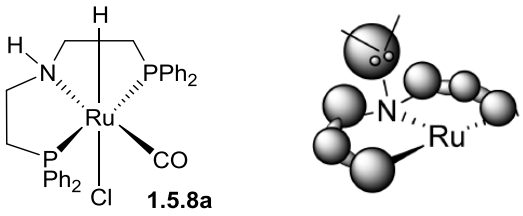

Figure 1.23 Ru-MACHO catalyst

Under their reaction conditions, aryl methanols were efficiently deuterated, however, slight deuterium incorporation at the *β*-carbon positions was observed when dealing with other kinds of primary alcohols. In the case of secondary alcohols, *β*-carbon positions were deuterated as efficiently as *α*-carbon positions. The authors explained that the different results might be due to the intermediate ketones which were more long-lived than aldehydes, resulting in the effective *β*-deuteration by H/D exchange via keto-enol tautomerism and the subsequent hydrogenation providing *α*,*β*-deuterated secondary alcohols. A mechanistic study indicated the formation of carbonyl species during the deuteration reactions, similar to that of Milstein's and Jia's cases.

As a complementary work of Milstein, Jia and Gunanathan, R. M. Gauvin and co-workers reported the deuterium labeling of alcohols using a series of ruthenium PNP pincer complexes in 2016.[46l] Through screening the ruthenium pincer catalysts, minor differences in terms of yield and regioselectivity were observed upon substitution of the chloride ligand by borohydride (**Figure 1.24**, ligand X); however, the nature of the substituents on the phosphorous atoms had an impact on both activity and selectivity (**Figure 1.24**, R group). Bulky *tert*-butyl substituent resulted in inactivation for deuterium labeling

[49] a) W. Kuriyama, T. Matsumoto, Y. Ino, O. Ogata, *PCT Int. Appl. WO/2011/048727 A1*, **2011**; b) W. Kuriyama; T. Matsumoto; O. Ogata; Y. Ino; K. Aoki; S. Tanaka; K. Ishida; T. Kobayashi; N. Sayo; T. Saito, *Org. Process Res. Dev.* **2012**, *16*, 166.

(**1.5.12b**), while cyclohexyl substituent (**1.5.8c** and **1.5.9c**) led to high regioselective activity for the *α*-selective deuteration of alcohols.

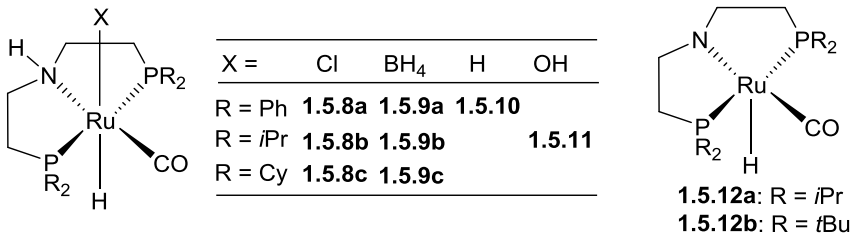

Figure 1.24 Ruthenium pincer catalysts screened by Gauvin

Apart from the deuteration of alcohols (including carbohydrates), the H/D exchange of carboxylic acids catalyzed by a ruthenium complex has been reported by S. Komiya and co-workers in 2013.[46d] However, this method suffered from the narrow substrate scope (only six examples were deuterated) and long reaction time (as long as 315 h), leading to few catalyst applications.

1.5.2 Ruthenium catalyzed deuteration involving nitrogen atom as directing groups

In 2012, M. Schnürch's group reported a Ru(0) catalyzed deuteration of aza-heterocycles using *t*-BuOD as deuterium source.[46a] Using $Ru_3(CO)_{12}$ (5 mol%) as catalyst, both electron-rich and electron-poor *N*-heteroarenes such as (aza)indoles, deazapurines, benzimidazole, (iso)quinolines, and pyridines were selectively deuterated at specific positions (**Scheme 1.15**). Indoles were selectively deuterated at C-3 position; pyridines were labeled at *α* position of N; interestingly, benzylic positions could also be deuterated when it existed in the substrate. The isotopic enrichment could also be improved by repeating an additional catalytic cycle. By synthesizing *t*-BuOD from *t*-BuONa and CF_3CO_2D, the authors also claimed that the method could be applied to tritium labeling by the synthesis of *t*-BuOT from *t*-BuONa and CF_3CO_2T. However, no example was given by the authors.

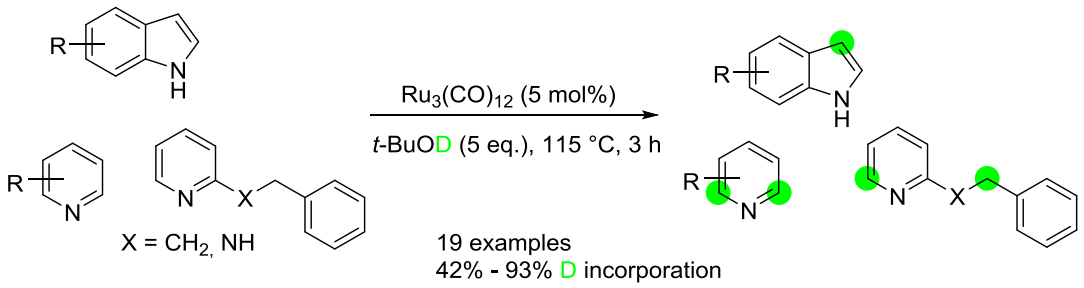

Scheme 1.15 Examples of deuteration by Schnürch's group

In 2012, M. Beller and co-workers reported a ruthenium catalyzed selective *α*, *β*-deuteration of bioactive amines using Shvo catalyst,[41f] a commercially available catalyst for transfer hydrogenation (**Figure 1.25**).[50] The selective deuteration could be explained by the so-called "borrowing hydrogen mechanism" involving the formation of an enamine intermediate (**Figure 1.26**).

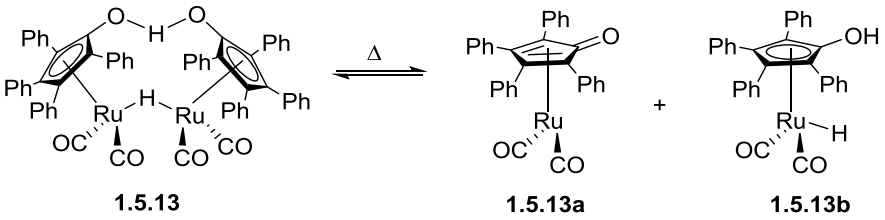

Figure 1.25 Different forms of Shvo's catalyst

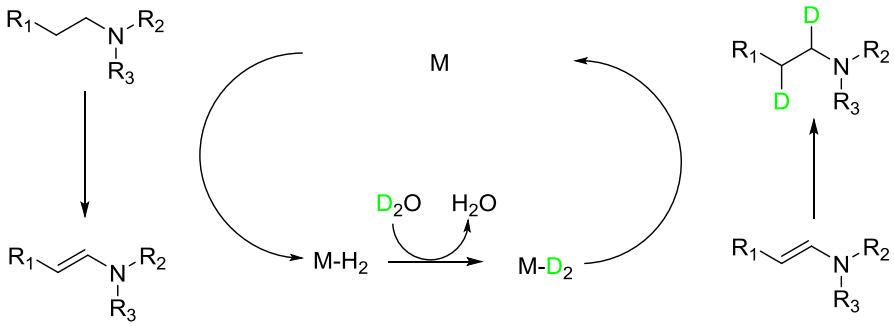

Figure 1.26 H/D exchange mechanism involving the "borrowing hydrogen mechanism"

Reactions could be carried out by either heating or microwave irradiation, both with high levels of deuterium incorporation. The authors also demonstrated the possibility of using different deuterated solvents to conduct the reaction, which could possibly enlarge the substrate scope. Moreover, the authors applied their method to the labeling of several bioactive compounds, including three actual marketed drugs (**Figure 1.27**). However, substrates with the presence of primary aliphatic amines were not able to be labeled by this method, owing to the side reactions of the formation of the corresponding imine. More importantly, the high reaction temperature and the use of D_2O or deuterated alcohols as isotopic source limited the method for tritium labeling.

[50] Y. Shvo, D. Czarkie, Y. Rahamim, *J. Am. Chem. Soc.* **1986**, *108*, 7400.

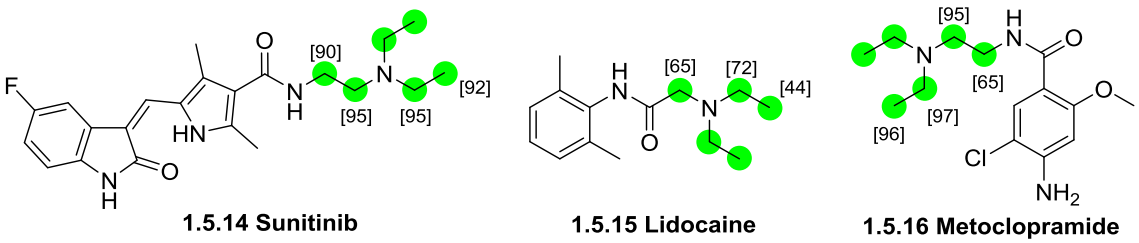

Figure 1.27 Deuterated drugs achieved with Shvo's catalyst

More recently, Gunanathan's group also developed a method allowing the deuterium labeling of amines and amino acids.[46o] Using a monohydrido-bridged ruthenium complex (**1.5.17**, **Figure 1.28**), *α*-selective deuteration of primary and secondary amines was achieved successfully. However, the deuterium labeling of amino acids failed due to the reaction between the proton of the amino acid and the hydride of the catalyst. Therefore the preparation of potassium salts was needed to allow the labeling of amino acids. However, the existence of potassium carboxylate might affect the deuteration process, as in the case of the labeling of pregabalin.

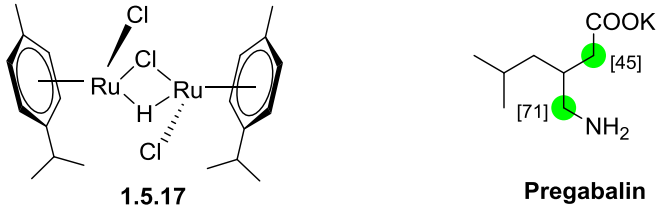

Figure 1.28 Monohydrido-bridged ruthenium complex

Similar to the mechanism of the deuterium labeling of alcohols, the deuterium labeling of amines and amino acids went through an imine intermediate. As a result, this protocol could be used to label primary and secondary amines, but not tertiary amines. Moreover, they were unable to label amino acids enantiospecifically. This fact strongly limited the application of this method to the life science, because the chirality of amino acids is of great importance for peptides and proteins.

Later, a stereoretentive deuteration of primary amines catalyzed by Ru-bMepi (**Scheme 1.16**, bMepi = 1,3-(6'-methyl-2'-pyridylimino)isoindolate) complex was reported by N. K. Szymczak.[46p] This method was the first example of stereoretentive H/D exchange catalyzed by a homogeneous catalyst. It was an efficient and stereoretentive deuteration process, despite the poor regioselectivity. Moreover, the isolated yields of deuterated products were generally low to moderate, although the authors claimed that the workup was convenient, performing a simple acidic workup to remove the ruthenium catalyst.

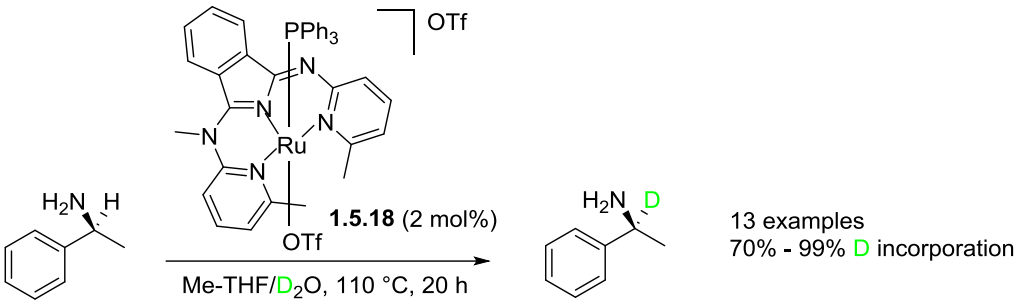

Scheme 1.16 Ru-bMepi catalyzed stereoretentive deuteration

The authors also tested the functional group tolerance of their method by adding additives to the deuteration procedures. According to the results, the deuterium incorporation of amines decreased significantly in the presence of a competitive coordinating ligand, such as heterocycles and ester group; and the deuteration was totally blocked in presence of a double bond. It meant that the method is not able to efficiently deuterate more complex molecules that contain other coordinating functional groups. The low isolated yields, poor functional group tolerance, together with inapplicability to tritium labeling (D_2O as the isotopic source) may limit the application of the method.

In addition to the works above, our research group is interested in the development of new methods of labeling by catalytic H/D and H/T exchange reactions. The research group of B. Chaudret at INSA Toulouse is a specialist in the synthesis of various well-characterized nanoparticles.[51] In 2001, Chaudret reported the synthesis of RuNp@PVP (polyvinylpyrrolidone) from the decomposition of the precursor Ru(cot)(cod) in THF and in the presence of polymer PVP (Ru/polymer = 5% by weight) under 3 bar of H_2 (**Scheme 1.17**).[52] The obtained nanoparticles, containing 7.6% by mass of ruthenium, was then characterized by infrared (IR) spectroscopy after CO adsorption, transmission electron microscopy (TEM), high resolution electron microscopy (HREM), X-ray diffraction (XRD), wide-angle X-ray scattering (WAXS) and X-ray photoelectron spectroscopy (XPS). In IR, the nanoparticles exhibited an absorption band at 2014 cm^{-1}, which corresponds to the end groups of CO adsorbed on Ru(0). High resolution microscopy showed that the particle size distribution was homogeneous [about 1.1 nm in diameter and hexagonal close packed (hcp) crystal structure] (**Figure 1.29**).

[51] P. Lara, K. Philippot, B. Chaudret, *ChemCatChem* **2013**, *5*, 28.

[52] C. Pan, K. Pelzer, K. Philippot, B. Chaudret, F. Dassenoy, P. Lecante, M.-J. Casanove, *J. Am. Chem. Soc.* **2001**, *123*, 7584.

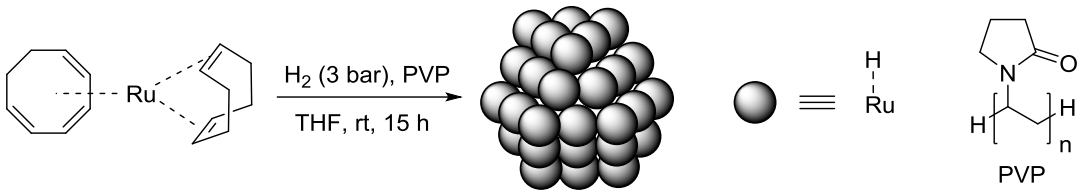

Scheme 1.17 Synthesis of RuNp@PVP

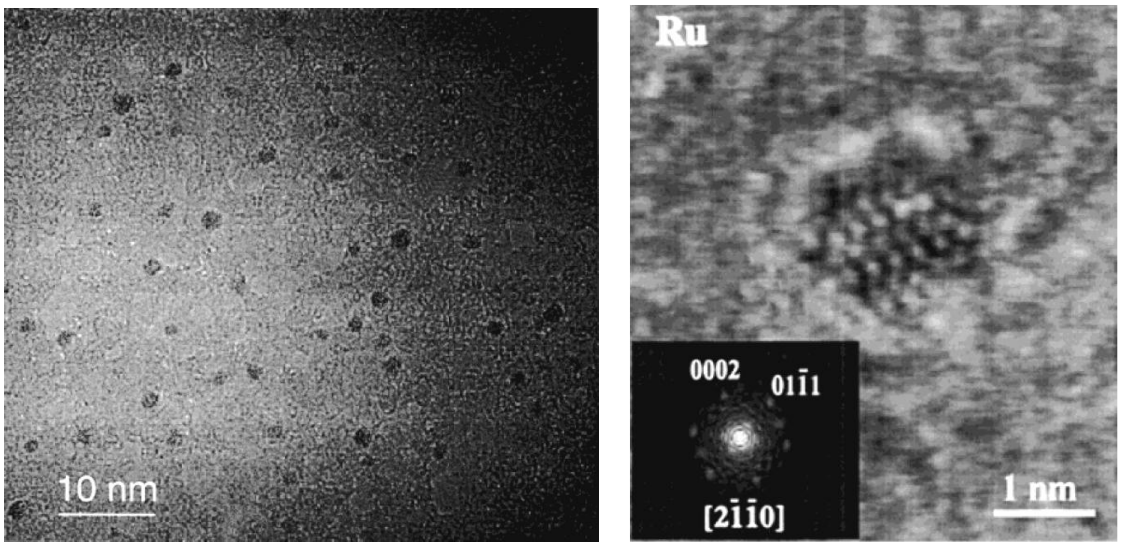

Figure 1.29 TEM (left) and HREM (right) analysis of RuNp@PVP

By hydrogenation of the organometallic precursor Ru(cod)(cot) in THF at room temperature in the presence of 1,4-bis(diphenylphosphino)butane (dppb, **Figure 1.30**), another heterogeneous ruthenium nanoparticle RuNp@dppb stabilized by the bidentate diphosphine ligand dppb was synthesized by Chaudret's group.[53] The synthesized nanoparticle was found to have a mean size of 1.5±0.3 nm and a hcp structure, which was characterized by NMR spectroscopies, WAXS and TEM (**Figure 1.31**).

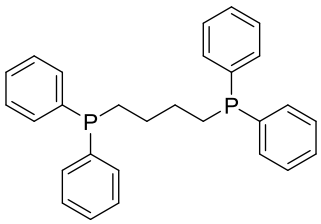

Figure 1.30 Structure of dppb

[53] J. García-Antón, M. R. Axet, S. Jansat, K. Philippot, B. Chaudret, T. Pery, G. Buntkowsky, H.-H. Limbach, *Angew. Chem. Int. Ed.* **2008**, *47*, 2074.

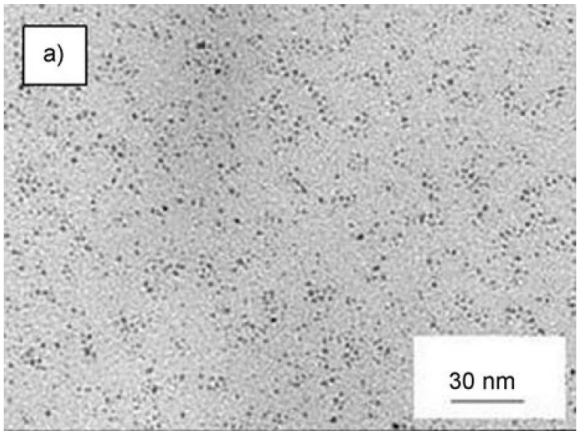

Figure 1.31 TEM images of RuNp@dppb

Two different heterogeneous ruthenium nanoparticles, RuNp@I*tBu* stabilized by *N*-heterocyclic carbene (NHC) ligand *N*,*N*-di(*tert*-butyl)imidazol-2-ylidene (**Figure 1.32**, L_1) and RuNp@IPr stabilized by 1,3-bis(2,6-diisopropylphenyl)imidazol-2-ylidene (**Figure 1.32**, L_2), were also synthesized by Chaudret.[54] The ruthenium nanoparticles were prepared by decomposition of Ru(cod)(cot) in pentane under 3 bar H_2 at room temperature in the presence of two different carbenes as stabilizing agents. The mean size of the nanoparticles varied with the equivalent of carbene ligands employed: when using 0.2 eq. of L_2 or 0.5 eq. of L_1, the mean size of the nanoparticles was 1.7 nm; when using 0.5 eq. of L_2, the mean size was 1.5 nm. The nanoparticles were homogeneous in size and shape and presented the hcp structure, and they were characterized by IR, TEM, HREM, WAXS and NMR spectroscopies.

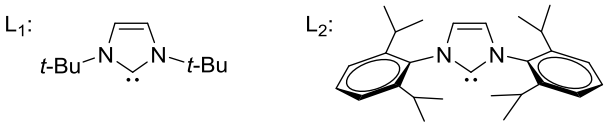

Figure 1.32 NHC ligands employed as stabilizers for the ruthenium nanoparticles

[54] P. Lara, O. Rivada-Wheelaghan, S. Conejero, R. Poteau, K. Philippot, B. Chaudret, *Angew. Chem. Int. Ed.* **2011**, *50*, 12080.

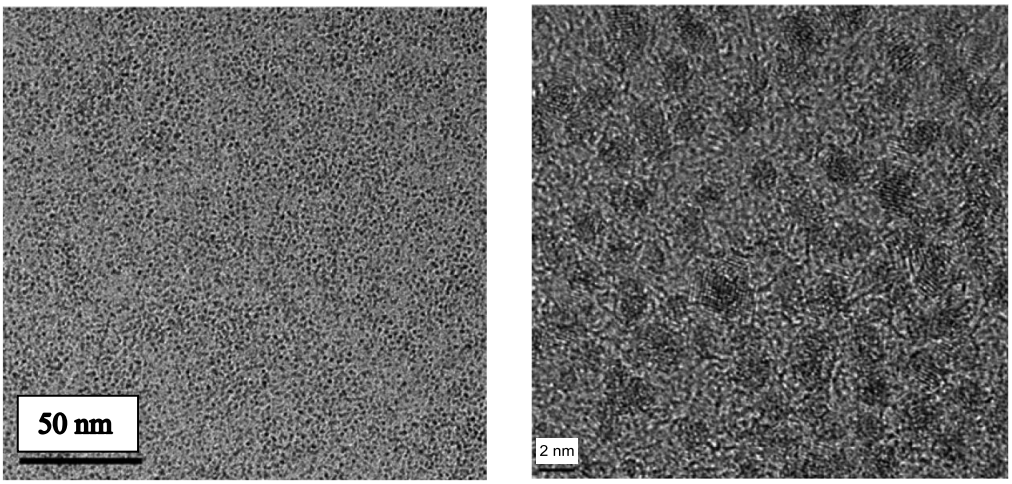

Figure 1.33 TEM image (left) and HREM image (right) of RuNp@I*t*Bu (L_1/Ru = 0.5)

In order to study the influence of the nanoparticle surface on the catalytic properties, two tin-decorated ruthenium nanoparticles Ru-SnNp@PVP and Ru-SnNp@dppb were synthesized by reacting RuNp@PVP and RuNp@dppb with tributyltin hydride respectively.[55] These particles were fully characterized by IR, TEM, HREM, WAXS and NMR spectroscopies (**Figure 1.34**). By this modification, the coordination of CO to the nanoparticles and their reactivity toward catalytic hydrogenation of styrene were changed, thus indicating the different surface properties of the tin-decorated ruthenium nanoparticles.

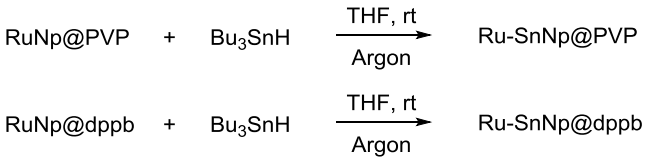

Scheme 1.18 Synthesis of tin-decorated ruthenium nanoparticles

[55] E. Bonnefille, F. Novio, T. Gutmann, R. Poteau, P. Lecante, J.-C. Jumas, K. Philippot, B. Chaudret, *Nanoscale* **2014**, *6*, 9806.

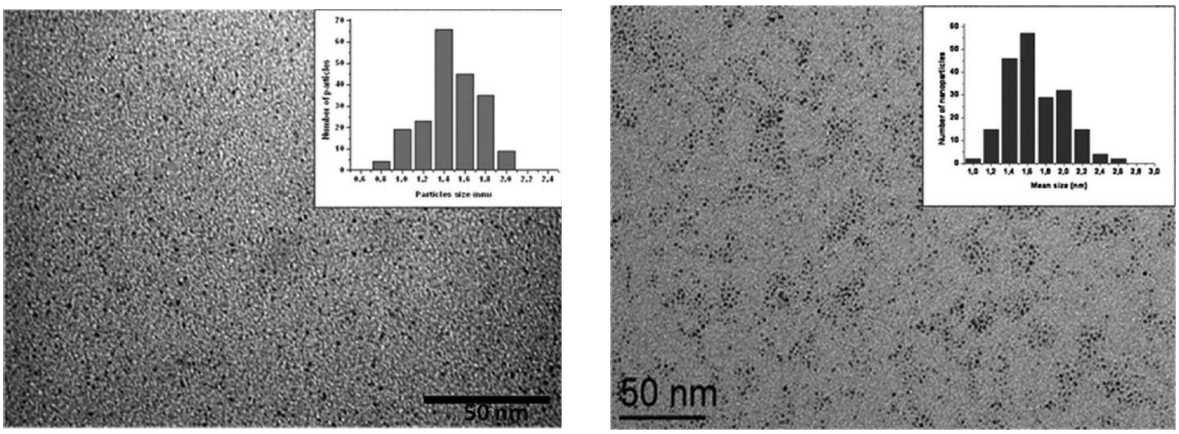

Figure 1.34 TEM image of Ru-SnNp@PVP (left) and Ru-SnNp@dppb (right)

In collaboration with Chaudret's group, we have demonstrated the exceptional capacity of ruthenium nanoparticles to catalyze H/D exchange.[29, 46j] In 2014, our group developed an efficient H/D exchange method allowing the deuteration of pyridines, quinolines, indoles, and alkyl amines using D_2 and RuNp@PVP nanoparticles (**Scheme 1.19**).[29] By a general and simple procedure involving mild reaction conditions (3 mol% RuNp@PVP, 1-2 bar D_2, 20-55 °C in THF) and simple filtration to recover the labeled product, the isotopic labeling of 22 compounds, including eight biologically active compounds, proceeded in good yield with high chemo- and regioselectivity (**Scheme 1.19**). Remarkably, the labeled compounds were obtained with conservation of the enantiomeric purity, even though the labeling took place in the vicinity of the asymmetric center. Furthermore, our method was readily applicable to tritium labeling because it used gas as an isotopic source.

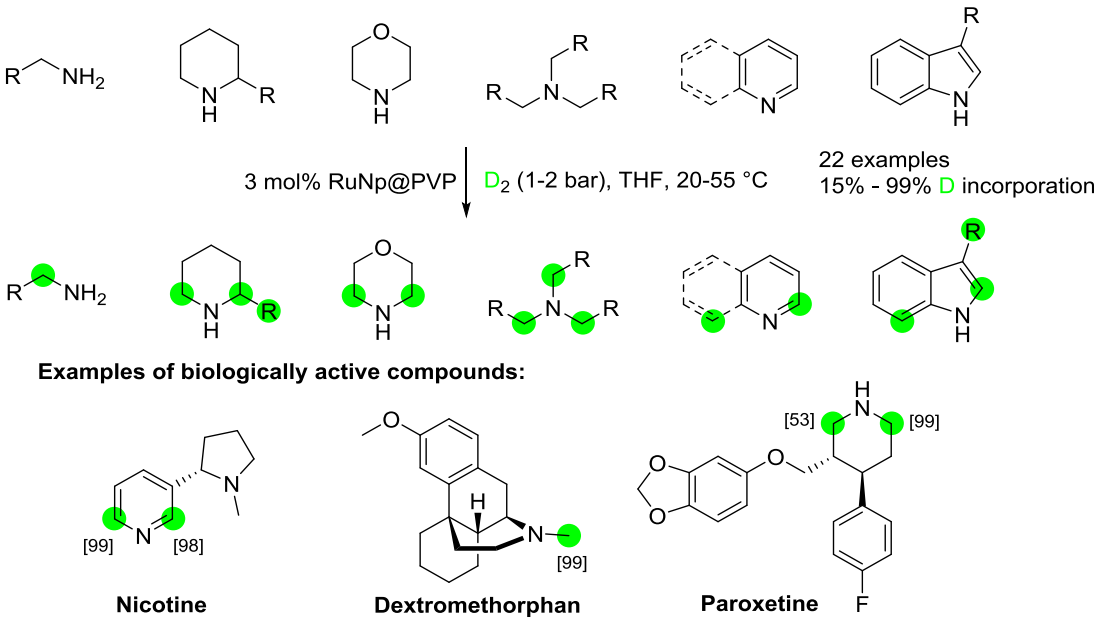

Scheme 1.19 H/D exchange reactions catalyzed by RuNp@PVP

Encouraged by the results above, and to further explore the reactivity of RuNp@PVP, the same group examined the catalytic ability of RuNp@PVP in the H/D exchange of amino acids and peptides.[46j] To our delight, three different chiral amines used as model compounds were efficiently deuterated with high isotopic enrichment (99%) and full retention of configuration (**Scheme 1.20**).

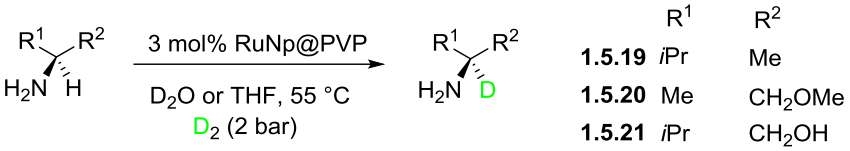

Scheme 1.20 Enantiospecific deuteration of chiral amines by RuNp@PVP

After obtaining the encouraging results, our group started to test the H/D exchange on amino acids. Gratifyingly, this reaction occurred enantiospecifically at the $C_{\alpha}(sp^3)$ position with full retention of configuration. Further investigations demonstrated that the reaction proceeded with high regioselectivity and full enantiospecificity in different solvents (D_2O, THF, DMF), thus demonstrating the broad potential of the C-H activation process catalyzed by this ruthenium nanocatalyst. Application of this method to the deuterium labeling of peptides were also achieved without detectable epimerization of the substrates (**Figure 1.35**).

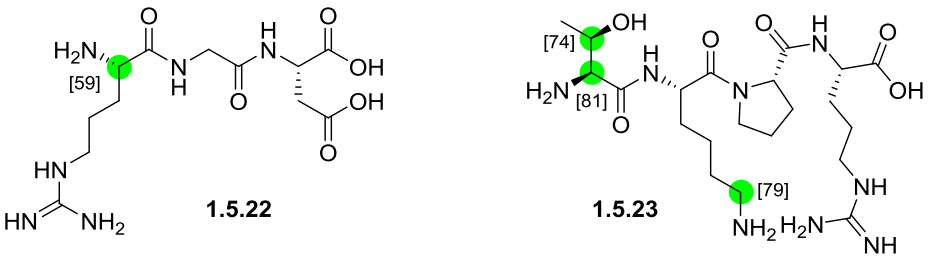

Figure 1.35 Enantiospecific deuteration of peptides by RuNp@PVP

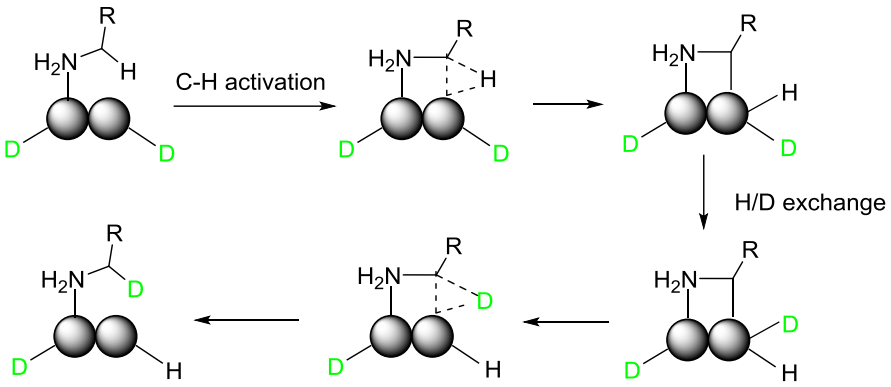

Figure 1.36 Mechanism for H/D exchange of amines

Regarding the deuteration mechanism, DFT calculations carried out by R. Poteau's group revealed a four-membered dimetallacycle as the key intermediate (**Figure 1.36**). The active metal center could keep its formal oxidation state during oxidative addition due to the facile diffusion of surface deuterides on nanoparticles, suggesting that a collective motion of surface species can optimize the C-H activation step by modulating the local electronic structure. The novel deuteration mechanism, different from the dehydrogenation/deuteration mechanism, explained the enantiospecificity of the reaction process because of the rigidity of the dimetallacycle. These findings clearly demonstrate the great potential of nanoparticles for the catalysis of C-H bond activation and pave the way for the rational development of new enantiospecific C-H functionalization reactions.

1.5.3 Ruthenium catalyzed deuteration of various compounds with distinct functional groups

In 2014, S. P. Nolan reported a ruthenium catalyzed regioselective H/D exchange of organic compounds with *N*- and *O*-containing directing groups.[46g] Using an organosilicon ruthenium complex (**Scheme 1.21**, **1.5.25**), which could be synthesized in one step starting from a commercially available ruthenium complex (**Scheme 1.21**, **1.5.24**), the authors succeeded to label various heteroarenes and aryl carbonyl compounds (**Scheme 1.21**). However, this method didn't permit to label benzaldehyde and alkyl aryl ketones, probably due to the tautomerization of the ketones to the corresponding enols. The authors also applied their method to the labeling of (*S*)-ketoprofen, an anti-inflammatory drug. As a result, complete and regioselective labeling was achieved with only a slight decrease of the enantiomeric excess (from 99% to 95%).

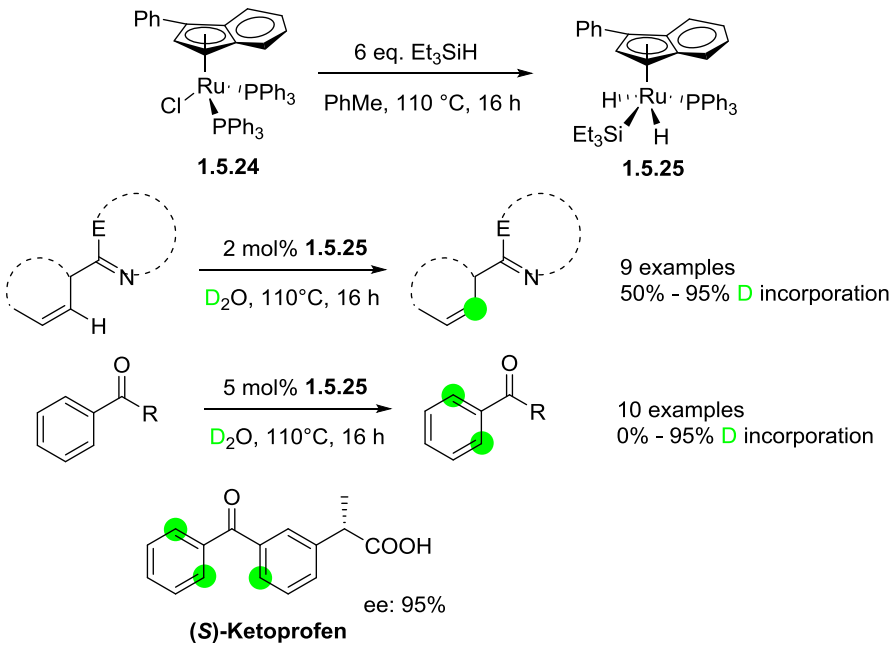

Scheme 1.21 Organosilicon ruthenium complex and its application in H/D exchange reactions

Later in 2016, a stereoretentive H/D exchange of amines and alcohols catalyzed by an electroactivated heterogeneous ruthenium particle was reported by J. E. Jackson's research group.[46m] This publication applied electrochemistry to the deuterium labeling of various organic compounds by using ruthenium particles supported on activated carbon cloth (Ru/ACC) as cathode, platinum wire as a counter electrode and 0.01 *M* phosphate buffer (pH 7) prepared in D_2O as the electrolyte (**Figure 1.37**). Deuterium gas was produced simultaneously as the reaction proceeded. This method resulted in high deuterium incorporation for most substrates, and the catalyst retained its catalytic activity over multiple runs; however, the yields of the deuterated products were extremely low (as low as 5%, mostly below 50%). The authors explained the low yield by substrate migration to the anodic cell compartment through the Nafion® membrane and substrate adsorption by the activated carbon cloth. Whatever, the low yields of the deuterated products had strongly limited the application of this method.

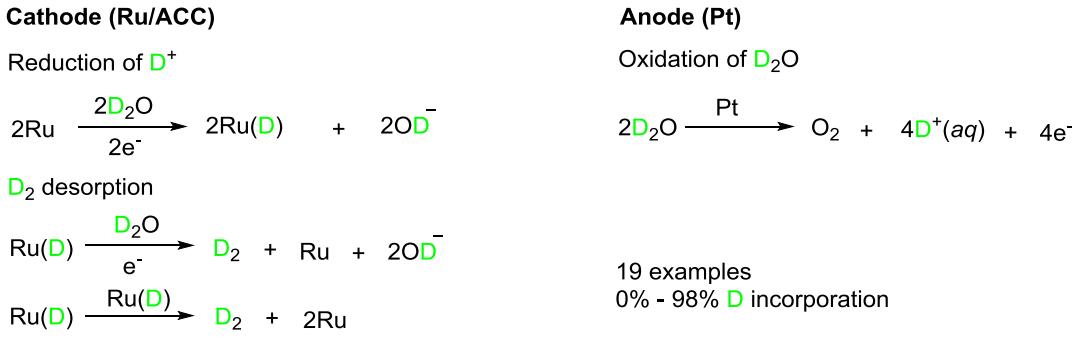

Figure 1.37 Electrochemical reactions at the electrode

1.5.4 Ruthenium catalyzed deuteration of other types of organic molecules

In addition to the works mentioned above, there are some other ruthenium based catalytic systems reported to catalyze H/D exchanges with different kinds of organic compounds. For example, G. I. Nikonov reported the catalytic H/D exchange of unactivated aliphatic C-H bonds of various types of molecules ((hetero)arenes, ethers, alkanes, alkyl nitriles…) by ruthenium hydride complex using C_6D_6 or D_2O as the deuterium source.[46e] Despite the broad substrate scope, this method suffered a general limitation that it needed a long reaction time (as long as 33 d) and high reaction temperature (100 ℃). Besides, only (hetero)arenes gave good deuterium incorporation under the reaction conditions, other substrates gave poor deuterium incorporation even with long reaction time.

B. Chaudret also reported an application of RuNp@PVP in the catalytic H/D exchange for phosphines in 2015.[46k] Under the reaction conditions (3.3 mol% RuNp@PVP, 2 bar D_2, THF, 80 ℃, 48 h or 88 h), phenyl rings in phenyl- or phenyl-alkylphosphines were selectively deuterated at the *ortho* positions, while full reduction of aryl rings was detected in the case of arylphosphine oxide derivatives and no reaction occurred in the case of arylphosphite (**Scheme 1.22**). This different behavior provided information about the coordination mode of each ligand. In the case of phosphine, the selective deuteration of *C2* carbons indicated that the ligand was coordinated through the phosphorus atom, similarly to what had been previously observed for nitrogen donors[46j] and that the C–H bond could approach the nanoparticle surface, which favored an H/D exchange. For phosphine oxides, the phenyl ring reduction could be explained considering that coordination to the nanoparticle took place through the aromatic rings. Triphenylphosphite was neither labeled nor reduced. The authors suggested that this result might be due to the aryl moieties being driven away from the surface of the catalyst by oxygen atoms, thus impeding the H/D exchange.

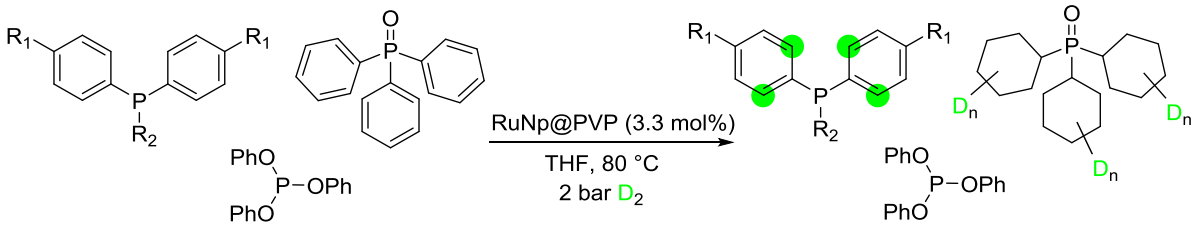

Scheme 1.22 H/D exchange of phosphorus ligands catalyzed by RuNp@PVP

Concerning the deuteration of phosphine ligand, M. Grellier and co-workers reported a case study of the H/D exchange of a polyhydride ruthenium phosphine complex using C_6D_6 as the deuterium

source.[56] The deuteration occurred at the phosphine ligand of the catalyst, thus it was not a catalytic process. Besides, there was no universality of this method because only tricyclopentyl phosphine was studied for the H/D exchange.

With the same Ru-MACHO catalyst for the deuteration of alcohols, Gunanathan also succeeded to apply it to the H/D exchange of terminal alkynes.[46n] Using similar reaction conditions to the deuteration of alcohols (0.5 mol% catalyst, 1 mol% *t*-BuOK, D_2O), the terminal alkynes were deuterated with high chemoselectivity for various functional groups (amine, alcohol, unactivated double bond…). A mechanistic study showed that the reaction intermediate was the Ru-acetylide species (**1.5.26**, **Scheme 1.23**). The deuteration took place after the H/D exchange of **1.5.26** with D_2O followed by reductive elimination.

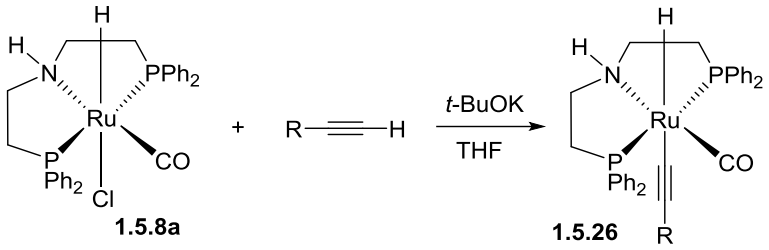

Scheme 1.23 Formation of Ru-acetylide intermediate

1.6 H/D exchange reactions catalyzed by other metals

Apart from the great achievements of H/D exchange process obtained using iridium and ruthenium complexes, there are still many excellent works accomplished with other transition metals such as palladium[57], rhodium[58], platinum[59], even some specific examples with tungsten[60] and iron[38b] recently.

---

[56] M. Grellier, S. A. Mason, A. Albinati, S. C. Capelli, S. Rizzato, C. Bijani, Y. Coppel, S. Sabo-Etienne, *Inorg. Chem.* **2013**, *52*, 7329.

[57] a) V. P. Shevchenko, I. Y. Nagaev, G. A. Badun, M. G. Chernysheva, K. V. Shevchenko, N. F. Myasoedov, *Dokl. Chem.* **2012**, *442*, 42; b) N. Modutlwa, H. Tada, Y. Sugahara, K. Shiraki, N. Hara, Y. Deyashiki, T. Maegawa, Y. Monguchi, H. Sajiki, *Heterocycles* **2012**, *84*, 419 ; c) V. P. Shevchenko, I. Yu. Nagaev, N. F. Myasoedov, *Dokl. Chem.* **2013**, *448*, 66; d) V. P. Shevchenko, I. Y. Nagaev, K. V. Shevchenko, N. F. Myasoedov, *Radiochemistry* **2013**, *55*, 346 ; e) V. P. Shevchenko, I. Y. Nagaev, K. V. Shevchenko, N. F. Myasoedov, *Radiochemistry* **2013**, *55*, 545; f) Y. A. Zolotarev, A. K. Dadayan, V. S. Kozik, E. V. Gasanov, I. V. Nazimov, R. K. Ziganshin, B. V. Vaskovsky, A. N. Murashov, A. L. Ksenofontov, O. N. Kharybin, E. N. Nikolaev , N. F. Myasoedov *Russ. J. Bioorg. Chem.* **2014**, *40*, 26; g) V. P. Shevchenko, I. Y. Nagaev, N. F. Myasoedov, *Radiochemistry* **2014**, *56*, 292; h) S. Ma, G. Villa, P. S. Thuy-Boun, A. Homs, J.-Q. Yu, *Angew. Chem. Int. Ed.* **2014**, *53*, 734; i) G. V. Sidorov, N. F. Myasoedov, S. N. Lomin, G. A. Romanov, *Radiochemistry* **2015**, *57*, 108; j) V. P. Shevchenko, G. A. Badun, I. A. Razzhivina, I. Y.Nagaev, K. V. Shevchenko, N. F. Myasoedov, *Dokl. Phys. Chem.* **2015**, *463*, 182; k) V. P. Shevchenko, I. A. Razzhivina, M. G. Chernysheva, G. A. Badun, I. Y. Nagaev, K. V. Shevchenko, N. F. Myasoedov, *Radiochemistry* **2015**, *57*, 312; l) R. Giles, G. Ahn, K. W. Jung, *Tetrahedron Lett.* **2015**, *56*, 6231.

[58] a) J. B. Gary, T. J. Carter, M. S. Sanford, *Top. Catal.* **2012**, *55*, 565; b) J. L. Rhinehart, K. A. Manbeck, S. K. Buzak, G. M. Lippa, W. W. Brennessel, K. I. Goldberg, W. D. Jones, *Organometallics* **2012**, *31*, 1943; c) A. D. Giuseppe, R. Castarlenas, J. J. Pérez-Torrente, F. J. Lahoz, L. A. Oro, *Chem. Eur. J.* **2014**, *20*, 8391; d) M. S. Webster-Gardiner, R. Fu, G. C. Fortman, R. J. Nielsen, T. B. Gunnoe, W. A. Goddard, *Catal. Sci. Technol.* **2015**, *5*, 96; e) S. R. Pollack, D. J. Schenk, *J. Label. Compd. Radiopharm* **2015**, *58*, 433.

[59] a) A. J. Hickman, M. A. Cismesia, M. S. Sanford, *Organometallics* **2012**, *31*, 1761; b) Y. Sawama, T. Yamada, Y. Yabe, K. Morita, K. Shibata, M. Shigetsura, Y. Monguchi, H. Sajiki, *Adv. Synth. Catal.* **2013**, *355*, 1529; c) M. Benedetti, C. R. Barone, C. R. Girelli, F. P. Fanizzi, G. Natile, L. Maresca, *Dalton Trans.* **2014**, *43*, 3669.

[60] J. Roth, T. Schwarz-Selinger, V. K. Alimov, E. Markina, *J. Nucl. Mat.* **2013**, *432*, 341.

1.6.1 Palladium catalyzed H/D exchange reactions

Palladium is one of the most common transition metals used in C–H activation, and there are many recent applications of palladium catalyzed H/D exchange reactions reported.[57] Among the recent developments for Pd-catalyzed hydrogen isotope exchanges, one of the most remarkable work is the high-temperature solid-state catalytic isotope exchange (HSCIE) method developed by Myasoedov *et al.*, which is based on the action of gaseous deuterium/tritium on a solid at high temperature (130-260 ℃). The solid phase is a highly dispersed mixture composed of the substrate and the transition-metal catalyst (mostly applying an inorganic carrier such as $CaCO_3$, $BaSO_4$ and so on) without solvent.[57a, c-g, i-k] This isotope exchange method was stereoretentive for deuteration/tritiation of amino acids and peptides; however, the regioselectivity was poor. It has also been applied in the tritiation of D-ribose,[61] maraviroc, an agent of new generation for HIV treatment blocking chemokine receptors CCR-5,[62] MK-801, a selective channel blocker of the glutamate receptor of the NMDA subtype, and 7-OH-DPAT, a selective agonist of the D3 dopamine receptor,[63] ataluren (PTC124),[64] serotonin (5-methoxytryptamine) and diazepam,[57a] brassinolide,[57c] GABA (γ-aminobutyric acid),[57d] SB258585, a potent, selective and orally active 5-HT_6 receptor antagonist,[57e] and isopentenyladenine[57i] (**Figure 1.38**).

[61] a) A. A. Baitov, G. V. Sidorov, N. F. Myasoedov, *Radiochemistry* **2005**, *47*, 201; b) A. A. Baitov, G. V. Sidorov, N. F. Myasoedov, *Radiochemistry* **2007**, *49*, 97; c) A. A. Baitov, G. V. Sidorov, N. F. Myasoedov, *Radiochemistry* **2007**, *49*, 100.

[62] V. P. Shevchenko, I. Y. Nagaev, N. F. Myasoedov, *Radiochemistry* **2009**, *51*, 175.

[63] Y. A. Zolotarev, Y. Y. Firsova, A. Abaimov, A. K. Dadayan, V. S. Kosik, A. V. Novikov, N. V. Krasnov, B. V. Vaskovskii, I. V. Nazimov, G. I. Kovalev, N. F. Myasoedov, *Russian J. Bioorg. Chem.* **2009**, *35*, 296.

[64] V. P. Shevchenko, Y. Nagaev, I. Yu, N. F. Myasoedov, *Radiochemistry* **2010**, *52*, 95.

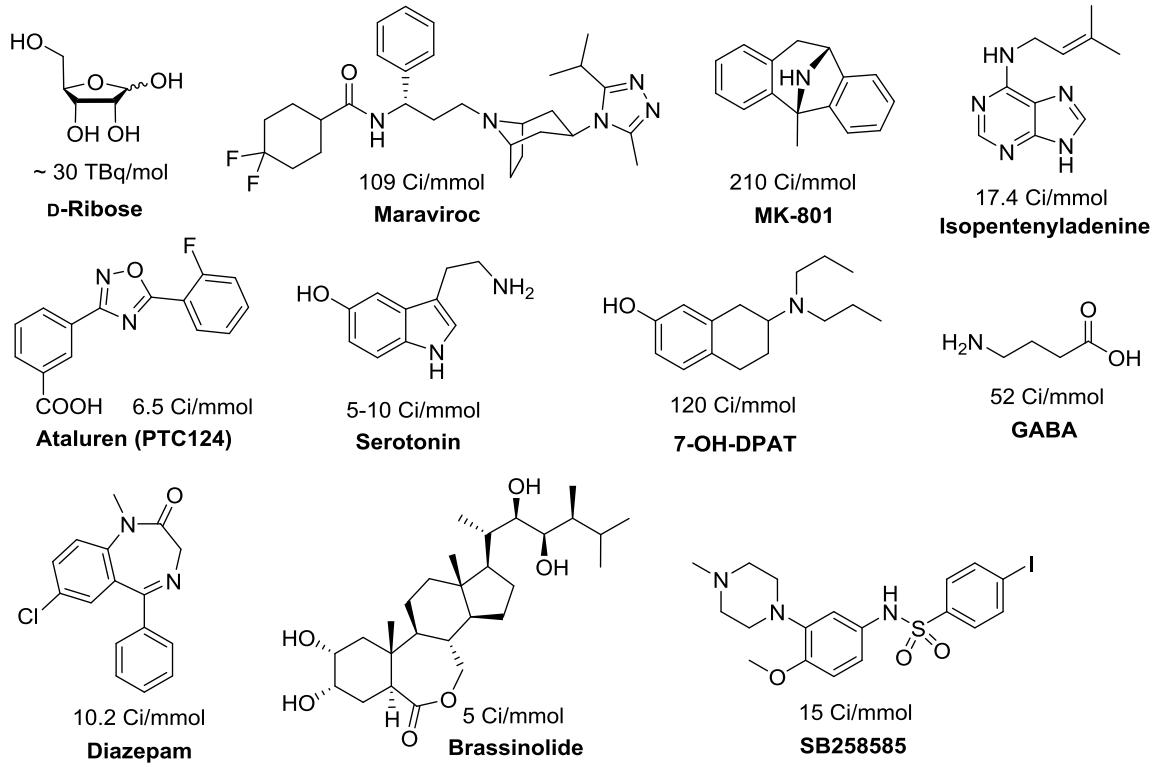

Figure 1.38 Applications of high-temperature solid-state catalytic isotope exchange (HSCIE)

Despite the broad applications of HSCIE, the harsh reaction conditions are not applicable to some sensitive substrates. Besides, for tritium labeling, the high reaction temperature was a potential risk for safety. In another example of Pd-catalyzed H/D exchange reaction, a modification of the catalyst surface by organic bases has been reported to accelerate the efficiency of deuteration against hydrogenolysis of benzyl ethers.[57b] However, it still required high reaction temperature (180 ℃) to achieve good level of deuterium incorporation, and poor regioselectivity was observed using these methods.

In 2014, a regioselective deuteration of arenes catalyzed by $Pd(OAc)_2$ was reported by J.-Q. Yu's group.[57h] Taking advantage of the weak coordination between the directing group of the substrate and the palladium catalyst, the authors realized the *ortho*-C-H deuteration of phenylacetic acids through protonolysis of palladacycles by using acetic acid-d_4 as solvent and deuterium source. Various substituted phenylacetic acids were deuterated efficiently with high deuterium incorporation. However, the benzylic positions were also deuterated under the reaction conditions, thus an additional reprotonation step of the benzylic positions was needed to obtain the *ortho*-deuterated phenylacetic acids (**Scheme 1.24**). Other substrates derived from benzoic acid also underwent H/D exchange under the reaction conditions. However, low deuterium incorporation was observed for substrates with

strong coordinating groups such as 2-phenylpyridine, suggesting that weakly coordinated palladacycle intermediates were more reactive towards protonolysis through an electrophilic-cleavage pathway.

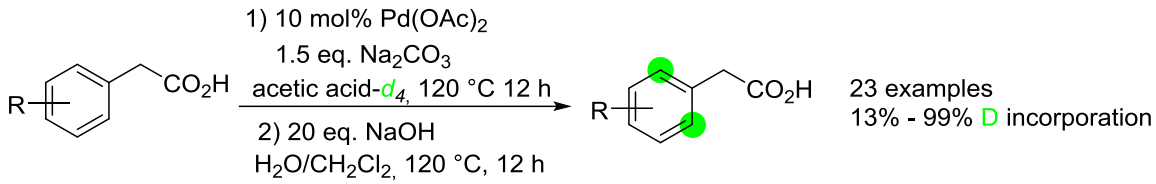

Scheme 1.24 *ortho*-Selective deuteration of phenylacetic acids

Overall, this method offered a one-step method to access *ortho*-deuterated phenylacetic acids and other related compounds. The major limitation of this method lay in the need of a reprotonation step, the high reaction temperature and the use of large amount of expensive deuterated solvent (5 mL acetic acid-d_4).

Later in 2015, K. W. Jung also reported an *ortho*-selective ligand-directed H/D exchange catalyzed by palladium catalyst with an NHC ligand.[57l] Using CF_3COOD as the deuterium source, this method was effective for the deuteration of aromatic substrates ranging from ketones to amides and amino acids. However, most substrates could be deuterated in the absence of the catalyst by acid-catalyzed electrophilic deuteration. The catalyst could just improve a little bit the deuterium incorporation in some cases. Moreover, for most substrates tested, poor deuterium incorporation was obtained with a poor regioselectivity, since multi-deuteration occurred in most cases.

Overall, despite the success of palladium achieved in the catalytic C-H functionalization, the application of palladium catalysts in the H/D exchange reactions remained less explored. The reaction conditions of palladium catalyzed deuteration processes were generally harsher than the ones using iridium and ruthenium catalysts.

1.6.2 Rhodium catalyzed H/D exchange reactions

Rhodium is another metal used for C-H activation reactions. It is usually used as a homogeneous catalyst, except for some cases of heterogeneous Rh/C or rhodium black.[58e]

In 2012, W. D. Jones reported the synthesis of two rhodium complexes and an iridium complex that contained a common core structure of **1.6.1** (**Figure 1.39**).[58b] The authors examined the catalytic activity of the rhodium complex **1.6.1a** for the H/D exchange reaction using AgOTf as additive and CF_3COOD as solvent and deuterium source. Moderate deuterium incorporations were obtained using this method for various substituted benzene derivatives. Interestingly, although no selectivity was observed in the deuteration of aryl rings, branched alkyl substituents showed an affinity toward

deuterium exchange in the *β*-alkyl position only (**Scheme 1.25**). DFT calculations suggested that the η^1-C-H bond of the arene coordinated to the metal center and the H/D exchange occurred by base-assisted C-H activation of the *β*-C-H bond.

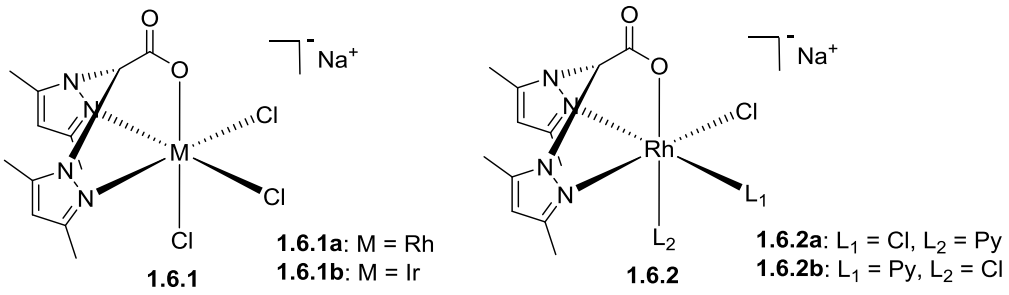

Figure 1.39 Structure of metal complexes synthesized by Jones *et al*

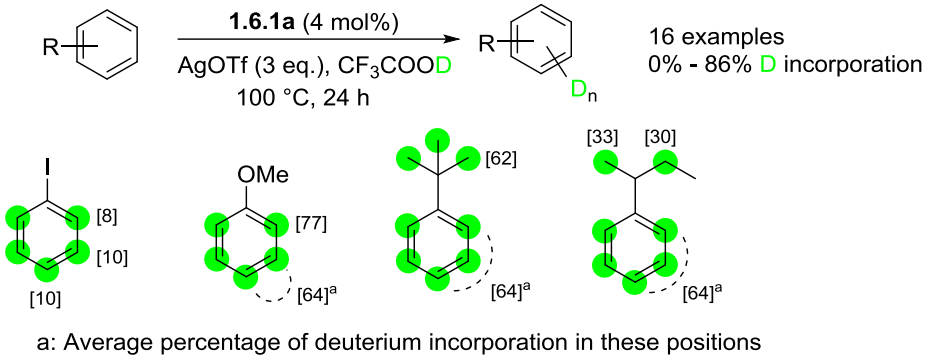

Scheme 1.25 H/D exchange reactions catalyzed by compound **1.6.1a**

Later the same year, M. S. Sanford reported the synthesis of rhodium(III) complexes, containing a cationic bipyridine ligand, and their catalytic activity toward the H/D exchange reactions.[58a] This new type of rhodium catalysts exhibited modest catalytic activity for the deuteration of benzene and 2-phenylpyridine using acetic acid-d_4 as the deuterium source. In spite of their low catalytic activity, they offered a new way to synthesize metal complexes with cationic ligands, which might have different reactivity from normal neutral ligands.

In 2014, L. A. Oro and co-workers reported the synthesis of a series of neutral and cationic Rh(III)-hydride and Rh(III)-ethyl complexes bearing a NHC ligand (**Figure 1.40**) and their application for H/D exchange of styrene using CD_3OD as the deuterium source.[58c] Most of the synthesized catalysts were able to selectively catalyze the H/D exchange of styrene at the vinyl *β*-position without concomitant deuteration of the aromatic ring. It had been observed that the NHC ligand played an important role in the catalytic activity and selectivity. According to the authors, the electronic property

and steric effect of the carbene ligand had a strong influence on the activity and selectivity of the catalyst; the existence of chloride ligand was essential for the catalyst; replacement of the chelating quinolinolate ligand by weakly bonded acetonitrile ligands increased the catalytic activity but decreased the selectivity of the catalyst. Overall, although the authors didn't show the catalytic activity of these catalysts for other substrates, this work represented an in-depth study for developing improved catalytic systems by ligand modification.

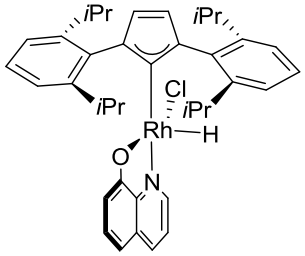

Figure 1.40 Example of Rh(III)-hydride complex synthesized by L. A. Oro and co-workers

In another example, the synthesis of two rhodium complexes with bidentate nitrogen ligands and their catalytic H/D exchange between benzene and CF_3CO_2D were accomplished by W. A. Goddard and co-workers.[58d] This method focused on the reactivity of the catalyst toward the deuteration of benzene by comparing the turnover frequency of the reaction with other reported metal catalysts. Since the authors didn't test the catalytic activity of the catalyst for the labeling of other substrates, the application of the catalyst remained to be explored.

Generally speaking, the substrate scope of rhodium cayalyzed H/D exchange process was not comparable to that of iridium or ruthenium catalyzed H/D exchange process; the reactivity of rhodium complexes have to be explored for more functionalized molecules.

1.6.3 Platinum catalyzed H/D exchange reactions

Platinum is one of the first metal catalysts used in H/D exchange reactions.[30] Many years after the work of Garnett, M. S. Sanford reported a similar process regarding the deuteration of benzene using a series of diimine Pt(II) complexes as catalysts (**Scheme 1.26**).[59a] Accordingly, substitution at the 2- and 6-positions of the *N*-aryl group, especially with halogens, led to significant increases in catalyst activity. The most active catalyst was bromo-substituted one, which was explained by the coordination and stabilization of the bromine atom to the metal center.

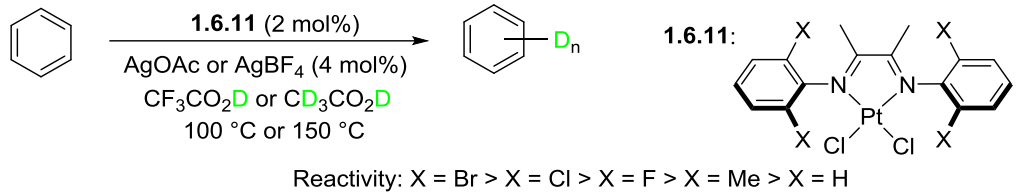

Scheme 1.26 H/D exchange of benzene catalyzed by Pt(II) complexes

A similar platinum catalyst with a nitrogen bidentate ligand was studied for H/D exchange reaction at the carbons sp^3 of the ligand.[59c] With a sterically strained nitrogen bidentate ligand (2,9-dimethyl-1,10-phenanthroline), the H/D exchange proceeded efficiently at the methyl groups; whereas with a more flexible nitrogen bidentate ligand (6,6'-dimethyl-2,2'-bipyridyl), the H/D exchange proceeded at a much slower rate and with lower deuteration incorporation at the methyl groups.

In 2013, H. Sajiki reported a Pt/C catalyzed H/D exchange reaction of various aromatic compounds using isopropyl alcohol and cyclohexane as co-solvent and D_2O as the deuterium source under an argon atmosphere.[59b] Using this method, deuterium-labeled compounds with high deuterium contents could be easily isolated by filtration of Pt/C and simple extraction, and various arenes possessing a variety of reducible functionalities could be effectively and directly deuterium-labeled without undesired reduction (**Scheme 1.27**).

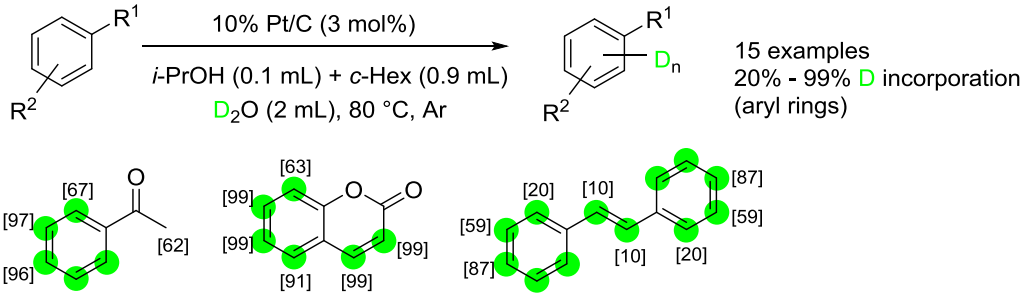

Scheme 1.27 Pt/C catalyzed H/D exchange reaction and selected examples

One possible limitation of this method was the poor selectivity. For all substrates tested, minor difference was observed regarding the regioselectivity on the aromatic rings. Lower deuterium incorporation was obtained at the positions adjacent to steric hindered substituent.

1.6.4 Iron catalyzed H/D exchange reactions

Among the metal catalysts used for isotopic labeling described above, the site selectivity of H/D exchange is either negligible or relies on directing groups to enable reactivity of the *ortho* positions in

aromatic and heteroaromatic rings. While in 2016, P. J. Chirik and co-workers described an iron-catalysed method for the direct deuterium and tritium labeling of pharmaceuticals by hydrogen isotope exchange, using deuterium/tritium gas as the isotopic source.[38b] Notably, the regioselectivity of the iron catalyst was orthogonal to currently used iridium or ruthenium catalysts and allowed isotopic labeling of complementary positions in drug molecules (**Scheme 1.28**), providing a new diagnostic tool in drug development. Using the iron catalyst **1.6.12**, a series of (hetero)arenes as well as several drug molecules were efficiently deuterated. Moreover, they applied their method successfully to the tritium labeling of some commercially available pharmaceuticals. The specific activities of labeled molecules were generally higher than the results got from the use of Crabtree's catalyst.

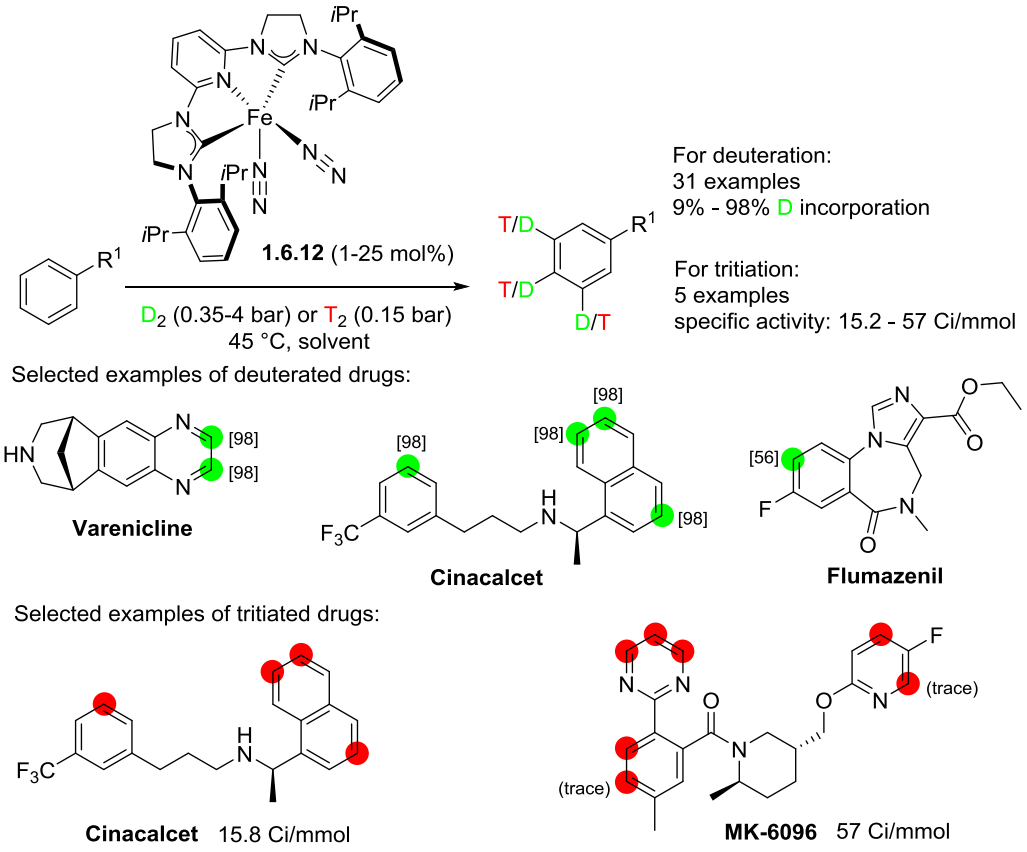

Scheme 1.28 Iron catalyzed selective deuterium/tritium labeling of drug molecules

1.6.5 H/D exchange reactions catalyzed by mixed metal catalysts

The deuteration reactions are usually catalyzed by a single metal catalyst; however, the use of mixed metal catalysts sometimes gives better results than a single catalyst.[36, 65] For example, S. C. Schou reported that the deuteration of compound **1.6.13** and **1.6.14** was achieved by using Crabtree's catalyst

[65] a) A. M. Krause-Heuer, N. R. Yepuri, T. A. Darwish, P. J. Holden, *Molecules* **2014**, *19*, 18604; b) S. Bijani, V. Jain, D. Padmanabhan, B. Pandey, A. Shah, *Tetrahedron Lett.* **2015**, *56*, 1211; c) T. Yamada, Y. Sawama, K. Shibata, K. Morita, Y. Monguchi, H. Sajiki, *RSC Adv.* **2015**, *5*, 13727.

and rhodium black as co-catalyst (**Scheme 1.29**). However, the use of either Crabtree's catalyst or rhodium black alone gave no deuteration of these two compounds. Therefore, the different combinations of catalysts give more possibilities to conduct reactions that are impossible to realize with a sole catalyst.

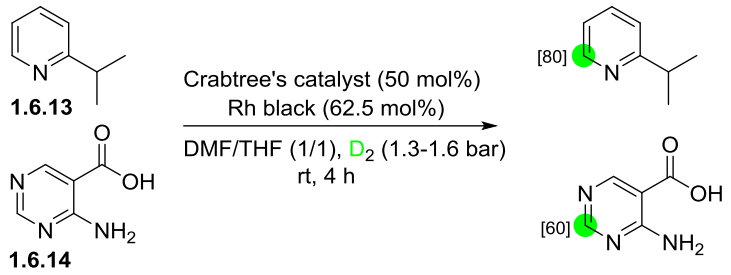

Scheme 1.29 Deuteration of compounds using co-catalyst

Using Pt/C (10 wt%) and Pd/C (10 wt%) as co-catalysts, T. A. Darwish and co-workers described a method allowing the H/D exchange of primary and secondary arylamines using D_2O as solvent and isotopic source at 80 ℃.[65a] Four arylamines were deuterated successfully on multi-gram scale (**Figure 1.41**), which could be used in the preparation of optoelectronic devices; while the attempts to deuterate tertiary arylamines failed.

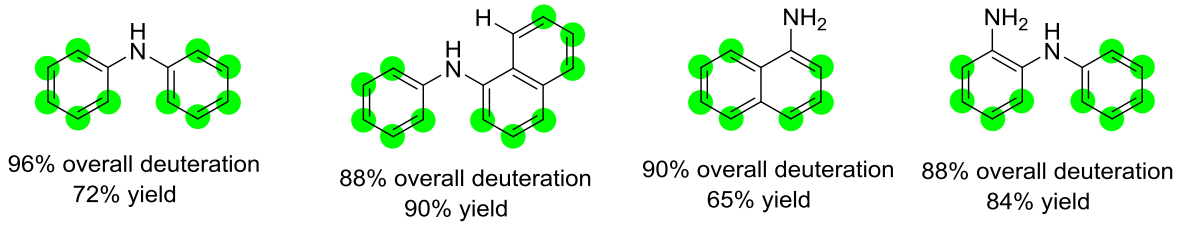

Figure 1.41 Pt/C and Pd/C catalyzed deuteration of arylamines

In 2015, A. Shah *et al.* reported the deuteration of mesalamine using Pd/C and Pt/C as co-catalysts and D_2O as the isotopic source under hydrogen atmosphere (**Scheme 1.30**).[65b] In Shah's protocol, the use of hydrogen atmosphere was essential for deuteration, since only trace of deuterium incorporation was observed without hydrogen atmosphere.

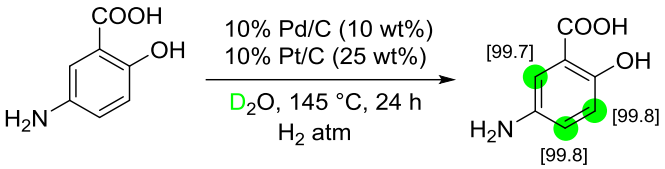

Scheme 1.30 Deuteration of mesalamine by Pd/C and Pt/C

Almost at the same time, H. Sajiki reported a multiple deuteration method for alkanes catalyzed by the combined use of heterogeneous Pt/C and Rh/C catalysts in *i*-PrOD-d_8 and D_2O as solvents.[65c] This method had been applied to the deuteration of wide variety of linear, branched and cyclic alkanes (**Scheme 1.31**). Interestingly, the combined use of Pt/C and Rh/C catalysts had a synergistic effect, since lower deuterium incorporation was obtained by using a single catalyst.

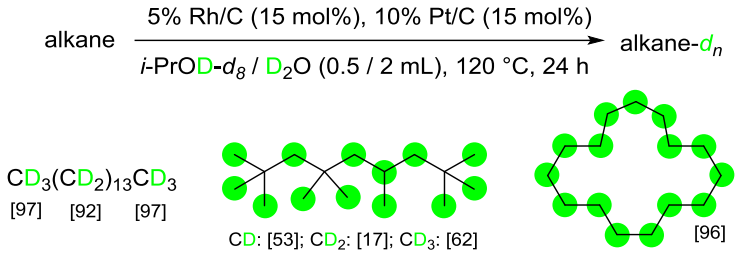

Scheme 1.31 Deuteration of alkanes by Rh/C and Pt/C

Thioether is an important substructure in various organic compounds, including bioactive compounds. For example, methionine is an essential amino acid in humans which contains a thioether moiety (**Figure 1.42**). It is important in angiogenesis, the growth of new blood vessels, and supplementation may benefit those suffering from Parkinson's disease, drug withdrawal, schizophrenia, radiation side effects, copper poisoning, asthma, allergies, alcoholism, or depression. Pergolide is an ergoline-based dopamine receptor agonist used in some countries for the treatment of Parkinson's disease. There is also a methio-moiety within pergolide (**Figure 1.42**). Benzthiazide is a thiazide diuretic used in the treatment of high blood pressure and edema. A sulfur atom is present between the bicyclic core structure and the benzyl group (**Figure 1.42**). These compounds are important to study their biological profiles and *in vivo* fates, thus a general method allowing the deuteration/tritiation of these compounds are highly desired.

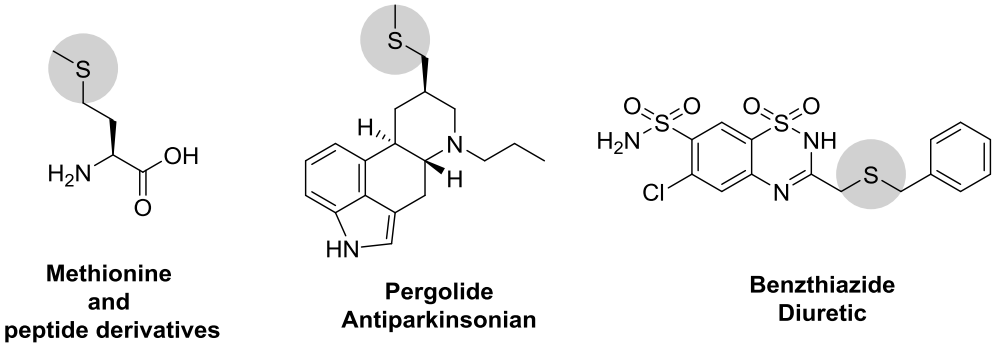

Figure 1.42 Examples of pharmaceutically relevant thioether-containing molecules

In spite of their occurrence in bioactive molecules (**Figure 1.42**), no general approach for the labeling of organosulfur compounds has been reported to date, only some limited examples describing the general H/D exchange process using directing groups involving a sulfonamide, which involved the coordination of either oxygen or nitrogen to the metal catalyst.[41d, 43q] One plausible reason for this lack of methods may be the propensity of sulfur atoms to poison noble metal catalysts. In this context, developing a general method allowing the deuteration of organosulfur compounds is of great importance and challenging work. Based on the results we have obtained from the labeling of nitrogen-containing compounds,[29, 46j] we decided to develop a general method allowing the labeling of organosulfur compounds.

2 Results and discussion

2.1 The investigation of the H/D exchange of thioethers

During the course of our studies toward the labeling of aza-compounds,[46j] when using methionine as substrate, we observed low (0.3 D) but exclusive deuterium incorporation at α-positions of the sulfur atom. Encouraged by this observation, we decided to examine the sulfur-directed C-H deuteration.

Using dihexylsulfide **2.1** as model substrate, the catalytic activity of various heterogeneous Ru sources towards this sulfur-directed C-H deuteration was examined under 2 bar of deuterium gas (**Table 2.1**). For all the reactions conducted, the ruthenium catalysts were stirred under 3 bar of D_2 for 3 hours before adding the substrates and solvents in order to remove the potential oxide species at the surface of the catalysts and do H/D exchange at the surface of the catalysts. The deuterium incorporation was quantified by the decrease of ^{1}H NMR integral intensities at the specified positions compared to the starting material. Integral intensities were calibrated against hydrogen signals that did not undergo H/D-exchange. For example, the ^{1}H NMR of unlabeled **2.1** was shown in **Figure 2.1**. After the deuteration process, the ^{1}H NMR of labeled **2.1** was shown in **Figure 2.2**. The protons at the α-positions of sulfur atom had a chemical shift around 2.5 ppm. After deuteration, we chose the hydrogen signal of terminal methyl group as the reference integral intensity since it was not labeled during the reaction. The integral intensity of the protons at position 1 decreased from 4 to 0.36, which meant that 91% of C-H bond was transformed into C-D bond. The isotopic enrichments obtained from ^{1}H NMR were compared to the results of mass spectrometry quantification analysis, which was performed by subtraction of the mean molecular masses of the product and substrate isotopologue clusters in order to eliminate the contribution of the natural isotope abundance to the total mass.

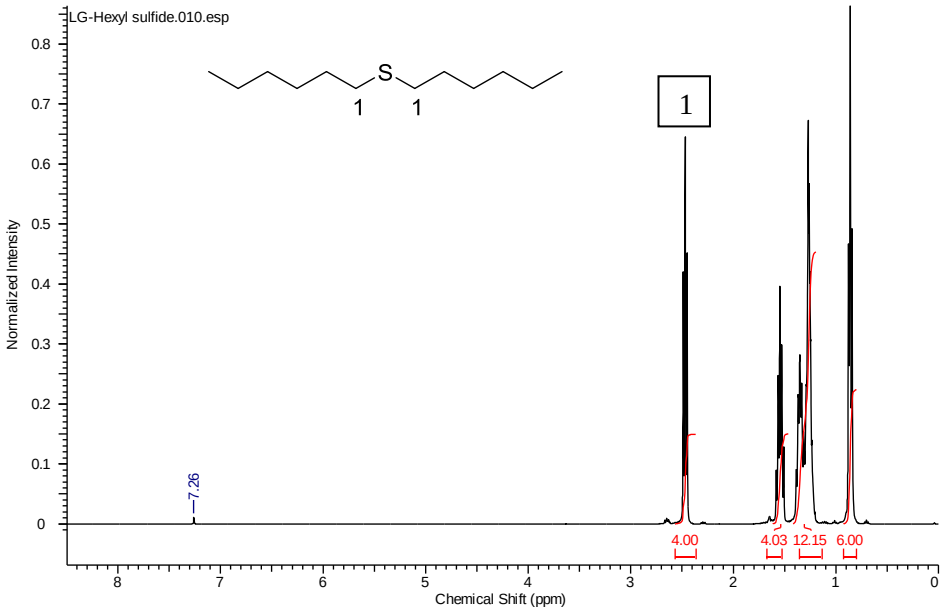

Figure 2.1 ^{1}H NMR of unlabeled dihexylsulfide **2.1**

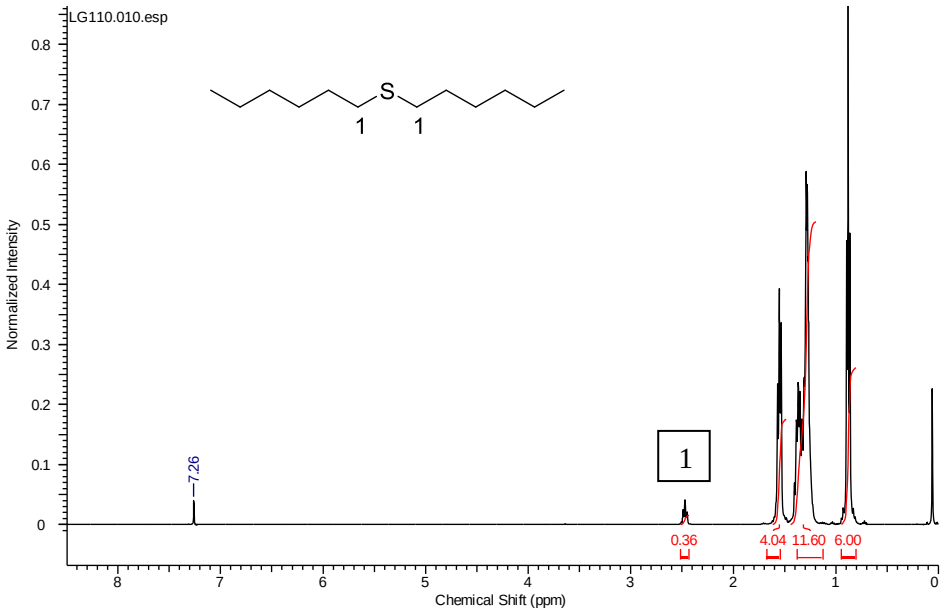

Figure 2.2 ^{1}H NMR of labeled dihexylsulfide **2.1**

We screened first the catalyst used for the labeling of nitrogen-containing compounds, RuNp@PVP. Unlike its good catalytic activity toward the labeling of nitrogen-containing compounds, this nano-catalyst gave only slight deuterium incorporation at the α-position of sulfur atom under the conditions used for the deuteration of aza-compounds (**Table 2.1**, Entry 1). The nano-catalyst with a phosphine ligand RuNp@dppb also gave a similar result (**Table 2.1**, Entry 2). To our delight, the use of commercially available catalyst Ru/C (from Aldrich) gave enhanced deuterium incorporation (**Table 2.1**, Entry 3). Furthermore, by increasing the catalyst loading and extending the reaction time, a high level of deuterium incorporation (91%) was obtained at the α-positions of the sulfur atom (**Table 2.1**, Entries 4 and 5). Other ruthenium catalysts and other metal catalysts supported on carbon gave lower deuterium incorporation under the same reaction conditions, demonstrating the robustness of Ru/C (**Table 2.1**, Entries 6-9). In order to explore the potential applications of the method, we also tested the deuteration reaction in other polar aprotic solvents, which gave positive results but lower deuterium incorporation (**Table 2.1**, Entries 10-12). The lower deuterium incorporation with these solvents might be due to the competitive H/D exchange with the solvents, which was observed by conducting the H/D exchange without any substrates. A decrease of the isotopic enrichment of the gas phase was detected after reaction. An attempt to run the reaction at room temperature gave much lower deuterium incorporation, with only 25% isotopic enrichment (**Table 2.1**, Entry 13), meaning that heating was essential to overcome the energy barrier of C-H bond activation. Thus, the best reaction conditions for the labeling of organosulfur compounds were as followed: 30 mol% of Ru/C as catalyst and reacted for 3 days in THF at 60 ℃ under 2 bar of D_2 gas.

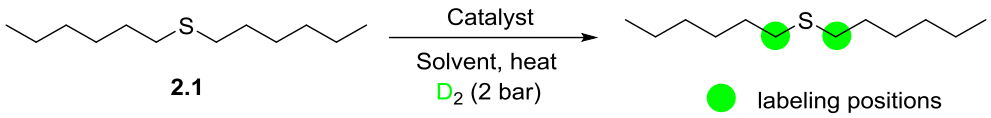

Entry	Catalyst	Solvent	T (℃)	Time (days)	Isotopic Enrichment
1	10 mol% RuNp@PVP	THF	55	1	3%
2	10 mol% RuNp@dppb	THF	55	1	4%
3	10 mol% Ru/C	THF	55	1	11%
4	30 mol% Ru/C	THF	60	1	77%
5	30 mol% Ru/C	THF	60	3	91%
6	30 mol% RuNp@PVP	THF	60	3	83%
7	30 mol% Ru-SnNp@PVP	THF	60	3	14%
8	30 mol% Rh/C	THF	60	3	14%
9	30 mol% Pd/C	THF	60	3	18%
10	30 mol% Ru/C	DMF	60	3	68%
11	30 mol% Ru/C	DMA	60	3	71%
12	30 mol% Ru/C	NMP	60	3	49%
13	30 mol% Ru/C	THF	rt	3	25%

Table 2.1 Screening conditions for the deuteration of dihexyl sulfide

With the best conditions in hand, we started to extend the substrate scope of the reaction (**Scheme 2.1**). For substrates **2.1**-**2.3**, THF was used as solvent. Regarding dibutylsulfide **2.2**, a higher deuterium incorporation (4.9 D) was obtained with a different regioselectivity. This might be due to the strong coordination of sulfur atom to the surface of the catalyst, and the butyl group was more feasible to coordinate to the particle surface. Other sulfides containing branched alkyl chains, such as bis(2-ethylhexyl)sulphide **2.3**, were also labeled with high isotopic enrichment and a selectivity in accordance with previously mentioned results.

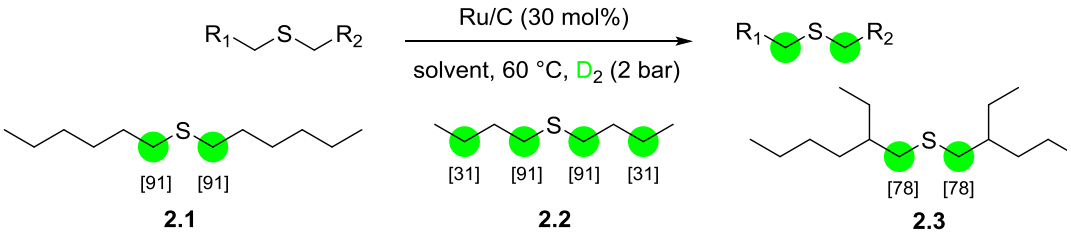

Scheme 2.1 Deuterium labeling of sulfur-containing compounds

Functionalized cyclic thioether **2.4** was successfully labeled at the α-positions of the sulfur atom using DMF as solvent, but low isotopic enrichment was obtained (**Table 2.2**, Entry 1). The use of THF as solvent gave a higher deuterium incorporation (**Table 2.2**, Entry 2), which was in accordance with the result for the deuteration of compound **2.1**. In order to know if Ru/C was the real catalyst and not other metals present in a trace amount in the catalyst, different commercial Ru/C sources were used for the labeling of this substrate. Interestingly, although Ru/C purchased from different commercial sources all catalyzed the H/D exchange of compound **2.4**, different catalytic activities were observed (**Table 2.2**, Entries 2-4). Unless otherwise noted, all the substrates were deuterated by using Ru/C purchased from Sigma-Aldrich. In this study, Ru/C purchased from Strem gave the best deuterium incorporation, with the incorporation of 2.3 deuterium atoms. It proved that the H/D exchange was catalyzed by Ru/C but not other metal impurities, and the physical properties such as particle sizes and shapes had an influence on the catalytic activities of Ru/C towards H/D exchange reactions. The use of ruthenium nanocatalyst stabilized by NHC ligand RuNp@ICy (ICy: *N*,*N*-dicyclohexylimidazol-2-ylidene) gave a lower isotopic enrichment (**Table 2.2**, Entry 5). Notably, performing a second run of H/D exchange with this molecule led to a significant increase of the isotopic enrichment (**Table 2.2**, Entry 6) for **2.4**, demonstrating the possibility of increasing deuterium incorporation when needed.

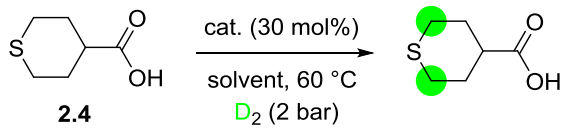

Entry	Catalyst	Solvent	Isotopic Enrichment
1	Ru/C	DMF	12%
2	Ru/C	THF	47%
3	Ru/C (from Strem)	THF	57%
4	Ru/C (from Alfa)	THF	55%
5	Ru@*i*Cy	THF	38%
6[a]	Ru/C	THF	82%

[a]: result got from second run of reaction using the product of Entry 2.

Table 2.2 Conditions screening for the deuteration of cyclic thioether **2.4**

We then explored the applicability of this transformation to the labeling of bioactive molecules, including amino acids and peptides derived from methionine and drugs containing a thioether substructure. Different solvents were used according to the solubility of the different substrates. Remarkably, in all cases, no racemization or epimerization occurred (checked by chiral HPLC analyses), and the deuterated products were obtained with retention of the stereochemistry.

Methionine **2.5** was deuterated in D_2O with an incorporation of 1.3 deuterium atoms using 30 mol% Ru/C as catalyst under 2 bar of D_2 gas at 60 ℃ (**Table 2.3**, Entry 1). Attempts to increase the isotopic enrichment by increasing either the catalyst loading or reaction temperature failed, both giving lower deuterium incorporation (**Table 2.3**, Entries 2 and 3), perhaps due to more side product formation under these conditions (see section 2.4, page 72 for more details). Considering the competing coordination to catalyst surface of nitrogen atom with sulfur atom, we transformed methionine into the corresponding hydrochloride salt so that the sulfur atom could coordinate more strongly to the surface of the catalyst. Pleasingly, the isotopic enrichment was improved significantly by this transformation (**Table 2.3**, Entry 4), proving that the coordination of the amino group to the surface of the catalyst had impeded the H/D exchange of methionine. Chiral high-performance liquid chromatography (HPLC) analyses were employed to determine the stereochemistry of the deuterated product. By injecting D,L-methionine into chiral HPLC, L-methionine and D-methionine could be separated (**Figure 2.3**, Run 3). The injection of optically pure L-methionine under the same conditions proved that the peak with a shorter retention time was the L-methionine (**Figure 2.3**, Run 2). Thus, the deuterated product was injected into chiral HPLC using the same analytical conditions. As shown in **Figure 2.3**, the labeled methionine contained only L-methionine (Run 1), no epimerization occurred under the reaction conditions. Therefore, the stereochemistry of methionine was retained after this C-H deuteration process.

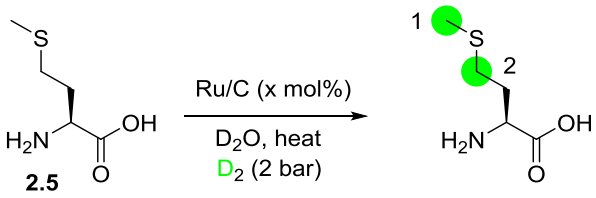

Entry	x	T (℃)	Isotopic Enrichment	
			1	2
1	30	60	37%	11%
2	50	60	21%	7%
3	30	100	28%	5%
4[a]	30	60	50%	20%

[a]: Hydrochloride salt of methionine was used as substrate.

Table 2.3 Conditions screening for the deuteration of methionine

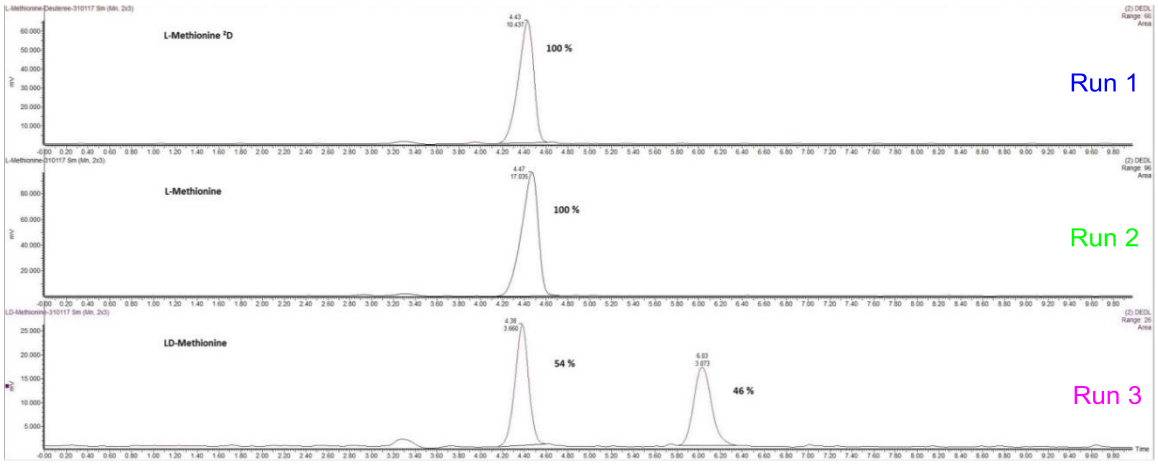

Figure 2.3 Chiral HPLC analysis of deuterated methionine

Different solvents were examined for the deuteration of *N*-Acetyl-L-methionine **2.6** (**Table 2.4**, Entries 1-3). By using DMF as solvent, moderate deuterium incorporation was obtained; while the use of D_2O or CD_3OD gave better results in this transformation, perhaps owing to the better solubility of compound **2.6** in D_2O and CD_3OD. Thus, in order to better solubilize the substrate, it was transformed into the corresponding sodium salt and then used as substrate under the same reaction conditions using D_2O as solvent. The deuterium incorporation at position 2 increased through this transformation; however, the deuterium incorporation at position 1 decreased at the same time (**Table 2.4**, Entry 4), which might be due to the different coordinating mode of the sodium salt to the surface of the catalyst. Increasing the D_2 pressure to 4 bar didn't lead to any increase of the isotopic enrichment (**Table 2.4**, Entry 5), demonstrating that the use of 2 bar D_2 was sufficient for the H/D exchange reactions.

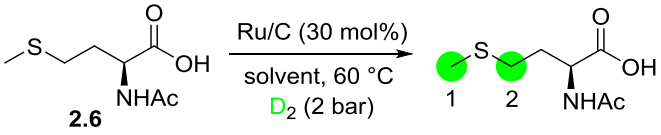

Entry	Solvent	Isotopic Enrichment	
		1	2
1	DMF	17%	5%
2	D_2O	67%	25%
3	CD_3OD	66%	31%
4[a]	D_2O	59%	32%
5[a, b]	D_2O	55%	36%

[a]: sodium salt was used as substrate; [b]: 4 bar D_2 was used for deuteration.

Table 2.4 Conditions screening for the deuteration of *N*-Acetyl-L-methionine

Dipeptide Pro-Met **2.7**, a substrate of prolinase, was regioselectively deuterated at the α-positions of the sulfur atom together with a slight deuteration at position 3 (which was due to the coordination of the nitrogen atom or amide group to the surface of the catalyst) (**Table 2.5**, Entry 1). In order to prevent the coordination of the nitrogen atom, the dipeptide was transformed into the corresponding hydrochloride salt. Surprisingly, by using the hydrochloride salt of **2.7** as substrate, a similar result was obtained, and the deuteration at position 3 was still observed (**Table 2.5**, Entry 2). Since the amine has been transformed into the corresponding hydrochloride salt, the deuteration at position 3 might be due to the coordination of the amide group to the surface of the catalyst. Increasing the catalyst loading to 50 mol% gave a higher deuterium incorporation at position 2 and 3, with totally 2.3 D incorporated (**Table 2.5**, Entry 3), which could be reasoned by the coordination of both amide group and sulfur atom to the surface of the catalyst, thus forming a rigid bidentate intermediate that promoted the H/D exchange at position 2 and 3.

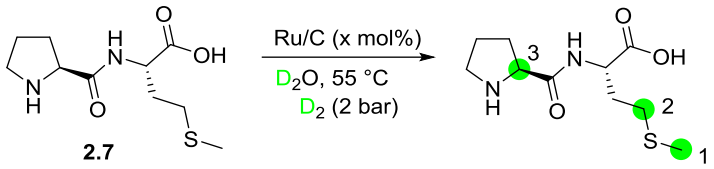

Entry	x	Isotopic Enrichment		
		1	2	3
1	30	41%	20%	5%
2[a]	30	43%	20%	8%
3[a]	50	43%	43%	17%

[a]: Hydrochloride salt of **2.7** was used as substrate.

Table 2.5 Conditions screening for the deuteration of dipeptide Pro-Met **2.7**

Remarkably, this method was found to be applicable to a tetrapeptide such as Leu-Trp-Met-Arg **2.8** (**Table 2.6**). Labeling of the thioether substructure of the methionine residue was observed by using 30 mol% Ru/C as catalyst in D_2O under 2 bar of D_2 gas with a moderate deuterium incorporation (**Table 2.6**, Entry 1). The use of well-defined nano-catalyst RuNp@dppb gave a comparable level of deuterium labeling (**Table 2.6**, Entry 2). Notably, deuteration with an elevated temperature of 100 ℃ led to an incorporation of 1.6 deuterium atoms in this complex structure (**Table 2.6**, Entry 3), without any observed degradation. The increased reaction temperature might promote the C-H activation process by providing more energy, thus the activation barrier was overcome and better results were obtained.

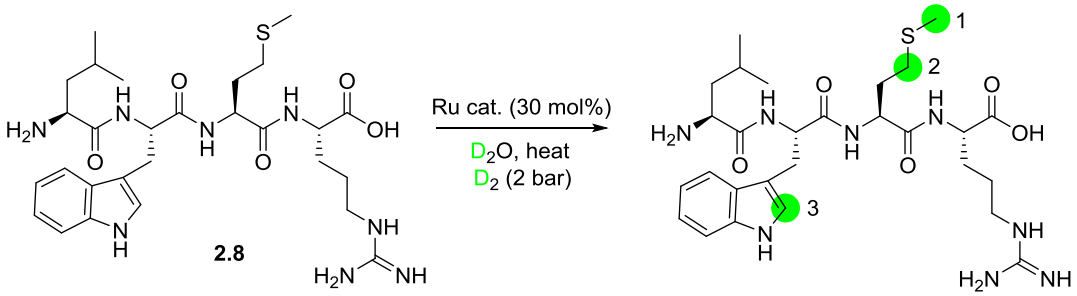

Entry	Ru cat.	T (℃)	Isotopic Enrichment		
			1	2	3
1	Ru/C	55	14%	7%	-
2	RuNp@dppb	55	9%	4%	-
3	Ru/C	100	30%	14%	43%

Table 2.6 Conditions screening for the deuteration of tetrapeptide **2.8**

For these two peptides **2.7** and **2.8**, the retention of stereochemistry of the labeled products was demonstrated by chiral HPLC analyses. Thus, acid catalyzed hydrolysis of the labeled peptides was performed, and the resulting amino acids obtained after hydrolysis were analyzed by chiral HPLC. For example, regarding peptide **2.7**, compared with D,L-methionine (**Figure 2.4**, Run 4), the amino acid resulting from the hydrolysis of the labeled peptide was L-methionine only (**Figure 2.4**, Run 1); compared with D,L-proline (**Figure 2.4**, Run 3), the amino acid resulting from the hydrolysis of the labeled peptide was L-proline only (**Figure 2.4**, Run 1). Same results were obtained from the hydrolysis of unlabeled peptide **2.7** (**Figure 2.4**, Run 2). Another experiment for the analysis of labeled peptide **2.8** also gave similar results, no racemization of the labeled product being detected. Therefore, these results demonstrated that the stereochemistry of labeled products was retained.

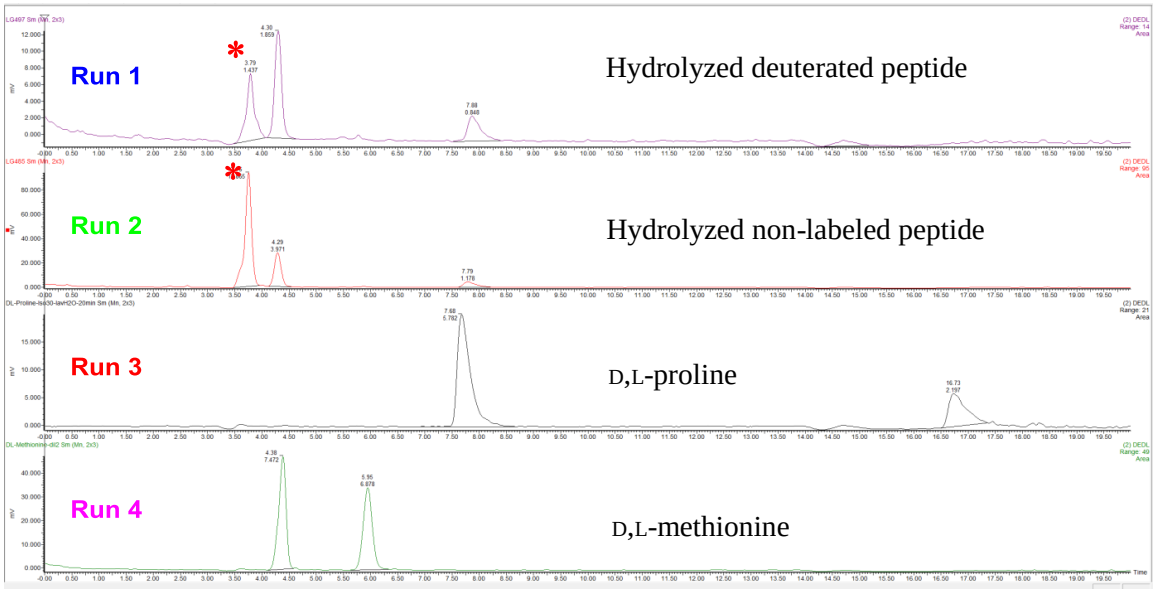

*Peak of unknown compound related to the polymerization of the peptide.

Figure 2.4 Chiral HPLC analyses of the amino acids obtained from the hydrolysis of **2.7**

Deuterated pergolide **2.9**, a dopamine receptor agonist used for the treatment of Parkinson's disease, has been prepared by the group of W. J. Wheeler in four steps (**Scheme 2.2**), with a total yield of 29% and an incorporation of 0.85 deuterium atoms.[66] The low deuterium incorporation obtained by this method was due to the use of protic solvent, which could undergo H/D exchange with D_2 to form H_2 or HD and thus decrease the isotopic enrichment of the gas phase. By contrast, using the commercially available catalyst Ru/C, our method resulted in a total of 2.1 deuterium atoms incorporation in a single step with 91% yield (**Scheme 2.3**), once again without racemization {starting compound: $[\alpha]_D^{20}$ -31.0 (*c* 0.1, CH_3OH), labeled compound: $[\alpha]_D^{20}$ -30.0 (*c* 0.1, CH_3OH)}. The labeled product could be obtained by a simple filtration after reaction, thus saving time and resources. The deuteration of compound **2.9** could also be accomplished with organic solvents, while the use of D_2O gave the best results. Detail studies for the tritium labeling of pergolide would be described later at section 2.3, page 69.

[66] W. J. Wheeler, D. L. K. Kau, N. J. Bach, *J. Label. Compd. Radiopharm.* **1990**, *28*, 273.

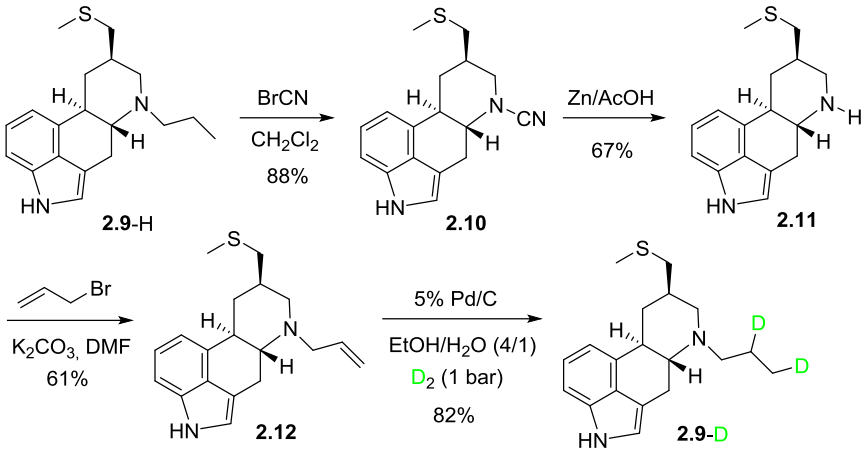

Scheme 2.2 Synthesis of deuterated pergolide

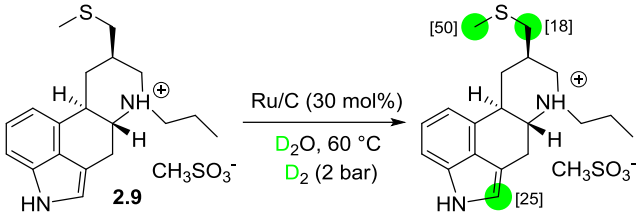

Scheme 2.3 Deuteration of pergolide by Ru/C catalyzed H/D exchange

The labeling of benzthiazide **2.13**, a diuretic used in the treatment of high blood pressure and edema, was quite tricky (**Table 2.7**). Selective labeling on the methylene group adjacent to the sulfur atom was observed using 30 mol% Ru/C as catalyst in DMF under 2 bar of D_2 gas (**Table 2.7**, Entry 1). However, it was worth noting that deuterated 1-methylchlorothiazide **2.14**, formed through the cleavage of C-S bond, was identified as a side product with a ratio of about 1:3.3 to **2.13**. The crude product was purified by column chromatography, giving pure deuterated benzthiazide. However, a significant decrease of isotopic enrichment (61% labeling at position 1 and 0% labeling at position 2) was observed after the purification, perhaps due to the reprotonation of labeled product during the purification process due to the acidity of the C-H bonds. Changing the solvent with THF/D_2O resulted in a lower deuterium incorporation (**Table 2.7**, Entry 2) and higher ratio of side product (**2.13**:**2.14** = 1.2:1). The uses of DMA and THF as solvents were even worse, giving poorer deuterium incorporation (**Table 2.7**, Entries 3 and 4) and/or more side product formation (**2.13**:**2.14** = 1:1.2 and 1.4:1 respectively), perhaps due to poorer solubility of **2.13** in these solvents. Reaction ran at a higher temperature using 2-MeTHF as solvent gave complex results (**Table 2.7**, Entry 5), perhaps due to more degradation of the substrate. In order to explore the mechanism of the C-S bond cleavage, more experiments were done using THF/D_2O as co-solvents (**Table 2.7**, Entries 6-8). The use of higher

catalyst loading (60 mol%) led to the formation of more side product (**2.13**:**2.14** = 1:10). Replacing D_2 by H_2 with high catalyst loading (60 mol%) also led to the formation of side product **2.14**; however, the ratio was lower than the use of D_2 (**2.13**:**2.14** = 1:3.4). Notably, although no D_2 was used, a high deuterium incorporation was observed from the undegraded benzthiazide (**Table 2.7**, Entry 7), which might be due to the formation of D_2 or HD from the H/D exchange between H_2 and D_2O or the labeling of **2.13** directly by D_2O. To confirm this observation, the reaction was conducted under an argon atmosphere. Surprisingly, the deuteration of benzthiazide proceeded efficiently without the formation of any side product (**Table 2.7**, Entry 8). Thus, we could conclude that: 1) the cleavage of C-S bond happened with the assistance of D_2 or H_2; 2) the ratio of side product **2.14** had a positive correlation with the amount of catalyst; 3) the C-H bonds at position 1 were more reactive, it could be exchanged with D_2O in the presence of Ru/C to form C-D bonds.

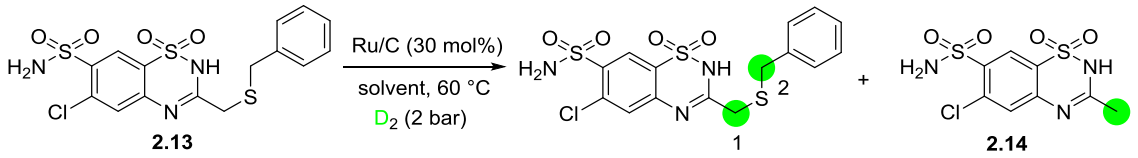

Entry	Solvent	Isotopic Enrichment		Ratio of **2.13**:**2.14**
		1	2	
1	DMF	80%	5%	3.3 : 1
2	THF/ D_2O	71%	4%	1.2 : 1
3	DMA	54%	5%	1 : 1.2
4	THF	19%	5%	1.4 : 1
5[a]	2-MeTHF	-	-	-
6[b]	THF/ D_2O	76%	5%	1 : 10
7[b,c]	THF/ D_2O	100%	3%	1 : 3.4
8[d]	THF/ D_2O	52%	7%	100% **2.13**

[a]: Run at 80 ℃; [b]: 60 mol% Ru/C was used; [c]: 2 bar H_2 was used instead of D_2; [d]: Run under Ar.

Table 2.7 Conditions screening for the deuteration of benzthiazide **2.13**

Biotin **2.15** was also labeled by means of a diastereoselective C-H deuteration process using DMF as solvent {starting compound: $[\alpha]_D^{20}$ +71.0 ° (*c* 0.1, CH_3OH), labeled compound: $[\alpha]_D^{20}$ +73.0 ° (*c* 0.1, CH_3OH)}. Only H_α proton was exchanged (**Table 2.8**, Entry 1), leading to an isotopic enrichment of 42%. The determination of the labeling position was done according to the analysis of ^1H NMR of the labeled product. As shown in **Figure 2.5**, the chemical shifts of proton 1, proton 2 and proton 3 could be identified from the ^1H NMR of unlabeled biotin. By comparing the ^1H NMR of labeled biotin with

the unlabeled one, we could see that only proton 2 was labeled with deuterium (**Figure 2.6**). The diastereoselective labeling might be due to the steric effect of the carboxylic acid side train and/or the hydrogen bonding between the carboxylic acid and proton 1, thus only the proton 2 was accessible to the catalyst surface. Reaction under an elevated temperature gave no improvement of isotopic enrichment (**Table 2.8**, Entry 2). In order to have a better solubility of the substrate, we transformed biotin into the corresponding sodium salt. Interestingly, conducting the deuteration process with the corresponding sodium salt of biotin in D_2O yielded multi-labeled product with a higher isotopic enrichment (**Table 2.8**, Entry 3), perhaps due to the better solubility of the sodium salt in D_2O.

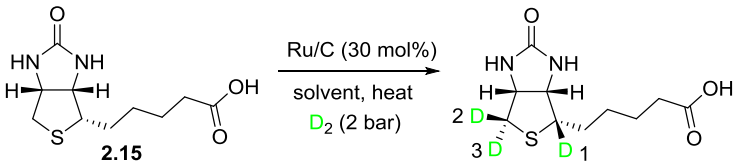

Entry	Solvent	T (℃)	Isotopic Enrichment		
			1	2	3
1	DMF	60	-	42%	-
2	DMF	80	-	42%	-
3[a]	D_2O	60	20%	80%	16%

[a]: Biotin sodium salt was used as substrate.

Table 2.8 Conditions screening for the deuteration of biotin **2.15**

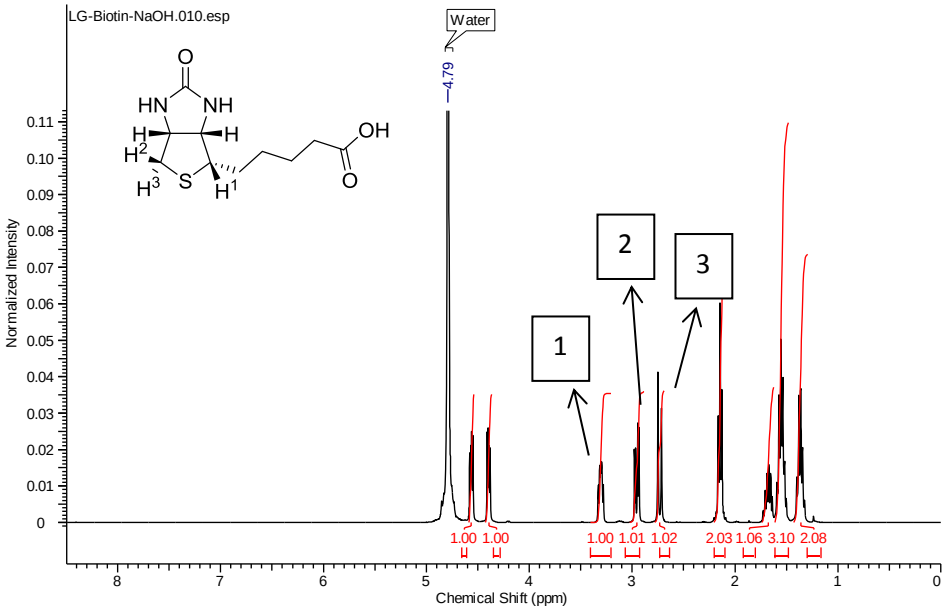

Figure 2.5 ^{1}H NMR of unlabeled biotin

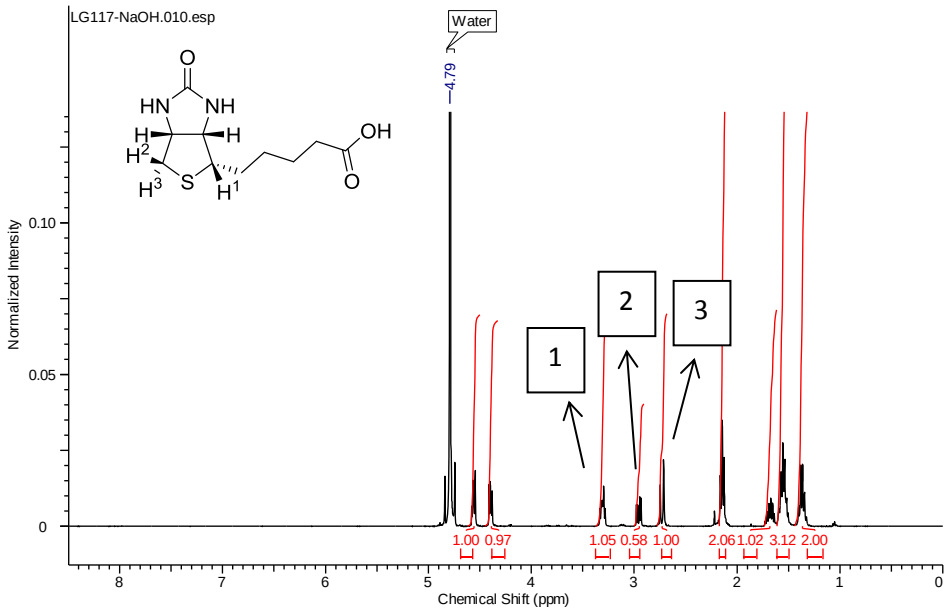

Figure 2.6 ^{1}H NMR of labeled biotin

2.2 Attempts to apply our method in quantitative LC-MS analysis

As mentioned above, one of the most important applications of deuterated compounds is related to their use as internal standards for quantitative LC-MS analysis, which requires an incorporation of 3-5 deuterium atoms and where the remaining amount of unlabeled (D0) compound is negligible.[9a] In this context, dipeptide **2.7** and pergolide **2.9** were selected as examples to conduct the deuteration process with a modified procedure: 0.2 mmol of substrate in D_2O were stirred at 60 ℃ for 24 h under 2 bar of D_2 gas. Then the crude product was filtered to remove the catalyst, dried and the deuteration procedure was repeated for twice. Pleasingly, for both substrates tested, significant improvement in deuterium incorporations were observed after the third cycle of deuteration (**Figure 2.7**): 3.8 deuterium atoms were incorporated in compound **2.7**, while 4.3 deuterium atoms were incorporated in compound **2.9** (determined by ^{1}H NMR). Moreover, both labeled products were obtained with negligible amounts of unlabeled compounds, and the amounts of monodeuterated (D1) and dideuterated (D2) materials were also detected within the system resolution (±5%) (**Table 2.9**), which meant that they were able to be used as internal standards in quantitative LC-MS analysis. The small differences of deuterium incorporation between ^{1}H NMR and MS analyses might be due to system resolution, which could be disregarded. The fact that the isotopic enrichment could be improved by repeating the deuteration procedure could be due to the poisoning of the catalyst by sulfides, which were derived from the cleavage of the C-S bonds of the substrates. Thus, the use of new batch of Ru/C reactivated the H/D exchange process, hence improving the isotopic enrichments. The cleavage of C-S bonds of the

substrates was confirmed by the observation of small amounts of degraded products together with the desired deuterated products after reaction. Thus, the final deuterated products were purified by preparative HPLC and the isotopic enrichments were recorded from the purified products.

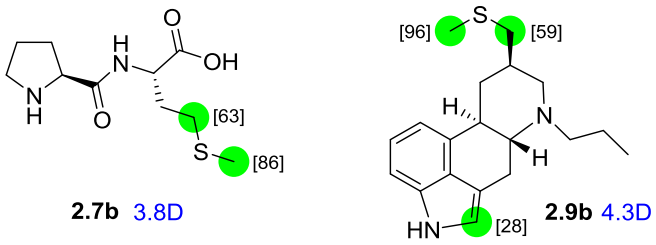

Figure 2.7 Results after third run of deuteration

Product	D0	D1	D2	D3	D4	D5	D6	D7	Total D
2.7	0.5%	1.5%	4.7%	18.6%	33.7%	33.4%	6.0%	1.3%	4.0
2.9	0.4%	0.7%	3.0%	17.8%	36.8%	30.0%	9.1%	1.7%	4.2

Table 2.9 Mass analyses of labeled products

2.3 Application of our method in tritium labeling

In order to further demonstrate the practicality of our method, we tried to label pergolide with tritium atoms because of its important medicinal properties and structural complexity. Besides, no direct exchange method on pergolide has been reported, only an example of multi-step synthesis.[66] Tritium labeling is more challenging than deuterium labeling, because: 1) aprotic solvent should be used instead of tritiated water to prevent the isotopic exchange between tritium gas and the solvent; 2) lower volume of tritium gas should be used for tritiation due to safety concerns; 3) with a lower volume and lower T_2 gas pressure, an incorporation of at least 0.5 tritium atom should be achieved in order to satisfy the need of specific activity for biological applications. In this context, optimization of the reaction conditions was conducted. D_2 was used instead of T_2 in the optimization for convenience. The results were shown in **Table 2.10**.

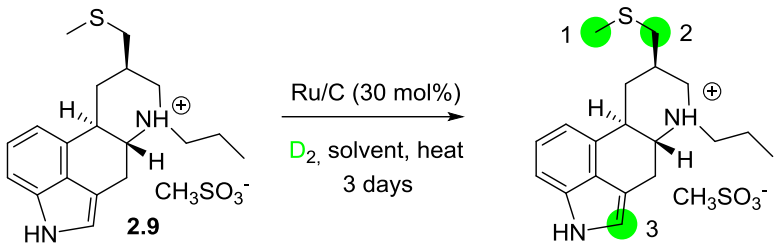

Entry	D_2 pressure	Solvent	T (℃)	Isotopic Enrichment			Total D
				1	2	3	
1	2 bar	D_2O	60	50%	18%	25%	2.1
2[a]	1.4 bar	DMF	60	59%	15%	-	2.1
3[a, b]	1 bar	DMF	rt	-	-	-	-
4[a, c]	1.4 bar	DMF	80	31%	6%	-	1.1
5[a, c]	1.4 bar	DMA	80	26%	12%	-	1.0
6[a, b]	1.4 bar	DMA	80	-	-	-	0.8[d]
7[a, b]	1.4 bar	2-MeTHF	80	-	-	-	0.6[d]
8[a, b, c, e]	1 bar	DMF	80	-	-	-	2.1[d]

[a]: Ru/C was used without prior activation; [b]: reaction run in a 5 mL flask; [c]: reaction run for 1d; [d]: determined directly by MS; [e]: 80 mol% Ru/C was used.

Table 2.10 Optimizing the reaction conditions for the tritium labeling of pergolide **2.9**

As mentioned above, all the H/D exchange reactions were conducted by using pre-activated Ru/C (by 3 bar of D_2 gas for 2 hours) as catalyst. However, to simplify the operations for tritium labeling, an attempt to use unactivated Ru/C for deuteration of pergolide was conducted using DMF as solvent under 1.4 bar of D_2 gas at 60 ℃ for 3 days. Pleasingly, with the lower D_2 pressure, a similar isotopic enrichment was obtained (**Table 2.10**, Entry 2). Encouraged by this result, we tried to run the reaction under a lower D_2 pressure at room temperature in a 5 mL flask. However, no deuteration was observed in this case (**Table 2.10**, Entry 3), suggesting that heating was essential for the activation of C-H bond. We then tried to run the reaction for a shorter reaction time in order to optimize the reaction conditions. Lower deuterium incorporation was obtained even if the reaction was run at a higher temperature (80 ℃) for 1 day (**Table 2.10**, Entry 4), suggesting that the kinetics of the H/D exchange was slow and the reaction was more dependent on time than on temperature. Changing the solvent with DMA slightly decreased the isotopic enrichment at the methyl group, while significantly increased the isotopic enrichment at the methylene group, leading to a similar deuterium incorporation (**Table 2.10**, Entry 5). These conditions could be applied to tritium labeling already, however, in order to decrease the amount of labeled waste, we tried to conduct the reaction in a 5 mL flask with smaller amount of

substrate (3 mg). The deuterium incorporation decreased a little in this case using DMA as solvent (**Table 2.10**, Entry 6), perhaps due to the use of lower volume of D_2. Considering that THF was a good solvent in the deuteration of many substrates, we tried 2-MeTHF as solvent. However, the deuterium incorporation was even lower compared with the use of DMA (**Table 2.10**, Entry 7). Since we used a very small amount of substrate for tritium labeling, the corresponding amount of catalyst was also little. Thus, we decided to conduct the deuteration of pergolide with a higher catalyst loading to improve the isotopic enrichment because higher isotopic enrichment was observed by using higher amount of catalyst for the labeling of compound **2.7**. The reaction was conducted using 3 mg of pergolide mesylate with 80 mol% Ru/C in 0.5 mL DMF under 1 bar of D_2 gas in a 5 mL Fisher-Porter bottle for 24 h. As a result, a total of 2.1 D was incorporated by this means (**Table 2.10**, Entry 8), suggesting that the use of higher amount of Ru/C would promote the C-H activation process. Thus, the best conditions for the tritium labeling of pergolide mesylate were: 80 mol% Ru/C as catalyst, DMF as solvent and reacted under 1 bar of D_2 gas for 24 h at 80 ℃.

With the best conditions in hand, the tritium labeling of pergolide mesylate was conducted. Thus, starting with 3 mg of pergolide mesylate and using 80 mol% of Ru/C as catalyst in DMF under 0.9 bar of T_2 gas, tritiated pergolide with a total activity of 18 mCi and a specific activity of 15.6 Ci/mmol (>0.5 T incorporated) was obtained after purification using preparative HPLC. The tritium NMR spectrum showed regioselective tritium incorporation (more than 96%) on the methyl group at the α-position of the sulfur atom (**Figure 2.8**). The three peaks observed were attributed to the 3 isotopologues CTH_2 (2.13), CT_2H (2.11) and CT_3 (2.08). These different chemical shifts were due to the isotope effect of the tritium atom.[67] A small additional tritium incorporation was also observed at the α-position of the sulfur moiety (CH_2 group). The obtained tritiated product had a specific activity high enough for most of the experiments required for ADME studies, demonstrating the usefulness of our method.

[67] P. G. Williams, H. Morimoto, D. E. Wemmer, *J. Am. Chem. Soc.* **1988**, *110*, 8038.

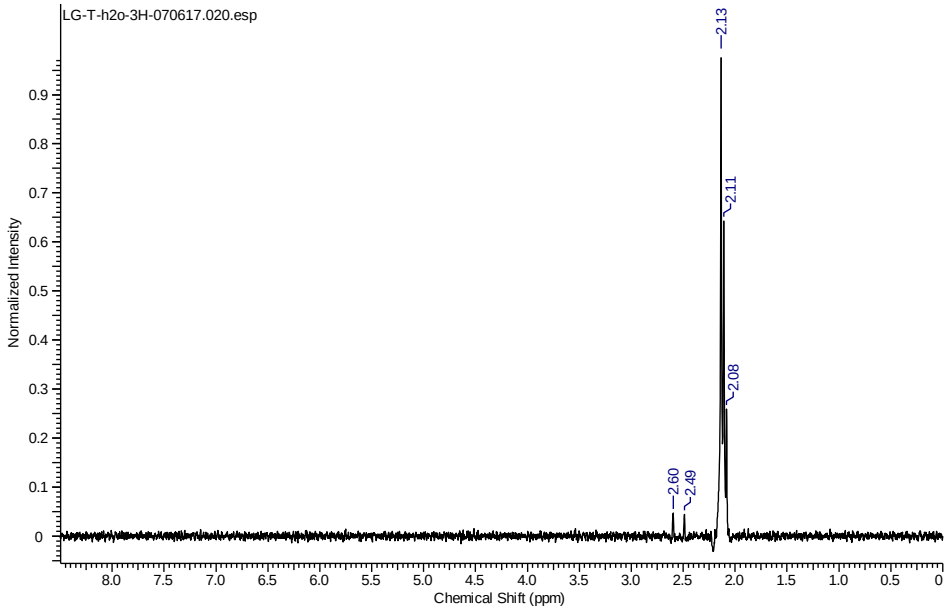

Figure 2.8 ^{3}H NMR spectrum of tritiated Pergolide

2.4 Mechanistic studies of the H/D exchange of thioethers

In order to understand the mechanism of our HIE process, several experiments were conducted. First of all, we studied the kinetics of the H/D exchange reaction using dihexylsulfide **2.1** as substrate. Using the same reaction conditions except the reaction time, the isotopic enrichments of labeled products were obtained by ^{1}H NMR and shown in **Table 2.11** and **Chart 2.1**. As we could see, the isotopic enrichment increased quickly at the beginning; while after 1 day, the deuteration rate slowed down. This observation indicated that the catalyst was deactivated after a certain period of time, which might be due to the cleavage of C-S bond of the substrate and the resulting sulfur compound poisoned the catalyst. The results also suggested that the H/D exchange occurred at the surface of the catalyst, and the observation that Ru/C purchased from different commercial sources displayed different catalytic activities (see the deuteration of compound **2.4**) also supported a surface catalytic mechanism, since the particle sizes, shapes, surface chemistry and other physical properties of Ru/C might be different from different commercial sources.

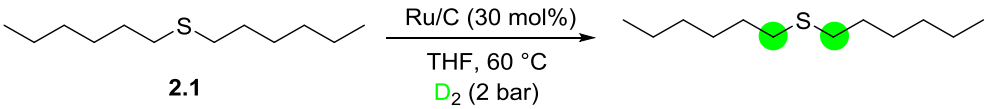

Entry	Reaction time	Isotopic Enrichment
1	0	0%
2	3 h	17%
3	6 h	39%
4	22 h	83%
5	66 h	92%

Table 2.11 Kinetic studies of the deuteration of dihexylsulfide **2.1**

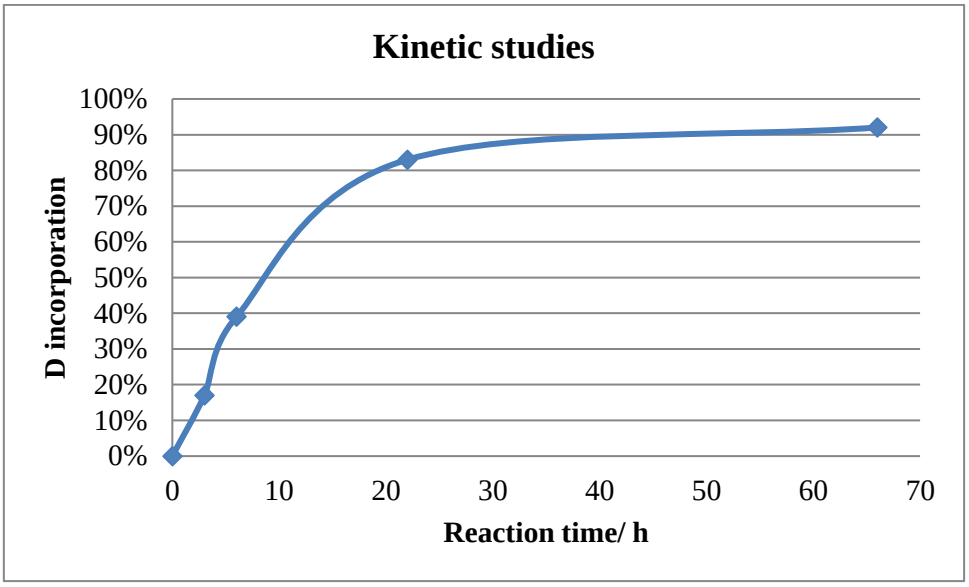

Chart 2.1 Kinetic studies of the deuteration of dihexylsulfide **2.1**

Interestingly, during the course of improving the isotopic enrichment for the application of quantitative LC-MS analysis, when using methionine **2.5** as the substrate, most of the substrate was transformed into compound **2.16** as the side product after conducting the deuteration procedure for a second run (**Scheme 2.4**). The side product was formed through the cleavage of C-S bond of the substrate. This observation could explain the need of relatively large amount of catalyst loading of our reaction procedure, since the methyl sulfide could poison the catalyst and thus block the catalytic cycle. In fact, other substrates that underwent a second run of deuteration (compound **2.6**, **2.7** and **2.9**) also gave the corresponding side products, but only small amount of them were observed. The cleavage of the C-S bond of methionine was much more significant than the other substrates, which might be due

to the strong coordination of both sulfur atom and nitrogen atom, similar to the case for the deuteration of benzthiazide **2.13**, thus slowing down the desorption process and increasing the possibility of C-S bond cleavage.

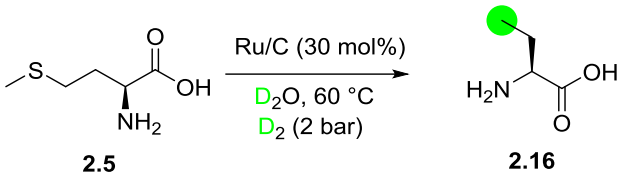

Scheme 2.4 C-S bond cleavage of methionine

Overall, combining the kinetic studies and the observation of side product formation by C-S bond cleavage, the mechanism for the H/D exchange of thioethers could be proposed as follow: first of all, the substrate reversibly coordinated to the surface of the catalyst by the sulfur atom; then the C-H bond adjacent to sulfur atom was activated by ruthenium atom, followed by the H/D exchange at the metal center; finally, the deuterated product was reversibly dissociated by elimination from the metal center and then another catalytic cycle could start (**Scheme 2.5**). According to this proposed mechanism, the mechanism for C-S bond cleavage of methionine was also proposed as shown in **Scheme 2.6**: the reversible coordination of both sulfur atom and nitrogen atom to the surface of the catalyst was the first step; then the C-H bond of the CH_2 group was activated by ruthenium, which was followed by deuterium assisted C-S bond cleavage; the degraded product was formed and then dissociated from the surface of the catalyst.

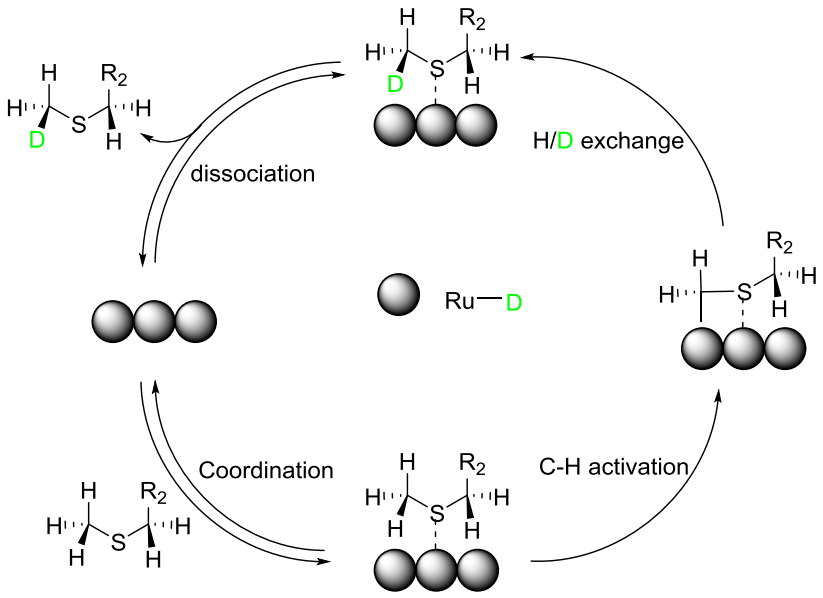

Scheme 2.5 Proposed mechanism for the H/D exchange of thioethers

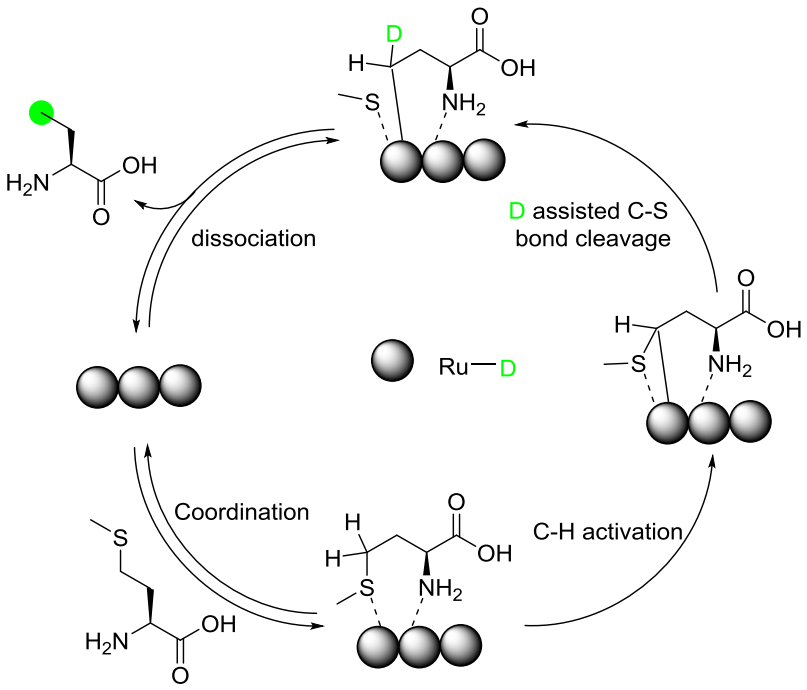

Scheme 2.6 Proposed mechanism for the cleavage of C-S bond

2.5 Summary and perspective

In summary, through the optimization of reaction conditions, we have realized the isotopic labeling of a series of thioethers through H/D exchange reactions. In all cases, high isolated yields were obtained and pure deuterated compounds were recovered after simple filtration to remove the catalyst. Different solvents were tolerated under our reaction conditions, while the choice of appropriate solvent could permit the deuteration process. Different commercial sources of Ru/C were found to have different catalytic activities; the amount of catalyst also had an influence on the deuterium incorporation. Besides, the isotopic enrichment could be improved by repeating deuteration procedures, providing the access to labeled compounds with high isotopic enrichment. Two bioactive compounds, dipeptide **2.7** and pergolide **2.9**, were deuterated with high isotopic enrichments by repeating the deuteration procedure for 3 times and could be used as internal standards for quantitative LC-MS analyses, which provided a simple and practical method for the preparation of internal standards for quantitative LC-MS analyses. Application of our method to tritium labeling was also achieved after optimization of reaction conditions using pergolide **2.9** as the substrate, and a high specific activity of 15.6 Ci/mmol was obtained. The results obtained from the labeling of thioether compounds under optimized reaction conditions were depicted in **Figure 2.9**.

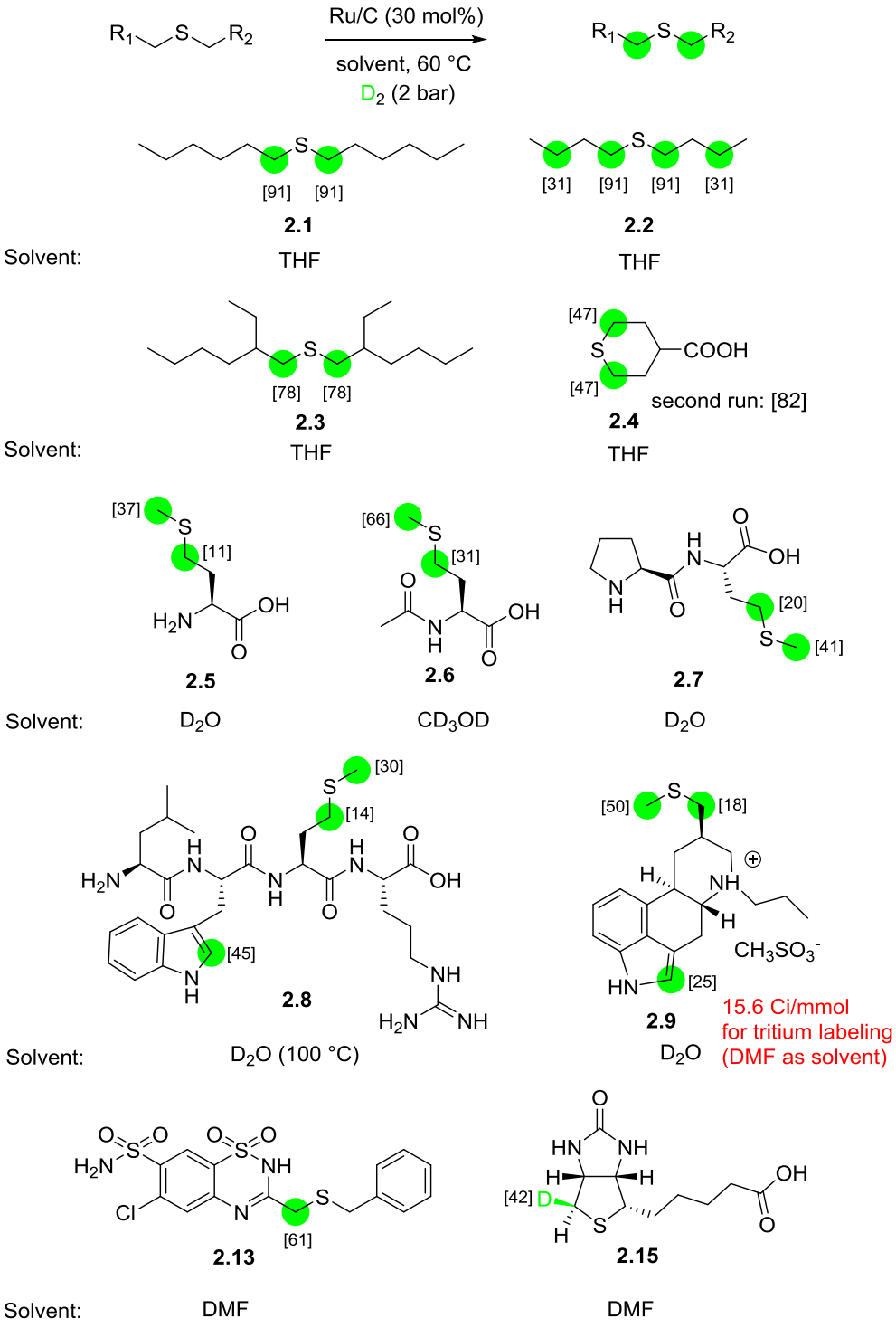

Figure 2.9 Summary of Ru/C catalyzed deuteration of thioethers

Besides the important substrate scope efficiently deuterated using our reaction conditions, there were some substrates that gave no deuteration or quite low deuterium incorporation under our reaction conditions, which were listed in **Figure 2.10**. For compound **2.17**, no deuteration was observed after standard reaction conditions using D_2O as solvent, and all the starting material was recovered after

removing the catalyst by filtration. Total degradation was observed for the labeling of compound **2.18** in D_2O, which might be due to a similar C-S bond cleavage mechanism as methionine **2.5** to give complex results. Albendazole **2.19**, a medication used for the treatment of a variety of parasitic worm infestations, was labeled on the phenyl ring and at the *α*-position of sulfur using THF as solvent at 60 ℃. However, the isotopic enrichment was low, perhaps due to the competition of coordination between the sulfur atom, the nitrogen atom and the carbamoyl group to the surface of the catalyst. No deuterium incorporation was observed when using peptide **2.20** as the substrate in D_2O at 55 ℃, while a small amount of deuterium incorporation (0.47 D) was observed by MS when the reaction was conducted at 100 ℃. Similarly, peptide **2.21** was not deuterated in D_2O at 55 ℃, while a detectable amount of deuterium incorporation was observed when the reaction was conducted at 100 ℃ (**Figure 2.10**). The reason that peptides **2.20** and **2.21** couldn't be labeled at a lower temperature might be due to the steric effect of the molecules or the coordination of other functional groups such as the amine group to the surface of the catalyst.

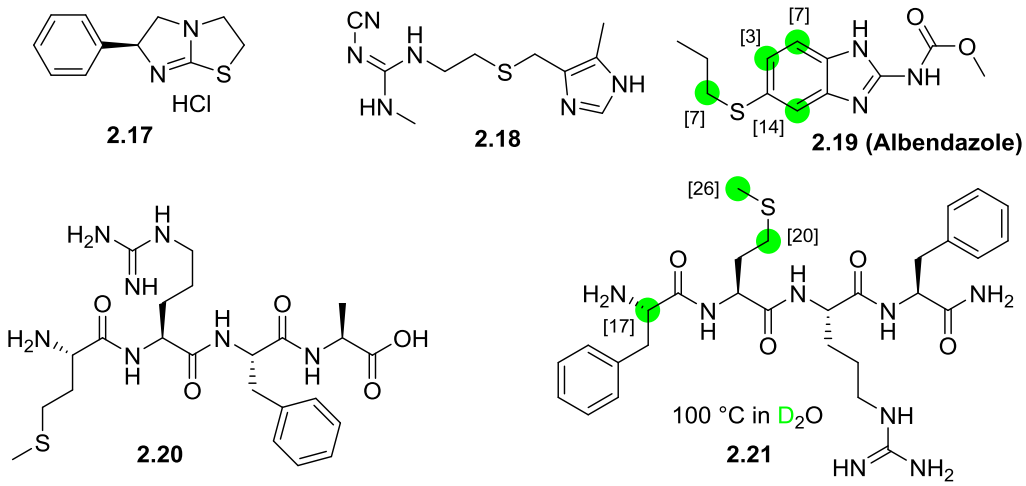

Figure 2.10 Substrate limitation of our method

In perspective, our future work will concentrate on the detailed mechanism of this H/D exchange process, by combination of computational studies and experimental studies. Moreover, deep investigation for the mechanism of the cleavage of C-S bond will be explored as well as more examples for tritium labeling. Besides, we are trying to find new catalysts allowing the efficient deuteration of thioethers with a lower catalyst loading and without the cleavage of C-S bonds.

2.6 Exploring the catalytic activities of different kinds of ruthenium catalysts

As we observed the robust catalytic activity of Ru/C in the deuteration reactions of sulfur containing compounds, we wanted to explore the catalytic activities of different kinds of ruthenium catalysts in order to further investigate the C-H activation reactions. In this context, we studied the catalytic activities of different ruthenium catalysts on H/D exchange reactions using 2,4-lutidine **2.6.1** as the substrate (**Chart 2.2**). The H/D exchange was conducted using 0.2 mmol of substrate with 5 mol% ruthenium catalyst and THF as solvent under 2 bar of D_2 gas at room temperature. As shown in **Chart 2.2**, both Ru/C and RuNp@PVP gave high deuterium incorporation at position 1 of the labeled product, while Ru/C also deuterated the 2-methyl group at position 2 with a low isotopic enrichment; Ru/alumina gave only negligible deuteration at position 1, and no deuteration was observed at position 2. Thus, we decided to investigate the influence of D_2 pressure on H/D exchange reactions by using both Ru/C and RuNp@PVP as catalysts for the H/D exchange of this substrate.

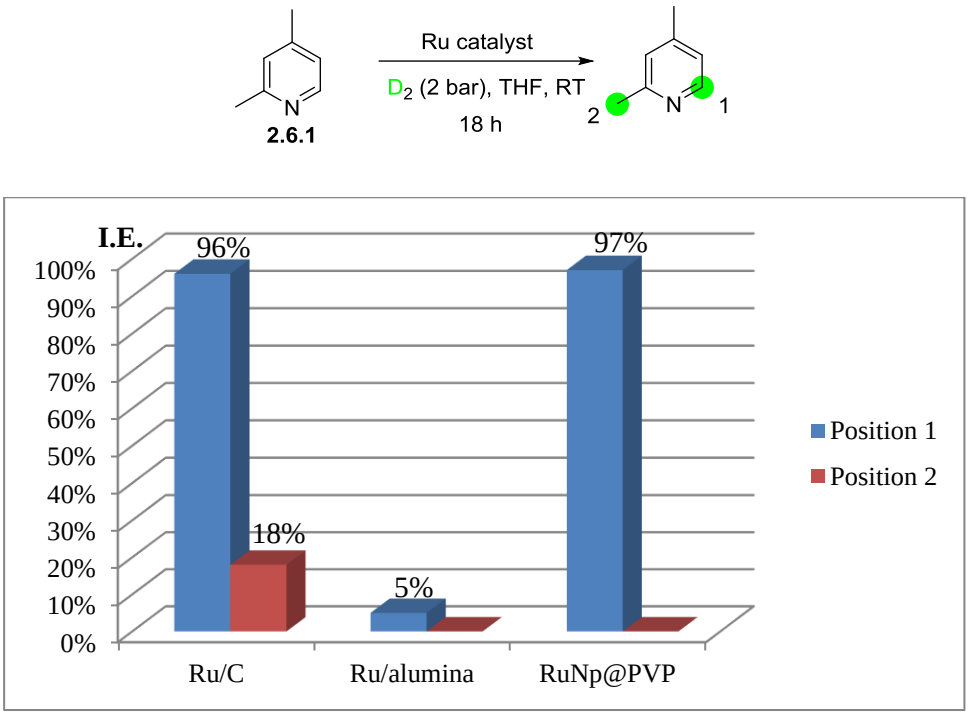

Chart 2.2 The influence of different ruthenium catalysts on the deuteration of 2,4-lutidine

As depicted in **Chart 2.3** and **Chart 2.4**, the H/D exchange reaction was strongly influenced by D_2 pressure. Generally, the isotopic enrichment of the product decreased with the decrease of D_2 pressure. Both RuNp@PVP and Ru/C gave high deuterium incorporation with 2 bar of D_2 gas; however, the catalytic activities of the two catalysts became different with the decrease of D_2 pressure: both catalysts remained active with a D_2 pressure of 1 bar; while RuNp@PVP lost its catalytic activity

when using 0.5 bar of D_2 gas, Ru/C still gave moderate deuterium incorporation under this pressure. It suggested that Ru/C could efficiently activate the C-H bond at position 1 under low D_2 pressure.

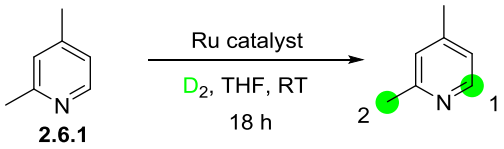

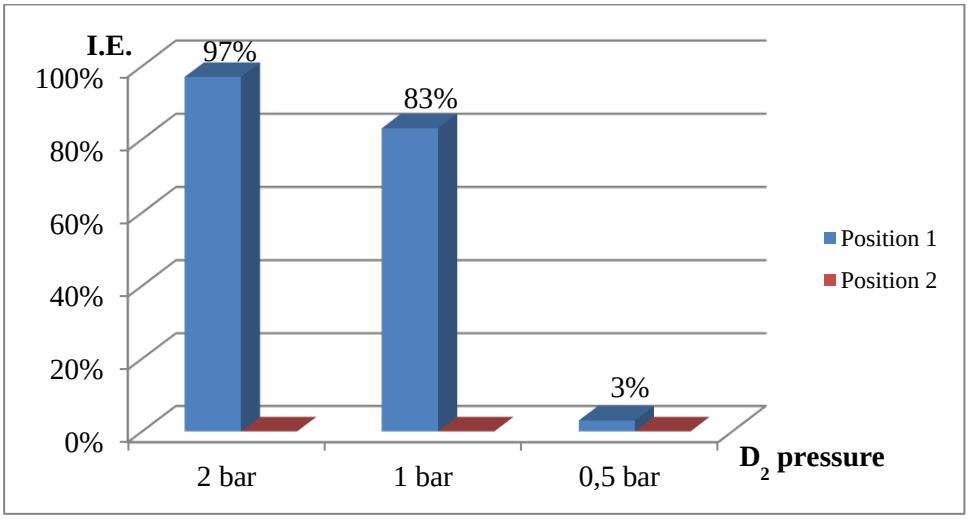

Chart 2.3 The influence of D_2 pressure on the deuteration of 2,4-lutidine catalyzed by RuNp@PVP

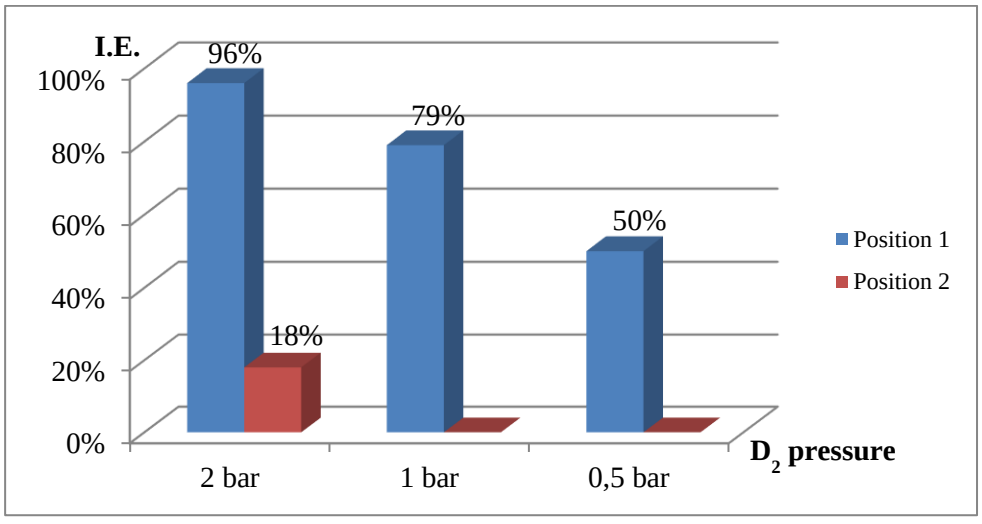

Chart 2.4 The influence of D_2 pressure on the deuteration of 2,4-lutidine catalyzed by Ru/C

In order to check the results we got from the labeling of compound **2.6.1**, we selected four different substrates to investigate their H/D exchange reactions, including pyridine derivative **2.6.2**, indole **2.6.3**,

quinoline **2.6.4** and alkyl amine **2.6.5** (**Figure 2.11**), because these substrates represented a large number of naturally occurring bioactive compounds. Different ruthenium catalysts were employed for the H/D exchange of these compounds under different D_2 pressures.

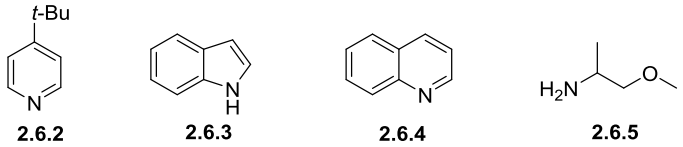

Figure 2.11 Substrates used in the H/D exchange reactions

For the labeling of compound **2.6.2**, the desired *ortho*-deuterated product **P1** was obtained together with small amount of the reduced product **P2** when using RuNp@PVP and Ru/C as catalyst (**Table 2.12**, Entries 1-4). With a D_2 pressure of 2 bar, both RuNp@PVP and Ru/C gave high deuterium incorporation of the desired product **P1**, while Ru/C gave a higher ratio of reduced product **P2**. The isotopic enrichment of **P1** and the ratio of **P2** both decreased with a lower D_2 pressure of 0.5 bar. Interestingly, when using tin-decorated ruthenium nanoparticle Ru-SnNp@PVP as catalyst,[55] the labeled product **P1** was obtained as the only product, although the isotopic enrichment was lower (**Table 2.12**, Entries 5 and 6). Besides, Ru-SnNp@PVP displayed different catalytic activity compared with RuNp@PVP and Ru/C: its catalytic activity was slightly improved when using a lower D_2 pressure. These results suggested that the surface chemistry of Ru-SnNp@PVP was quite different compared with RuNp@PVP, which might be due to the modification of active sites on the ruthenium nanoparticles by tin, and it might have new catalytic activity for C-H activation reactions.

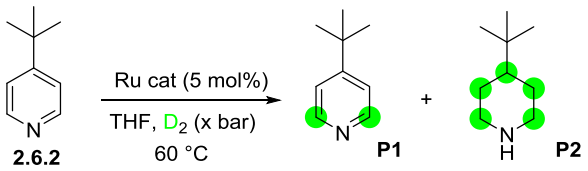

Entry	Ru cat	x bar	D incorporation (**P1**)	**P1** :**P2**
1	RuNp@PVP	2	99%	6.90 :1
2	RuNp@PVP	0.5	-[a]	-
3	Ru/C	2	98%	1.05 :1
4	Ru/C	0.5	20%	16 :1
5	Ru-SnNp@PVP	2	30%	100% **P1**
6	Ru-SnNp@PVP	0.5	37%	100% **P1**

[a]: crude product was removed by vacuum.

Table 2.12 H/D exchange of 4-*tert*-butylpyridine

Indole **2.6.3** was labeled at three positions: C1 position (position 1) and C2 position (position 2) in the pyrrole ring and C6 position (position 3) in the benzene ring. The labeling of position 1 and position 3 could be attributed to the coordination of nitrogen atom to the surface of the catalyst, while the labeling of position 2 could be reasoned by the coordination of pyrrole ring to the ruthenium centers. With a D_2 pressure of 2 bar, both RuNp@PVP and Ru/C deuterated position 1 and position 2 of indole with high isotopic enrichment, while the deuterium incorporation of position 3 was lower (**Table 2.13**, Entries 1 and 3). Trace amount of reduced product **I2** was also observed by LC-MS. These results indicated that the coordination of pyrrole ring to the ruthenium centers was comparable to the coordination of nitrogen to the surface of the catalyst. With a lower D_2 pressure of 0.5 bar, Ru/C displayed a stronger catalytic activity than RuNp@PVP (**Table 2.13**, Entries 2 and 4), suggesting that Ru/C could catalyze the H/D exchange reactions at lower D_2 pressure. Tin-decorated ruthenium nanoparticle Ru-SnNp@PVP displayed unique catalytic activity for the labeling of indole (**Table 2.13**, Entries 5 and 6): no reduced product **I2** was observed with the use of 2 bar D_2 pressure, although the isotopic enrichment of labeled product **I1** was lower; no labeling was observed at position 3, indicating that the coordinating mode was probably different; decreasing the D_2 pressure to 0.5 bar also decreased the isotopic enrichment at position 1, but the isotopic enrichment at position 2 was increased significantly, indicating that at lower D_2 pressure, pyrrole was easier to coordinate to the ruthenium centers than nitrogen atom.

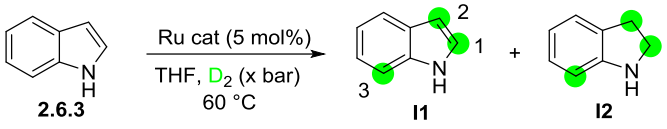

Entry	Ru cat	x bar	D^1 incorporation	D^2 incorporation	D^3 incorporation	**I1** :**I2**
1	RuNp@PVP	2	99%	87%	30%	trace **I2**
2	RuNp@PVP	0.5	57%	14%	0%	100% **I1**
3	Ru/C	2	99%	93%	32%	trace **I2**
4	Ru/C	0.5	100%	70%	4%	trace **I2**
5	Ru-SnNp@PVP	2	61%	5%	0%	100% **I1**
6	Ru-SnNp@PVP	0.5	29%	42%	0%	100% **I1**

Table 2.13 H/D exchange of indole

Quinoline was efficiently deuterated with RuNp@PVP under 2 bar of D_2 gas, providing the desired labeled product **Q1** together with reduced product **Q2** (**Table 2.14**, Entry 1). However, the use of Ru/C as catalyst under 2 bar of D_2 gas gave only reduced product **Q2**, indicating that Ru/C was more active in the reduction (**Table 2.14**, Entry 3). Decreasing the D_2 pressure to 0.5 bar strongly decrease

the isotopic enrichment of **Q1** using RuNp@PVP as catalyst (**Table 2.14**, Entry 2); however, high deuterium incorporation of **Q1** was observed using Ru/C as catalyst under 0.5 bar D_2 (**Table 2.14**, Entry 4), suggesting that Ru/C was more active for H/D exchange reactions at low D_2 pressure. The use of Ru-SnNp@PVP as catalyst gave higher ratio of desired labeled product **Q1** under 2 bar of D_2 gas with high deuterium incorporation at position 1 and moderate deuterium incorporation at position 2 (**Table 2.14**, Entry 5); however, it lost its catalytic activity with lower D_2 pressure of 0.5 bar (**Table 2.14**, Entry 6), indicating that the catalytic activity of Ru-SnNp@PVP was strongly influenced by the D_2 pressure.

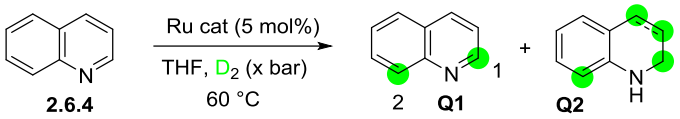

Entry	Ru cat	x	D^1 incorporation	D^2 incorporation	**Q1** :**Q2**
1	RuNp@PVP	2	98%	93%	1 :1.4
2	RuNp@PVP	0.5	14%	0%	100% **Q1**
3	Ru/C	2	-	-	100% **Q2**
4	Ru/C	0.5	91%	73%	1 :1
5	Ru-SnNp@PVP	2	98%	44%	3 :1
6	Ru-SnNp@PVP	0.5	4%	0%	100% **Q1**

Table 2.14 H/D exchange of quinoline

Alkyl amine **2.6.5** was more sensitive to D_2 pressure: with a D_2 pressure of 2 bar, both RuNp@PVP and Ru/C gave high deuterium incorporation of the desired product at the α-position of nitrogen (**Table 2.15**, Entries 1 and 3); however, both catalysts lost their catalytic activity when the D_2 pressure was decreased to 0.5 bar (**Table 2.15**, Entries 2 and 4). These results suggested that the activation of $C(sp^3)$-H bond was more difficult than the activation of $C(sp^2)$-H bond. The use of Ru-SnNp@PVP gave low deuterium incorporation even with high D_2 pressure of 2 bar (**Table 2.15**, Entry 5), indicating that this catalyst hardly activated the $C(sp^3)$-H bond. Thus, there was no need to conduct the reaction under a lower D_2 pressure.

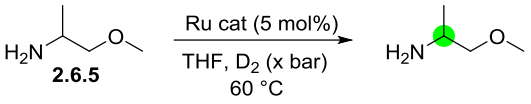

Entry	Ru cat	x bar	D incorporation
1	RuNp@PVP	2	93%
2	RuNp@PVP	0.5	0%
3	Ru/C	2	90%
4	Ru/C	0.5	5%
5	Ru-SnNp@PVP	2	10%

Table 2.15 H/D exchange of alkyl amine **2.5**

From the H/D exchange of compounds **2.6.1** to **2.6.5**, we can conclude that: 1) the D_2 pressure is a key parameter in the H/D exchange reactions, the use of 2 bar of D_2 gas is suitable to obtain deuterated product with high isotopic enrichment in most cases; 2) RuNp@PVP is more selective than Ru/C with a D_2 pressure of 2 bar, while Ru/C tend to produce more reduced product; 3) Ru/C is more active than RuNp@PVP under low D_2 pressure; 4) Ru-SnNp@PVP has unique catalytic activity compared with RuNp@PVP, which has a better selectivity for H/D exchange reactions in most cases, while the activity is usually weaker; 5) the activation of C(sp^3)-H bond is more difficult than the activation of C(sp^2)-H bond, and it requires relatively higher D_2 pressure to achieve high deuterium incorporation for RuNp@PVP and Ru/C.

Based on the results above and the previous studies about the H/D exchange reactions,[29, 46j] we decided to explore more C-H activation reactions based on Ru/C, because it has good catalytic activity towards C-H bond activation, and it is commercially available and relatively cheap compared with other transition metal complexes. Besides, it is easy to remove Ru/C from the reaction mixture after reaction using a simple filtration. In fact, Ru/C has already been used as catalyst for several transformations: deuteration of alcohols[68] and sugars,[69] oxidation of alcohols[70] and amides,[71] oxidative cyclization,[72] hydrogenation[73] and coupling reactions.[74] These results indicate that Ru/C has potential catalytic

[68] T. Maegawa, Y. Fujiwara, Y. Inagaki, Y. Monguchi, H. Sajiki, *Adv. Synth. Catal.* **2008**, *350*, 2215.

[69] a) Y. Fujiwara, H. Iwata, Y. Sawama, Y. Monguchi, H. Sajiki, *Chem. Commun.* **2010**, *46*, 4977; b) Y. Sawama, Y. Yabe, H. Iwata, Y. Fujiwara, Y. Monguchi, H. Sajiki, *Chem. Eur. J.* **2012**, *18*, 16436.

[70] S. Mori, M. Takubo, K. Makida, T. Yanase, S. Aoyagi, T. Maegawa, Y. Monguchi, H. Sajiki, *Chem. Commun.* **2009**, *45*, 5159.

[71] S.-I. Murahashi, T. Naota, T. Kuwabara, T. Saito, H. Kumobayashi, S. Akutagawa, *J. Am. Chem. Soc.* **1990**, *112*, 1820.

[72] T. M. Gädda, X.-Y. Yu, A. Miyazawa, *Tetrahedron* **2010**, *66*, 1249.

[73] a) H. Wan, A. Vitter, R. V. Chaudhari, B. Subramaniam, *J. Catal.* **2014**, *309*, 174; b) Y. J. Kim, J. H. Lee, V. T. Widyaya, H. S. Kim, H. Lee, *Bull. Korean Chem. Soc.* **2014**, *35*, 1117.

[74] a) S. Imoto, T. Uemura, F. Kakiuchi, N. Chatani, *Synlett* **2007**, 170 ; b) K. H. V. Reddy, G. Satish, V. P. Reddy, B. S. P. A. Kumar, Y. V. D. Nageswar, *RSC Adv.* **2012**, *2*, 11084; c) K. H. V. Reddy, B. S. P. A. Kumar, V. P. Reddy, R. U. Kumar, Y. V. D. Nageswar, *RSC Adv.* **2014**, *4*, 45579.

activities towards many types of reactions. In this context, some experiments were conducted to examine the potential catalytic activities of Ru/C, and the results will be shown in Chapter 2.

3 Experimental section

3.1 Reagents and General Procedures

All operations were carried out in a Fischer-Porter glassware. Commercially available substrates were used without further purification. Ru/C was purchased from Aldrich, Alfa Aesar and Strem Chemicals Inc. and used as received. THF was dried over sodium and benzophenone, distilled and then thoroughly degassed before use. DMF anhydrous was purchased from Aldrich and used without further purification. ^{1}H NMR (400 MHz), ^{13}C NMR (100 MHz) spectra were recorded on a Bruker Avance 400 MHz spectrometer. Chemical shifts are reported in parts per million (ppm) downfield from residual solvent peaks and coupling constants are reported in Hertz (Hz). Splitting patterns are designated as singlet (s), doublet (d), triplet (t). Splitting patterns that could not be interpreted or easily visualized are designated as multiplet (m). Electrospray mass spectra were recorded using an ESI/TOF Mariner Mass Spectrometer. Optical rotations were measured using a Perkin Elmer Polarimeter 341. Centrifugation was performed on a VWR Galaxy Ministar Mini Centrifuge. Chiral HPLC were recorded using Astec Chirobiotic T chiral column (25 cm × 4.6 mm × 5 μm). Preparative HPLC were recorded using Phenomenex Luna PFP column (15 cm × 21.2 mm × 5 μm) for compound **2.7** and Waters X-bridge Phenyl column (15 cm × 19 mm × 5 μm) for compound **2.9**.

H/D exchange quantification:

Deuterium incorporation was quantified by the decrease of ^{1}H NMR integral intensities at the specified positions compared to the starting material. Integral intensities were calibrated against hydrogen signals that do not undergo H/D-exchange. Mass spectrometry quantification was performed by subtraction of the mean molecular masses of the product and substrate isotopologue clusters in order to eliminate the contribution of the natural isotope abundance to the total mass.

General Procedure A for H/D exchanges:

A 93 mL Fischer-Porter glassware was charged with Ru/C (Aldrich, 30 mol%) and a magnetic stirrer under air. The Fischer-Porter glassware was then left under vacuum for 5 min and pressurized with D_2 gas (3 bar) during 2 hours. A solution of the substrate (0.2 mmol) in degassed DMF or THF or D_2O or CD_3OD (2 mL) was added under argon. The reaction mixture was magnetically stirred at 60 °C (sand bath) under pressure of D_2 (2 bar) during 72 hours. The solution was then cooled down to room temperature, filtered through syringe filter and evaporated under vacuum. Deuterated products were obtained mostly in quantitative yield except extra mention.

General Procedure B for H/D exchanges:

A 47 mL Fischer-Porter glassware was charged with Ru/C (Aldrich, 30 mol%) and a magnetic stirrer under air. The Fischer-Porter glassware was then left under vacuum for 5 min and pressurized with D_2 gas (3 bars) during 2 hours. A solution of the substrate (15 mg) in degassed D_2O (1 mL) was added under argon. The reaction mixture was magnetically stirred at 60 °C (sand bath) under pressure of D_2 (2 bar) during 72 hours. The solution was then cooled down to room temperature, filtered through syringe filter and evaporated under vacuum. Deuterated products were obtained mostly in quantitative yield except extra mention.

General Procedure C for H/D exchanges:

Same as General Procedure A, except that the reaction was run for 24 hours. After that, the substrate was filtered, dried and the deuteration procedure was repeated for two more runs. Small amount of side product was observed after the final run of deuteration, so the product was purified by preparative HPLC. The isotopic enrichment was recorded after the purification by ^1H NMR and MS.

3.2 Experimental details and characterization for compounds **2.1** to **2.15'**

Dihexyl sulfide (2.1) :

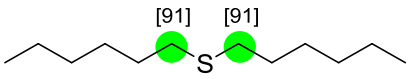

Following the General Procedure A and using THF as solvent. After the final evaporation an ^{1}H NMR spectrum of the residue was recorded.

^{1}H NMR (400 MHz, $CDCl_3$) δ 2.47 (t, J = 7.4 Hz, 0.4H), 1.61-1.48 (m, 4H), 1.46-1.16 (m, 12H), 0.88 (t, J = 6.8 Hz, 6H). ^{13}C NMR (100 MHz, $CDCl_3$) δ 31.5, 29.5, 28.6, 22.6, 14.0.

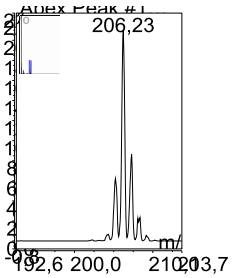

Figure 3.1 GC-MS spectrum of compound **2.1**

Dibutyl sulfide (2.2) :

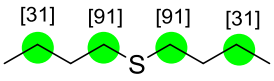

Following the General Procedure A and using THF as solvent. After the final evaporation an ^{1}H NMR spectrum of the residue was recorded.

^{1}H NMR (400 MHz, $CDCl_3$) δ 2.48 (t, J = 7.3 Hz, 0.4H), 1.58-1.50 (m, 4H), 1.45-1.34 (m, 2.8H), 0.91 (t, J = 7.3 Hz, 6H). ^{13}C NMR (100 MHz, $CDCl_3$) δ 31.6, 22.0, 13.7.

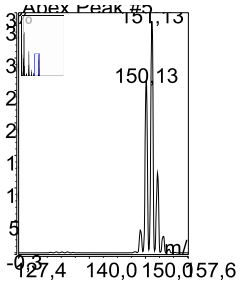

Figure 3.2 GC-MS spectrum of compound **2.2**

Bis(2-ethylhexyl)sulfide (2.3) :

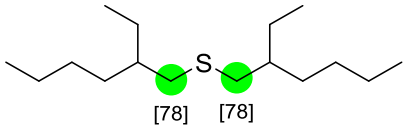

Following the General Procedure A and using THF as solvent. After the final evaporation an ^{1}H NMR spectrum of the residue was recorded.

^{1}H NMR (400 MHz, $CDCl_3$) δ 2.47-2.38 (m, 0.9H), 1.49-1.20 (m, 18H), 0.99-0.72 (m, 12H). ^{13}C NMR (100 MHz, $CDCl_3$) δ 39.2, 37.2, 32.4, 28.9, 25.5, 23.0, 14.1, 10.8.

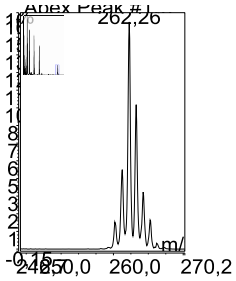

Figure 3.3 GC-MS spectrum of compound **2.3**

Tetrahydro-2*H*-thiopyran-4-carboxylic acid (2.4):

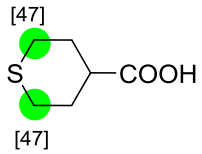

Following the General Procedure A and using THF as solvent. After the final evaporation an ^{1}H NMR spectrum of the residue was recorded. Repeating the reaction with this material (using standard conditions) has led to higher deuterium incorporation (82%, product **2.4'**).

2.4: ^{1}H NMR (400 MHz, CD_3OD) δ 2.76-2.60 (m, 2.1H), 2.41 (tt, J = 11.0, 3.3 Hz, 1H), 2.28-2.17 (m, 2H), 1.87-1.73 (m, 2H). ^{13}C NMR (100 MHz, CD_3OD) δ 178.8, 43.7, 31.3, 28.5.

2.4': ^{1}H NMR (400 MHz, CD_3OD) δ 2.73-2.60 (m, 0.7H), 2.41 (tt, J = 11.0, 3.4 Hz, 1H), 2.28-2.15 (m, 2H), 1.88-1.71 (m, 2H). ^{13}C NMR (100 MHz, CD_3OD) δ 178.8, 43.7, 31.3.

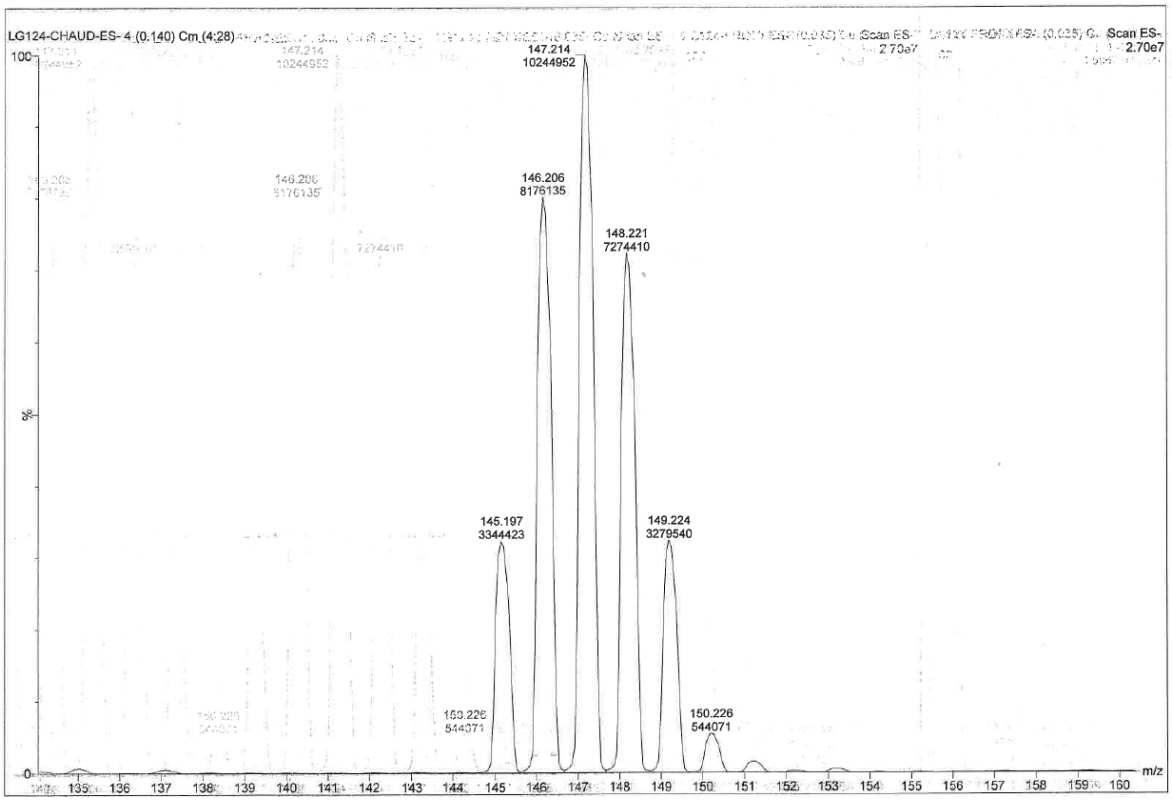

Figure 3.4 LC-MS spectrum of compound **2.4**

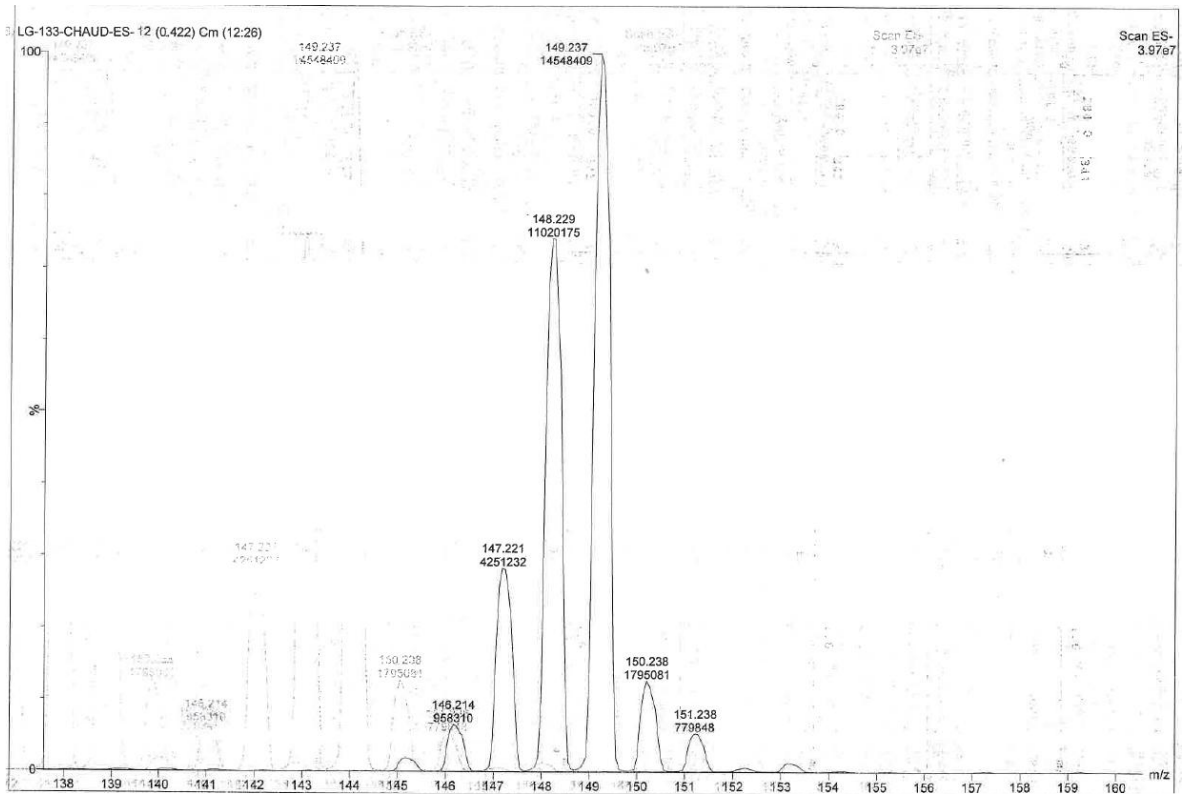

Figure 3.5 LC-MS spectrum of compound **2.4'**

L-Methionine (2.5) :

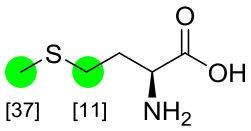

Following the General Procedure A and using D_2O as solvent. After the final evaporation an ^1H NMR spectrum of the residue was recorded.

^1H NMR (400 MHz, D_2O) δ 3.85 (t, J = 6.1 Hz, 1H), 2.62 (t, J = 7.3 Hz, 1.8H), 2.25-2.02 (m, 3.9H).
^{13}C NMR (100 MHz, D_2O) δ 174.3, 53.9, 29.7, 28.7, 13.9.

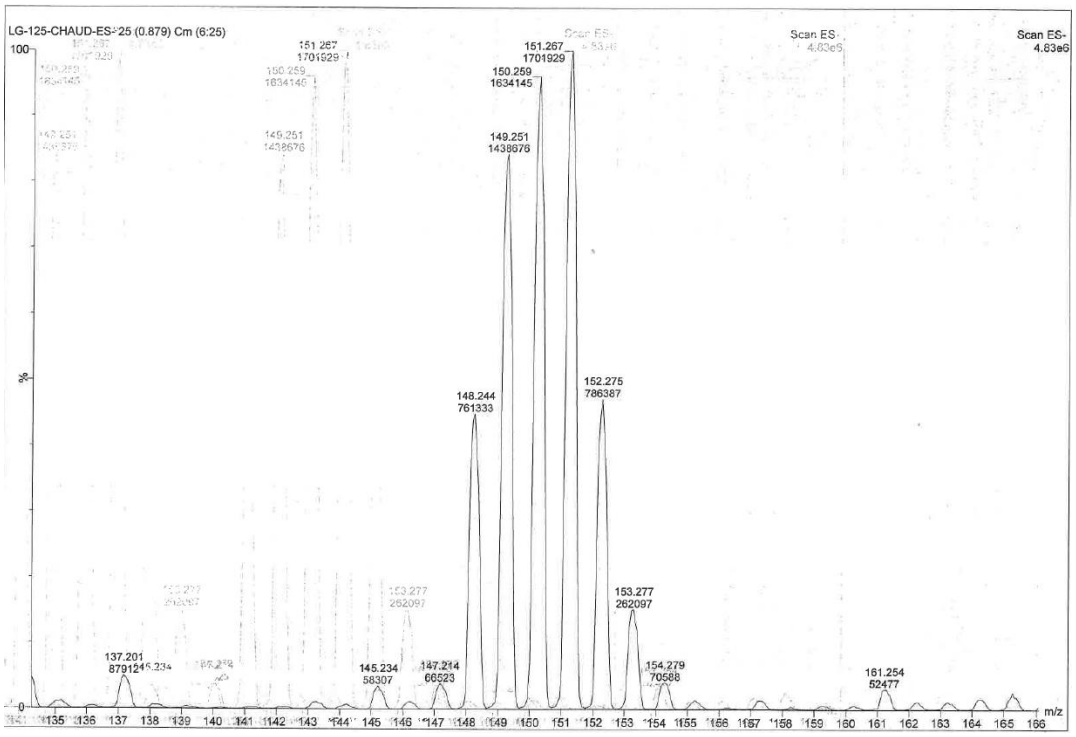

Figure 3.6 LC-MS spectrum of compound **2.5**

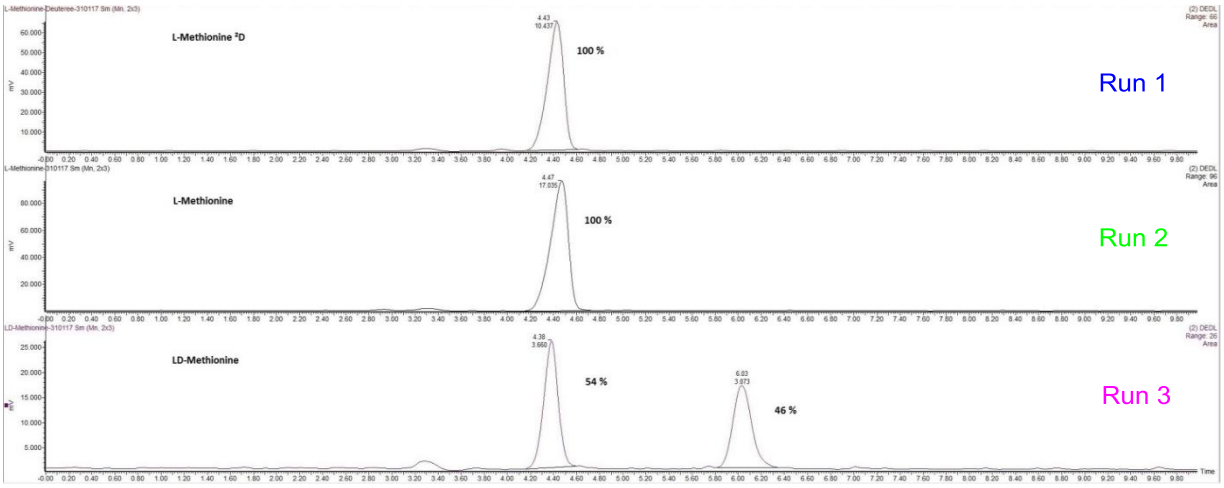

Figure 3.7 Chiral HPLC analysis of compound **2.5**

1.1.1

Run	Substrate	L-Methionine	D-Methionine
1	Deuterated L-methionine	100%	0%
2	L-Methionine	100%	0%
3	D,L-Methionine	54%	46%

Conditions :

Column : Astec Chirobiotic T n °89930-02 250mm*4.6mm*5 µm

Eluent : Iso30 15min (H_2O / MeOH / HCOOH; 30 / 70 / 0.2)

Debit : 1mL/min

Temperature : Room temperature

Injection : 20 µL

Acetyl-L-methionine (2.6) :

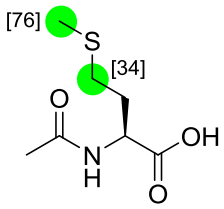

2.6

Following the General Procedure A and using CD_3OD as solvent. After the final evaporation an ^1H NMR spectrum of the residue was recorded.

^1H NMR (400 MHz, CD_3OD) δ 4.53 (dd, J = 9.0, 4.6 Hz, 1H), 2.65-2.48 (m, 1.3H), 2.20-2.06 (m, 1.7H), 2.05-1.91 (m, 4H). ^{13}C NMR (100 MHz, CD_3OD) δ 175.8, 173.5, 53.3, 32.6, 31.2, 22.6, 15.3.

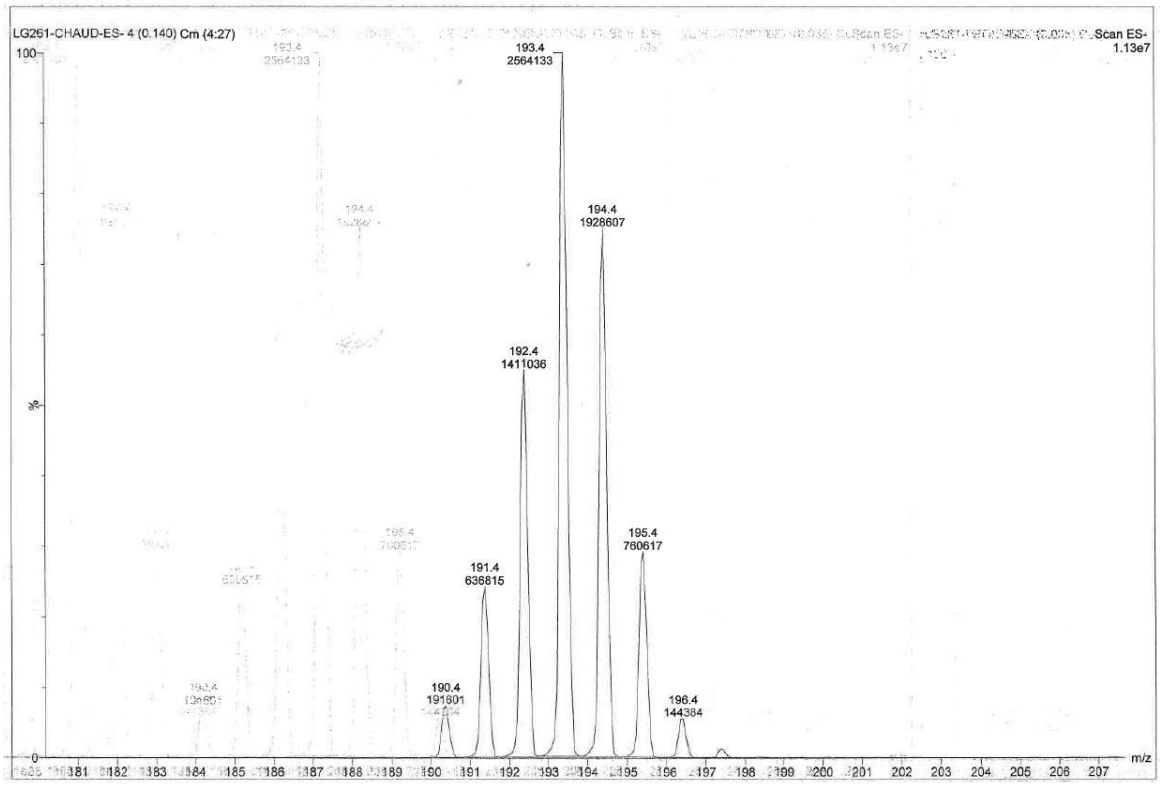

Figure 3.8 LC-MS spectrum of compound **2.6**

H-Pro-Met-OH (2.7):

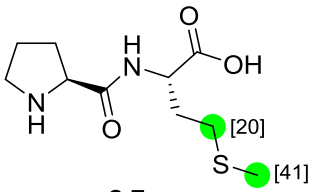

2.7a

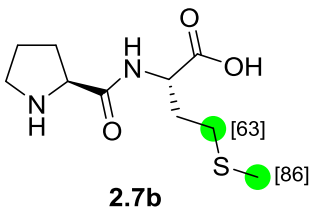

2.7b

Following the General Procedure B for **2.7a** and General Procedure C for **2.7b** using D_2O as solvent. After the final evaporation an ^1H NMR spectrum of the residue was recorded.

Conditions for preparative HPLC:

Column : Phenomenex Luna PFP 150*21.2 mm*5µm

Eluent : A : H_2O + 0.1% HCOOH; B : MeOH + 0.1% HCOOH

t(min)	%A	%B
0	95	5
24	80	20
25	0	100
30	0	100
30.1	95	5
35	95	5

2.7a: ^1H NMR (400 MHz, D_2O) δ 4.38 (dd, J = 8.4, 7.0 Hz, 1H), 4.26 (dd, J = 8.9, 4.7 Hz, 1H), 3.52-3.27 (m, 2H), 2.64-2.39 (m, 2.6H), 2.19-1.90 (m, 6.8H). ^{13}C NMR (100 MHz, D_2O) δ 178.0, 169.0, 59.8, 54.9, 46.5, 30.7, 29.7, 29.6, 23.8, 14.1.

2.7b: ^1H NMR (400 MHz, D_2O) δ 4.39 (dd, J = 8.4, 7.0 Hz, 1H), 4.28 (dd, J = 8.9, 4.7 Hz, 1H), 3.51-3.31 (m, 2H), 2.62-2.41 (m, 1.8H), 2.20-1.90 (m, 5.4H).

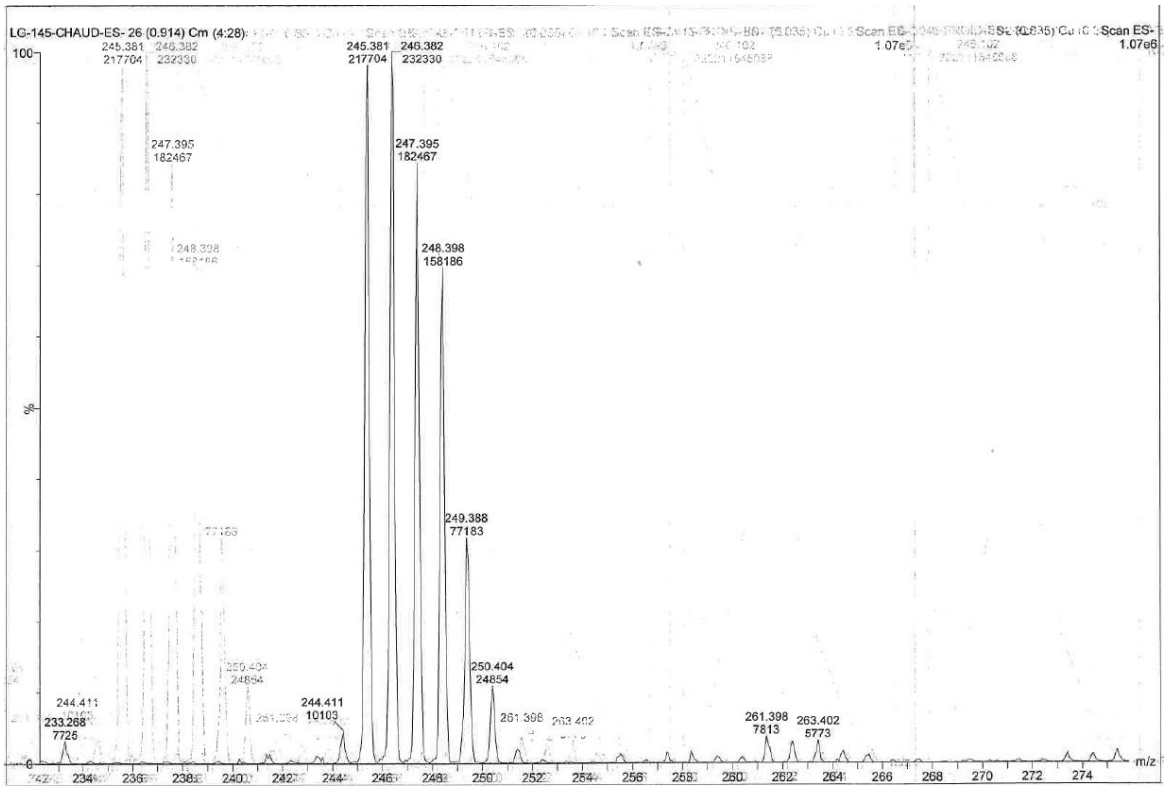

Figure 3.9 LC-MS spectrum of compound **2.7a**

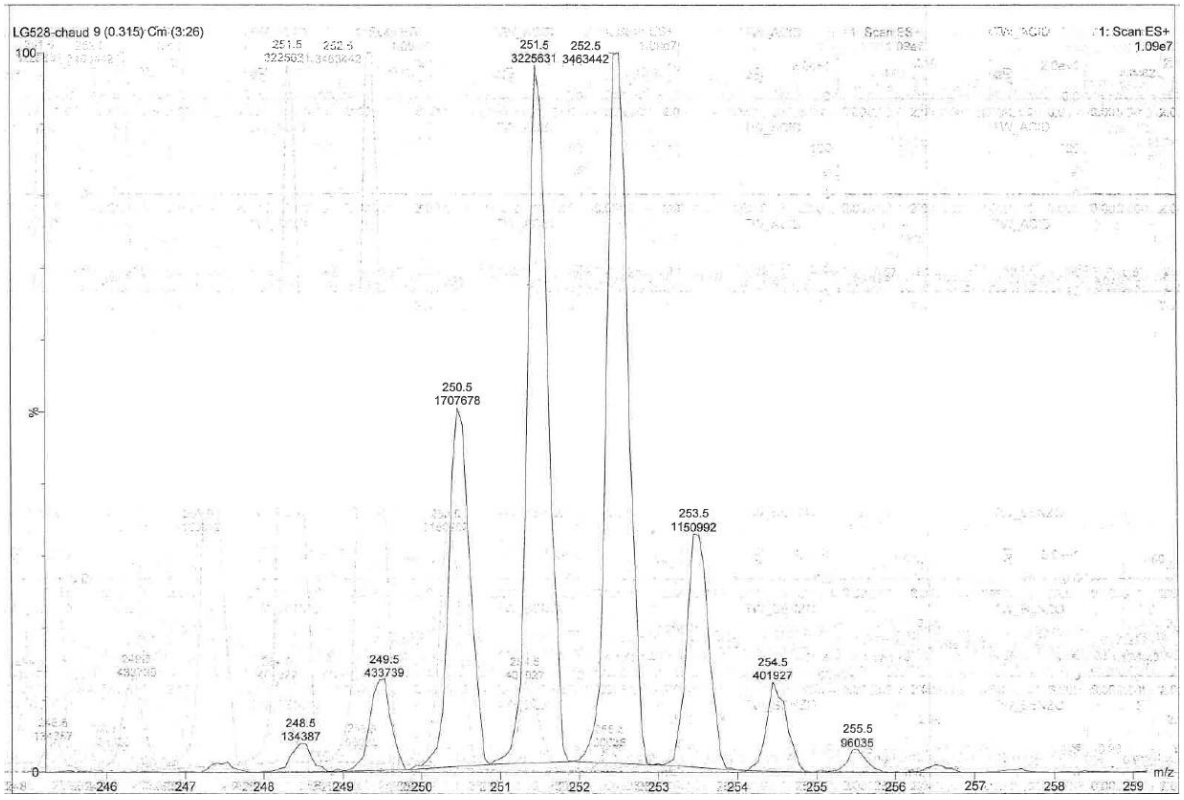

Figure 3.10 LC-MS spectrum of compound **2.7b**

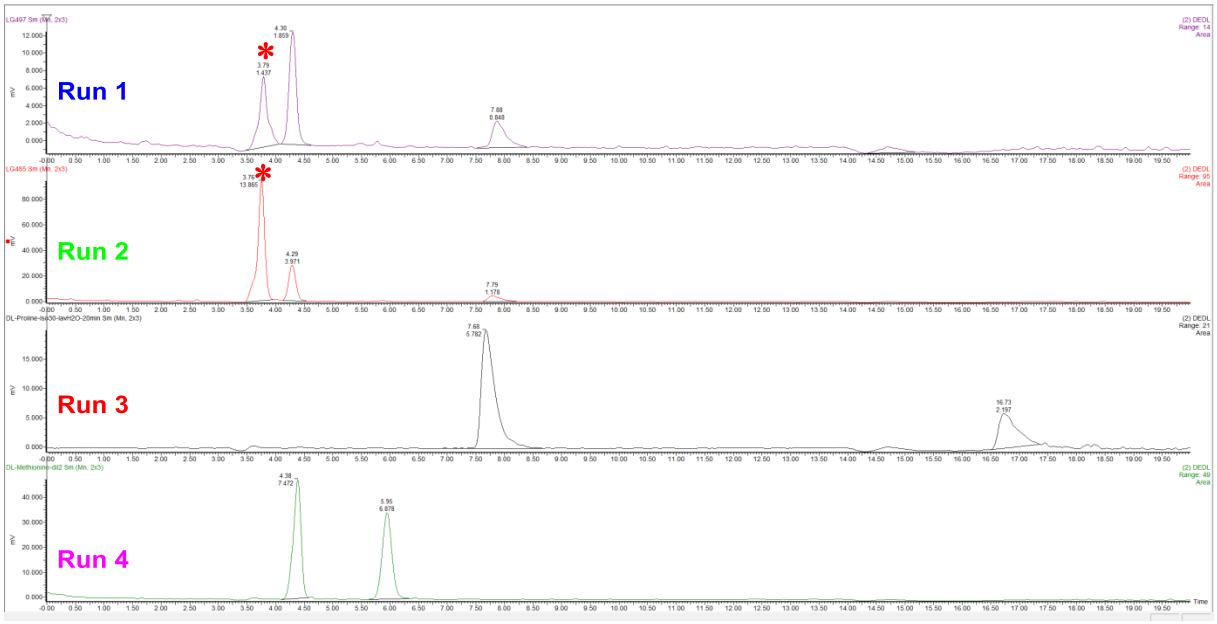

Figure 3.11 Chiral HPLC analyses of the amino acids obtained from the hydrolysis of compound **2.7a**

Run 1	Amino acids obtained from the hydrolysis of **2.7a**, only deuterated L-methionine and L-proline were detected
Run 2	Amino acids obtained from the hydrolysis of unlabeled **2.7**, only L-methionine and L-proline were detected
Run 3	D,L-Proline, the peak on the left is L-proline
Run 4	D,L-Methionine, the peak on the left is L-methionine

*Peak of unknown compound related to the polymerization of the peptide.

Conditions :

Column : Astec Chirobiotic T n °89930-02 250mm*4.6mm*5 µm

Eluent : Iso30 10min (H_2O / MeOH / HCO_2H; 30 / 70 / 0,2) + lavage 100 % H_2O 5min

Debit : 1mL/min

Temperature : Room temperature

Injection : 10 µL

H-Leu-Trp-Met-Arg-OH (2.8):

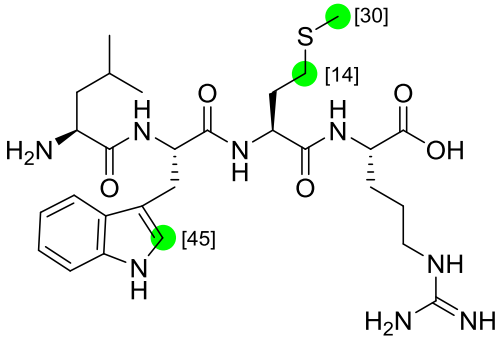

Following the General Procedure B and using D_2O as solvent. After the final evaporation an ^1H NMR spectrum of the residue was recorded. Note that the reaction was conducted at 100 ℃.

^1H NMR (400 MHz, D_2O) δ 7.57 (d, J = 7.9 Hz, 1H), 7.44 (d, J = 8.1 Hz, 1H), 7.22 (s, 0.6H), 7.19 (t, J = 7.9 Hz, 1H), 7.10 (t, J = 7.5 Hz, 1H), 4.67 (t_{app}, J = 7.8 Hz, 1H), 4.31 (dd, J = 8.4, 5.5 Hz, 1H), 4.05-3.92 (m, 2H), 3.26-3.17 (m, 2H), 3.13-3.04 (m, 2H), 2.45-2.29 (m, 1.7H), 2.03-1.97 (m, 2.1H), 1.96-1.87 (m, 1H), 1.85-1.71 (m, 2H), 1.68-1.55 (m, 4H), 1.53-1.44 (m, 2H), 0.89 (t, J = 6.8 Hz, 6H). ^{13}C NMR (100 MHz, D_2O) δ 172.5, 172.0 (s, 2C), 170.0, 156.7, 136.0, 126.8, 124.3, 121.9, 119.3, 118.2, 111.9, 108.6, 54.8, 52.2, 51.7, 40.5, 39.9, 30.6, 28.9, 27.9, 26.8, 24.4, 23.8, 21.7 (s, 2C), 21.2, 14.1.

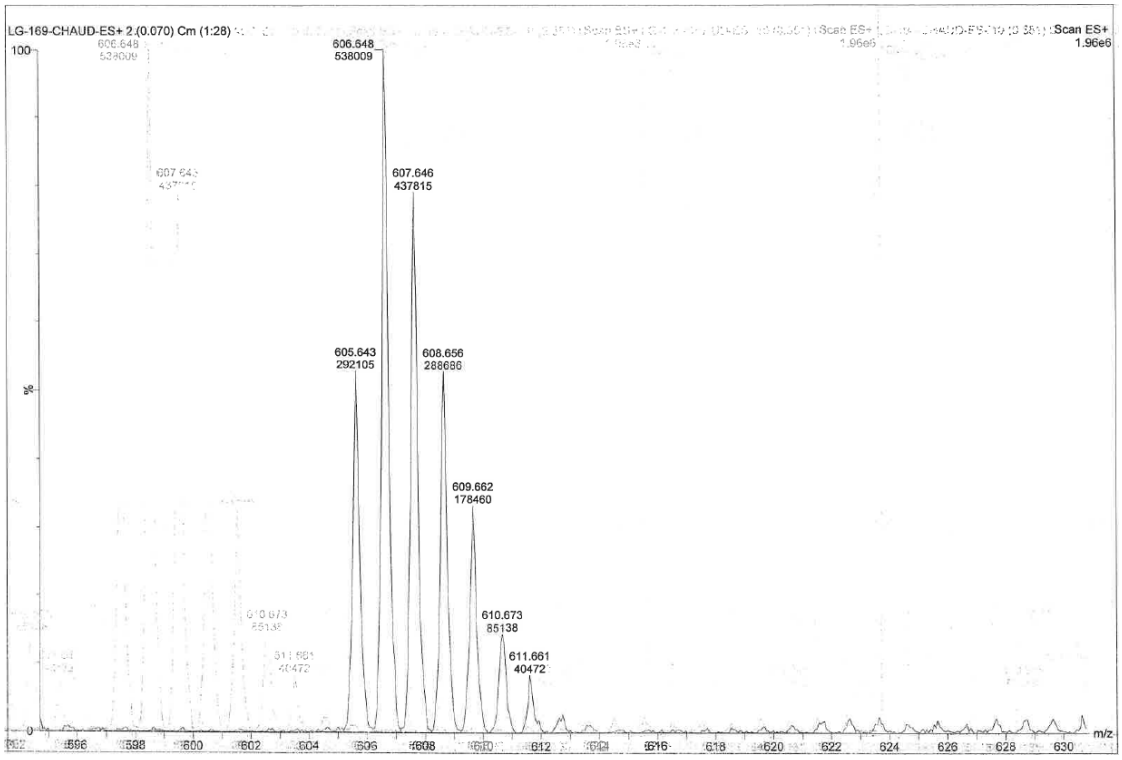

Figure 3.12 LC-MS spectrum of compound **2.8**

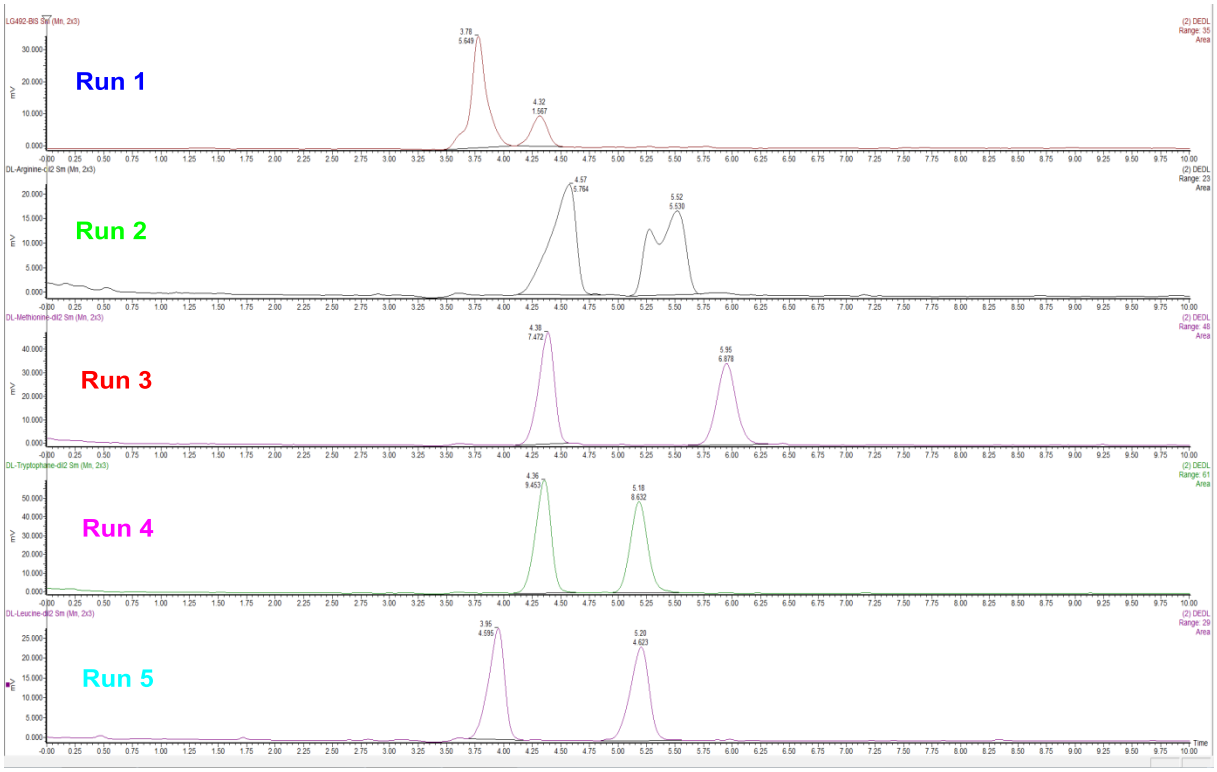

Figure 3.13 Chiral HPLC analyses of the amino acids obtained from the hydrolysis of compound **2.8**

Run 1	Amino acids obtained from the hydrolysis of **2.8**, only L-amino acids were obtained
Run 2	D,L-Arginine, the peak on the left is L-arginine
Run 3	D,L-Methionine, the peak on the left is L-methionine
Run 4	D,L-Tryptophane, the peak on the left is L-tryptophane
Run 5	D,L-Leucine, the peak on the left is L-leucine

Conditions :

Column : Astec Chirobiotic T n °89930-02 250mm*4.6mm*5 µm

Eluent : Iso30 10min (H_2O / MeOH / HCO_2H; 30 / 70 / 0,2) + lavage 100 % H_2O 5min

Debit : 1mL/min

Temperature : Room temperature

Injection : 10 µL

Pergolide (2.9):

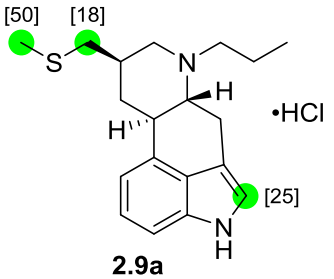

2.9a

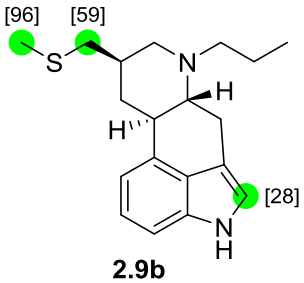

2.9b

Following the General Procedure B for **2.9a** using D_2O as solvent and General Procedure C for **2.9b** using D_2O as solvent. Note that the starting compound was pergolide mesylate.

In order to better analyze the result, the product **2.9a** was transformed into hydrochloride salt. After evaporation the crude product was dissolved in ethyl acetate and aqueous Na_2CO_3 was added. The mixture was stirred for 15 min and extracted with ethyl acetate. Then organic layer was dried over $MgSO_4$, evaporated to dryness and dissolved in THF and HCl (1M, 1 mL). After 30 min of stirring, the solution was evaporated to afford a brown solid (12 mg, 91% yield). Before deuteration $[\alpha]_D^{20}$ -31.0 °(*c* 0.1, CH_3OH), after deuteration $[\alpha]_D^{20}$ -30.0 °(*c* 0.1, CH_3OH).

Product **2.9b** was obtained after repeating the deuteration procedure for 3 times, and the crude product was purified by preparative HPLC to give pure **2.9b**.

Conditions for preparative HPLC:

Column : Waters X-bridge Phenyl 150*19mm*5 µm

Eluent : A : H_2O + 0.1% HCOOH; B : MeCN + 0.1% HCOOH

t(min)	%A	%B
0	95	5
24	60	40
25	0	100
30	0	100
30.1	95	5
35	95	5

2.9a: ^{1}H NMR (400 MHz, CD_3OD) δ 7.25 (d, *J* = 8.1 Hz, 1H), 7.15 (t, *J* = 7.6 Hz, 1H), 7.08 (s, 0.75H), 6.95 (d, *J* = 7.1 Hz, 1H), 3.83 (d, *J* = 10.8 Hz, 1H), 3.70 (dd, *J* = 14.2, 3.2 Hz, 1H), 3.53-3.36 (m, 4H), 3.11-2.92 (m, 3H), 2.75 (dd, *J* = 13.5, 6.0 Hz, 0.8H), 2.62 (dd, *J* = 13.5, 7.8 Hz, 0.8H), 2.43 (br s, 1H), 2.28-2.16 (m, 1.5H), 1.98-1.76 (m, 2H), 1.54-1.41 (m, 1H), 1.13 (t, *J* = 7.3 Hz, 3H). ^{13}C NMR (100

MHz, CD_3OD) δ 135.9, 131.2, 127.5, 124.7, 121.2, 114.8, 111.6, 109.1, 67.6, 58.5, 55.7, 39.1, 34.2, 31.7, 26.8, 18.4, 17.4, 16.9, 12.1.

2.9b: ^1H NMR (400 MHz, CD_3OD) δ 7.23 (d, J = 8.1 Hz, 1H), 7.14 (t, J = 7.6 Hz, 1H), 7.05 (s, 0.8H), 6.94 (d, J = 7.1 Hz, 1H), 3.74 (d, J = 11.7 Hz, 1H), 3.67-3.58 (m, 1H), 3.45-3.22 (m, 4H), 3.00-2.85 (m, 3H), 2.73 (dd, J = 13.5, 6.0 Hz, 0.6H), 2.60 (dd, J = 13.5, 7.6 Hz, 0.9H), 2.37 (br s, 1H), 2.24-2.16 (m, 0.7H), 1.91-1.75 (m, 2H), 1.47-1.36 (m, 1H), 1.10 (t, J = 7.3 Hz, 3H).

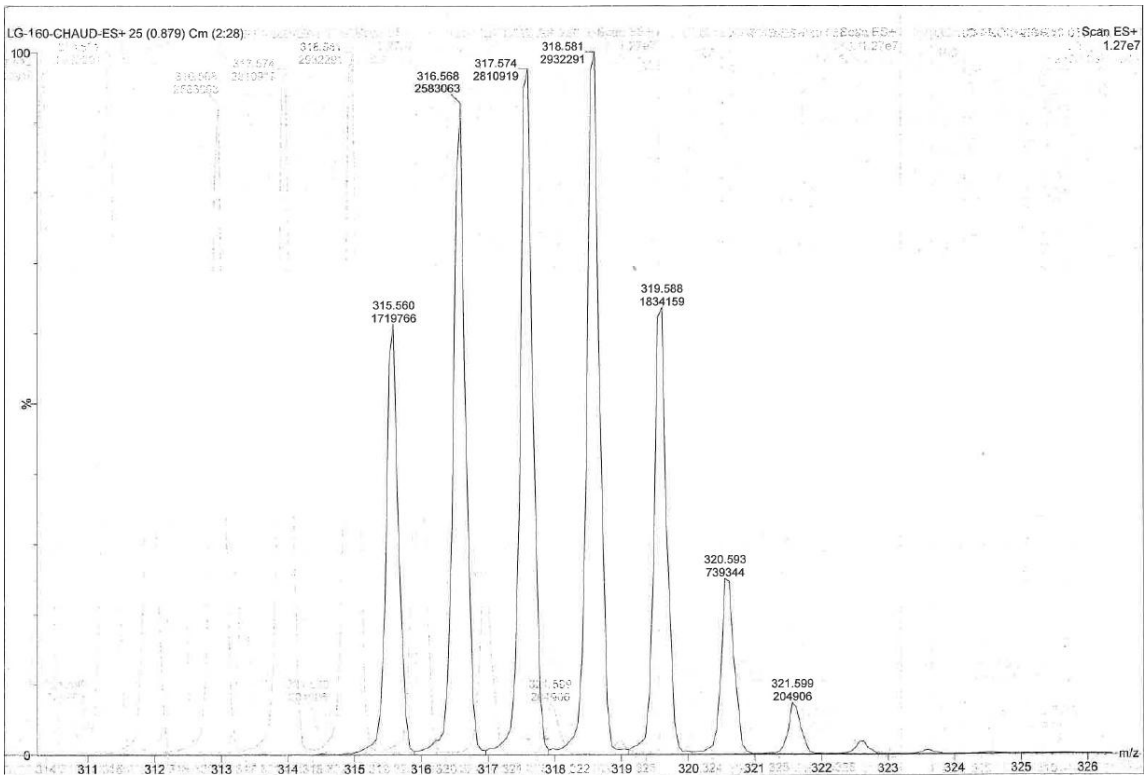

Figure 3.14 LC-MS spectrum of compound **2.9a**

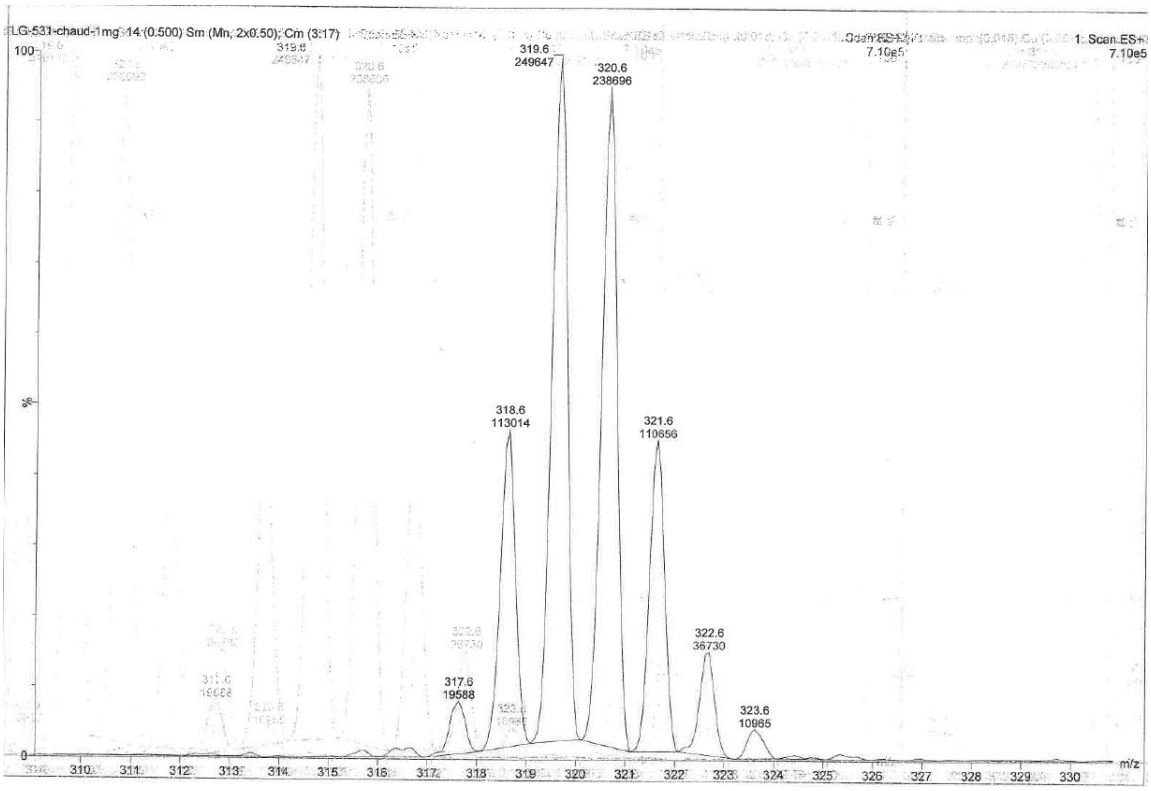

Figure 3.15 LC-MS spectrum of compound **2.9b**

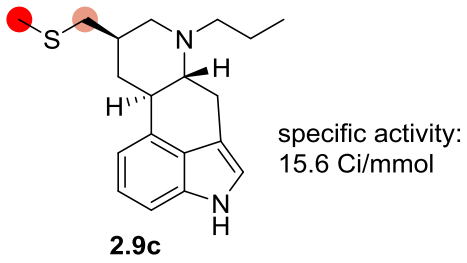

2.9c

Experimental procedure for tritium labeling:

A 5 mL Fischer-Porter glassware with a magnetic stirrer was charged with pergolide mesylate (3.0 mg, 0.0073 mmol), Ru/C (4.4 mg, 30 mol %) and DMF (0.5 mL) under air. The Fischer-Porter glassware was then frozen using a liquid nitrogen bath, left under vacuum for 5 min and then pressurized with T_2 gas (0.9 bar at room temperature). The reaction mixture was magnetically stirred and heated at 80 ℃ (sand bath) overnight. The solution was then cooled down to room temperature, further cooled using a liquid nitrogen bath, the extra T_2 gas was then removed and replaced by N_2. Then the solution was warmed to room temperature and filtered through syringe filter and evaporated under vacuum. The crude product was purified by preparative HPLC and the specific activity was determined on purified product **2.9c**.

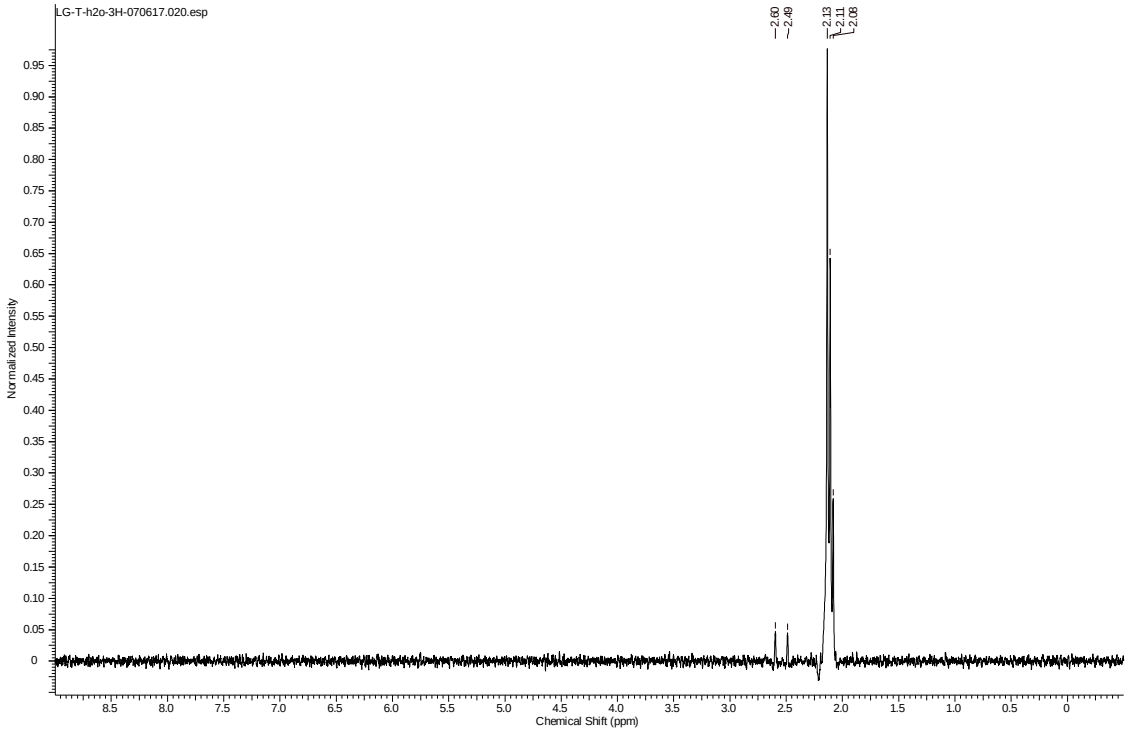

Figure 3.16 ^{3}H NMR of Pergolide **2.9c**

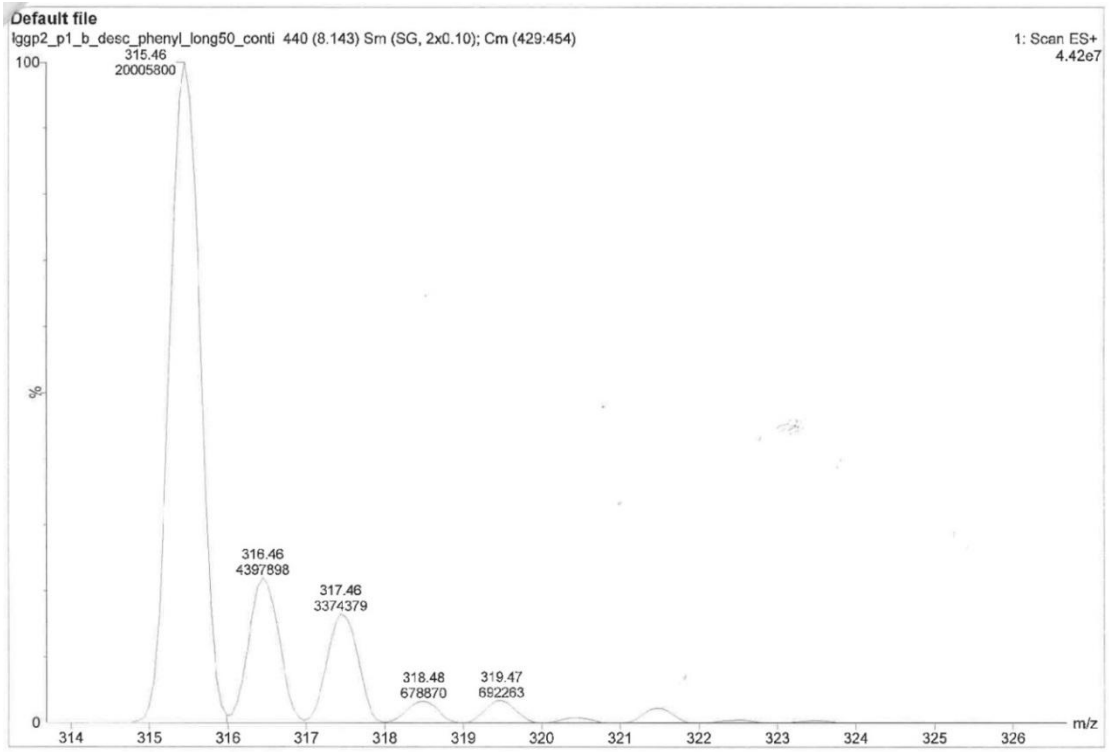

Figure 3.17 LC-MS spectrum of compound **2.9c**

Benzthiazide (2.13):

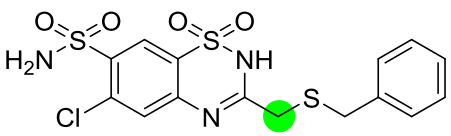

[61]

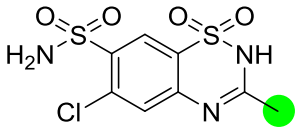

2.14 [41]

Following the General Procedure A and using THF/D_2O (1:1) as solvent. After the final evaporation an ^1H NMR spectrum of the residue was recorded. Note that degraded product (**2.14**) was detected after the reaction, leading to the product that contained deuterated methyl. After purification by column chromatography (eluent: ethyl acetate/cyclohexane = 1/1), the NMR spectra were recorded.

2.13: ^1H NMR (400 MHz, D_2O) δ 8.45 (s, 1H), 7.46-7.32 (m, 3H), 7.22 (t, J = 7.6 Hz, 2H), 7.10 (t, J = 7.6 Hz, 1H), 3.93 (s, 1.9H), 3.52-3.48 (m, 1.1H). ^{13}C NMR (100 MHz, D_2O) δ 160.5, 140.3, 140.0, 139.1, 137.0, 130.4 (s, 2C), 129.7 (s, 2C), 128.2, 127.2, 121.3, 120.6, 37.1.

2.14: ^1H NMR (400 MHz, D_2O) δ 8.47 (s, 1H), 7.44 (s, 1H), 2.39 (t, J = 2.2 Hz, 1.8H).

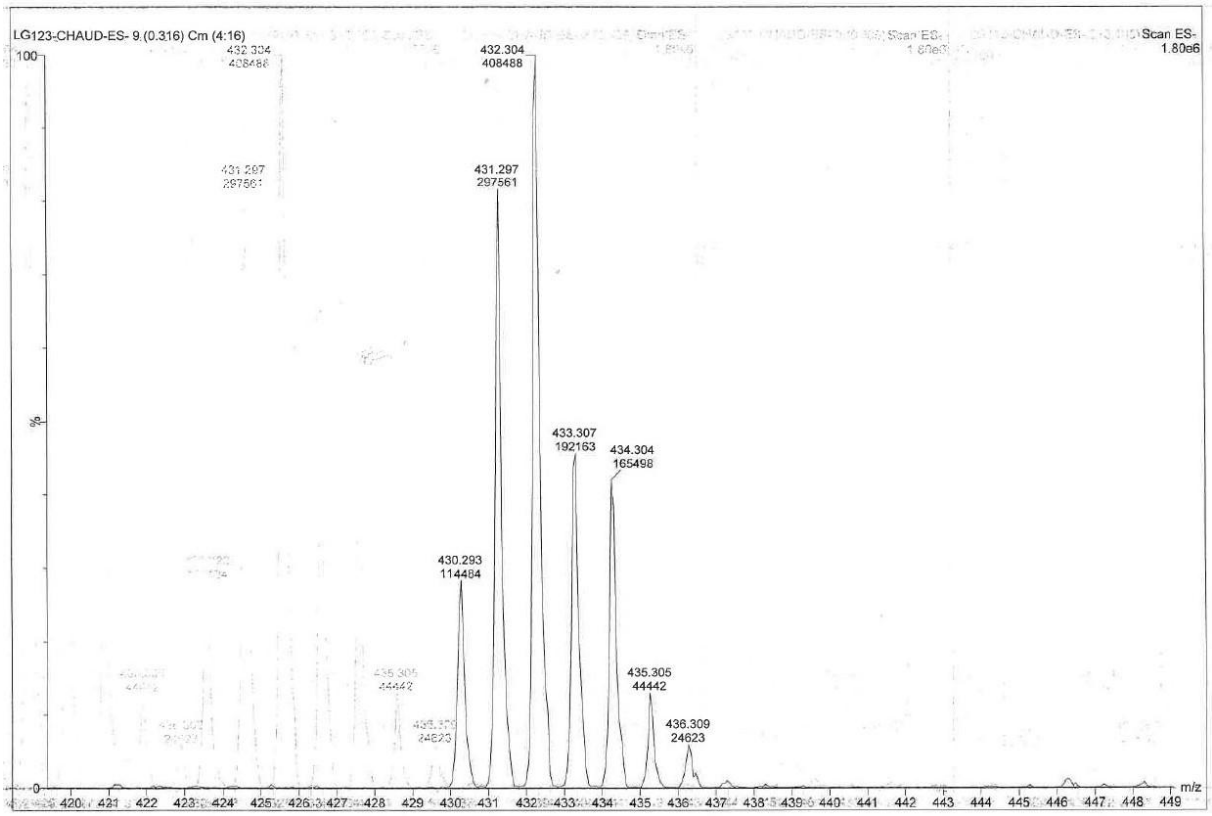

Figure 3.18 LC-MS spectrum of compound **2.13**

Biotin (2.15):

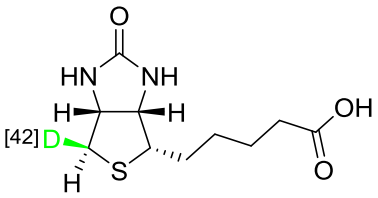

Following the General Procedure A and using DMF as solvent. After evaporation the crude product was dissolved in methanol and centrifuged (2000 G). Supernatant was collected and evaporated *in vacuo* to afford the desired product in quantitative yield. The NMR spectrum was obtained by adding 1 eq. NaOH into the D_2O solution of biotin. Before deuteration $[\alpha]_D^{20}$ +71.0 ° (*c* 0.1, CH_3OH), after deuteration $[\alpha]_D^{20}$ +73.0 °(*c* 0.1, CH_3OH).

^{1}H NMR (400 MHz, D_2O) δ 4.56 (dd, *J* = 7.9, 4.6 Hz, 1H), 4.39 (dd, *J* = 8.0, 4.5 Hz, 1H), 3.37-3.23 (m, 1H), 2.95 (dd, *J* = 13.1, 5.0 Hz, 0.6H), 2.73 (d_{app}, *J* = 13.1 Hz, 1H), 2.14 (t, *J* = 8.0 Hz, 2H), 1.74-1.62 (m, 1H), 1.61-1.49 (m, 3H), 1.44-1.28 (m, 2H). ^{13}C NMR (100 MHz, D_2O) δ 183.8, 165.4, 62.0, 60.3, 55.4, 39.8, 37.4, 28.3, 27.7, 25.7.

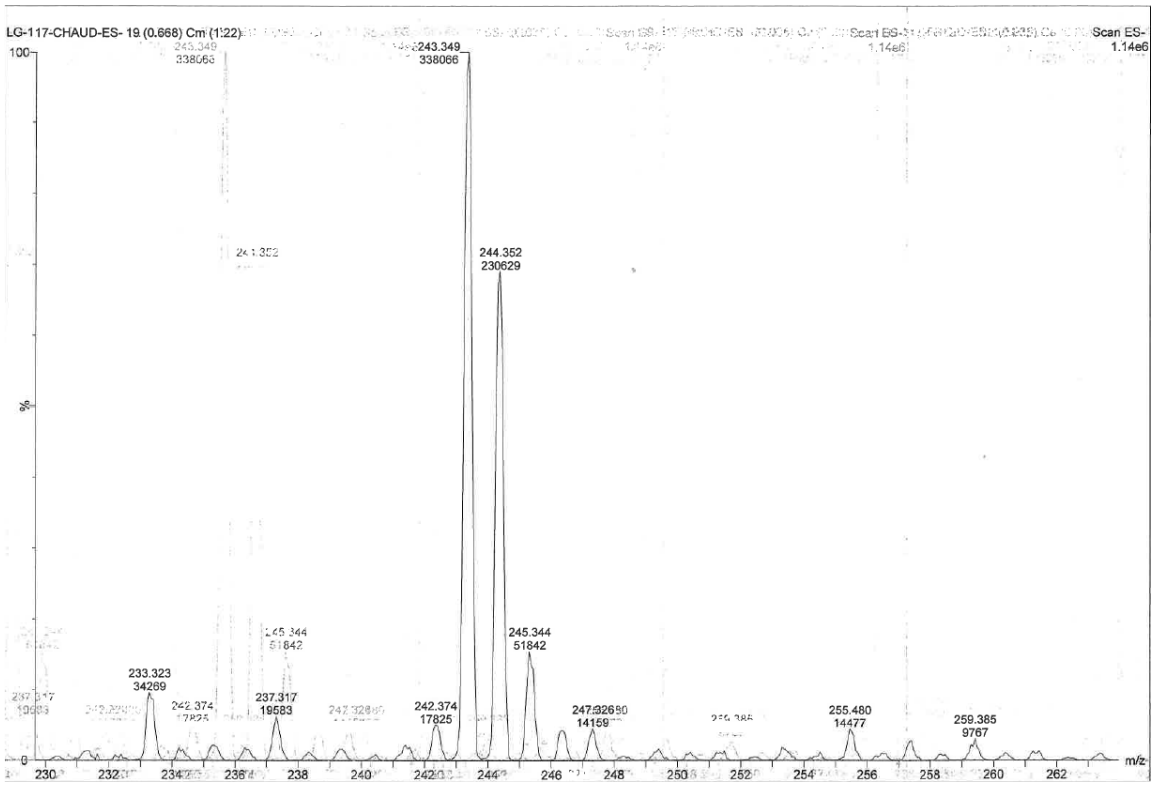

Figure 3.19 LC-MS spectrum of compound **2.15**

Biotin sodium salt (2.15'):

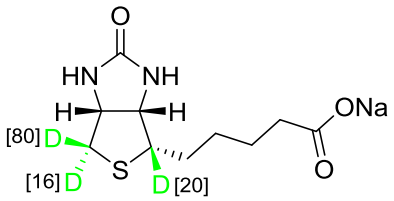

Following the General Procedure A and using D_2O as solvent. Note that the starting compound was biotin sodium salt. After the final evaporation an ^1H NMR spectrum of the residue was recorded. Before deuteration $[\alpha]_D^{20}$ +71.0 °(*c* 0.1, CH_3OH), after deuteration $[\alpha]_D^{20}$ +75.0 °(*c* 0.1, CH_3OH).

^1H NMR (400 MHz, D_2O) δ 4.59 (d, *J* = 7.9 Hz, 1H), 4.43 (dd, *J* = 8.0, 4.5 Hz, 1H), 3.40-3.29 (m, 0.8H), 2.99 (dd, *J* = 13.0, 4.9 Hz, 0.2H), 2.76 (d, *J* = 13.0 Hz, 0.8H), 2.23-2.12 (m, 2H), 1.78-1.22 (m, 6H). ^{13}C NMR (100 MHz, D_2O) δ 183.8, 165.4, 62.0, 60.3, 55.4, 39.8, 37.3, 28.3, 27.7, 25.7.

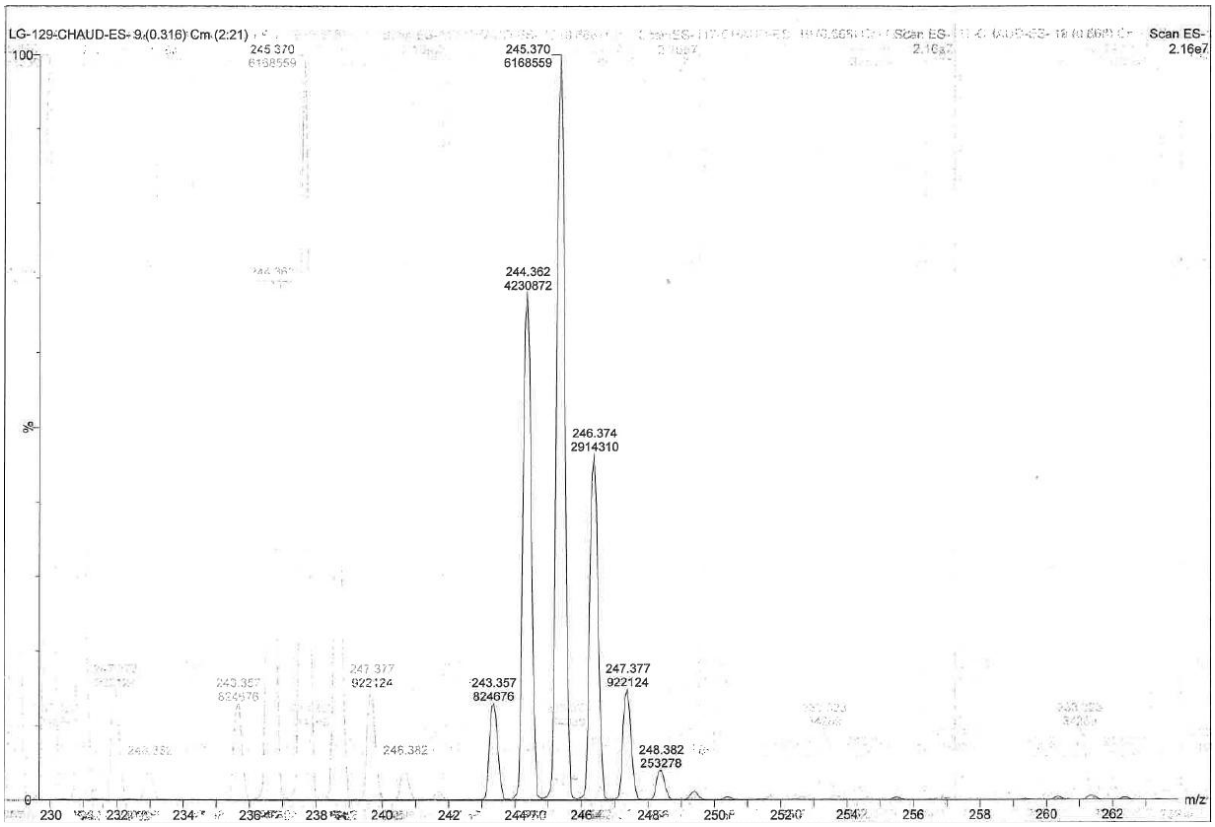

Figure 3.20 LC-MS spectrum of compound **2.15'**

3.3 Data of mass analyses for compounds **2.1** to **2.15'**

Compound	M_0	M_{+1}	M_{+2}	M_{+3}	M_{+4}	M_{+5}	M_{+6}	M_{+7}	M_{+8}	Total D incorporation
2.1	0.3%	0.2%	2.2%	19.4%	59.7%	15.6%	2.3%	0.4%		3.9
2.2	0.0%	0.0%	0.1%	3.2%	25.8%	52.1%	17.8%	0.6%	0.4%	4.9
2.3	0.2%	0.8%	7.6%	21.1%	39.0%	22.1%	6.1%	3.7%	0.2%	4.0
2.4	11.4%	27.1%	32.4%	21.0%	8.0%					1.9
2.4'	0.9%	3.1%	13.9%	35.7%	45.3%					3.2
2.5	13.0%	23.4%	25.3%	25.7%	10.2%	2.4%				2.0
2.6	2.9%	9.2%	20.1%	36.0%	24.5%	7.2%				2.9
2.7a	28.9%	27.1%	19.0%	16.8%	6.8%	1.3%				1.5
2.7b	0.5%	1.5%	4.7%	18.6%	33.7%	33.4%	6.0%	1.3%		4.0
2.8	23.6%	34.4%	20.0%	11.4%	6.9%	2.4%	1.2%			1.6
2.9a	17.4%	22.1%	22.1%	23.0%	11.7%	3.2%				2.0
2.9b	0.4%	0.7%	3.0%	17.8%	36.8%	30.0%	9.1%	1.7%		4.2
2.13	11.0%	41.1%	47.9%							1.4
2.15	63.2%	35.2%	1.6%							0.4
2.15'	6.4%	31.8%	43.2%	15.2%						1.6

Chapter 2 Ru/C catalyzed homocoupling of 2-arylpyridines

1 Introduction and background

The rapid synthesis of complex molecules with various functional groups is one of the most important challenges in organic chemistry. For this purpose, metal catalyzed C-H bond activation followed by functionalization has been proved to be a predominant way.[75] Compared with multistep synthesis and traditional cross-coupling methods such as Suzuki, Stille, Hiyama, and Negishi reactions that involved pre-functionalization of substrates,[76] C-H activation/functionalization is preferred because it is more environmentally-benign and economically attractive.

During the last decade, C-H activation/functionalization has been broadly applied for the preparation of pharmaceuticals, the synthesis of biologically active natural products, agrochemicals and molecules used in material science.[77] Although numerous advances have been achieved in C-H activation field, it remains a challenge to solve the site selectivity in such process. One common solution to attain this goal is the employment of a directing group. Taking advantage of the coordination abilities of functional groups to various metal catalysts, a considerable amount of C-H activation processes have been developed for the construction of various useful structures.

According to the nature of the catalysts used in such reactions, they can be divided into two kinds of categories: homogeneous and heterogeneous catalyses. Homogeneous catalysis refers to the catalytic reactions where the catalyst is in the same phase as the reactants. Heterogeneous catalysis is the alternative to homogeneous catalysis, where the catalysis occurs at the interface of two phases, such as liquid-solid phases. So far, the majority of C-H activation processes have been achieved with

---

[75] For selected reviews on C-H bond functionalizations, see: a) D. Alberico, M. E. Scott, M. Lautens, *Chem. Rev.* **2007**, *107*, 174; b) R. Giri, B.-F. Shi, K. M. Engle, N. Maugel, J.-Q. Yu, *Chem. Soc. Rev.* **2009**, *38*, 3242; c) X. Chen, K. M. Engle, D.-H. Wang, J.-Q. Yu, *Angew. Chem. Int. Ed.* **2009**, *48*, 5094; d) L. Ackermann, R. Vicente, A. Kapdi, *Angew. Chem. Int. Ed.* **2009**, *48*, 9792; e) O. Daugulis, *Top. Curr. Chem.* **2010**, *292*, 57; f) P. Sehnal, R. J. K. Taylor, I. J. S. Fairlamb, *Chem. Rev.* **2010**, *110*, 824; g) T. Satoh, M. Miura, *Chem. Eur. J.* **2010**, *16*, 11212; h) C. S. Yeung, V. M. Dong, *Chem. Rev.* **2011**, *111*, 1215; i) J. Schipper, K. Fagnou, *Chem. Mater.* **2011**, *23*, 1594; j) J. Wencel-Delord, F. Glorius, *Nat. Chem.* **2013**, *5*, 369; k) G. Rouquet, N. Chatani, *Angew. Chem. Int. Ed.* **2013**, *52*, 11726; l) S. A. Girard, T. Knauber, C.-J. Li, *Angew. Chem. Int. Ed.* **2014**, *53*, 74; m) S. Tani, T. N. Uehara, J. Yamaguchi, K. Itami, *Chem. Sci.* **2014**, *5*, 123; n) M. Zhang, Y. Zhang, X. Jie, H. Zhao, G. Li, W. Su, *Org. Chem. Front.* **2014**, *1*, 843; o) T. Mesganaw, J. A. Ellman, *Org. Process Res. Dev.* **2014**, *18*, 1097; p) L. Ackermann, *J. Org. Chem.* **2014**, *79*, 8948; q) Y. Segawa, T. Maekawa, K. Itami, *Angew. Chem. Int. Ed.* **2015**, *54*, 66; r) K. Shin, H. Kim, S. Chang, *Acc. Chem. Res.* **2015**, *48*, 1040; s) O. Daugulis, J. Roane, L. D. Tran, *Acc. Chem. Res.* **2015**, *48*, 1053; t) B. Ye, N. Cramer, *Acc. Chem. Res.* **2015**, *48*, 1308; u) B. Liu, F. Hu, B.-F. Shi, *ACS Catal.* **2015**, *5*, 1863; v) J. Yang, *Org. Biomol. Chem.* **2015**, *13*, 1930; w) Z. Huang, H. N. Lim, F. Mo, M. C. Young, G. Dong, *Chem. Soc. Rev.* **2015**, *44*, 7764; x) S. Santoro, S. I. Kozhushkov, L. Ackermann, L. Vaccaro, *Green Chem.* **2016**, *18*, 3471.

[76] a) N. Miyaura, *Cross-Coupling Reactions: A Practical Guide*; Springer: Berlin, **2002**; b) F. Diederich, P. J. Stang, *Metal-Catalyzed Cross-Coupling Reactions*; Wiley-VCH, Weinheim, Germany, **1998**; c) N. Miyaura, A. Suzuki, *Chem. Rev.* **1995**, *95*, 2457; d) A. Suzuki, *Angew. Chem., Int. Ed.* **2011**, *50*, 6722.

[77] For recent reviews, see: a) L. McMurray, F. O'Hara, M. J. Gaunt, *Chem. Soc. Rev.* **2011**, *40*, 1885; b) W. R. Gutekunst, P. S. Baran, *Chem. Soc. Rev.* **2011**, *40*, 1976; c) J. Yamaguchi, A. D. Yamaguchi, K. Itami, *Angew. Chem. Int. Ed.* **2012**, *51*, 8960; d) Y.-K. Chen, S. W. Youn, *Chem. Eur. J.* **2012**, *18*, 9452; e) J. Hong, *Chem. Eur. J.* **2014**, *20*, 10204; f) L. Ackermann, *Org. Process Res. Dev.* **2015**, *18*, 260; g) Y. Kuninobu, S. Sueki, *Synthesis* **2015**, 3823; h) F. J. Lombard, M. J. Coster, *Org. Biomol. Chem.* **2015**, *13*, 6419.

homogeneous catalysis. However, for industrial purpose, heterogeneous catalysis is preferable, due to the easier separation of products from the reaction mixture and the possibility to recover the catalyst. Moreover, the possibility to have different catalytic activity and achieve different site selectivity compared with homogeneous catalysis also makes heterogeneous catalysis an attractive research hotspot. Despite the fact that heterogeneous catalysts can generally be easily separated from the products by filtration or centrifugation, the recovered catalysts are not always reusable. A decrease in catalytic efficacy or even completely loss of catalytic activity may be observed in some cases. Therefore, the development of recyclable heterogeneous catalysts is highly desirable and challenging.

Traditional C-H activation reactions involve the activation of one C-H bond, and it needs a pre-functionalized coupling partner such as halocarbons, boronic acids/esters, triflate ester or organometallic reagents and so on (**Scheme 1.1**). Recently, many works based on heterogeneously catalyzed C-H activation reactions have been reported, dealing with the formation of C-C bond, C-O bond, C-N bond and C-X bond (X represents halides). In this context, selected examples concerning the formation of C-C bonds through C-H activation processes are reviewed herein.

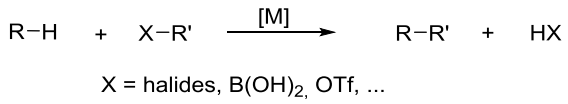

Scheme 1.1 Usual C-H activation coupling reactions

1.1 C-C bond formation through heterogeneously catalyzed C-H functionalization

1.1.1 C-C bond formation based on heterogeneous palladium catalysts

Among the reported methods describing heterogeneously catalyzed C-C coupling reactions, catalysts based on palladium are the most studied. The most practical palladium-based heterogeneous catalyst may be Pd/C, which is commercially available and relatively cheap compared with other palladium catalysts. Recently, Pd/C was reported to catalyze C-C coupling reactions through C-H activation. In this field, F. Glorius is one of the pioneering researchers.[78]

In 2013, Glorius reported the first completely selective C-H arylation of benzo[*b*]thiophenes at C3 position using Pd/C and CuCl as co-catalyst (**Scheme 1.2**).[78a] No ligand was required for this transformation, and the reaction was insensitive to air and moisture. Aryl chlorides with various functional groups were tolerated under the reaction conditions. Good yields were obtained with electron-rich and electron-neutral aryl chlorides, while electron-deficient aryl chlorides with nitro- and

[78] a) D.-T. D. Tang, K. D. Collins, F. Glorius, *J. Am. Chem. Soc.* **2013**, *135*, 7450; b) D.-T. D. Tang, K. D. Collins, J. B. Ernst, F. Glorius, *Angew. Chem. Int. Ed.* **2014**, *53*, 1809; c) K. D. Collins, R. Honeker, S. Vásquez-Céspedes, D.-T. D. Tang, F. Glorius, *Chem. Sci.* **2015**, *6*, 1816.

ester-substituents gave low yields of the corresponding products. Good yields were obtained when using sterically encumbered aryl chlorides (such as 2-chloro-*m*-xylene) as substrate, although an extended reaction time (96 h) was required.

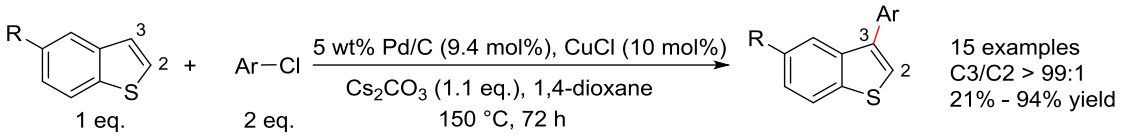

Scheme 1.2 Regioselective C-H arylation of benzo[*b*]thiophenes

The authors have conducted a series of experiments in order to identify the active catalytic species of the reaction. Although it is difficult to evaluate the homo/heterogeneous nature of an active catalyst,[79] several methods are usually used to determine the active catalytic species of such reactions:

1) The three-phase test: This consists to run the reaction with the substrates supported on solids such as resins under the standard reaction conditions. If the reaction proceeds smoothly, then the active catalytic species should be homogeneous; if the reaction is completely inhibited, then the active catalytic species should be heterogeneous.

2) The hot-filtration test: This consists to remove the catalyst by hot-filtration after a certain time of the reaction, and then continue to run the reaction with the filtrate. If the reaction stops at the point when removing the catalyst, then the active catalytic species should be heterogeneous; if the reaction is not affected, the active catalytic species should be homogeneous.

3) The mercury test: This consists to add elemental mercury into the standard reaction mixture during the reaction process. Elemental mercury is a powerful poison for both heterogeneous and colloidal catalysts,[80] because it covers the surface of these catalysts and blocks their activity. If the reaction continues to run, then the active catalytic species should be homogeneous; if the reaction stops at the point when adding mercury, then the active catalytic species should be heterogeneous.

4) Other methods: by comparing the physical properties and catalytic efficacies of the recycled catalyst and the original catalyst; by detecting the amount of leaching metal in the filtrate after the reaction; by adding metal scavenger into the standard reaction mixture.

Experiments including three-phase tests, mercury poisoning, hot-filtration tests and other methods such as detecting the leaching Pd in the filtrate by X-ray fluorescence spectroscopy (XRF) and so on were all conducted by the authors, which supported a heterogeneous catalysis of the reaction process.

[79] a) R. H. Crabtree, *Chem. Rev.* **2012**, *112*, 1536; b) J. A. Widegren, R. G. Finke, *J. Mol. Catal. A: Chem.* **2003**, *198*, 317.
[80] C. Paal, W. Hartmann, *Chem. Ber.* **1918**, *51*, 711.

The good regioselectivity, the use of simple Pd/C and CuCl as co-catalyst, the tolerance of air and water formed the advantages of this method. Besides, detailed investigations about the active catalytic species were conducted by the authors, indicating a heterogeneous catalysis of the reaction process. However, the limited scope of substituted benzo[*b*]thiophenes and the harsh reaction conditions were the limitations of the method.

Based on the work above, the same group developed a method for completely C3-selective arylation of thiophenes by using Pd/C as catalyst without ligands or additives (**Scheme 1.3**).[78b] Same as the previous method, this method was insensitive to air and water. Moreover, the reaction conditions were milder (ethanol as solvent, lower reaction temperature and shorter reaction time). Besides, this reaction is also applicable to the arylation of benzo[*b*]thiophenes, with the same regioselectivity, thus the substrate scope of this method is broader. In addition, nitrogen- and oxygen-containing heterocycles could be functionalized regioselectively at *C2* positions (**Figure 1.1**, compounds **1.1.1**-**1.1.3**), which further increased the substrate scope of this method. Moreover, the authors demonstrated the chemoselectivity of this method by the sequential functionalization of compounds **1.1.4** and **1.1.8**, which contained two reactive heteroaromatic systems under the reaction conditions (**Scheme 1.4**).

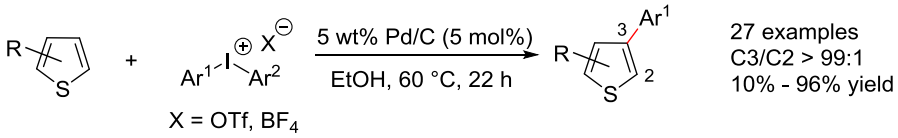

Scheme 1.3 Regioselective C-H functionalization of thiophenes

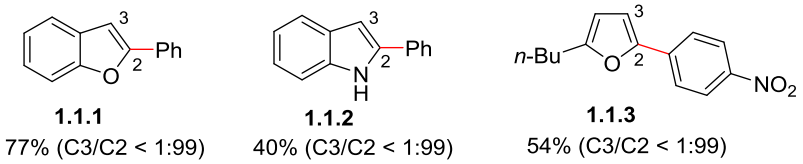

Figure 1.1 Products from regioselective C-H functionalization of heterocycles

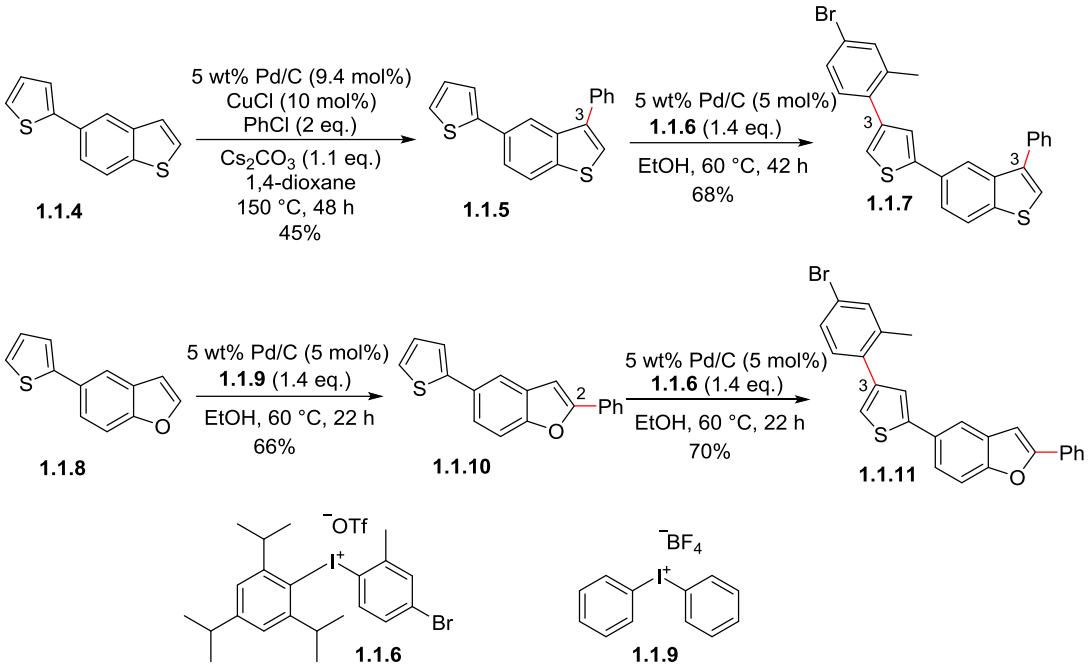

Scheme 1.4 Chemoselective arylation of compounds **1.1.4** and **1.1.8**

Several experiments, including three-phase tests, mercury poisoning and hot-filtration test, were conducted by the authors to identify the active catalytic species of the reaction. As a result, these experiments suggested a heterogeneous active catalytic species, which was the same as their previous reported method.

The mild reaction conditions, broad substrate scope and good regio- and chemoselectivities were the advantages of this method. However, the required iodonium salts as arylation reagents limited its application. Moreover, the catalysts used in the two methods described above could not be recycled.

In 2015, the same group developed a method allowing the C-H arylation of triphenylene, naphthalene and related arenes with aryliodonium salts using Pd/C as catalyst and dimethoxyethane (DME) as solvent (**Scheme 1.5**).[78c] It was the first method for the C-H functionalization of triphenylene (type **I**), and it proceeded at the most sterically hindered position. Other related arenes were also functionalized with good regioselectivity. Various aryliodonium salts with diverse electronical and sterical effects were tolerated under the reaction conditions, giving generally moderate yields.

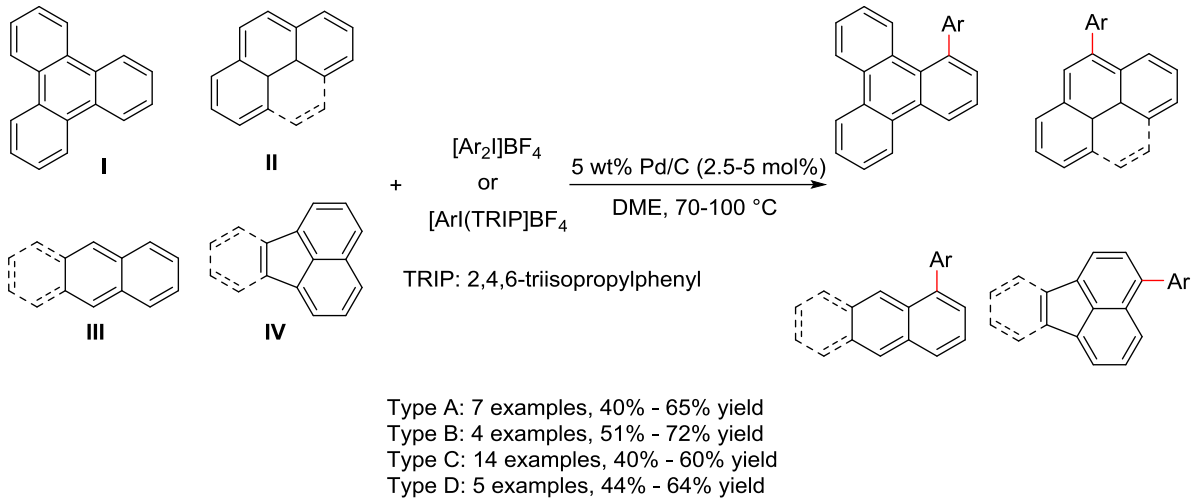

Scheme 1.5 Pd/C catalyzed arylation of polyaromatic hydrocarbons

To identify the active catalytic species, mercury poisoning and hot-filtration tests were conducted, which indicated a heterogeneous active catalytic species. Further mechanism studies suggested the *in situ* formation of catalytically active insoluble nanoparticles from Pd/C, and the reaction was suggested to proceed through a Pd(0)/Pd(II) pathway (**Scheme 1.6**). As shown in **Scheme 1.6**, the active catalytic species **A** was formed upon heating Pd/C in the presence of oxidants, then the surface of **A** saturated with naphthalene through π-interactions to form **B**. Reversible dissociation of naphthalene from **B** could create a vacant coordination site to give species **C**, which transferred a single electron to the iodonium salt to form a phenyl radical and Pd(I) species. Then Pd(II) species **D** was formed by recombination of the phenyl radical and the Pd(I) species. Finally, an electrophilic palladation followed by re-aromatization and reductive elimination, or an insertion and subsequent *β*-hydride elimination gave the product and re-generated the Pd(0) species.

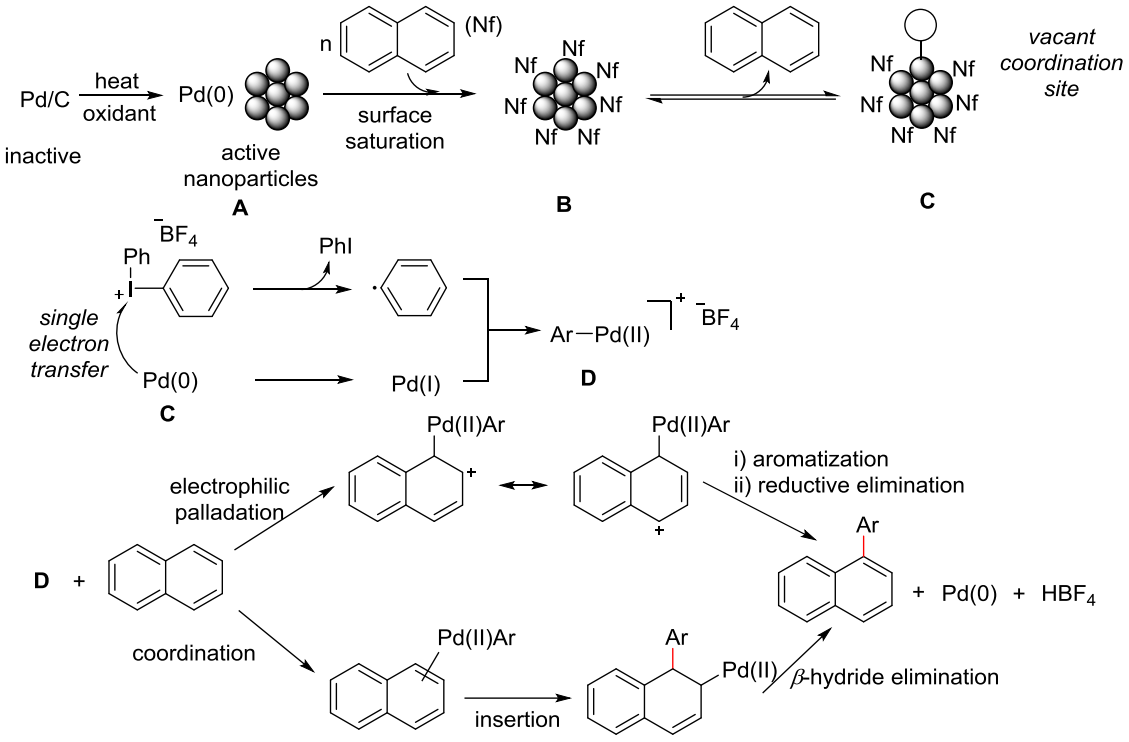

Scheme 1.6 Proposed reaction mechanisms for the arylation of polyaromatic hydrocarbons

In addition to the work of Glorius, Pd/C was reported to catalyze the polycondensation of 2-bromo-3-hexylthiophene to give linear and highly regioregular thiophene-based π-conjugated polymer poly(3-hexylthiophene-2,5-diyl) (compound **1.1.13**) with high molecular weight (**Scheme 1.7**),[81] which further demonstrated the broad application of Pd/C.

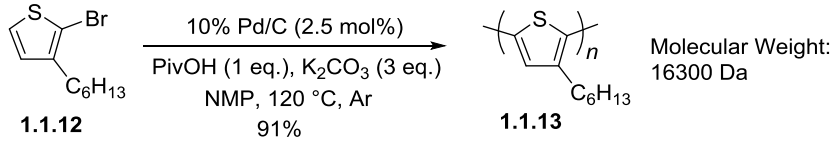

Scheme 1.7 Pd/C catalyzed polycondensation of 2-bromo-3-hexylthiophene

Besides the applications of Pd/C, there were some C-H activation processes accomplished with Pd-nanoparticles. In 2011, Vorotyntsev, Hierso and co-workers reported the synthesis of highly dispersed palladium based polypyrrole (PPy) nanocomposites PdNp@PPy and its applications for the C2-arylation of *n*-butyl furan and *n*-butyl thiophene with bromoarenes and bromoquinoline (**Scheme**

[81] S. Hayashi, Y. Kojima, T. Koizumi, *Polym. Chem.* **2015**, *6*, 881.

1.8).[82] This nanocatalyst had a mean size of 2.4 nm and a high palladium content of 35 wt%, which was characterized by means of Fourier transform infrared spectroscopy (FTIR), X-ray photoelectron spectroscopy (XPS), X-ray diffraction (XRD), scanning electron microscopy (SEM), and transmission electron microscopy (TEM) techniques. Based on preliminary kinetic and post-catalysis studies, the authors suggested that the active catalytic species of the reaction were soluble molecular or colloidal species, which were delivered by the nanocomposites and were susceptible to a uniform redeposition within the polypyrrole support.

Scheme 1.8 C-H arylation of furan and thiophene catalyzed by PdNp@PPy

The absence of organic ligand, the easy recovery of PdNp@PPy nanocomposites by simple filtration were the advantages of this method. However, the substrate scope of the heterocycles was limited to only two examples, and steric hindered bromoarenes such as 2-bromomesytilene were not reactive, which limited the application of the method.

In 2014, a silicon nanowire array-stabilized palladium nanoparticle catalyst, SiNA-Pd, was developed by Yamada's group. Its catalytic activities towards Mizoroki-Heck reaction (**Scheme 1.9**) and C-H bond functionalization reactions of thiophenes and indoles were investigated.[83] With a low catalyst loading (0.3 mol%), various electron-rich and electron-deficient iodoarenes were readily coupled with butyl acrylate and styrene, resulting in good yields of the corresponding products. The use of aryl bromides as substrates led to the formation of the corresponding cinnamates with good yields using optimized reaction conditions.

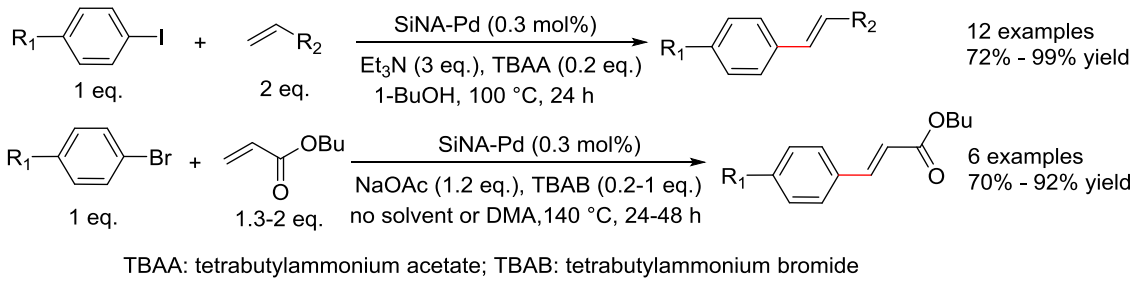

Scheme 1.9 Mizoroki-Heck reaction catalyzed by palladium nanocatalyst SiNA-Pd

[82] V. A. Zinovyeva, M. A. Vorotyntsev, I. Bezverkhyy, D. Chaumont, J.-C. Hierso, *Adv. Funct. Mater.* **2011**, *21*, 1064.

[83] Y. M. A. Yamada, Y. Yuyama, T. Sato, S. Fujikawa, Y. Uozumi, *Angew. Chem. Int. Ed.* **2014**, *53*, 127.

Using the same catalyst, the authors also realized the C-H arylation of thiophenes and indoles using iodobenzene as the arene source (**Figure 1.2**). Thus, 2-alkylthiophenes were regioselectively functionalized at *C5* positions (compounds **1.1.14** and **1.1.15**) with high yields, while 1-methylindole was arylated with poor regioselectivity (the ratio of 2-arylated, 3-arylated and 2,3-diarylated products was 4:2:1). Moreover, by using 490 mol ppb of SiNA-Pd (0.000049 mol% Pd) for the Mizoroki-Heck reaction, high turnover number (TON) of 2000 000 and turnover frequency (TOF) of 40000 h^{-1} were obtained.

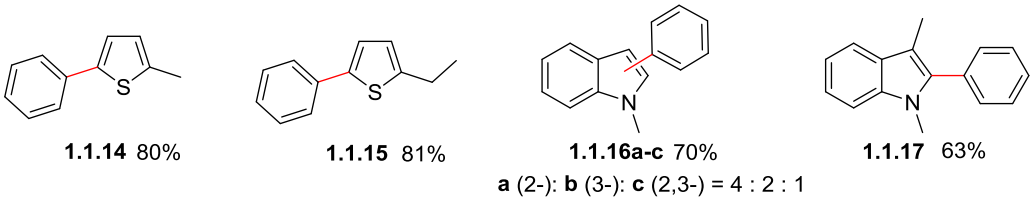

Figure 1.2 C-H functionalization products using SiNA-Pd as catalyst

The recyclability of SiNA-Pd was investigated by the authors, and the recovered catalyst was found to remain its activity after ten cycles, giving 98% yield of the coupling product in the tenth use of the catalyst. Inductively coupled plasma atomic emission spectrometry (ICP-AES) analysis of the reaction mixture showed no leaching of Pd; the hot-filtration test showed the termination of the reaction upon removing the catalyst. These results suggested a heterogeneous catalysis of the reaction process.

Besides the works described above, there are some other C-H activation processes accomplished with Pd-based nanoparticles.[84] These works all concerned with the C-H arylation reactions, and most of the catalysts could be reused for several cycles, demonstrating the advantages of using heterogeneous catalysts.

1.1.2 C-C bond formation based on heterogeneous ruthenium catalysts

In addition to the use of Pd-based heterogeneous catalysts, some Ru-based heterogeneous catalysts were developed for the C-H functionalization of various compounds. Among them, Ru/C showed strong activity towards some transformations based on C-H activation.[85]

[84] a) T. J. Williams, I. J. S. Fairlamb, *Tetrahedron Lett.* **2013**, *54*, 2906; b) J. Lee, J. Chung, S. M. Byun, B. M. Kim , C. Lee, *Tetrahedron* **2013**, *69*, 5660; c) J. Malmgren, A. Nagendiran, C.-W. Tai, J.-E. Bäckvall, B. Olofsson, *Chem. Eur. J.* **2014**, *20*, 13531; d) M. Cao, D. Wu, W. Su, R. Cao, *J.Catal.* **2015**, *321*, 62; e) S. Vásquez-Céspedes, M. Holtkamp, U. Karst, F. Glorius, *Synlett*, **2017**, *28*, *asap* (doi: 10.1055/s-0036-1589007).

[85] a) S. Imoto, T. Uemura, F. Kakiuchi, N. Chatani, *Synlett* **2007**, 170 ; b) K. H. V. Reddy, G. Satish, V. P. Reddy, B. S. P. A. Kumar, Y. V. D. Nageswar, *RSC Adv.* **2012**, *2*, 11084.

In 2007, N. Chatani's group developed a method for the C-H carbonylation of 2-phenylpyridine derivatives using Ru/C as catalyst (**Scheme 1.10**).[85a] Regardless of the electronical nature of the substituents on the phenyl ring, various functional groups were tolerated under the reaction conditions, although electron-deficient substituents gave lower yields of products. Moreover, regioselective carbonylation at the less hindered C-H bonds was observed for *meta*-substituted substrates, showing the good regioselectivity of the reaction. Other *N*-heterocycles such as 1-phenylpyrazole and 2-phenylpyrimidine also underwent regioselective C-H carbonylation to give the corresponding ketones, increasing the substrate scope of the reaction.

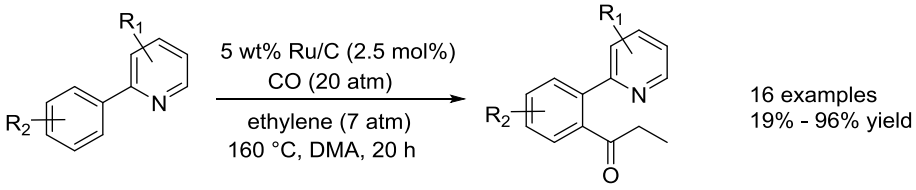

Scheme 1.10 Ru/C catalyzed carbonylation of 2-arylpyridine

Performing the reaction with recovered catalyst gave no reaction at all, indicating the loss of catalytic activity of the recovered catalyst. Meanwhile, the filtrate obtained from heating the Ru/C under the reaction conditions in the absence of any substrates showed comparable catalytic activity (90% yield of the product). These results clearly indicated that the active ruthenium species leached from the Ru/C into the solvent under the reaction conditions. Based on the observations, the authors suggested that the active catalytic species could be $Ru_3(CO)_{12}$, which was reported to catalyze the same reactions under the reaction conditions.[86]

In 2012, Y. V. D. Nageswar reported a Ru/C catalyzed oxidative α-cyanation of tertiary amines with ethyl cyanoformate by using *tert*-butylhydroperoxyde (TBHP) as oxidant.[85b] Various α-aminonitriles were synthesized from *N*,*N*-dialkylanilines in good to excellent yields with high selectivity. Besides, the use of ethyl cyanoformate as cyanide source was less toxic, and the reaction conditions were mild (low catalyst loading, methanol as solvent, short reaction time). Moreover, the use of recovered Ru/C as catalyst showed no significant loss of catalytic activity after four reaction cycles. TEM analysis showed no significant differences on the morphology, shape and size between the recovered catalyst and original Ru/C.

[86] N. Chatani, Y. Ie, F. Kakiuchi, S. Murai, *J. Org. Chem.* **1997**, *62*, 2604.

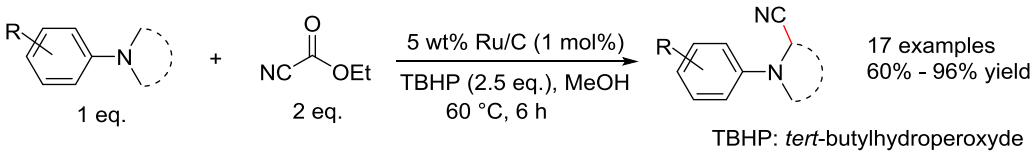

Scheme 1.11 Ru/C catalyzed oxidative α-cyanation of tertiary amines

Despite the broad substrate scope of the reaction, this method could not be applied to the cyanation of trialkylamines, which limited the application of the method. Regarding the reaction mechanism, the authors proposed the following one (**Scheme 1.12**) according to the experimental observations: Ru/C was oxidized by TBHP to give the Ru-oxo species **A**, which reacted with tertiary amine to produce an iminium ion intermediate **B** by electron transfer and subsequent hydrogen transfer. The iminium ion intermediate then reacted with the *in situ* generated cyanide to form the α-aminonitrile product and regenerated the Ru/C species.

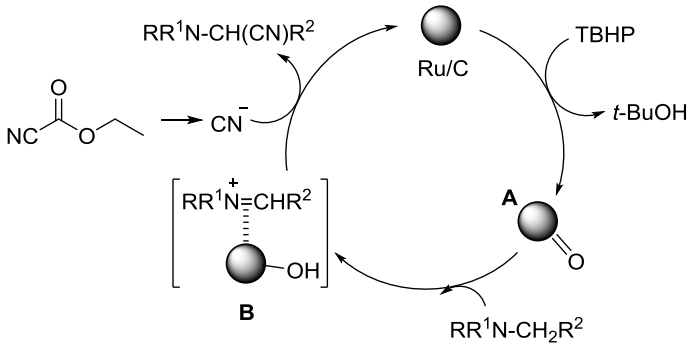

Scheme 1.12 Proposed reaction mechanism for Ru/C catalyzed oxidative α-cyanation

In 2010, K. Wada and co-workers reported the first example of Ru/CeO_2-catalyzed nitrogen-directed C-H arylation with aryl halides (**Scheme 1.13**).[87] The different Ru precursors used for the preparation of Ru/CeO_2 strongly affected the catalytic activity, and the best Ru precursor was $Ru_3(CO)_{12}$, which gave quantitative yield of the arylated product. Besides, the catalytic activity was greatly increased when the catalyst was modified by PPh_3 (treatment of Ru/support at 100 ℃ for 20 min in the presence of PPh_3 under an H_2 atmosphere), and the best ratio of PPh_3 was 3 equivalents relative to the molar amount of Ru (designated as $3PPh_3$-Ru/CeO_2). In addition, the type of the solid support and the precipitant used for the preparation of the CeO_2 support also affected the catalytic activity, and $3PPh_3$-Ru/CeO_2 showed the highest catalytic activity using KOH as the precipitant for the preparation of the CeO_2 support.

[87] H. Miura, K. Wada, S. Hosokawa, M. Inoue, *Chem. Eur. J.* **2010**, *16*, 4186.

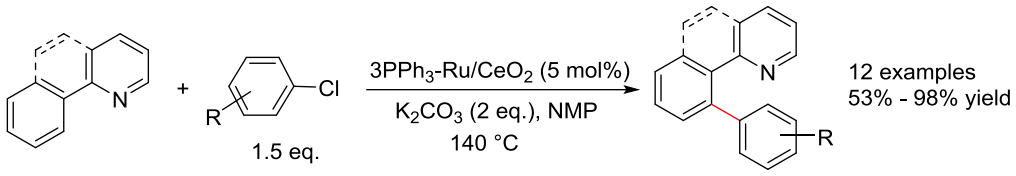

Scheme 1.13 Ru/CeO_2-catalyzed C-H arylation with aryl halides

Various electron-rich and electron-deficient aryl chlorides were tolerated under the reaction conditions. Heteroaryl chlorides such as 2-chlorothiophene and 2-chloropyridine also gave good yields of the arylated products. ICP-AES analysis of the solution after the reaction showed 2.6% of Ru species leaching in the solution, and the catalyst could be recycled and reused for 3 reaction cycles without loss of catalytic activity. The active catalytic species in the reactions were considered to be low-valent Ru species generated from Ru(IV) species on CeO_2, which was observed from FTIR study from the fresh Ru/CeO_2 catalyst (a distinct band at 975 cm^{-1}, which corresponded to a ruthenium-oxo species). Notably, aryl bromides and aryl iodides could also be used as arylation reagents. However, most arylation reactions used benzo[*h*]quinoline as the substrate, and the use of 2-phenylpyridine and 1-phenylpyrrole as the substrates gave a mixture of mono- and diarylated compounds as the product. The narrow substrate scope and harsh reaction conditions limited the application of the method.

In the same year, the same group reported that Ru/CeO_2 was able to catalyze the addition of a C-H bond of aromatic ketones to vinylsilanes in the presence of PPh_3 (**Scheme 1.14**).[88] Similarly to the previous method, the reaction efficiency was greatly affected by the nature and amount of phosphorus additives, which might serve as ligands for active catalytic species of Ru (the best additive was 4 equivalents of PPh_3). The reaction temperature also strongly affected the reaction process, since a lower yield was obtained if the reaction was conducted below 160 ℃. The authors suggested that high temperatures were essential for transforming Ru(IV) species on CeO_2 into active catalytic species. Interestingly, the use of PPh_3-modified catalyst 4PPh_3-Ru/CeO_2 (treatment of Ru/CeO_2 at 100 ℃ for 20 min in the presence of 4 equivalents of PPh_3 under an H_2 atmosphere) resulted in completion of the reaction within 90 min at a lower temperature of 140 ℃.

[88] H. Miura, K. Wada, S. Hosokawa, M. Inoue, *ChemCatChem* **2010**, *2*, 1223.

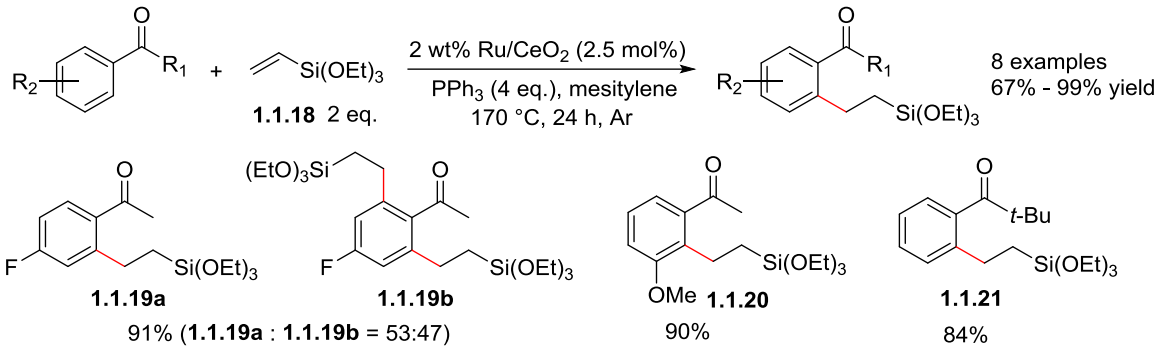

Scheme 1.14 Ru/CeO_2-catalyzed hydroarylation of vinylsilanes

Various (hetero)aromatic ketones were efficiently coupled with the vinylsilane **1.1.18**. Interestingly, when using 4-fluoro-acetophenone as the substrate, monoalkylated product **1.1.19a** and dialkylated product **1.1.19b** were obtained with a ratio of almost 1:1, while 3-methoxy-acetophenone gave monoalkylated compound **1.1.20** as the sole product, which might be due to the interaction between the ruthenium and lone pair electrons of the oxygen in methoxy group.[89] In the case of using phenyl *tert*-butyl ketone as the substrate, compound **1.1.21** was obtained as the sole product, probably due to the steric hindrance of the *tert*-butyl group. The solid catalysts were readily separated from the product by simple filtration, and the filtrate contained only 2% of ruthenium species as detected by ICP-AES. However, the recovered catalysts showed no catalytic activity, due to the irreversible deposition of silicon residues derived from vinylsilanes on the surface of Ru species.

As described above, heterogeneous Ru-based catalysts showed potential catalytic activities towards various C-H activation processes. In particularly, Ru/C is a promising heterogeneous catalyst because it is commercially available and inexpensive, and it is usually easy to separate it from the reaction mixture by simple filtration. Moreover, ligand is not necessary for Ru/C catalyzed C-H activation reactions, and it can be recycled in some cases. Thus, the development of more C-H activation reactions based on Ru/C is of great interest.

1.1.3 C-C bond formation based on heterogeneous platinum catalysts

In addition to Pd/C and Ru/C, Pt/C was also reported to catalyze C-H perfluoroalkylation of (hetero)arenes with R_fI or R_fBr (R_f = perfluoroalkyl group).[90] In this publication, various arenes and heteroarenes, including nucleobase derivatives such as caffeine, were perfluoroalkylated with moderate to good yields using Pt/C as catalyst with a low regioselectivity (compounds **1.1.22** and **1.1.23**, **Scheme 1.15**). The reaction was blocked after hot-filtration of the solid catalyst, and

[89] M. Sonoda, F. Kakiuchi , N. Chatani, S. Murai, *Bull. Chem. Soc. Jpn.* **1997**, *70*, 3117.

[90] L. He, K. Natte, J. Rabeah, C. Taeschler, H. Neumann, A. Brückner, M. Beller, *Angew. Chem. Int. Ed.* **2015**, *54*, 4320.

inductively coupled plasma (ICP) analysis showed no detectable Pt present in the filtrate. Moreover, the recovered catalyst could be used at least for three reaction cycles without significant loss of catalytic activity. These results strongly indicated a heterogeneous active catalytic species of the reaction.

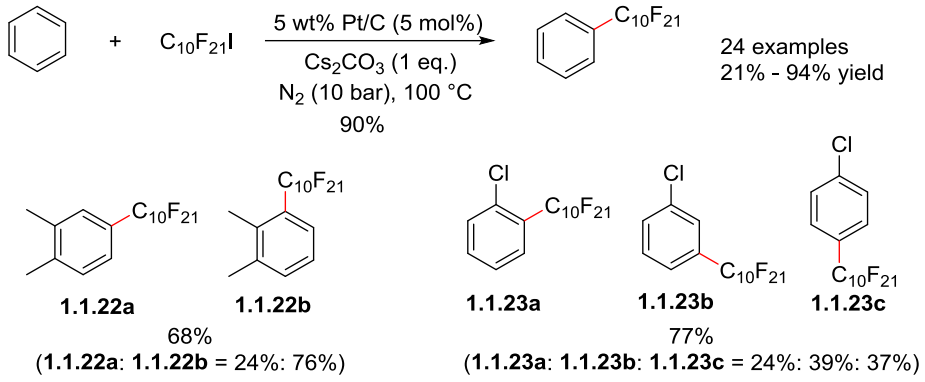

Scheme 1.15 Pt/C catalyzed C-H perfluoroalkylation of (hetero)arenes

Despite the remarkable importance and considerable advances on C-H activation reactions in organic synthesis, traditional C-H activation processes require the use of a pre-functionalized coupling partner, such as halocarbons, boronic acids/esters, triflate ester or organometallic reagents and so on (**Scheme 1.1**). These C-H activation processes are quite efficient to obtain various structures. However, large quantities of wastes such as halide salt, boronic acids or organo-residues are formed with the desired products. These wastes may cause significant environmental pollution, which must be considered in industrial productions.

A more environmentally friendly and more economical way is the cross-dehydrogenative coupling (CDC) reactions (**Scheme 1.16**).[91] This protocol requires no pre-synthesis of any reactants, and the only by-product is formally H_2. Thus, it is more environmentally friendly and potentially applicable to more substrates. Recently, numerous advances have been achieved with the CDC reactions using heterogeneous catalysis involving the formation of C-C, C-O[92] or C-N bonds.[93] In this context, selected examples concerning the formation of C-C bonds through CDC reactions are reviewed herein.

[91] For selected reviews on CDC reactions, see *ref 75h, 75l* and: a) S.-I. Murahashi, D. Zhang, *Chem. Soc. Rev.* **2008**, *37*, 1490; b) C. J. Scheuermann, *Chem. Asian J.* **2010**, *5*, 436; c) C. Liu, H. Zhang, W. Shi, A. Lei, *Chem. Rev.* **2011**, *111*, 1780; d) A. E. Wendlandt, A. M. Suess, S. S. Stahl, *Angew. Chem. Int. Ed.* **2011**, *50*, 11062.

[92] For publications involving C-O bond formation through CDC reactions, see: a) A. M. Voutchkova, R. H. Crabtree, *J. Mol. Catal. A: Chem.* **2009**, *312*, 1; b) N. T. S. Phan, P. H. L. Vu, T. T. Nguyen, *J. Catal.* **2013**, *306*, 38; c) N. T. S. Phan, T. T. Nguyen, P. H. L. Vu, *ChemCatChem* **2013**, *5*, 3068 ; d) L. Panahi, M. R. Naimi-Jamal, J. Mokhtari, A. Morsali, *Microporous Mesoporous Mater.* **2017**, *244*, 208.

[93] For publications involving C-N bond formation through CDC reactions, see: a) N. T. T. Tran, Q. H. Tran, T. Truong, *J. Catal.* **2014**, *320*, 9; b) P. Pal, A. K. Giri, H. Singh, S. C. Ghosh, A. B. Panda, *Chem. Asian J.* **2014**, *9*, 2392; c) S. Priyadarshini, P. J. A. Joseph, M. L. Kantam, *Tetrahedron* **2014**, *70*, 6068; d) T. Truong, K. D. Nguyen, S. H. Doan, N. T. S. Phan, *Appl. Catal. A* **2016**, *510*, 27; e) K. D. Nguyen, S. H. Doan, A. N. V. Ngo, T. T. Nguyen, N. T. S. Phan, *J. Ind. Eng. Chem.* **2016**, *44*, 136; f) T. N. Tu, K. D. Nguyen, T. N. Nguyen, T. Truong, N. T. S. Phan, *Catal. Sci. Technol.* **2016**, *6*, 1384.

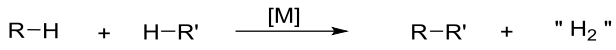

Scheme 1.16 Cross-dehydrogenative coupling reactions

1.2 C-C bond formation through heterogeneously catalyzed CDC reactions

1.2.1 C-C bond formation through heterogeneously catalyzed dehydrogenative alkylation

Heterogeneously catalyzed intermolecular dehydrogenative alkylation has been rarely reported in the literature. Only several research groups have reported a similar process involving the α-C(sp^3)-H bond activation of *N*-aryl-1,2,3,4-tetrahydroisoquinoline (compound **1.2.1**).[94] By using Fe_3O_4 nanoparticles as catalyst, C.-J. Li and co-workers reported the C(sp^3)-C(sp^3) coupling between compound **1.2.1** and nitroalkanes **1.2.2** (**Scheme 1.17**).[94a, e]

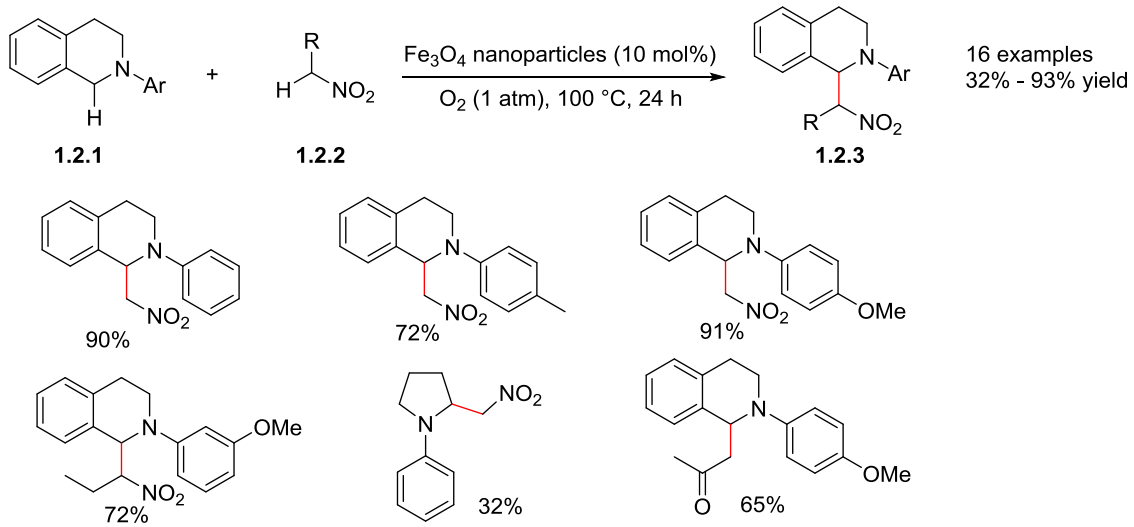

Scheme 1.17 CDC reactions catalyzed by Fe_3O_4 nanoparticle

In Li's protocol, both electron rich and electron deficient aryl groups attached to the nitrogen were tolerated, while higher yield was obtained with electron rich arenes. Nitroalkanes were used both as reactant and solvent; the chain length of nitroalkanes strongly influenced the yield: nitromethane gave the best yield, nitroethane gave a lower yield, and nitropropane gave the lowest yield. Other type of tertiary amine such as 1-phenylpyrrolidine was also tested, giving a much lower yield of desired

[94] a) T. Zeng, G. Song, A. Moores, C.-J. Li, *Synlett* **2010**, 2002; b) P. Liu, C.-Y. Zhou, S. Xiang, C.-M. Che, *Chem. Commun.* **2010**, *46*, 2739; c) M. Rueping, J. Zoller, D. C. Fabry, K. Poscharny, R. M. Koenigs, T. E. Weirich, J. Mayer, *Chem. Eur. J.* **2012**, *18*, 3478; d) Q.-Y. Meng, Q. Liu, J.-J. Zhong, H.-H. Zhang, Z.-J. Li, B. Chen, C.-H. Tung, L.-Z. Wu, *Org. Lett.* **2012**, *14*, 5992; e) R. Hudson, S. Ishikawa, C.-J. Li, A. Moores, *Synlett* **2013**, *24*, 1637; f) H. E. Ho, Y. Ishikawa, N. Asao, Y. Yamamotoab, T. Jin, *Chem. Commun.* **2015**, *51*, 12764.

product. In addition to nitroalkanes, the authors also tried acetone as the coupling partner. The reaction proceeded but with a lower yield.

The reusability of the nanoparticles was tested by the authors. It was shown that the catalyst could be easily recovered and reused nine times without significant loss of catalytic activity. However, despite the robust catalytic activity of the nanoparticles, the use of largely excess nitroalkanes and the limited substrate scope constituted the limitations of this method. Although the authors developed a new $CuFe_2O_4$ nanoparticle that could catalyze the same reaction with higher yields,[94e] the limitation of this reaction was not solved.

Further substrate scope extension of this CDC reaction was achieved by M. Rueping and co-workers through the use of commercially available TiO_2 nanoparticles (Evonik-Degussa Aeroxide P25) as catalyst.[94c] Using this photocatalyst, the authors were able to realize the coupling between compound **1.2.1** and both nitromethane and acetone that Li had accomplished.[94a] Besides, cyanation of compound **1.2.1** was also achieved with the same catalyst, giving high chemical yields (**Scheme 1.18**). Moreover, by replacing TiO_2 with ZnO as the photocatalyst, the authors also succeeded to couple compound **1.2.1** with diethylphosphite, providing the amino-phosphonates **1.2.5** (**Scheme 1.18**).

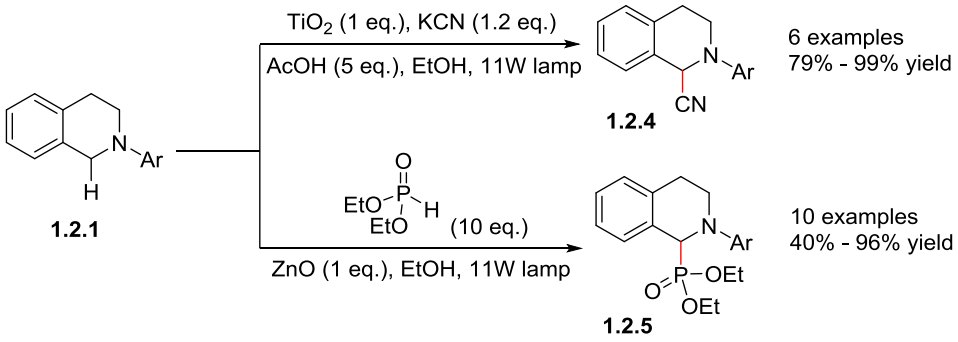

Scheme 1.18 Photocatalyzed CDC reactions

Compared with Li's method, this method used a cheaper and more readily available photocatalyst, which could catalyze the CDC reactions at ambient temperature using ethanol as solvent. Besides, both TiO_2 and ZnO could be recycled by simple centrifugal separation, and they could be reused in the catalytic reactions in consecutive catalytic cycles without loss in reactivity and selectivity. However, this protocol suffered a limitation of the need of stoichiometric amount of catalysts. Decreasing the catalyst loading of TiO_2 resulted in lower yields of the products.

By using the *in situ* generated graphene-supported RuO_2 nanoparticles as catalyst, L.-Z. Wu and co-workers realized the CDC reaction between compound **1.2.1** and **1.2.2**.[94d] Compared with Li's protocol, the graphene-supported RuO_2 nanoparticles required less equivalents of nitroalkanes and lower

reaction temperature. Besides, the use of water as the reaction solvent also made it more environmentally friendly. Moreover, the catalyst could be recycled by simple filtration, and it could be reused for five consecutive catalytic cycles, although a decrease of catalytic activity was observed for the recycled catalyst (89% yield for the first run, 64% yield for the fifth run).

In another publication, various tertiary amines were successfully coupled with a series of nucleophiles catalyzed by a heterogeneous zero-valent nanoporous gold catalyst (AuNPore), which was developed by T. Jin's group.[94f] Using the reaction conditions similar to the work of Li,[94a] Jin was able to realize the same transformation that Li had accomplished for the coupling of compound **1.2.1** and **1.2.2** (**Scheme 1.17**). Besides, more nucleophiles such as dialkyl malonates, methyl ketones, indole derivatives, TMSCN and diethylphosphite were subjected to the CDC reactions with compound **1.2.1a** (Ar = phenyl), yielding the corresponding CDC products. More importantly, Jin extended the CDC reactions to various cyclic and acyclic tertiary amines (**Scheme 1.19**), which largely magnified the substrate scope of this reaction. The reusability of the catalyst was also tested. As a result, the catalytic activity remained unchanged after ten cycles for the reaction of compound **1.2.1a** and nitromethane, yielding 99% of the corresponding product after the tenth cycle.

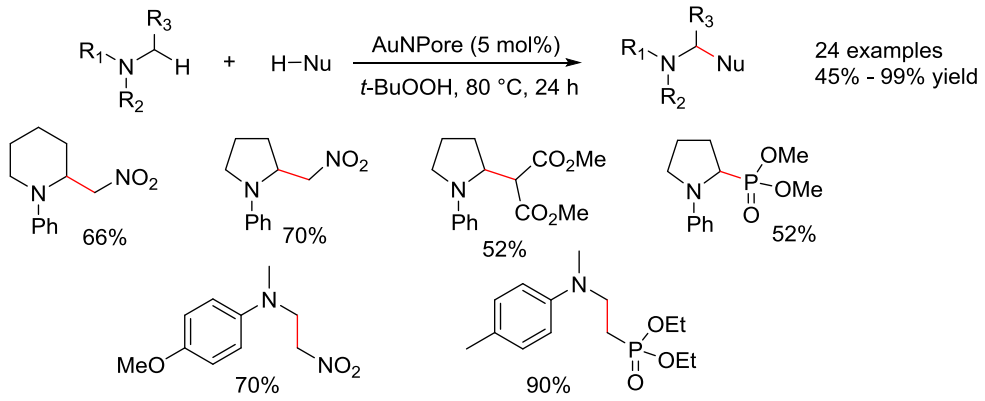

Scheme 1.19 Gold catalyzed CDC reactions of tertiary amines

1.2.2 C-C bond formation through heterogeneously catalyzed dehydrogenative alkenylation

In 2011, J. Y. Ying *et al.* reported a method for the C(sp^2)-C(sp^2) bond formation between anilides and acrylates through a heterogeneous palladium-polyoxometalate (Pd-POM) catalyst with the formula Pd-$H_6PV_3Mo_9O_{40}$/C (Pd-PV_3Mo_9/C) using O_2 as the terminal oxidant.[95] In Ying's protocol, the coupling reactions were strongly depended on the electronic nature of the anilide: the best results were obtained with unsubstituted anilide or methylsubstituted anilides; both electron-withdrawing and electron-donating substituents on the phenyl group gave lower yields (**Scheme 1.20**).

[95] L. L. Chng, J. Zhang, J. Yang, M. Amoura, J. Y. Ying, *Adv. Synth. Catal.* **2011**, *353*, 2988.

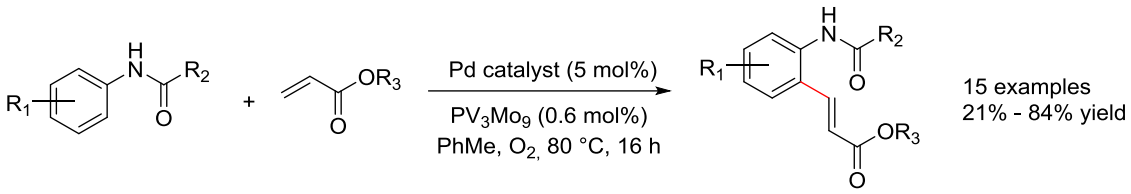

Scheme 1.20 Ying's protocol for the Fujiwara-Moritani reactions

15 substrates were tested by this method, providing moderate to good yields. However, the substrate scope of Ying's protocol was quite narrow, only applicable to the coupling of anilides and acrylates. To determine the active catalytic species, a hot filtration test was done by the authors. After removal of solid catalyst, no further formation of product was observed by heating the filtrate. Inductively coupled plasma-mass spectrometry (ICP-MS) analysis of the filtrate showed a low amount of leaching palladium in the solution (7 ppm), thus confirming the heterogeneous nature of the catalyst. The catalyst could also be separated by centrifugation and reused at least for four times, although reloading of PV_3Mo_9 to the recovered solid should be done prior to the next run and a fractional loss of catalytic activity was observed from the recovered catalyst (76% yield for the first run, 60% yield for the fourth run). It was worth noting that Ying's method was also applied to the C-N bond formation between diarylamines and acrylates, yielding to the corresponding enamines.

1.2.3 C-C bond formation through heterogeneously catalyzed dehydrogenative arylation

The cross-dehydrogenative arylation (CDA) reaction is the most efficient and economic synthetic strategy for the synthesis of arylated compounds. However, the vast majority of CDA reactions were accomplished with homogeneous catalyst, only a handful of examples being reported with heterogeneous catalyst very recently.[96]

In 2016, H. Yoshida and co-workers reported a $C(sp^3)$-$C(sp^2)$ coupling method allowing the arylation of dialkylethers using Pd/TiO_2 as a bifunctional photocatalyst.[96a] The catalyst was obtained by loading palladium nanoparticles on the TiO_2 photocatalyst, and the two metals worked synergistically. Thus, the photocatalyst could activate the $C(sp^3)$-H bond at the α-position of the oxygen atom in various ethers to form a radical species, then the palladium catalyst would promote the formation of the a $C(sp^3)$-$C(sp^2)$ bond between the radical species and benzene to produce the α-arylated ethers (**Scheme 1.21**).

[96] a) A. Tyagi, T. Matsumoto, T. Kato, H. Yoshida, *Catal. Sci. Technol.* **2016**, *6*, 4577; b) K. Matsumoto, M. Yoshida, M. Shindo, *Angew. Chem. Int. Ed.* **2016**, *55*, 5272; c) C. Rajendran, G. Satishkumar, *ChemCatChem* **2017**, *9*, 1284.

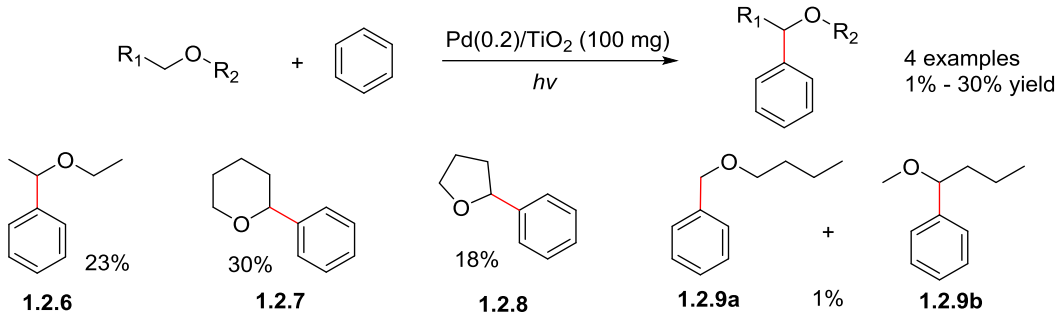

Scheme 1.21 Arylation of dialkylethers catalyzed by bifunctional Pd/TiO_2 photocatalyst

As depicted in **Scheme 1.21**, although this method allowed the quick synthesis of α-arylated ethers, the yields were generally low. Besides, the substrate scope was quite narrow, only benzene was tested as the aromatic source. Therefore, applications of this method were strongly limited.

The first heterogeneous Rh/C catalyzed aerobic oxidative CDC reactions of aryl amines allowing the synthesis of nonsymmetrical biaryls was achieved by M. Shindo's group recently.[96b] Based on their former work on the homocoupling of arylamines,[97] by using sterically hindered substituents on the amino group to prevent homocoupling reactions, the authors succeeded to realize the heterocoupling between aminonaphthalenes and electron-rich arenes (**Scheme 1.22**). Various phenol derivatives and aniline derivatives were coupled with *N*,*N*-dialkyl-2-naphthylamine with moderate to good yields. Gram-scale synthesis of compound **1.2.11** gave a good isolated yield compared with small scale synthesis; moreover, the synthesis of **1.2.11** using a recovered Rh/C also proceeded efficiently, giving a high yield of 93%. Notably, 2-amino-2'-hydroxy-1,1'-binaphthyl (NOBIN) analogue **1.2.13** was synthesized by this method, which could possibly be used in asymmetric catalysis after resolution and act as a source of various ligands.[98]

[97] K. Matsumoto, K. Dougomori, S. Tachikawa, T. Ishii, M. Shindo, *Org. Lett.* **2014**, *16*, 4754.
[98] K. Ding, X. Li, B. Ji, H. Guo, M. Kitamura, *Curr. Org. Synth.* **2005**, *2*, 499.

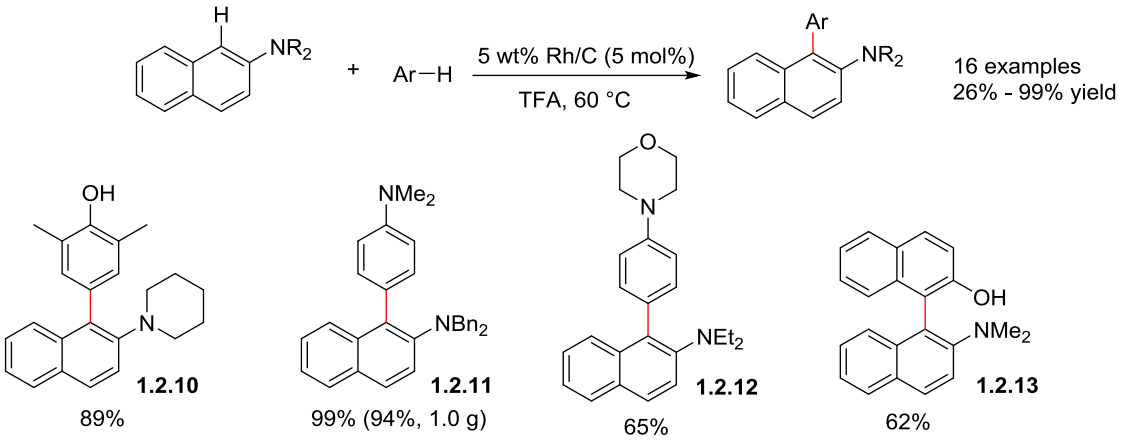

Scheme 1.22 Synthesis of nonsymmetrical biaryls catalyzed by Rh/C

Shindo's protocol provided a mild and operationally simple approach for the synthesis of biaryl amines; the reactions were conducted under an air or oxygen atmosphere with high regioselectivity, some reactions could even be accomplished at room temperature. Unfortunately, the substrate scope of this reaction was narrow (only with *N*,*N*-dialkyl-2-naphthylamines), which was a limitation of this reaction.

Recently, G. Satishkumar developed a method for the coupling between biphenylmethane and various substituted anisole by using a heterogeneous iron catalyst Fe/SBA-15 (iron grafted over mesoporous silica).[96c] Ten examples were presented using the iron catalyzed CDA reactions with moderate isolated yields (**Scheme 1.23**). The coupling occurred regioselectively at the *para* position of the methoxy group, or *meta* position if *para* position was blocked.

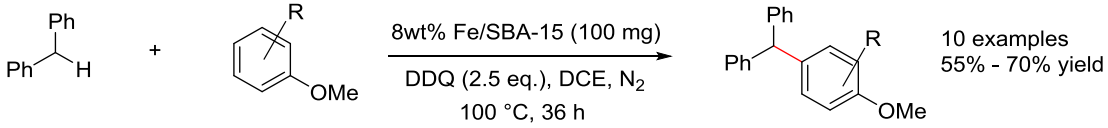

Scheme 1.23 Iron catalyzed arylation of biphenylmethane

Notably, the iron catalyst was also effective for the coupling of arenes and arylboronic acids. A recycling study of the catalyst was performed for this coupling reaction. As a result, the catalyst could be successfully recycled for 5 times without significant loss in its activity. Overall, Satishkumar's protocol offered a practical way to construct C(sp^3)-C(sp^2) bond through dehydrogenative coupling. However, only diarylmethanes were used as substrates in this publication, which limited the substrate scope of this reaction.

1.2.4 C-C bond formation through heterogeneously catalyzed dehydrogenative alkynylation

In 2013, A. Corma *et al.* developed a method allowing the coupling between electron-rich arenes and propiolate in the presence of O_2 by gold nanoparticles (**Scheme 1.24**).[99] However, this method was effective only with a quite limited number of substrates, and the propiolate underwent cyclotrimerization to form benzene derivatives without the presence of molecular oxygen or Michael addition to form styrene derivatives with cationic gold species. A hot filtration test was carried out for the dehydrogenative coupling, revealing that no active species were present in the solution after filtration. Thus, the reaction might occur at the surface of the catalyst.

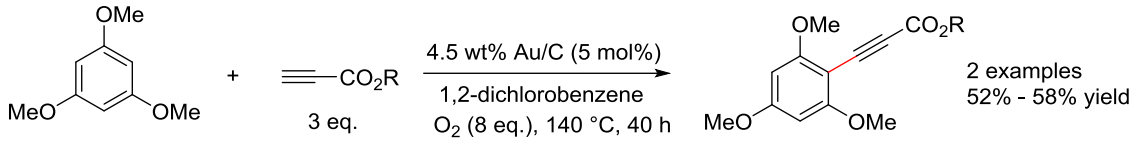

Scheme 1.24 Gold catalyzed dehydrogenative alkynylation of electron-rich arenes

As mentioned above, Li and co-workers developed two heterogeneous catalysts, Fe_3O_4 nanoparticles and $CuFe_2O_4$ nanoparticles, allowing the formation of C(sp^3)-C(sp^3) bonds.[94a, e] In fact, the latter could also catalyze the formation of C(sp^3)-C(sp) bond (**Scheme 1.25**).[94e] Thus, the copper activated the terminal C(sp)-H bond of the alkyne, then it was coupled with the iminium (formed by the oxidation of compound **1.2.1**) to form the propargylamine product (**Scheme 1.26**).

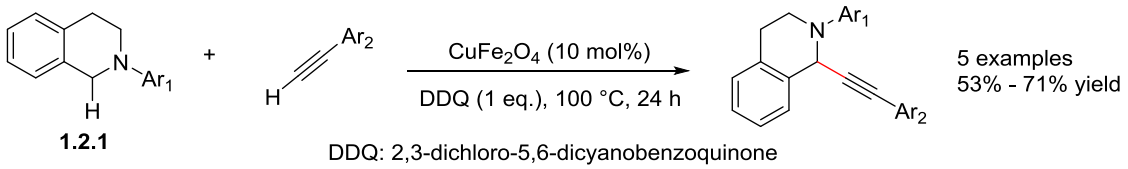

Scheme 1.25 $CuFe_2O_4$ nanoparticle catalyzed dehydrogenative alkynylation

[99] A. Leyva-Pérez, J. Oliver-Meseguer, J. R. Cabrero-Antonino, P. Rubio-Marqués, P. Serna, S. I. Al-Resayes, A. Corma, *ACS Catal.* **2013**, *3*, 1865.

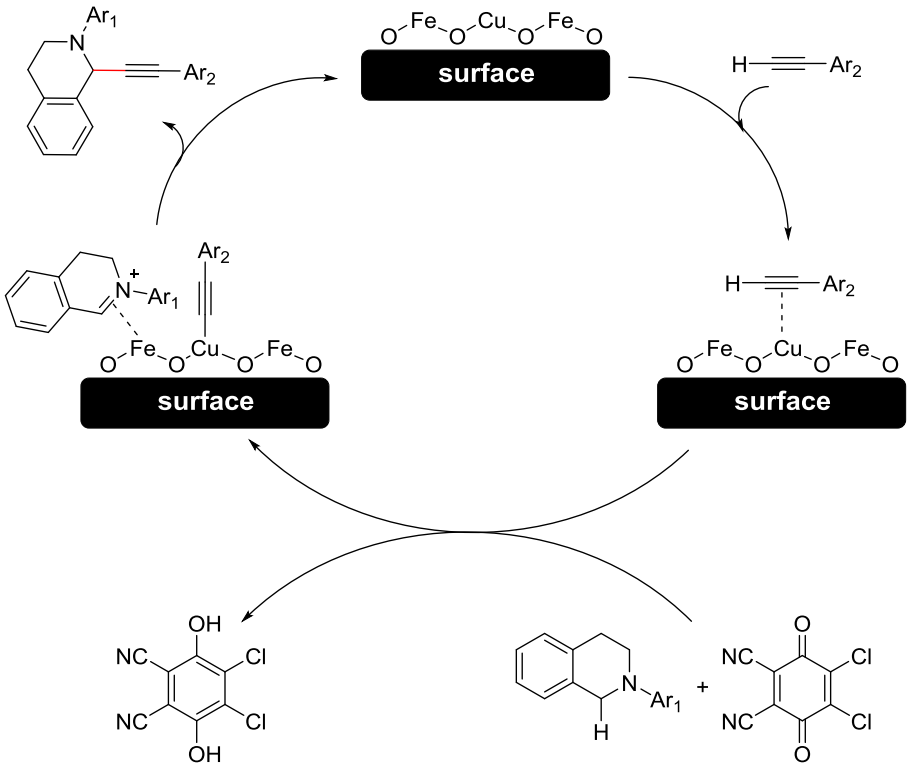

Scheme 1.26 Proposed reaction mechanism for $CuFe_2O_4$ catalyzed alkynylation

In order to establish the active catalytic species of the reaction, a hot filtration test was conducted by the authors. No further reaction was observed after the removal of the solid catalyst, suggesting that no homogeneous catalyst was produced by leaching during the reaction. In addition, ICP analysis of the filtrate showed that less than 0.39 ppm of dissolved copper was present in solution. The reusability of the catalyst was also examined, showing that the catalyst was still active after ten runs without significant loss of catalytic activity. These results strongly suggested a heterogeneous mechanism of the reaction.

A commercially available metal-organic framework MOF-199, a highly porous metal-organic framework based on copper ions which is formerly used in the field of gas separation and storage, was used as heterogeneous catalyst for the C(sp^3)-C(sp) coupling between *N*,*N*-dimethylanilines and terminal alkynes by T. Truong, N. T. S. Phan and co-workers (**Scheme 1.27**).[100] According to the authors, copper was essential for the C(sp^3)-C(sp) bond formation, since no product was detected when using cobalt or nickel complexes as catalysts. Besides, the solvent and oxidant also had an influence on the reaction conversion. The MOF-199 catalyst was easily recovered by filtration, and it remained active after ten catalytic cycles without a significant loss of catalytic activity. The reaction

[100] G. H. Dang, D. T. Nguyen, D. T. Le, T. Truong, N. T. S. Phan, *J. Mol. Catal. A: Chem.* **2014**, *395*, 300.

was blocked after removal of the solid catalyst, since no further conversion was observed when heating the filtrate under the same reaction conditions, supporting thus a heterogeneous catalysis.

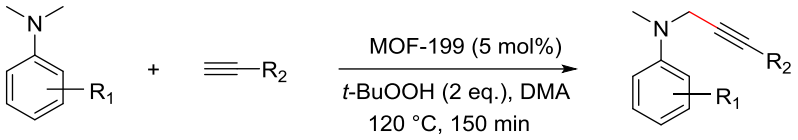

Scheme 1.27 C(sp^3)-C(sp) bond formation catalyzed by MOF-199

Generally speaking, the heterogeneously catalyzed dehydrogenative alkynylation reactions were less explored, and the substrate scope remained very limited. Only a handful of methods were developed dealing with some specific substrates. The development of methods for the coupling between various amines and terminal alkynes is still challenging for synthetic chemists.

1.2.5 C-C bond formation through heterogeneously catalyzed dehydrogenative homocoupling

Intermolecular dehydrogenative homocoupling of (hetero)arenes is one of the most useful tools for the preparation of symmetrically substituted 1,1'-biaryls. These 1,1'-biaryls are usually used as ligands for various transformations, including asymmetric catalysis.[101] Despite the usefulness of 1,1'-biaryls, there are only few methods to synthesize them. Among the methods reported, some of them were achieved using heterogeneous catalysts.[102, 103] However, although these 1,1'-biaryls were all obtained using dehydrogenative coupling, most of them were obtained through radical coupling reactions, but not a C-H activation process.[102] The only reaction involving the C-H activation process is the homocoupling of pyridine derivatives.[103]

In 2008, H. E. Hagelin-Weaver reported a method for the synthesis of 4,4'-dimethyl-2,2'-bipyridine through C-H activation by using palladium catalysts supported on nanoparticle alumina [Pd/nano-Al_2O_3(+)] (**Scheme 1.28**).[103c] Although previous methods were available to obtain 2,2'-bipyridines through dehydrogenative homocoupling of pyridine derivatives, the yields were generally quite low (less than 10%).[103a,b] In this context, through the preparation of various Pd/nano-Al_2O_3(+) synthesized from different methods, the authors discovered that the catalyst obtained from palladium precipitated onto nano-Al_2O_3(+) gave the best yield (75% or more of the raw yields). Interestingly, the

[101] a) L. Pu, *Chem. Rev.* **1998**, *98*, 2405 ; b) P. Kočovský , Š. Vyskočil , M. Smrčina, *Chem. Rev.* **2003**, *103*, 3213; c) Y. Chen, S. Yekta, A. K. Yudin, *Chem. Rev.* **2003**, *103*, 3155.

[102] a) T. Sakamoto, H. Yonehara, C. Pac, *J. Org. Chem.* **1997**, *62*, 3194; b) M. L. Kantam, B. Kavita, F. Figueras, *Catal. Lett.* **1998**, *51*, 113; c) H. Fujiyama, I. Kohara, K. Iwai, S. Nishiyama, S. Tsuruya, M. Masai, *J. Catal.* **1999**, *188*, 417; d) E. Armengol, A. Corma, H. García, J. Primo, *Eur. J. Org. Chem.* **1999**, 1915; e) P. Mastrorilli, F. Muscio, G. P. Suranna, C. F. Nobile, M. Latronico, *J. Mol. Catal. A* **2001**, *165*, 81; f) M. R. Prasad, G. Kamalakar, S. J. Kulkarni, K. V. Raghavan, *J. Mol. Catal. A* **2002**, *180*, 109; g) K. Iwai, T. Yamauchi, K. Hashimoto, T. Mizugaki, K. Ebitani, K. Kaneda, *Chem. Lett.* **2003**, *32*, 58; h) M. Matsushita, K. Kamata, K. Yamaguchi, N. Mizuno, *J. Am. Chem. Soc.* **2005**, *127*, 6632; i) K. Matsumoto, K. Dougomori, S. Tachikawa, T. Ishii, M. Shindo, *Org. Lett.* **2014**, *16*, 4754.

[103] a) G. D. F. Jackson, W. H. F. Sasse, C. P. Whittle, *Aust. J. Chem.* **1963**, *16*, 1126; b) P. E. Rosevear, W. H. F. Sasse, *J. Heterocycl. Chem.* **1971**, *8*, 483; c) L. M. Neal, H. E. Hagelin-Weaver, *J. Mol. Catal. A: Chem.* **2008**, *284*, 141.

homocoupling reaction was very sensitive to the quality of the 4-methylpyridine, which must be distilled over KOH in order to achieve high yields.

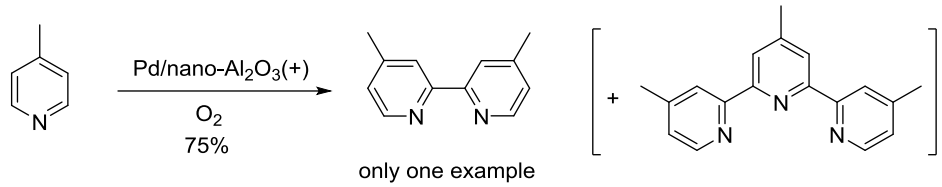

Scheme 1.28 Homocoupling of 4-methylpyridine catalyzed by Pd/nano-Al_2O_3(+)

Hagelin-Weaver's method improved significantly the efficiency for the homocoupling of 4-methylpyridine. However, according to the authors, this method was probably not applicable to other pyridine derivatives, since the yield was strongly dependent on the quality of substrate. Thus, the application of this method was limited.

1.3 Summary and perspectives of CDC reactions through heterogeneous catalysis

The development of heterogeneous catalysis is important and it is urgent to fulfil the growing need of green chemistry processes. The recyclability and reusability of heterogeneous catalysts make them more environmentally friendly and economic. However, compared with homogeneous catalysis, it remains to be explored more deeply, especially in the field of C-H activation. As reviewed above, the more attractive CDC processes are still rarely reported. The existing works also have a general drawback of limited substrate scope and low isolated yields compared with similar transformations catalyzed by homogeneous catalysts. Thus, the development of new methods using heterogeneous catalysts, especially commercially available and less expensive ones, is a challenging and promising field.

2 The discovery of new C-H activation reactions

2.1 Exploring new C-H activation reactions catalyzed by ruthenium heterogeneous catalyst

Based on our previous C-H deuteration experiments (Chapter1, section 2.6), we found that several heterocycles, such as pyridine derivatives, indoles and quinoline, were very good substrates for deuterium labeling. Thus, we chose these compounds as model substrates to explore the potential reactivity of ruthenium nanoparticles in cross coupling reactions with various coupling partners (**Scheme 2.1**).

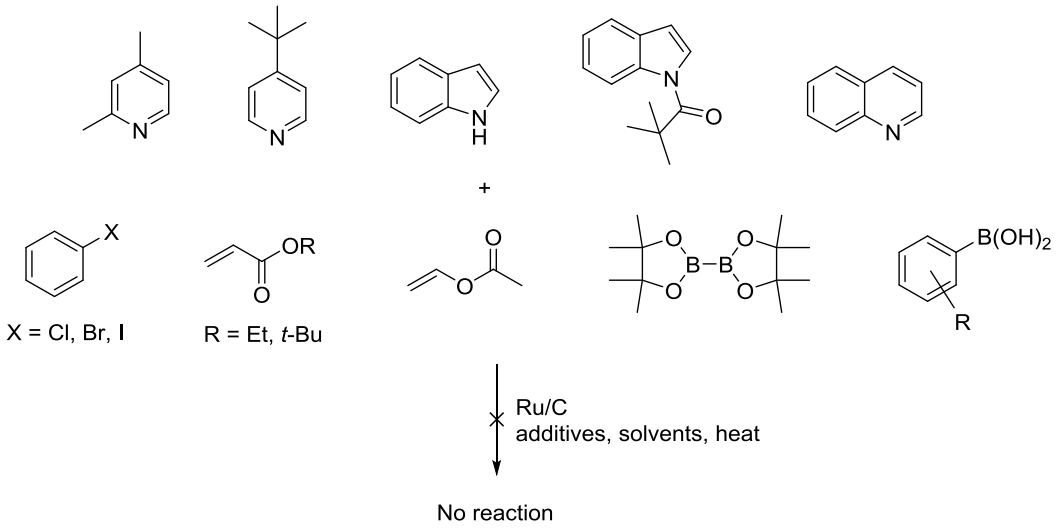

Scheme 2.1 Substrates used for the coupling reactions catalyzed by Ru/C

Since the deuteration proceeded efficiently with these substrates, the C-H bonds of these compounds should be able to be activated. As shown in **Scheme 2.1**, despite the use of various coupling partners, including aryl halides, acrylates, vinyl ester, bis(pinacolato)diboron and aryl boronic acids, and the screening of reaction conditions including solvents, additives and reaction temperature, no desired coupling products were detected by LC-MS analysis of the crude reaction mixtures. Thus, the results might be due to two possible reasons: one was that for deuteration, the catalyst surface was reduced under D_2 atmosphere; while for coupling reactions, the catalyst surface remained unchanged and might contain some Ru-oxo species.[87] The other reason might be due to the different mechanisms of deuteration and coupling reactions: for deuteration, the deuterium gas was dissociated at the surface of Ru-particles, and our group has found that the high mobility and diffusion of hydrides/deuterides on the surface of ruthenium nanoparticles could lower down the energy barrier of C-H activation, thus promoting the activation of C-H bonds.[104] As soon as the C-H bond was activated by the ruthenium

[104] C. Taglang, L. M. Martínez-Prieto, I. del Rosal, L. Maron, R. Poteau, K. Philippot, B. Chaudret, S. Perato, A. S. Lone, C. Puente, C. Dugave, B. Rousseau, G. Pieters, *Angew. Chem. Int. Ed.* **2015**, *54*, 10474.

catalyst, the H/D exchange could take place and then be followed by reductive elimination to form deuterated molecules. In the case of coupling reactions, the energy barrier of C-H activation was higher due to the lack of hydrides/deuterides, and the coupling partners might have weaker affinities to ruthenium centers than the heterocycles, thus the formation of C-C bond was hindered even if the C-H activation occurred.

More positive results were obtained using 2-phenylpyridine as substrate, which was also a good substrate for deuterium labeling. The phenyl ring of compound **2.1.1** was efficiently deuterated at position 1, thus confirming the activation of phenyl C-H bonds by ruthenium nanoparticles. In this context, several coupling partners were tested with 2-phenylpyridine, including phenyl halides, vinyl esters and *N*-bromosuccinimide (NBS). To our delight, when treating NBS with 2-phenylpyridine using 10 mol% of Ru/C in dichloroethane (DCE) at 80 ℃, we observed the formation of trace amount of brominated product by LC-MS analysis of the crude product (**Scheme 2.2**). Thus, an attempt to increase the conversion of bromination product was conducted, including the screening of additives, solvents and reaction temperatures.

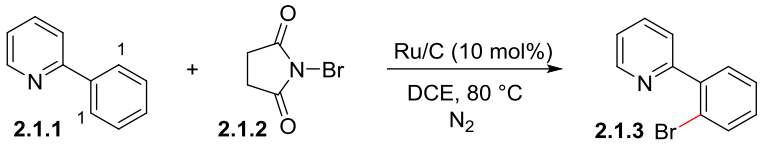

Scheme 2.2 Ru/C catalyzed bromination of 2-phenylpyridine

Interestingly, when using AcOH as solvent, we detected a trace amount of homocoupling product **2.1.4** together with trace amount of brominated product **2.1.3** (**Scheme 2.3**). To the best of our knowledge, there has never been described using a heterogeneous species as catalyst or pre-catalyst for such kind of dehydrogenative homocoupling reactions. Thus, we diverted our attention to the investigation of this reaction.

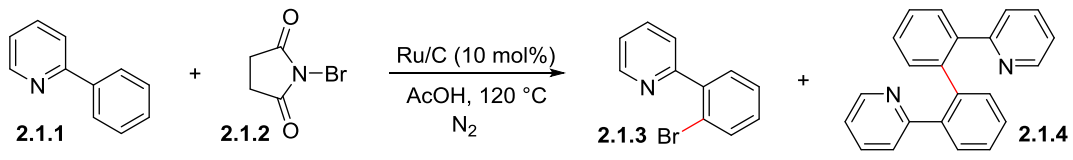

Scheme 2.3 Formation of homocoupling product

Firstly, we run the homocoupling reaction without the use of NBS. Interestingly, more homocoupling product was detected. In order to obtain the isolated yield of this reaction, a reaction using 1 mmol of

substrate was conducted. As a result, homocoupling product **2.1.4** was isolated with 21% yield (**Table 2.1**, Entry 2). Encouraged by this result, optimization of reaction conditions was conducted for this transformation (**Table 2.1**). Conducting the reaction under air gave no desired product (Entry 3); the use of other organic solvents also gave no conversion of the reaction (Entry 4-7); the reaction didn't proceed by replacing Ru/C with ruthenium nanoparticle RuNp@PVP or Rh/C (Entry 8, 9), demonstrating the robust catalytic activity of Ru/C. Considering that an oxidant might accelerate the homocoupling process, 1 equivalent of oxone was added to the reaction mixture. However, no desired product was observed (Entry 10). When using 1 equivalent of $FeCl_3$ as the oxidant, a much higher conversion was detected by ^1H NMR of the crude reaction mixture (Entry 11). No reaction was observed without the use of Ru/C as catalyst (Entry 12), indicating that the active catalyst was the ruthenium species and not the iron one. Having this encouraging result in hands, we started to investigate carefully this transformation. Thus, a detailed literature study was first carried out prior to further experimental investigations.

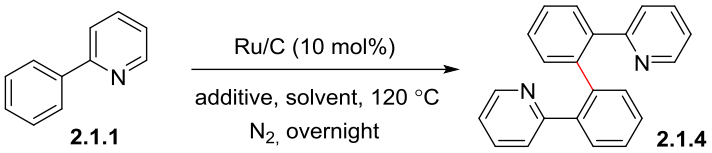

Entry	Additive	Solvent	Conversion [a]
1	2 eq. NBS	AcOH	Trace
2	-	AcOH	21% [b]
3[c]	-	AcOH	0%
4	-	MeOH	0%
5	-	MeCN	0%
6	-	PhMe	0%
7	-	Pyridine	0%
8[d]	-	AcOH	0%
9[e]	-	AcOH	0%
10	1 eq. Oxone	AcOH	0%
11	1 eq. $FeCl_3$	AcOH	1:0.92 [f]
12[g]	1 eq. $FeCl_3$	AcOH	0%

Table 2.1 Optimization of reaction conditions for homocoupling of 2-phenylpyridine

[a]: conversion was determined by ^1H NMR; [b]: isolated yield using 1 mmol of 2-phenylpyridine; [c]: reaction run under air; [d]: 10 mol% of RuNp@PVP was used as catalyst; [e]: 10 mol% of Rh/C was used as catalyst; [f]: ratio of **2.1.1**:**2.1.4** determined by ^1H NMR; [g]: no catalyst was added.

2.2 Literature review for the homocoupling of 2-arylpyridines

There are several research groups that have reported the homocoupling of 2-arylpyridines.[105] Among them, M. S. Sanford reported the first method which used $Pd(OAc)_2$ as catalyst and oxone as oxidant for this transformation (**Scheme 2.4**).[105a] Using 2-*o*-tolylpyridine **2.2.1** as substrate, the authors optimized the reaction conditions by investigating a variety of oxidants, solvents and catalysts, finding that $Pd(OAc)_2$ was the most active catalyst and oxone was the best oxidant. Interestingly, Sanford discovered that the homocoupling reaction gave a better yield when the reaction was conducted at room temperature rather than elevated temperature (60 ℃) in most solvents, because significant amounts of *ortho*-functionalization products were formed through the reaction between 2-arylpyridine and the solvent as a function of temperature.[106]

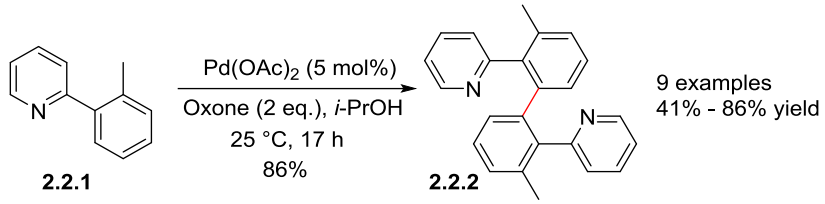

Scheme 2.4 Sanford's protocol for the homocoupling of 2-arylpyridines

Despite the mild reaction conditions of Sanford's protocol, the homocoupling of 2-phenylpyridine gave a much lower yield (42%) due to further oligomerization of the product. Besides, when *meta*-substituted substrates were used, a poor regioselectivity was observed. For example, the homocoupling of compound **2.2.3** gave two regioisomers, the symmetrical product **2.2.4a** from the coupling at 6,6-positions and the unsymmetrical product **2.2.4b** from the coupling at 2,6-positions, with a ratio of 1.7:1 (**Scheme 2.5**). Mechanistic studies were performed by the authors (**Scheme 2.6**),[105a, 107] suggesting that the coupling product was obtained by two sequential C-H activation processes involving a Pd^{II} and a Pd^{IV} complexes, respectively. Firstly, the C-H bond at 2-position of the phenyl ring was activated by $Pd(OAc)_2$ through oxidative addition to form intermediate **M1**, which was subsequently oxidized by oxone to give Pd^{IV} species **M2**. Ligand exchange followed by a second C-H

[105] a) K. L. Hull, E. L. Lanni, M. S. Sanford, *J. Am. Chem. Soc.* **2006**, *128*, 14047; b) X. Chen, G. Dobereiner, X.-S. Hao, R. Giri, N. Maugel, J.-Q. Yu, *Tetrahedron* **2009**, *65*, 3085; c) X. Guo, G. Deng, C.-J. Li, *Adv. Synth. Catal.* **2009**, *351*, 2071; d) L. Ackermann, P. Novák, R. Vicente, V. Pirovano, H. K. Potukuchi, *Synthesis* **2010**, 2245; e) F. Saito, H. Aiso, T. Kochi, F. Kakiuchi, *Organometallics* **2014**, *33*, 6704; f) W. Liu, Y. Zhu, C.-J. Li, *Synthesis* **2016**, *48*, 1616; g) Y. Xie, D. Xu, W.-W. Sun, S.-J. Zhang, X.-P. Dong, B. Liu, Y. Zhou, B. Wu, *Asian J. Org. Chem.* **2016**, *5*, 961.

[106] a) A. R. Dick, K. L. Hull, M. S. Sanford, *J. Am. Chem. Soc.* **2004**, *126*, 2300; b) L. V. Desai, H. A. Malik, Melanie S. Sanford, *Org. Lett.* **2006**, *8*, 1141.

[107] a) S. R. Whitfield, M. S. Sanford, *J. Am. Chem. Soc.* **2007**, *129*, 15142; b) J. M. Racowski, A. R. Dick, M. S. Sanford, *J. Am. Chem. Soc.* **2009**, *131*, 10974.

activation gave intermediate **M3**, which gave homocoupling product **2.2.6** through reductive elimination.

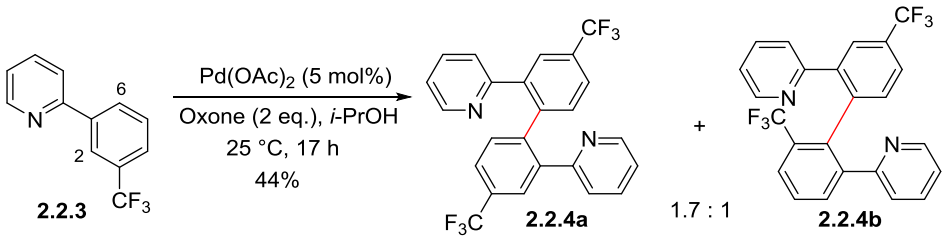

Scheme 2.5 Homocoupling of *m*-substituted compound **2.2.3**

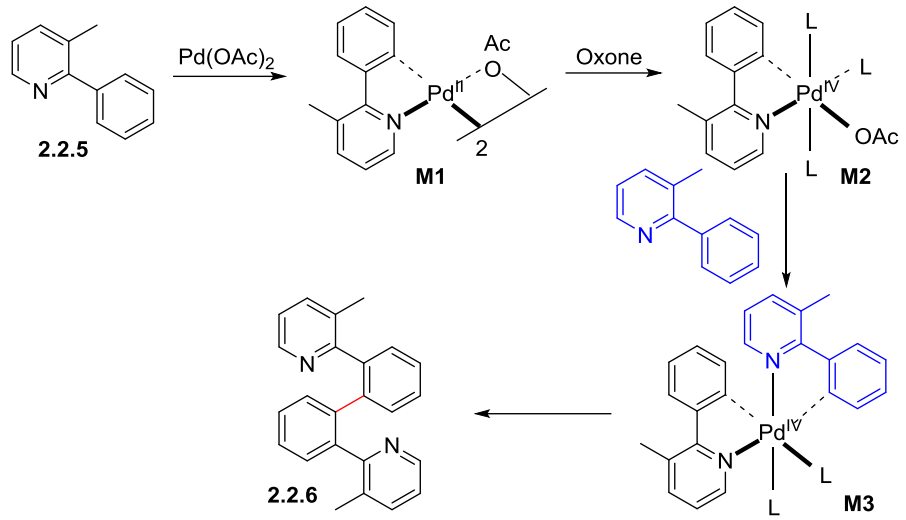

Scheme 2.6 Proposed mechanism for the homocoupling of 2-arylpyridines

Later in 2009, J.-Q. Yu *et al.* reported a similar homocoupling reaction by an *in situ* iodination followed by a $Cu(OAc)_2$ mediated Ullmann coupling to give the homocoupling products (**Scheme 2.7**).[105b] In Yu's protocol, stoichiometric amount of $Cu(OAc)_2$ and I_2 were employed. Interestingly, the solvent strongly affected the reaction outcome: when using iodobenzene as solvent, the homocoupling reaction proceeded smoothly; while the use of tetrachloroethane as solvent resulted in iodination product only.[108] Besides, decreasing the amount of either the solvent, $Cu(OAc)_2$ or I_2 led to lower yields of the product. The regioselectivity of this reaction was demonstrated by the homocoupling of *m*-fluorinated substrate and 2-(naphthalen-2-yl)pyridine: the former gave a single regioisomer product **2.2.7** derived from the homocoupling of less steric hindered C-H bonds, while the latter gave two regioisomer products, symmetrical product **2.2.8a** from the coupling of less steric hindered 3,3-positions and unsymmetrical product **2.2.8b** from the coupling at 1,3-positions, with a ratio of 2:1.

[108] X. Chen, X.-S. Hao, C. E. Goodhue, J.-Q. Yu, *J. Am. Chem. Soc.* **2006**, *128*, 6790.

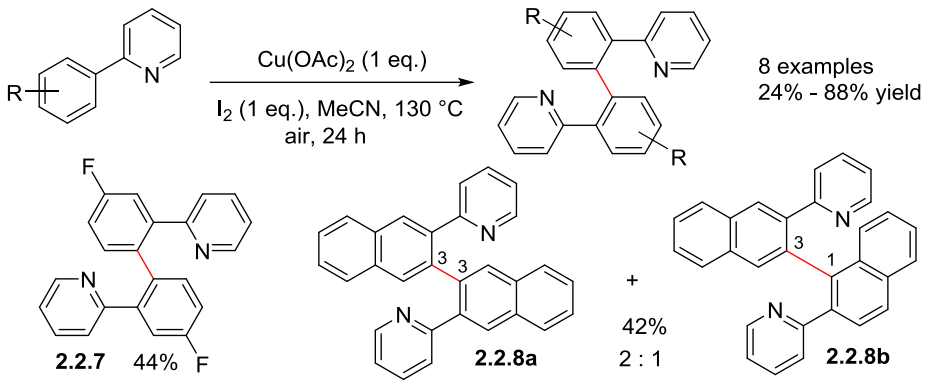

Scheme 2.7 Yu's protocol for the homocoupling of 2-arylpyridines

Although no experiment was conducted to demonstrate the reaction mechanism, the authors proposed that the homocoupling product was formed through the Ullmann coupling of iodinated 2-phenylpyridine, which was formed by a single electron transfer (SET) or electrophilic metalation. The advantage of this method is the use of cheap reagents such as $Cu(OAc)_2$ and I_2, and the fact that the reaction is not air sensitive. However, the narrow substrate scope and the generally low yields limited the application of this method. Moreover, the use of stoichiometric amount of metal catalyst does not fit the requirement of green chemistry.

A ruthenium catalyzed oxidative homocoupling reaction of 2-arylpyridines was developed by G. Deng and C.-J. Li *et al.* (**Scheme 2.8**).[105c] Under their reaction conditions, the yield of homocoupling product was influenced by the amount of oxidant used: the yield decreased both with a lower amount (0.5 equiv.) or a higher amount (1 equiv.) of the oxidant. The authors explained that with more $FeCl_3$ being added, it coordinated with the nitrogen atom in 2-phenylpyridine, which prevented the coordination of ruthenium at the same site, thus reducing the efficiency of the coupling process. Various substituted 2-arylpyridines were used as substrates under their reaction conditions, giving moderate to good yields. No obvious influence of the electronic effects on the phenyl ring was observed, while steric effects played an important role. For example, high yields were obtained for the homocoupling of 2-(*m*-tolyl)pyridine and 2-(*p*-tolyl)pyridine (**Scheme 2.8**, compound **2.2.9** and **2.2.10**), while the use of 2-(*o*-tolyl)pyridine as substrate resulted in very low yield even with a longer reaction time (**Scheme 2.8**, compound **2.2.2**). A methyl substituent at the 2-position of the pyridine ring completely blocked the reaction because the methyl group prevented ruthenium from coordinating to the nitrogen atom (**Scheme 2.8**, compound **2.2.11**). The regioselectivity of this method was demonstrated by the homocoupling of 3-methylated substrate, which yielded in a single regioisomer product **2.2.9** derived from the homocoupling of less steric hindered C-H bonds.

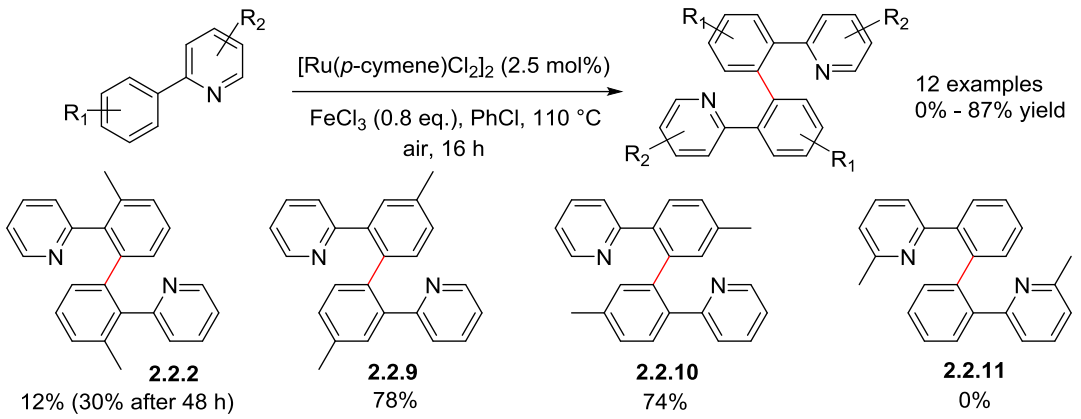

Scheme 2.8 Deng and Li's protocol for the homocoupling of 2-arylpyridines

Same as Yu's work, no experiment was conducted to demonstrate the reaction mechanism. The advantage of this method was the good regioselectivity when dealing with *meta*-substituted substrates, despite only one example was described by the authors.

Later in 2016, Li reported a new method for this transformation.[105f] The new method combined the works of Sanford and Yu, using $Pd(OAc)_2$ as catalyst and I_2 as oxidant (**Scheme 2.9**). Using this method, 2-(2-naphthyl)pyridine was regioselectively homocoupled at the less steric hindered 3,3-positions to give compound **2.2.8a** as product (**Scheme 2.7**). However, the reaction did not take place using a *para*-acetyl substituted substrate, probably due to the competing coordination of the carbonyl group to the catalyst. Moreover, low yield (28%) was obtained when *p*-chloro substituent at the phenyl group was employed as the substrate.

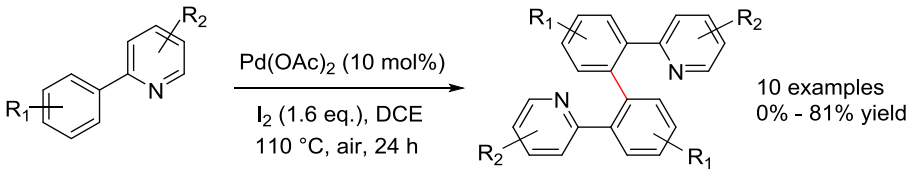

Scheme 2.9 Li's protocol for the homocoupling of 2-arylpyridines

A plausible mechanism was proposed by the authors. Similar to Yu's proposed mechanism, Li's one involved the formation of 2-(2-iodophenyl)pyridine. However, different from the proposed Ullmann coupling mechanism by Yu, Li indicated that the homocoupling product was formed through the reductive elimination of the Pd^{IV} species, which was formed by the addition of the 2-(2-iodophenyl)pyridine to Pd^{II} species. However, the 2-(2-iodophenyl)pyridine intermediate was not isolated by the authors, making the proposed mechanism less reliable. Compared with the pervious

method developed by Deng and Li, this method had no obvious advantage: no improvement of the yields; no better regioselectivity; no wider substrate scope. It could only be considered as an alternative method for the homocoupling of 2-arylpyridines.

The ruthenium complex $[Ru(p\text{-cymene})Cl_2]_2$ was also employed by L. Ackermann's group for the oxidative homocoupling of 2-arylpyridines.[105d] In Ackermann's protocol, 2,4,6-trimethylbenzoic acid ($MesCO_2H$) was used as an additive, while aryl chloride **2.2.12** was used as the oxidant, which acted as a hydrogen acceptor. Several *o*-substituted 2-phenylpyridines were successfully homocoupled using these reaction conditions. Arenes with other heterocycles such as pyrazole and 1,2,3-triazole also reacted to give the homocoupling products **2.2.14** and **2.2.15** with good yields. However, 1,2,3-triazole derivative with a methoxy substituent at the *ortho*-position of the phenyl ring didn't react under the reaction conditions, and no explanation was given by the authors. Notably, only electron-rich *ortho*-alkylated arenes gave good yields of products using this method, since poor yields were obtained when using electron-deficient substrates (**Scheme 2.10**, compound **2.2.13**).

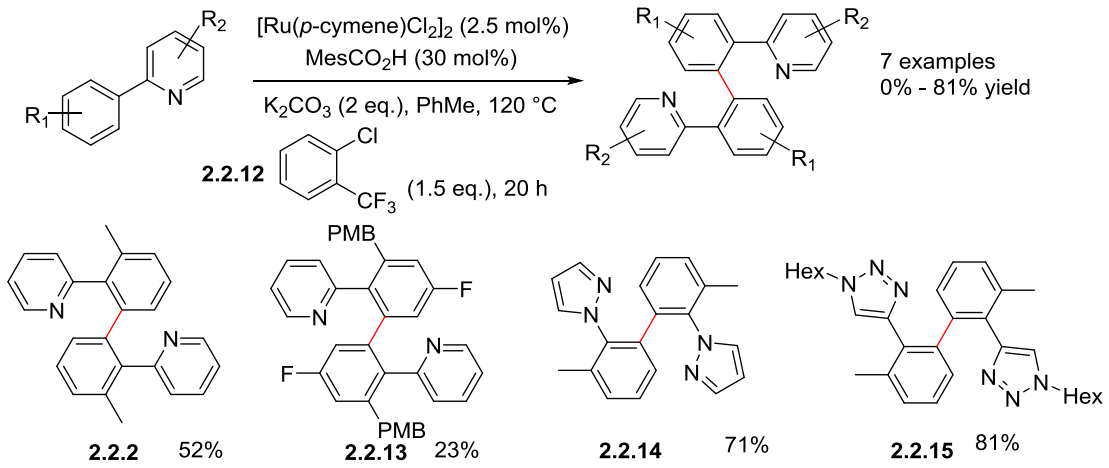

Scheme 2.10 Ackermann's protocol for the homocoupling of 2-arylpyridines

Taking advantage of electrochemistry, F. Kakiuchi and co-workers also developed a method for the homocoupling of 2-arylpyridines using $Pd(OAc)_2$ as catalyst in the presence of I_2 (**Scheme 2.11**).[105e] As shown in **Scheme 2.11**, Fakiuchi's method allowed the obtention of good regioselectivity for the homocoupling of *meta*-substituted substrates (only the products derived from the homocoupling of less steric hindered C-H bonds were obtained). According to these results, the authors proposed that the reaction mechanism was different from the one that Sanford had proposed: after the activation of the first C-H bond by $Pd(OAc)_2$, a second C-H bond was activated to form the doubly chelated Pd(II) species **M5**, which was followed by reductive elimination to form the homocoupling product (**Scheme 2.12**). This mechanism involved the formation of a doubly chelated Pd(II) intermediate **M5**, so a

higher substrate concentration might facilitate the formation of **M5**. Thus, the reaction was conducted under different substrate concentrations, finding that the yield of homocoupling product was increased with the increase of the substrate concentration, which supported the proposed mechanism.

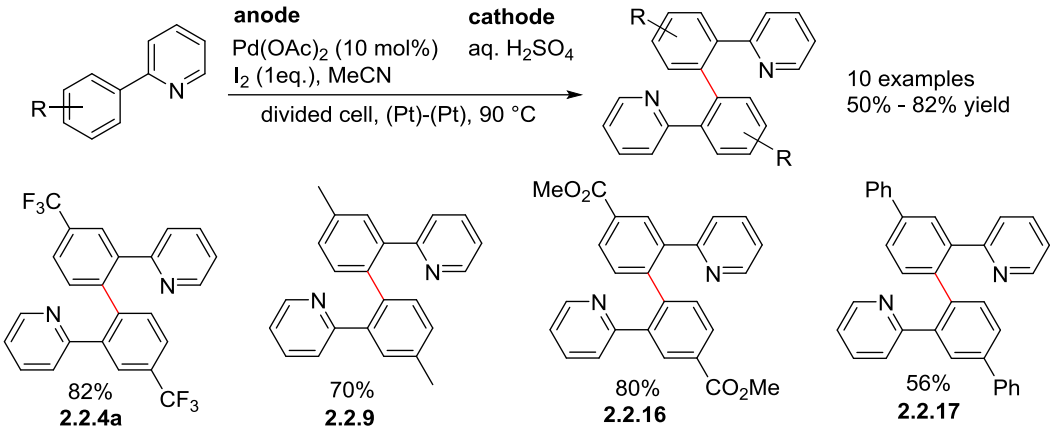

Scheme 2.11 Kakiuchi's protocol for the homocoupling of 2-arylpyridines

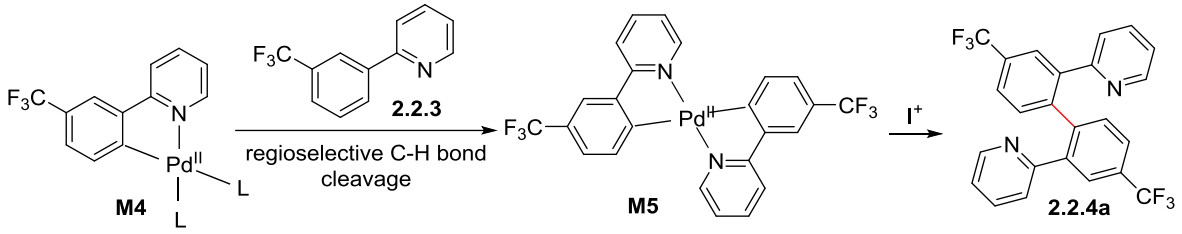

Scheme 2.12 Proposed reaction mechanism for the electrochemical homocoupling of **2.2.3** with I_2

The advantage of this method was the good regioselectivity of the reactions: a single regioisomer was obtained with *meta*-substituted substrates. Besides, this method tolerated a series of functional groups such as ester group, bromide and trifluoromethyl group. Unfortunately, the isolated yields of the products were generally moderate.

Recently, B. Liu, Y. Zhou and B. Wu reported a method allowing the homocoupling of 2-arylpyridines using $Co(OAc)_2$ as catalyst and $PhI(OAc)_2$ and O_2 as the co-oxidants in the presence of a base in acetic acid (**Scheme 2.13**).[105g] Three different reaction conditions were used for all substrates (**Scheme 2.13**, Conditions A-C). Substrates with different substituents were tested under the three reaction conditions, and the results indicated that the substrates with electron-withdrawing groups on the phenyl ring gave higher isolated yields of the homocoupling products than the ones containing electron-donating groups. Besides, the use of a lower catalyst loading sometimes led to higher isolated yields of the desired

homocoupling products than the use of a higher catalyst loading (**Scheme 2.13**, compounds **2.2.18-2.2.20**, yields from Condition A and C). The regioselectivity of the method was demonstrated by the homocoupling of substrate with *meta*-bromo group on the phenyl ring, giving the sole product **2.2.20** deriving from the homocoupling of less steric hindered C-H bonds. Moreover, the authors also conducted the cross-coupling reaction between two different 2-phenylpyridine derivatives **2.2.21** and **2.2.22** for the first time under Condition C (**Scheme 2.14**, the equivalents of the catalyst and reagents were calculated according to the total molar amount of **2.2.21** and **2.2.22**). As a result, the heterocoupling product **2.2.23** was obtained as the main product together with the two homocoupling products **2.2.18** and **2.2.24**, although the selectivity was moderate.

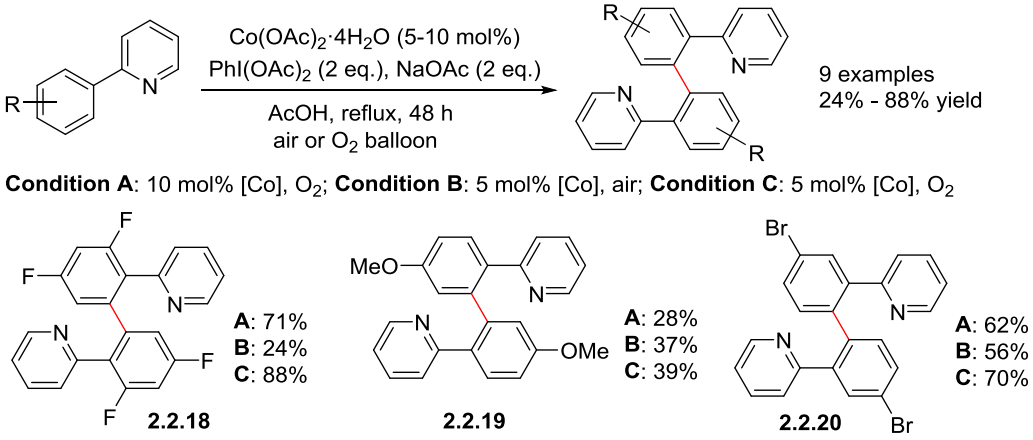

Scheme 2.13 Liu, Zhou and Wu's protocol for the homocoupling of 2-arylpyridines

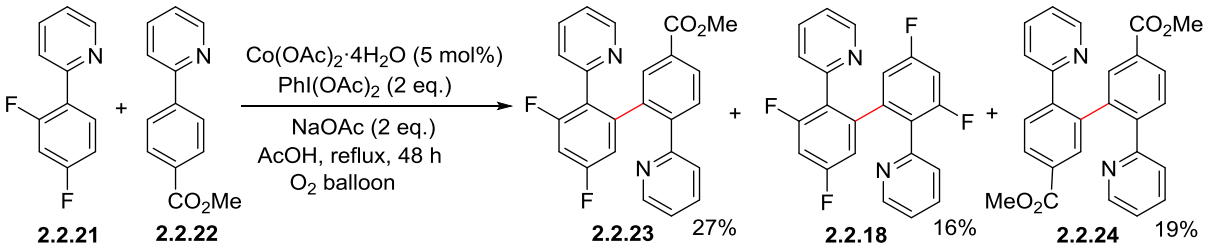

Scheme 2.14 Cross-coupling reaction between **2.3.21** and **2.3.22**

A mechanism was proposed by the authors to explain the reaction process, which involved the formation of Co^{III} species as the real catalyst by the oxidation of Co^{II} species. However, no further experiment was conducted to support the mechanism. The advantage of this method was the good functional group tolerance, including substituents such as halides, trifluoromethyl group, ester group and ether group. Besides, it presented the first example of heterocoupling between different 2-

arylpyridines, which may provide the access to more diverse structures of phenylpyridine dimers. Unfortunately, moderate yields were obtained in most cases.

In addition to the works described above, there were two related publications dealing with the homocoupling of 2-aryl-2-oxazolines (**Scheme 2.15**)[109] and 1-phenylpyrazoles (**Scheme 2.16**)[110] respectively. These two types of substrates contained *N*-heterocycles other than pyridine, but it was also the nitrogen atom that coordinated to the metal centers. Thus, it is possible that these two methods could be used for the homocoupling of 2-arylpyridines.

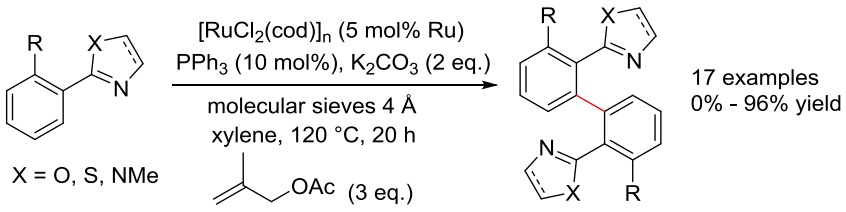

Scheme 2.15 Homocoupling of 2-aryl-2-oxazolines developed by Oi, Inoue and co-workers

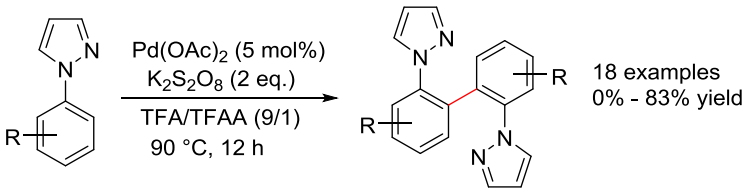

Scheme 2.16 Homocoupling of *N*-phenylpyrazoles developed by Batra and co-workers

In summary, although there are several methods developed for the homocoupling of 2-arylpyridines, they suffer the drawbacks of low isolated yields, poor regioselectivity and harsh reaction conditions. Besides, all the reported methods have employed homogeneous catalysts to conduct the reactions. To the best of our knowledge, no method has been developed using a heterogeneous source of catalyst or pre-catalyst. Based on the preliminary results obtained, detailed studies were conducted for the homocoupling of 2-arylpyridines using Ru/C as catalyst.

[109] S. Oi, H. Sato, S. Sugawara, Y. Inoue, *Org. Lett.* **2008**, *10*, 1823.

[110] H. Batchu, S. Bhattacharyya, R. Kant, S. Batra, *J. Org. Chem.* **2015**, *80*, 7360.

3 Results and discussions

3.1 Optimization of reaction conditions

After the bibliographical studies, we began to optimize the reaction conditions for the homocoupling reactions using 2-phenylpyridine **2.1.1** as the model compound. We first investigated the influence of the number of equivalent of the oxidant (**Table 3.1**). As shown in **Table 3.1**, when the equivalent of $FeCl_3$ was below 1.0, the conversion of the product increased with the increase of the oxidant (Entry 1-4); however, when the number of equivalents for oxidant was higher than 1.0, the conversion of the product decreased significantly (Entry 4-7). Moreover, when using 2.0 equivalents of the oxidant, the reaction was totally blocked (Entry 7). The possible reason for these observations might be that with the increase of the oxidant (below 1.0 equivalent), the C-H activation process was promoted to give the coupling product; while increasing the oxidant to more than 1.0 equivalent might inhibit the coupling reaction due to the competitive coordination of the iron atom to the nitrogen atom of the pyridine. As a result, when using 2.0 equivalents of the oxidant, the substrate was totally deactivated, thus blocking the reaction. Therefore, the optimized equivalent number of the oxidant was 1.0.

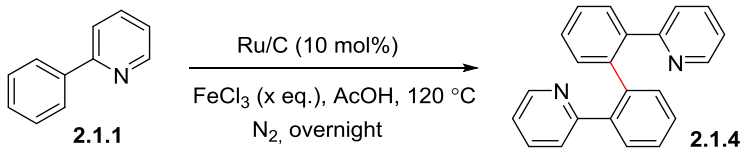

Entry	x eq.	SM:TM[a]
1	0.3	1:0.65
2	0.5	1:0.75
3	0.8	1:0.86
4	1.0	1:0.92
5	1.2	1:0.84
6	1.5	1:0.32
7	2.0	Trace TM

Table 3.1 Optimizing the reaction conditions: number of equivalent of the oxidant

[a]: SM=starting material; TM=target molecule; the ratio was determined by ^{1}H NMR, and the conversion was 50% when SM:TM = 1:0.5.

Next, different solvents were screened for the homocoupling reactions. As shown in **Table 3.2**, we first tried polar aprotic solvents such as acetonitrile (MeCN) and *N*,*N*-dimethylformamide (DMF) (Entry 2, 3). However, no desired product was detected using MeCN as solvent; only trace amount of product was observed using DMF. The use of dioxane also gave no desired product (Entry 4). This

might be due to the competing coordination of the solvent to the catalyst or the interaction with $FeCl_3$, since the solvent was largely in excess compared with the substrate. Taking this into account, we conducted the reaction with nonpolar solvents such as chlorobenzene (Entry 5). To our delight, the homocoupling product was obtained with more than 50% of conversion. Thus, more nonpolar solvents were investigated. For example, the use of toluene as solvent increased the product conversion (Entry 6), while the use of xylene and dichloroethane (DCE) gave a lower conversion of the starting material (Entry 7, 8). These results also supported the previous assumption that polar solvents might either coordinate to the catalyst or have an interaction with $FeCl_3$, preventing thus the homocoupling reactions. As a result, we could see that the use of acetic acid as solvent gave the best conversion of the product (Entry 1). However, the purification of the crude product when using acetic acid as solvent was problematic, leading to low isolated yield of the desired product. Besides, small amount of oligomer was detected when acetic acid was employed as solvent, while only the desired dimer product was observed using nonpolar solvents. Therefore, we chose toluene as the best solvent for our homocoupling reactions.

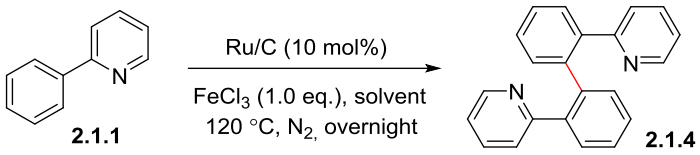

Entry	solvent	SM :TM
1	AcOH	1 :0.92
2	MeCN	No reaction
3	DMF	Trace TM
4	Dioxane	No reaction
5	PhCl	1 :0.56
6	PhMe	1 :0.67
7	Xylene	1 :0.20
8	DCE	1 :0.27

Table 3.2 Optimizing the reaction conditions: the solvent

Finally, we examined the effects of some other reaction conditions such as using different catalysts and changing the reaction time and temperature (**Table 3.3**). As shown in **Table 3.3**, decreasing the catalyst loading to 5 mol% resulted in the decease of the conversion (Entry 2); interestingly, increasing the catalyst loading to 20 mol% also led to a decrease of the conversion (Entry 3), perhaps owing to the aggregation of the catalyst. We then investigated the influence of the reaction temperature. Decreasing the reaction temperature to 80 ℃ gave no conversion of the product (Entry 4), indicating

that high temperature was required to generate the active catalytic species.[88] In contrast, increasing the reaction temperature to 150 ℃ strongly accelerated the homocoupling reaction, leading to a conversion of 86% and an isolated yield of 66% (Entry 5), indicating again that the formation of active catalytic species was promoted with high temperature. Extending the reaction time to 3 days further increased the isolated yield of the product to 86% (Entry 6). In order to know if Ru/C was the real catalyst and not another metal present in a trace amounts in the catalyst, different well-characterized ruthenium nanoparticles were used as catalysts for the homocoupling of 2-phenylpyridine (Entry 7-9). As a result, all the ruthenium nanoparticles were found to catalyze the homocoupling reaction and gave the desired product with acceptable isolated yields. The use of polyvinylpyrrolidone (PVP) supported ruthenium nanoparticles RuNp@PVP as catalyst resulted in low yield, which might be due to the loss of products during the work-up, since aggregated solids were observed after reaction completed and the subsequent filtration resulted in low yield of the crude product. According to these results, we could conclude that the active catalytic metal was the ruthenium one and not the potentially existing metal impurities. We also tried Pd/C as catalyst, but only trace amounts of product were detected (Entry 10). No reaction occurred without the use of $FeCl_3$, suggesting that it participated in the C-H activation process. The role of $FeCl_3$ in the catalytic cycle remained to be studied.

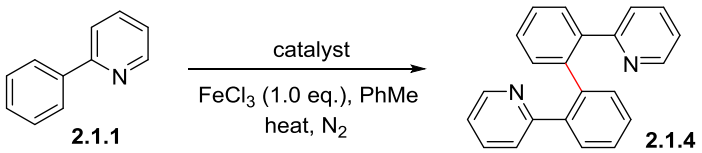

Entry	catalyst	Reaction time	Temperature / ℃	Result
1	10 mol% Ru/C	Overnight	120	SM:TM=1:0.67
2	5 mol% Ru/C	Overnight	120	SM:TM=1:0.48
3	20 mol% Ru/C	Overnight	120	SM:TM=1:0.42
4	10 mol% Ru/C	Overnight	80	No reaction
5	10 mol% Ru/C	Overnight	150	SM:TM=1:3.06 (66%)[a]
6	10 mol% Ru/C	3 days	150	86% [a]
7	10 mol% RuNp@PVP	3 days	150	21% [a]
8	10 mol% RuNp@dppb	3 days	150	59% [a]
9	10 mol% RuNp@ICy	3 days	150	56% [a]
10	10 mol% Pd/C	3 days	150	Trace TM
11[b]	10 mol% Ru/C	3 days	150	No reaction

Table 3.3 Optimizing the reaction conditions: catalyst, reaction time and temperature

[a]: isolated yield; [b]: reaction run without $FeCl_3$.

Therefore, the best reaction conditions for the homocoupling of 2-arylpyridines were figured out as the followings: 10 mol% of Ru/C as catalyst, 1.0 equivalent of $FeCl_3$ as oxidant and reacted in PhMe for 3 days at 150 ℃ under N_2 atmosphere.

3.2 Substrate scope of the homocoupling reactions

Having the best reaction conditions in hand, we began to explore the substrate scope of this reaction. Substrates bearing alkyl or aryl groups on the phenyl ring gave desired homocoupling products with moderate to good yields. The relatively low isolated yield obtained from the homocoupling of *ortho*-methyl substituted substrate was probably due to the steric effect of the methyl group (**Scheme 3.1**, compound **2.2.2**), since good yield was obtained with the methyl group substituted at *para*-position of the phenyl ring (**Scheme 3.1**, compound **2.2.10**). Substrate with a phenyl group at *para*-position of the phenyl ring also gave good yield of the homocoupling product (**Scheme 3.1**, compound **3.2.1**).

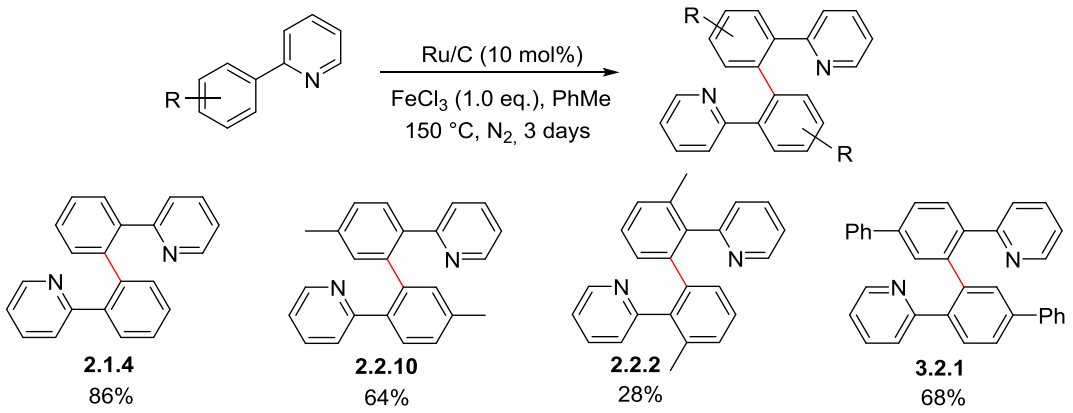

Scheme 3.1 Homocoupling of 2-phenylpyridines catalyzed by Ru/C

Substrates with electron-withdrawing substituents on the phenyl ring gave excellent yields of the corresponding homocoupling products (**Figure 3.1**). Halides such as fluoro- and bromo-substituted substrates underwent homocoupling reactions efficiently and gave 75% and 80% isolated yield for compound **3.2.2** and **3.2.3** respectively. Trifluoromethyl group was also tolerated, giving the homocoupling product **3.2.4** with an excellent isolated yield of 91%. Substrate with 2,4-difluoro substituent on the phenyl ring also efficiently homocoupled to give a good isolated yield of 63%.

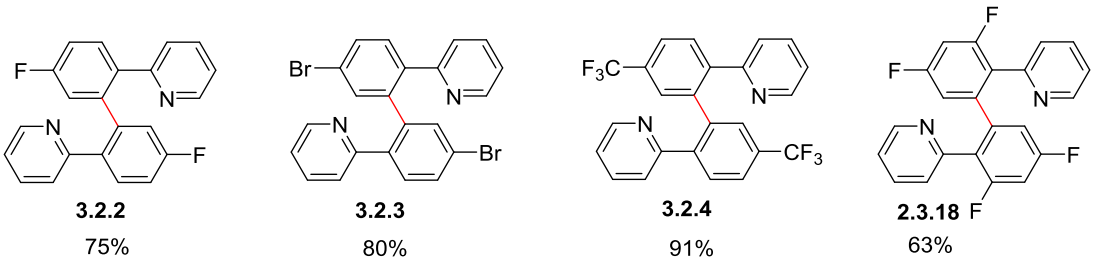

Figure 3.1 Homocoupling products with electron-withdrawing substituents

We then tested the homocoupling reactions using substrates with electron-donating substituents on the phenyl ring. As shown in **Figure 3.2**, both methoxy- and phenoxy-substituted substrates were successfully homocoupled to give the corresponding products **2.2.19** and **3.2.5**, with the isolated yield of 61% and 85% respectively. Thus, we were able to conduct the homocoupling reactions with both electron-withdrawing and electron-donating substrates of 2-phenylpyridines, which showed the broad substrate scope of our reaction.

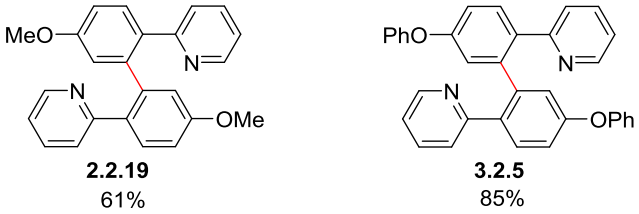

Figure 3.2 Homocoupling products with electron-donating substituents

Moreover, other 2-arylpyridine derivatives were used as substrates and subjected to our homocoupling reaction conditions. As shown in **Figure 3.3**, sterically more hindered 1-phenylisoquinoline was successfully homocoupled under our reaction conditions, giving an acceptable isolated yield of 59% for compound **3.2.6**. Replacing the phenyl ring with 1-naphthyl group in the substrate resulted in the formation of compound **3.2.7**, with a moderate isolated yield of 51%. The yields of compound **3.2.6** and compound **3.2.7** were lower than the one of compound **2.1.4**, perhaps owing to the steric effect of the substrates, as observed for the synthesis of compound **2.2.2**. We also conducted the homocoupling reactions using substrates with other heterocycles. The homocoupling of 2-(thiophen-2-yl)pyridine occurred chemoselectively and gave compound **3.2.8** as product with an isolated yield of 77%. Replacing the pyridine group of the substrate with other *N*-heterocycles such as pyrazole also gave the corresponding product of **3.2.9** with an isolated yield of 66%. These results further extended the substrate scope of our reaction conditions, and it provided a general method for the preparation of biaryl compounds.

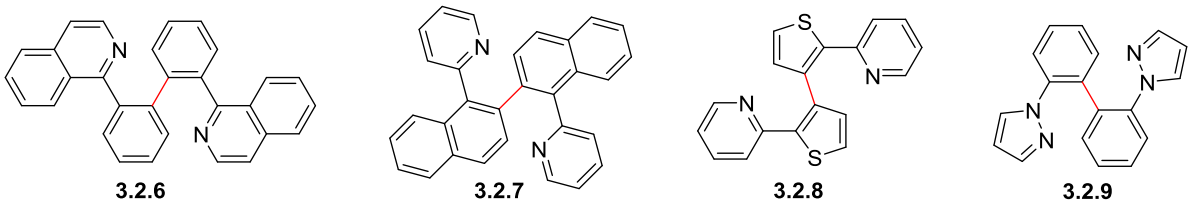

Figure 3.3 Homocoupling products of 2-arylpyridine derivatives

In order to examine the regioselectivity of our catalytic system, several unsymmetrical substrates were synthesized according to the literature method.[111] As a result, when employing these substrates to the homocoupling reaction conditions, the products resulting from the coupling of less steric hindered C-H bonds were obtained as sole products (**Figure 3.4**), which demonstrated the excellent regioselectivity obtained using our catalytic system. For example, compound **2.2.4a** was obtained by Sanford's group as one of the regioisomer under their reaction conditions, the ratio of compound **2.2.4a** and its regioisomer **2.2.4b** was 1.7:1 with a total yield of 44% (**Scheme 2.5**). However, **2.2.4a** was obtained as sole product with an isolated yield of 78% under our reaction conditions. Moreover, the homocoupling of 3,4-dimethoxy substituted substrate also occurred in a regioselective manner, giving compound **3.2.10** as sole product with an isolated yield of 43%. The relatively low yield of compound **3.2.10** might be due to the electronic effect of the two methoxy group on the phenyl ring, which might lead to a stronger C-H bond energy and thus slow down the C-H activation process. Interestingly, the homocoupling of 2-(thiophen-3-yl)pyridine also took place in a regioselective manner, giving 28% isolated yield of compound **3.2.11** as sole product. The possible reason for the good selectivity might be the electronic effect of the thiophene group, since the pK_a value of the C-H bond at the α-position of the sulfur atom is smaller than the one at β-position (33.5 and 39.0 respectively).[112]

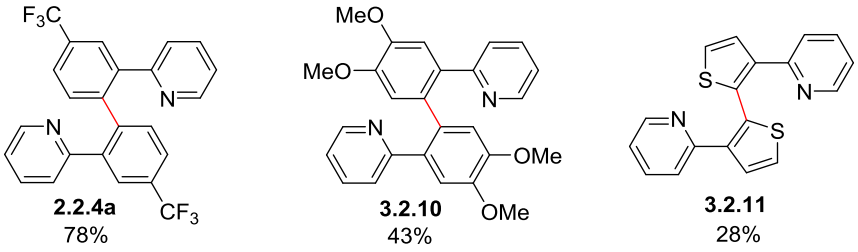

Figure 3.4 Regioselective homocoupling of 2-arylpyridines

[111] C. Liu, W. Yang, *Chem. Commun.* **2009**, 6267.

[112] K. Shen, Y. Fu, J.-N. Li, L. Liu, Q.-X. Guo, *Tetrahedron* **2007**, *63*, 1568.

Finally, in order to obtain more diverse structures of the biaryl compounds, we decided to conduct the heterocoupling reaction between two different 2-arylpyridines. In order to separate the products after the coupling reaction, the two substrates should have enough difference in terms of polarity. Thus, we chose two 2-phenylpyridines with different substituents on the phenyl ring, one with a methoxy group and the other with a bromo group. As shown in **Scheme 3.2**, the two substrates were employed with a molar ratio of 1:1, while the catalyst loading and the number of equivalents of $FeCl_3$ were calculated according to the total molar amount of the two substrates. After heating at 150 ℃ in toluene for 3 days, the desired heterocoupling product **3.2.14** was obtained as the main product together with the two homocoupling products **2.2.19** and **3.2.3**. Both starting compounds were recovered after the reaction (41% for compound **3.2.12**, 12% for compound **3.2.13**). The different conversions indicated that the C-H activation of compound **3.2.13** was easier than the one of compound **3.2.12**, which might be due to the electronic effect of the substituents. This experiment indicated that it was possible to synthesize various biaryl compounds with different functional groups, which was of great importance for both organic synthesis and ligand chemistry. Besides, the bromo substituent could be further transformed into other functional groups through metal catalyzed coupling reactions, providing more possibilities to the synthesis of biaryl compounds.

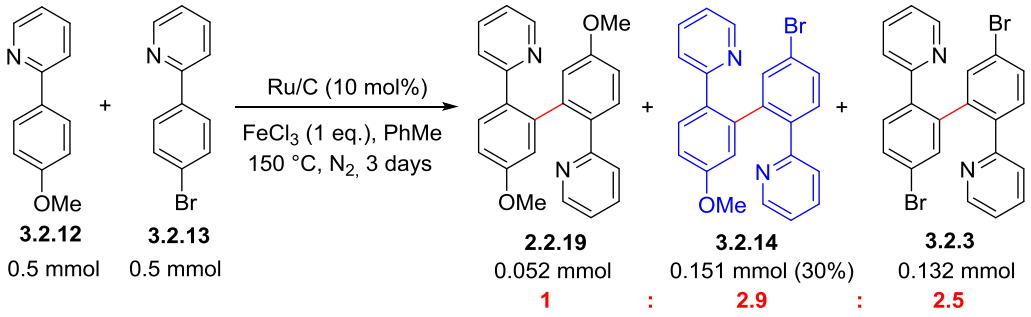

Scheme 3.2 Heterocoupling of two different 2-arylpyridines (1)

Another heterocoupling reaction was conducted to obtain more unsymmetrical biaryls. As shown in **Scheme 3.3**, compound **3.2.12** was remained as one of the coupling compound because of its polarity, and compound **3.2.15** was chosen as the other coupling compound. After the same catalytic process, the heterocoupling product **3.2.16** was obtained as the main product together with the two homocoupling products **2.2.19** and **3.2.2**. In this case, more starting compounds were recovered than the previous example (59% for compound **3.2.12**, 15% for compound **3.2.13**), indicating that the C-H activation of these two substrates was more difficult. Overall, we proved that the heterocoupling reactions was repeatable, and different biaryls with *N*,*N*-bidentate could be synthesized using our method.

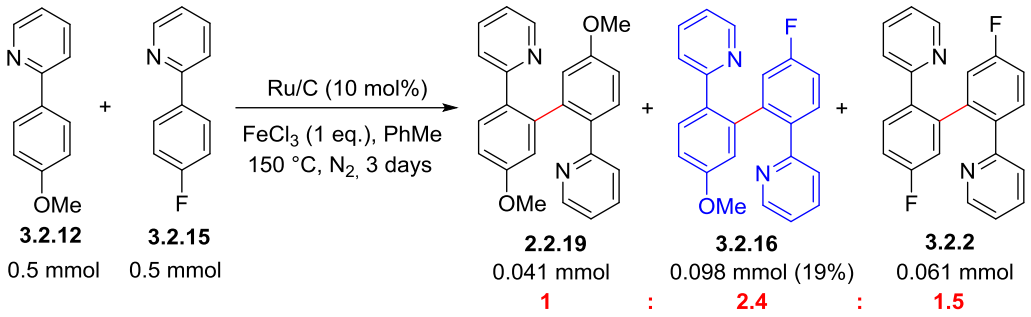

Scheme 3.3 Heterocoupling of two different 2-arylpyridines (2)

Just like a coin has two sides, the good regioselectivity of our method was accompanied with the limitation of the substrate scope. As described above, our method was sensitive to the steric effect of the substrates. As a result, the attempts to conduct the homocoupling reactions with some sterically hindered substrates failed. As shown in **Figure 3.5**, the homocoupling of compound **3.2.17** gave no product, probably due to the rigid structure of the substrate. The methyl group at the *α*-position of nitrogen in compound **3.2.18** blocked the coordination of the pyridine group to the ruthenium center, thus preventing the C-H activation process. Surprisingly, the homocoupling of 3,5-disubstituted substrate **3.2.19** also gave no product, indicating that the steric effect at 3-position of the phenyl ring also strongly affected the homocoupling reactions. This might explain the results of the regioselective homocoupling reactions (**Figure 3.4**), because only the less steric hindered positions were available for C-H activation in these substrates. In the case of the homocoupling reactions of compound **3.2.20** and **3.2.21**, the other nitrogen atom present in the molecules probably had the priority to coordinate to the ruthenium center because of the less steric hindrance, thus preventing the C-H activation process and resulting in no product. Compound **3.2.22** decomposed during the catalytic process, which was due to the poor stability of this substrate.

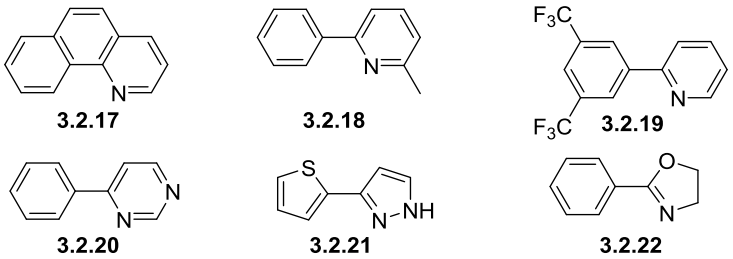

Figure 3.5 Substrate limitation of our catalytic system

3.3 Experiments for mechanism studies

In order to understand the reaction mechanism of the homocoupling reactions, we studied the kinetics of the homocoupling reaction using 2-phenylpyridine **2.1.1** as the model compound. Notably, the heater should be preheated to 150 ℃ before placing the reaction tubes in order to have the accurate reaction time. As shown in **Chart 3.1**, the conversion (determined by ^{1}H NMR of the crude product) increased quickly at the beginning of the homocoupling reaction, and the induction period of the reaction was very short (within 30 min), indicating that the formation of active catalytic species was fast under the reaction conditions. When the reaction was conducted for 4 hours, the conversion reached 64%, suggesting that the kinetics of the homocoupling reaction was fast at the beginning, and it slowed down significantly in the later period, since the reaction required 72 hours to reach high yield of the product. This could be explained by the better coordinating ability of the 2-arylpyridine dimers to the ruthenium center compared with the monomers, which resulted in the stronger coordination at the surface of the catalyst and thus slowed down the subsequent homocoupling reactions.

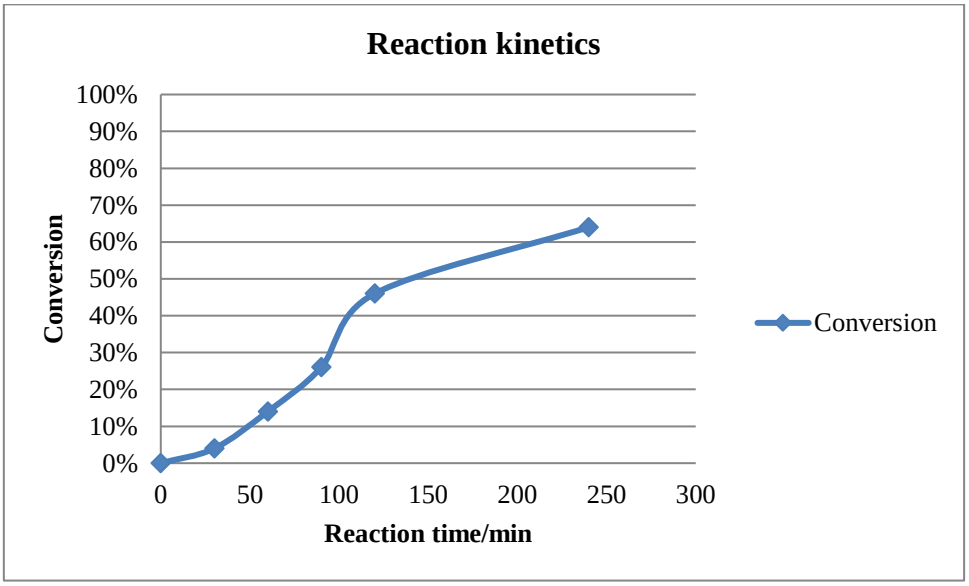

Chart 3.1 Reaction kinetics of the homocoupling of 2-phenylpyridine

According to the observations above, a plausible reaction mechanism was proposed as follow: first of all, the active catalytic species was generated by the heating of Ru/C. The formation of Ru(II) species was possible by the oxidation of Fe(III), since the standard electrode potential of Fe(III)/Fe(II) (+0.771 V) was larger than the one of Ru(II)/Ru(0) (+0.455 V). Then 2-phenylpyridine coordinated to the surface of the catalyst, and the *ortho*-C-H bond of the substrate was activated by ruthenium atom through oxidative addition to form the intermediate **3.3.1**. Then another molecule of the substrate coordinated to the same ruthenium center and the second C-H activation occurred to form intermediate

3.3.2, which underwent reductive elimination to give the desired homocoupling product **2.1.4** and regenerated the active catalytic species. The steric effects played an important role in this transformation because there were two molecules of substrate coordinated to the same ruthenium center, as we have observed in our experiments.

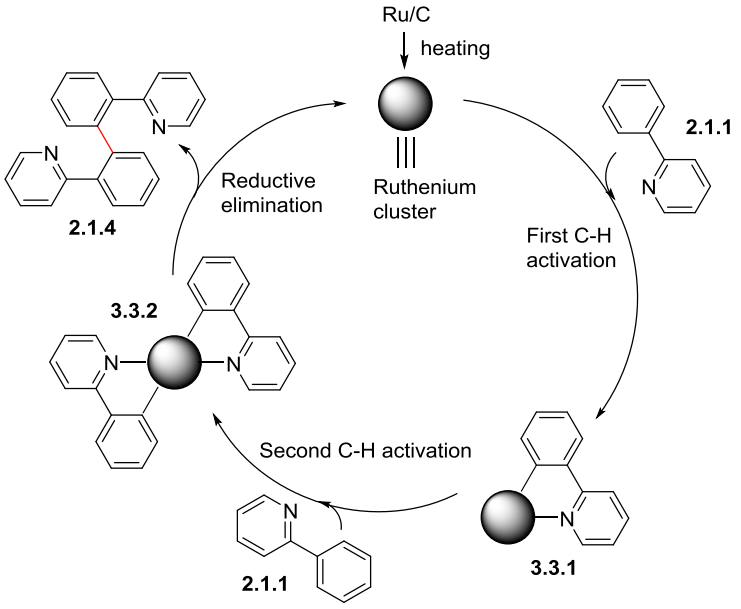

Scheme 3.4 Proposed reaction mechanism for the homocoupling of 2-phenylpyridine

The determination of the nature of the active catalyst is undergoing in our lab. Three-phase test, mercury poisoning, detection of leaching ruthenium and adding metal scavenger to the standard reaction conditions will be conducted in the future.

3.4 Applications of the homocoupling products

After obtaining the homocoupling products, possible applications of these compounds were envisioned. In 2010, M. Murakami reported a method for the synthesis of pyridine-borane complexes through an electrophilic aromatic borylation of 2-phenylpyridines with BBr_3 followed by alkylation/ arylation of the dibromoboranes (**Scheme 3.5**).[113] These pyridine-borane compounds were found to have interesting photophysical and electrochemical properties,[114] and they were patented for their use as air-

[113] N. Ishida, T. Moriya, T. Goya, M. Murakami, *J. Org. Chem.* **2010**, *75*, 8709.

[114] a) Y.-L. Rao, H. Amarne, S.-B. Zhao, T. M. McCormick, S. Martić, Y. Sun, R.-Y. Wang, S. Wang, *J. Am. Chem. Soc.* **2008**, *130*, 12898; b) H. Amarne, C. Baik, S. K. Murphy, S. Wang, *Chem. Eur. J.* **2010**, *16*, 4750; c) Y.-L. Rao, S. Wang, *Inorg. Chem.* **2011**, *50*, 12263; d) D. L. Crossley, J. Cid, L. D. Curless, M. L. Turner, M. J. Ingleson, *Organometallics* **2015**, *34*, 5767; e) A. C. Shaikh, D. S. Ranade, S. Thorat, A. Maity, P. P. Kulkarni, R. G. Gonnade, P. Munshid, N. T. Patil, *Chem. Commun.* **2015**, *51*, 16115; f) Y.-J. Shiu, Y.-C. Cheng, W.-L. Tsai, C.-C. Wu, C.-T. Chao, C.-W. Lu, Y. Chi, Y.-T. Chen, S.-H. Liu, P.-T. Chou, *Angew. Chem. Int. Ed.* **2016**, *55*, 3017; g) Y.-J. Shiu, Y.-T. Chen, W.-K. Lee, C.-C. Wu, T.-C. Lin, S.-H. Liu, P.-T. Chou, C.-W. Lu, I-C. Cheng, Y.-J. Lien, Y. Chi, *J. Mater. Chem. C* **2017**, *5*, 1452.

stable organic light-emitting materials.[115] Therefore, we decided to investigate the possible enhancement of the photophysical properties of such pyridine-borane complexes between the monomers and dimers. Inspired by the work of Murakami, a series of pyridine-borane complexes were synthesized according to the literature method.

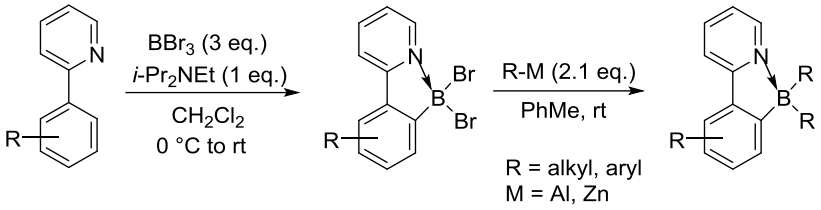

Scheme 3.5 Synthesis of pyridine-borane complexes reported by Murakami

As shown in **Scheme 3.6**, the pyridine-borane monomers were synthesized by electrophilic aromatic borylation of 2-arylpyridines followed by alkylation with $AlMe_3$. Substrates with different electronic properties were successfully synthesized with good to excellent isolated yields (the yields showed in **Scheme 3.6** were the combined yield of two steps). It was worth noting that an optimization of the reaction procedure was conducted: after the electrophilic aromatic borylation reactions in the first step, the crude intermediate 2-(2-dibromoborylaryl)pyridines were used immediately in the alkylation process without further purification. Using this more convenient protocol, the isolated yields of the pyridine-borane monomers were significantly improved (the synthesis of compound **3.4.1** was achieved with a combine yield of 81% by Murakami).

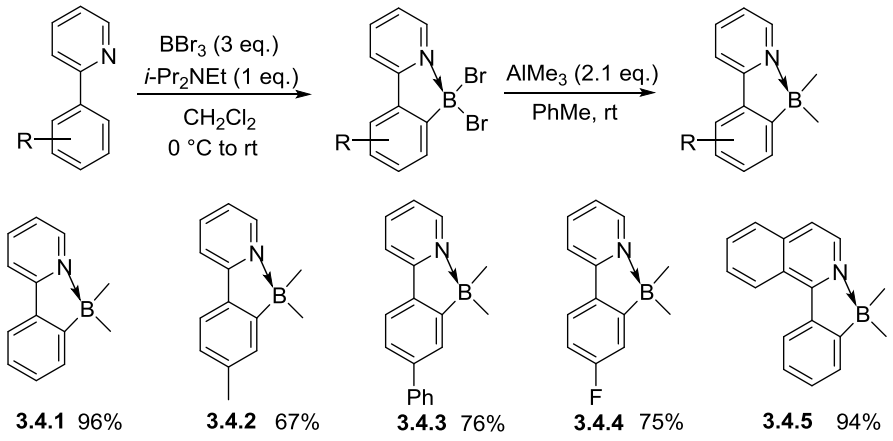

Scheme 3.6 Synthesis of pyridine-borane monomers

[115] a) M. Murakami, N. Ishida, T. Moriya, T. Goya, K. Morii, M. Hasegawa, Y. Arimoto, *WO 2011/099331 A1*. b) Z.-J. Zhao, Z.-F. Chang, P. Jiang, J. Chen, H.-Y. Qiu, *CN 102899027 A*.

Although the pyridine-borane monomers were synthesized smoothly, the syntheses of pyridine-borane dimers remained a challenging task because the dimers were more sterically hindered. Thus, we first conducted the reaction with compound **2.1.4** since there was no substituent on this molecule. Fortunately, by simply doubling the quantity of reagents, the borylation reaction proceeded smoothly using our optimized reaction procedures (**Scheme 3.7**). The desired pyridine-borane dimer **3.4.7** was obtained with an isolated yield of 82% after purification by column chromatography. Notably, we also tried Murakami's protocol with this molecule in the beginning, which has led to a low combine yield of 31%, demonstrating the advantage of our optimized reaction procedures. The polarity of the molecule decreased significantly from compound **2.1.4** to compound **3.4.7**, suggesting the presence of interaction between nitrogen and boron atoms.

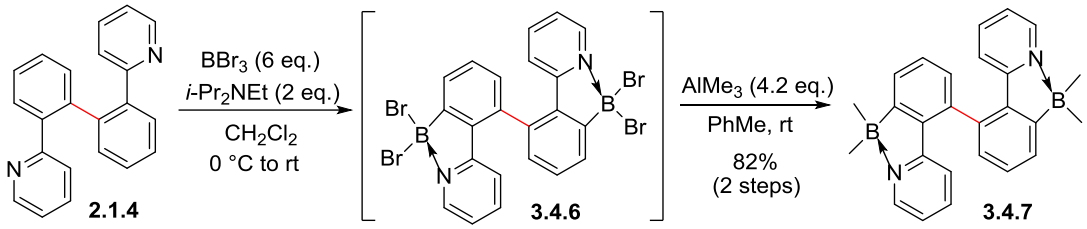

Scheme 3.7 Synthesis of pyridine-borane dimer **3.4.7**

Knowing that the borylation could be achieved under the same reaction conditions, other homocoupling dimers were subjected to the same reaction conditions. As shown in **Figure 3.6**, methyl-substituted substrate **2.2.10** was borylated to give compound **3.4.8** with a quantitative yield; phenyl-substituted substrate **3.2.1** also gave borylated product **3.4.9** with a high yield of 87% after two steps; electron-withdrawing substrate **3.2.2** gave borylated product **3.4.10** with a moderate yield of 69%, perhaps owing to the strong electron-withdrawing effect of the fluoro substituent, which resulted in the difficulty of the electrophilic aromatic borylation reaction; the more sterically hindered substrate **3.2.6** was also borylated under the reaction conditions, although the yield of compound **3.4.11** was much lower (due to the steric effect of the isoquinoline moiety). Indeed, the purification of compound **3.4.11** was more difficult than other pyridine-borane dimers (a part of the product was mixed with the starting compound).

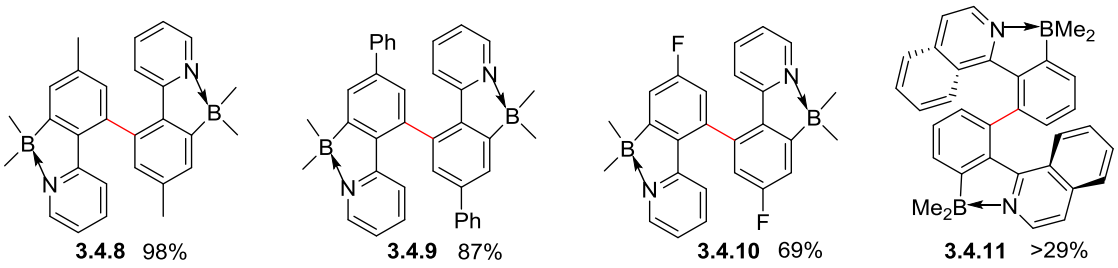

Figure 3.6 Synthesis of pyridine-borane dimers

Having these pyridine-borane complexes in hand, we studied their photophysical properties by performing the ultraviolet-visible (UV-Vis) absorption and fluorescence spectroscopies of these compounds (see **Chart 3.2** for example), and the results were shown in **Table 3.4**. All of these pyridine-borane compounds absorbed light within the wavelengths of ultraviolet. Generally, the maximum absorption wavelengths ($\lambda_{abs,\ max}$) of the pyridine-borane monomers were identical or very close to the corresponding dimers, which might be due to the structural similarity between the monomers and dimers. However, the maximum emission wavelengths ($\lambda_{em,\ max}$) of the dimers were larger than the ones of the corresponding monomers, which had resulted in the larger Stokes shifts of the dimers. The difference of Stokes shifts between monomers and dimers was significantly affected by the substituents: from 138 cm^{-1} for phenyl group (**Table 3.4**, Entry 5, 6) to 2560 cm^{-1} for isoquinoline substrate (**Table 3.4**, Entry 7, 8). Besides, the molar extinction coefficients (ε_{vis}) of the dimers were larger than the ones of the monomers, due to the larger conjugational structures of the dimers. The substituents on the phenyl ring strongly influenced the photophysical properties of the pyridine-borane compounds, as indicated by the quantum yields (Φ, calculated by using quinine dication as the standard) of the compounds with different functional groups. Notably, compound **3.4.3** and compound **3.4.9**, which contained biphenyl groups, showed much higher quantum yields compared with other analogues (**Table 3.4**, Entry 5, 6). The high quantum yields of these two compounds might be due to the conjugation effect of the phenyl group with the main structure. The fact that high quantum yield of the pyridine-borane compounds could be obtained by employing different substituents on the phenyl group also indicated that these compounds were promising materials for organic light-emitting diodes (OLEDs). In addition, the brightness of a fluorophore (defined as $\varepsilon_{vis} \times \Phi$ /1000) is another important characteristic to consider when applying fluorescence microscopy. In our case, the brightness of each pyridine-borane dimer was higher than the one of the corresponding monomer, which also represented an advantage of the pyridine-borane dimers.

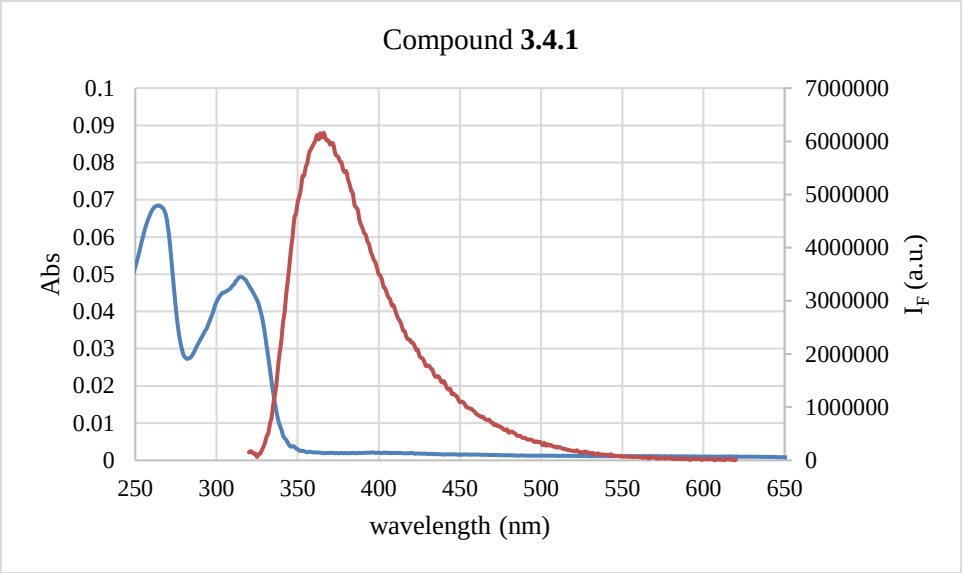

Chart 3.2 UV-Vis (blue) and fluorescence (red) spectra of compound **3.4.1**

Entry	Compound	$\lambda_{abs,\ max}$	$\lambda_{em,\ max}$	Stokes Shift/cm^{-1}	ε_{vis}	Φ	Brightness
1	**3.4.1**	315 nm	366 nm	4424	8.21×10^3	0.103	0.8
2	**3.4.7**	314 nm	387 nm	6007	1.65×10^4	0.223	3.7
3	**3.4.2**	321 nm	371 nm	4198	9.10×10^3	0.217	2.0
4	**3.4.8**	321 nm	381 nm	5043	2.09×10^4	0.323	6.8
5	**3.4.3**	330 nm	379 nm	3918	1.56×10^4	0.731	11.4
6	**3.4.9**	330 nm	381 nm	4056	3.43×10^4	0.607	20.8
7	**3.4.4**	367 nm	401 nm	2310	1.04×10^4	0.338	3.5
8	**3.4.10**	361 nm	438 nm	4870	1.65×10^4	0.246	4.1
9	**3.4.5**	313 nm	358 nm	4016	8.79×10^3	0.239	2.1
10	**3.4.11**	314 nm	372 nm	4965	1.81×10^4	0.134	2.4

Table 3.4 Photophysical properties of the pyridine-borane compounds

3.4.1 Perspectives

In addition to these pyridine-borane compounds, the homocoupling products are potential *N*,*N*-bidentate ligands that could be used in catalytic reactions. For example, in 2015, R. Irie and co-workers reported the synthesis of 2,2'-binaphthyl-1,1'-biisoquinoline (BINIQ, compound **3.4.14**) and used it as a new axially chiral bidentate ligand after the optical resolution of synthesized BINIQ by a

chiral HPLC method.[116] There were three chiral biaryl axes in BINIQ, two from naphthyl-isoquinoline moiety and one from 2,2'-binaphthyl moiety, which were denoted with α, β, and γ chiral axis as shown in **Scheme 3.8**. According to the authors, BINIQ was stereochemically stable for the *α*- and *γ*-axis to permit optical resolution by a chiral HPLC method; besides, the configuration at the β-axis could be dynamically changed at room temperature upon coordination to a copper(I) ion center. Thus, optically pure BINIQ could be obtained as a chiral ligand for catalytic asymmetric reactions.

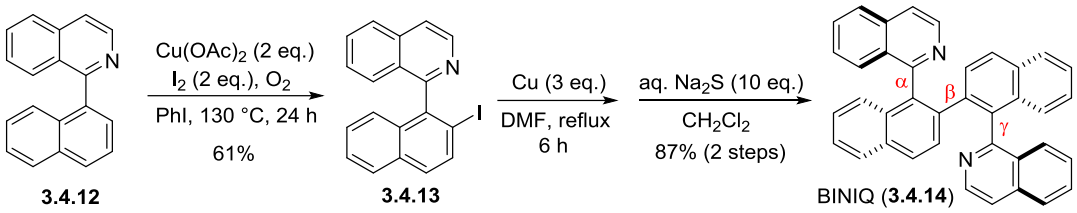

Scheme 3.8 Synthesis of NINIQ by Irie *et al.*

Compared with the synthetic method of Irie, which required 3 steps to obtain the desired product, it is possible to synthesize BINIQ by our method in a single step starting from the same compound **3.4.12**. Since we have succeeded to synthesize compounds **3.2.6** and **3.2.7**, which were very close to the structure of BINIQ, it is reasonable to synthesize BINIQ under our reaction conditions.

Moreover, the homocoupling products could also be applied in the synthesis of iridium complexes, which may have many applications in material science such as organic light-emitting diodes (OLEDs). The monomers of 2-phenylpyridines were widely used in the synthesis of iridium complexes (**Figure 3.7**), and these complexes were reported to have important photophysical and electrochemical properties, thus they could be prepared as phosphorescent OLEDs.[117]

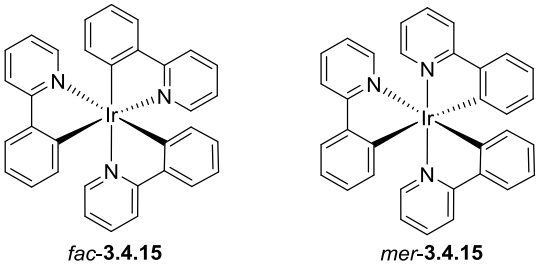

Figure 3.7 Reported example of iridium complexes

[116] T. Kawatsu, H. Tokushima, Y. Takedomi, T. Imahori, K. Igawa, K. Tomooka, R. Irie, *ARKIVOC* **2015**, *iv*, 161.

[117] a) F. 0. Garces, K. A. King, R. J. Watts, *Inorg. Chem.* **1988**, *27*, 3464; b) V. V. Grushin, N. Herron, D. D. LeCloux, W. J. Marshall, V. A. Petrov, Y. Wang, *Chem. Commun.* **2001**, 1494; c) A. Köhler, J. S. Wilson, R. H. Friend, *Adv. Mater.* **2002**, *14*, 701; d) C.-H. Yang, K.-H. Fang, C.-H. Chen, I-W. Sun, *Chem. Commun.* **2004**, 2232; e) Q. Zhao, S. Liu, M. Shi, C. Wang, M. Yu, L. Li, F. Li, T. Yi, C. Huang, *Inorg. Chem.* **2006**, *45*, 6152; f) Y. Liu, K. Ye, Y. Fan, W. Song, Y. Wang, Z. Hou, *Chem. Commun.* **2009**, 3699; g) T. Kim, H. Kim, K. M. Lee, Y. S. Lee, M. H. Lee, *Inorg. Chem.* **2013**, *52*, 160; h) A. Singh, K. Teegardin, M. Kelly, K. S. Prasad, S. Krishnan, J. D. Weaver, *J. Organomet. Chem.* **2015**, *776*, 51; Y. Kim, S. Park, Y. H. Lee, J. Jung, S. Yoo, M. H. Lee, *Inorg. Chem.* **2016**, *55*, 909.

By replacing one of the 2-phenylpyridine ligand with the homocoupling dimers, the corresponding iridium complexes are expected to have new photophysical and electrochemical properties compared with the monomers. The dimers can coordinate to iridium center by two different modes: as an *N*,*N*-bidentate ligand such as complex **3.4.16** or as an *N*, *C*-bidentate ligand such as complexes **3.4.17** and **3.4.18**. As we can see, there are two iridium centers in complex **3.4.18**, thus it may have unique properties compared with former reported complexes.

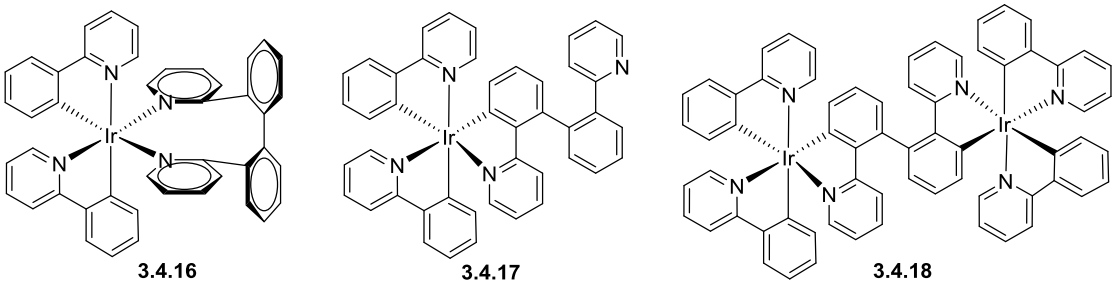

Figure 3.8 Iridium complexes with a dimer as the ligand

3.4.2 Conclusion

In conclusion, we have developed a method allowing the homocouping of 2-arylpyridines using Ru/C as catalyst and $FeCl_3$ as oxidant (**Scheme 3.9**). To the best of our knowledge, this is the first method for the homocoupling of 2-arylpyridines using a heterogeneous catalyst. Different functional groups such as alkyl, aryl, halides, trifluoromethyl group, methoxy group and phenoxy group on the phenyl ring were tolerated in our catalytic system. Moreover, substrates with other heterocycles such as thiophene, isoquinoline and pyrazole were also successfully homocoupled to give the desired products. Our method was highlighted by the regioselective homocoupling of unsymmetrical substrates, which only gave the products resulting from the homocoupling of less steric hindered C-H bonds. We also succeeded to conduct the heterocoupling of two different 2-phenylpyridines, giving the heterocoupling compound as the main product together with the two homocoupling products. According to the different conversions of the substrates, we suggested that the substrates with electron-withdrawing substituents were generally easier to undergo the C-H activation process under our reaction conditions, leading to higher yields of the homocoupling products. As an application of our method, a series of pyridine-borane complexes were synthesized and their photophysical properties (UV and fluorescence) were studied. Substrates with different substituents were found to have different quantum yields, and the phenyl substituted substrate showed high quantum efficiency of 73% for monomer and 61% for dimer. These pyridine-borane complexes are expected to be promising OLEDs, and more potential applications are shown for the homocoupling products. More efforts will be made to the identification of the active catalytic species of the reaction in the future.

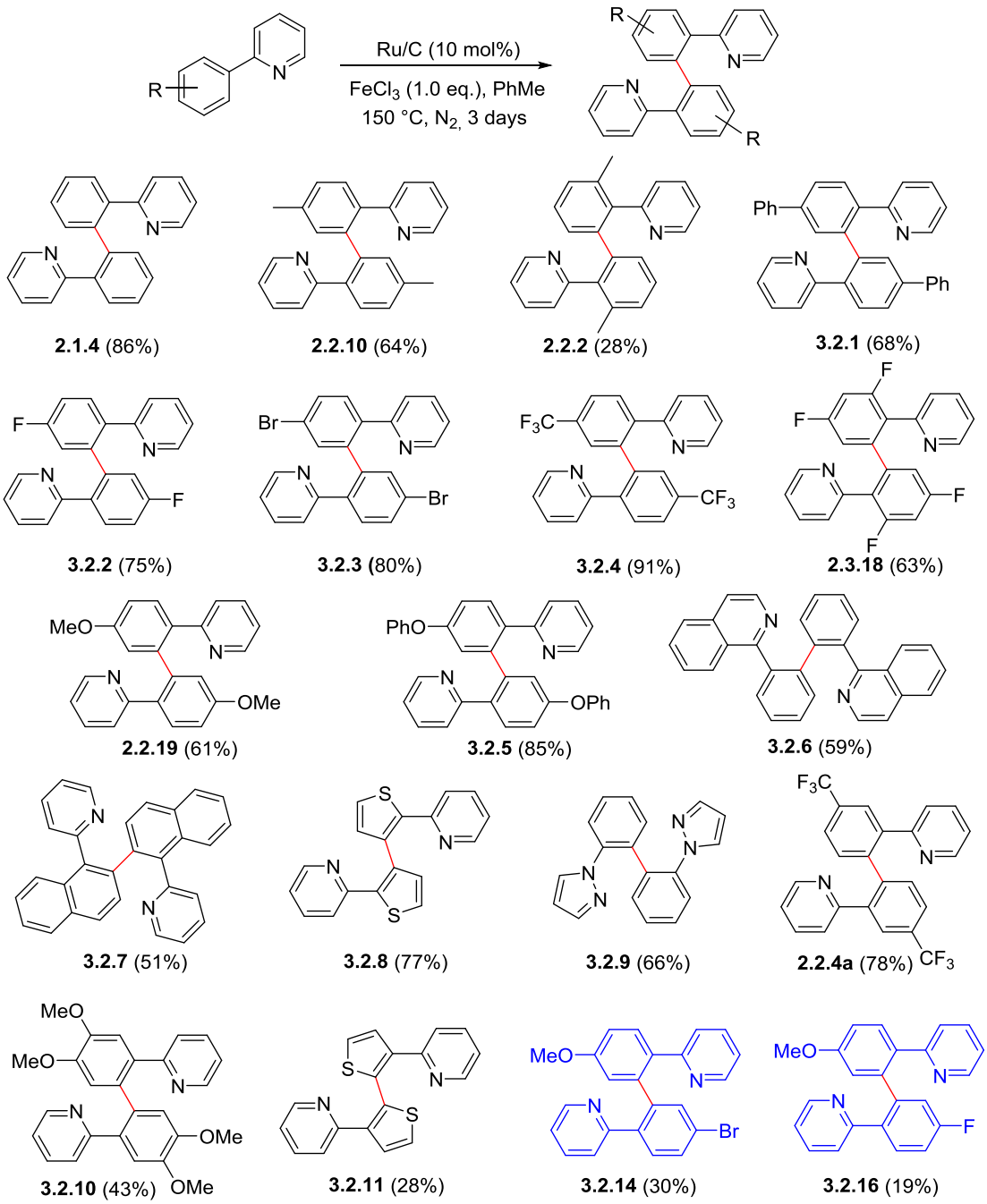

Scheme 3.9 Substrate scope of Ru-catalyzed homocoupling of 2-arylpyridines

4 Experimental section

4.1 Reagents and General Procedures

All reactions were carried out in a Fischer-Porter glassware. Commercially substrates were used without any further purification. Other phenylpyridines were synthesized by 2-bromopyridine and corresponding boronic acids according to reported literature.[111] All work-up and purification procedures were carried out with reagent-grade solvents. Toluene was purchased from VWR Chemicals (BDH Prolabo) and used without further purification. Flash column chromatography was performed using Merck silica gel 60 (0.040-0.063 mm). ^{1}H NMR (400 MHz), ^{13}C NMR (100 MHz) spectra were recorded on a Bruker Avance 400 MHz spectrometer. Chemical shifts are reported in parts per million (ppm) downfield from residual solvent peaks and coupling constants are reported in Hertz (Hz). Splitting patterns are designated as singlet (s), doublet (d), triplet (t). Splitting patterns that could not be interpreted or easily visualized are designated as multiplet (m). Electrospray mass spectra were recorded using an ESI/TOF Mariner Mass Spectrometer. UV-visible spectra were recorded on a Cary 400 (Agilent) double-beam spectrometer using a 10 mm path quartz cell. Emission spectra were measured on a Fluoromax-3 (Horiba) spectrofluorimeter. A right-angle configuration was used. High-resolution mass spectra (HRMS) were performed on a Bruker maXis mass spectrometer by the "Fédération de Recherche" ICOA/CBM (FR2708) platform.

General Procedure A: homocoupling of phenylpyridines:

A 80 mL Fischer-Porter glassware was charged with Ru/C (101 mg, 10 mol%), $FeCl_3$ (81 mg, 0.5 mmol) and phenylpyridines (0.5 mmol) with a magnetic stirring bar under air. The Fischer-Porter glassware was then left under vacuum for 5 min and pressurized with Ar gas. Then toluene (2 mL) was added under argon. The reaction mixture was magnetically stirred at 150 °C (sand bath) under Ar during 72 hours. The solution was cooled down to room temperature, then Et_3N (~2mL) was added and stirred at room temperature for 10 min before filtered through silica gel pad and washed with CH_2Cl_2 (30 mL). Then the filtrate was concentrated under vacuum and the crude product was purified by flash chromatography on silica gel (eluent: cyclohexane/AcOEt = 5/1 - 1/1).

General Procedure B: borylation of phenylpyridines[113]:

To a stirred solution of 2-phenylpyridine (78 mg, 0.5 mmol) and *i*-Pr_2NEt (65 mg, 0.5 mmol) in CH_2Cl_2 (0.5 mL) at 0 °C was added BBr_3 (1.0 M in CH_2Cl_2, 1.5 mL, 1.5 mmol). After being stirred at room temperature for 24 h, saturated aqueous K_2CO_3 solution was added to the reaction mixture. The organic layer was separated and the aqueous layer was extracted with CH_2Cl_2 (twice). The combined organic layers were washed with water (once) and brine (once), dried over $MgSO_4$, and concentrated. The resulting solid was dried under vacuum and used immediately in the next step without further purification.

To a stirred solution of the crude product in toluene (1.0 mL) at room temperature was added $AlMe_3$ (2 M in toluene, 0.55 mL, 1.1 mmol). After being stirred at this temperature for 5 min, the reaction was quenched by adding water. The organic layer was separated and the aqueous layer was extracted with AcOEt (twice). The combined organic layers were washed with water (once) and brine (once), dried over $MgSO_4$, and concentrated. The residue was purified by column chromatography on silica gel (eluent: cyclohexane/AcOEt = 5/1) to afford the corresponding methyl boron compound (94 mg, 0.48 mmol, 96% yield).

For the boronation of dimers, the number of equivalents for all reagents was doubled.

4.2 Experimental details and characterization for synthesized compounds

2,2'-Di(pyridin-2-yl)-1,1'-biphenyl (2.1.4):

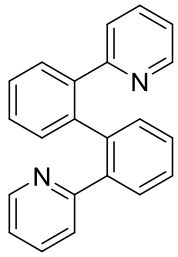

Following the General Procedure A. The product was isolated as a light yellow solid (66 mg, 86% yield). ^{1}H NMR (400 MHz, $CDCl_3$) δ 8.32 (d, J = 4.5 Hz, 2H), 7.57-7.49 (m, 2H), 7.45-7.36 (m, 6H), 7.31 (td, J = 7.7, 1.7 Hz, 2H), 7.00 (dd, J = 6.7, 5.1 Hz, 2H), 6.76 (d, J = 7.9 Hz, 2H). ^{13}C NMR (100 MHz, $CDCl_3$) δ 157.9, 148.9, 139.7(2C), 135.1, 131.2, 129.9, 128.4, 127.6, 124.3, 121.1.

The experimental data obtained are in accordance with the literature.[105g]

2,2'-(5,5'-Dimethyl-[1,1'-biphenyl]-2,2'-diyl)dipyridine (2.2.10):

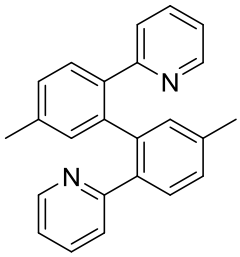

Following the General Procedure A. The product was isolated as a yellow solid (53 mg, 64% yield). ^{1}H NMR (400 MHz, $CDCl_3$) δ 8.27 (d, J = 4.2 Hz, 2H), 7.41 (d, J = 7.8 Hz, 2H), 7.34-7.25 (m, 4H), 7.21 (d, J = 7.8 Hz, 2H), 6.97 (dd, J = 6.6, 5.0 Hz, 2H), 6.67 (d, J = 7.9 Hz, 2H), 2.43 (s, 6H). ^{13}C NMR (100 MHz, $CDCl_3$) δ 157.9, 148.7, 139.7, 138.4, 137.1, 135.1, 131.8, 129.9, 128.5, 124.3, 120.9, 21.2.

The experimental data obtained are in accordance with the literature.[105g]

2,2'-(3,3'-Dimethyl-[1,1'-biphenyl]-2,2'-diyl)dipyridine (2.2.2):

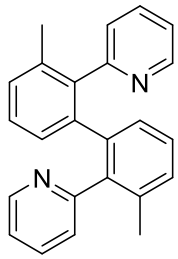

Following the General Procedure A. The product was isolated as a yellow solid (22 mg, 28% yield). ^{1}H NMR (400 MHz, $CDCl_3$) δ 8.57 (d, J = 3.9 Hz, 2H), 7.55 (t, J = 7.2 Hz, 2H), 7.39-7.27 (m, 2H), 7.11-7.02 (m, 4 H), 6.93 (t, J = 7.6 Hz, 2H), 6.76 (d, J = 7.6 Hz, 2H), 2.10 (s, 6H). ^{13}C NMR (100 MHz, $CDCl_3$) δ 159.4, 148.7, 140.2, 139.7, 135.9, 135.5, 128.8, 128.5, 126.6, 125.6, 121.2, 20.5.

2,2'-(5,5'-Diphenyl-[1,1'-biphenyl]-2,2'-diyl)dipyridine (3.2.1):

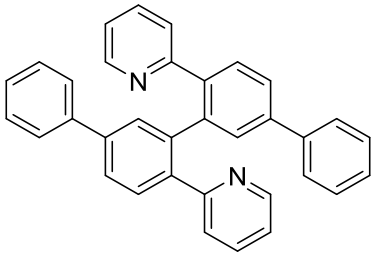

Following the General Procedure A. The product was isolated as a white solid (86 mg, 68% yield). ^{1}H NMR (400 MHz, $CDCl_3$) δ 8.39 (d, J = 4.4 Hz, 2H), 7.77 (s, 2H), 7.74-7.64 (m, 8H), 7.47 (t, J = 7.6 Hz, 4H), 7.38 (t, J = 7.4 Hz, 4H), 7.05 (dd, J = 6.9, 5.3 Hz, 2H), 6.91 (d, J = 7.9 Hz, 2H). ^{13}C NMR (100 MHz, $CDCl_3$) δ 157.5, 149.0, 141.1, 140.1, 140.0, 138.8, 135.2, 130.6, 129.8, 128.7(2C), 127.5, 127.0(2C), 126.3, 124.4, 121.2.

The experimental data obtained are in accordance with the literature.[105c]

2,2'-(5,5'-Difluoro-[1,1'-biphenyl]-2,2'-diyl)dipyridine (3.2.2):

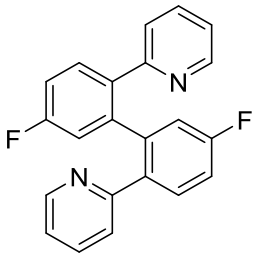

Following the General Procedure A. The product was isolated as a white solid (64 mg, 75% yield). ^{1}H NMR (400 MHz, $CDCl_3$) δ 8.31 (d, J = 4.3 Hz, 2H), 7.50 (dd, J = 8.1, 6.1 Hz, 2H), 7.36 (td, J = 7.7, 1.6 Hz, 2H), 7.14-7.06 (m, 4H), 7.03 (dd, J = 6.8, 5.1 Hz, 2H), 6.76 (d, J = 7.9 Hz, 2H). ^{13}C NMR (100 MHz, $CDCl_3$) δ 162.6 (d, $J_{C\text{-}F}$ = 248.8 Hz), 156.7, 149.0, 140.8 (d, $J_{C\text{-}F}$ = 7.7 Hz), 136.0 (d, $J_{C\text{-}F}$ = 3.1 Hz), 135.4, 132.0 (d, $J_{C\text{-}F}$ = 8.5 Hz), 124.1, 121.4, 117.6 (d, $J_{C\text{-}F}$ = 22.1 Hz), 115.0 (d, $J_{C\text{-}F}$ = 21.1 Hz). ^{19}F NMR (376 MHz, $CDCl_3$) δ -113.2 (s).

The experimental data obtained are in accordance with the literature.[105c]

2,2'-(5,5'-Dibromo-[1,1'-biphenyl]-2,2'-diyl)dipyridine (3.2.3):

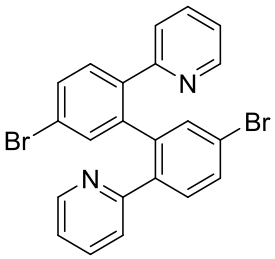

Following the General Procedure A. The product was isolated as a white solid (94 mg, 80% yield). ^{1}H NMR (400 MHz, $CDCl_3$) δ 8.28 (d, J = 4.5 Hz, 2H), 7.60 (d, J = 1.9 Hz, 2H), 7.55 (dd, J = 8.3, 1.9 Hz, 2H), 7.41-7.33 (m, 4H), 7.04 (dd, J = 6.9, 5.1 Hz, 2H), 6.71 (d, J = 7.9 Hz, 2H). ^{13}C NMR (100 MHz, $CDCl_3$) δ 156.4, 149.1, 140.3, 138.7, 135.5, 133.6, 131.7, 131.2, 124.1, 122.7, 121.6.

The experimental data obtained are in accordance with the literature.[105g]

2,2'-(5,5'-Bis(trifluoromethyl)-[1,1'-biphenyl]-2,2'-diyl)dipyridine (3.2.4) :

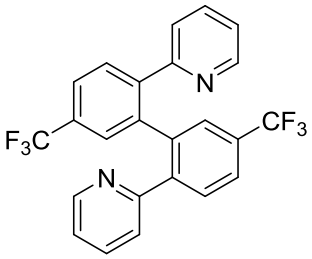

Following the General Procedure A. The product was isolated as a white solid (101 mg, 91% yield). ^{1}H NMR (400 MHz, $CDCl_3$) δ 8.35 (d, J = 4.7 Hz, 2H), 7.67 (s, 4H), 7.61 (s, 2H), 7.42 (td, J = 7.7, 1.4 Hz, 2H), 7.10 (dd, J = 7.4, 5.0 Hz, 2H), 6.83 (d, J = 7.9 Hz, 2H). ^{13}C NMR (100 MHz, $CDCl_3$) δ 156.4, 149.3, 143.2, 139.3, 135.7, 130.69 (q, $J_{C\text{-}F}$ = 32.2 Hz), 130.68, 128.0 (q, $J_{C\text{-}F}$ = 3.7 Hz), 124.8 (q, $J_{C\text{-}F}$ = 3.6 Hz), 124.2, 123.8 (d, $J_{C\text{-}F}$ = 271.4 Hz), 122.0. ^{19}F NMR (376 MHz, $CDCl_3$) δ -62.5 (s).

The experimental data obtained are in accordance with the literature.[105g]

2,2'-(3,3',5,5'-Tetrafluoro-[1,1'-biphenyl]-2,2'-diyl)dipyridine (2.2.18)

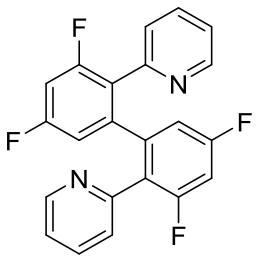

Following the General Procedure A. The product was isolated as a white solid (59 mg, 63% yield). ^{1}H NMR (400 MHz, $CDCl_3$) δ 8.47 (d, J = 4.4 Hz, 2H), 7.54 (td, J = 7.8, 1.7 Hz, 2H), 7.23-7.09 (m, 4H), 6.88-6.75 (m, 2H), 6.66 (d, J = 8.8 Hz, 2H). ^{13}C NMR (100 MHz, $CDCl_3$) δ 161.6 (dd, $J_{C\text{-}F}$ = 250.0, 13.8 Hz), 160.2 (dd, $J_{C\text{-}F}$ = 250, 13.8 Hz), 152.1, 149.1, 142.1, 135.8, 126.0, 124.3 (dd, $J_{C\text{-}F}$ = 15.3, 4.6 Hz), 122.2, 113.9 (dd, $J_{C\text{-}F}$ = 22.1, 3.6 Hz), 103.5 (dd, $J_{C\text{-}F}$ = 26.7, 25.3 Hz). ^{19}F NMR (376 MHz, $CDCl_3$) δ -109.8 (s), -111.8 (d, J = 6.1 Hz).

The experimental data obtained are in accordance with the literature.[105g]

2,2'-(5,5'-Dimethoxy-[1,1'-biphenyl]-2,2'-diyl)dipyridine (2.2.19) :

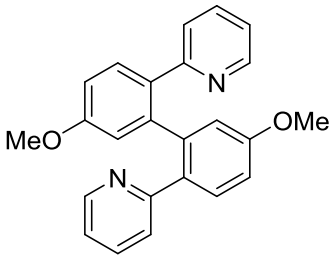

Following the General Procedure A. The product was isolated as a white solid (56 mg, 61% yield). ^{1}H NMR (400 MHz, $CDCl_3$) δ 8.29 (d, J = 4.6 Hz, 2H), 7.50 (d, J = 8.1 Hz, 2H), 7.30 (td, J = 7.9, 1.3 Hz, 2H), 7.01-6.91 (m, 6H), 6.73 (d, J = 7.9 Hz, 2H), 3.82 (s, 6H). ^{13}C NMR (100 MHz, $CDCl_3$) δ 159.6, 157.5, 148.7, 141.0, 135.2, 132.6, 131.4, 124.2, 120.7, 116.1, 113.6, 55.3.

The experimental data obtained are in accordance with the literature.[105g]

2,2'-(5,5'-Diphenoxy-[1,1'-biphenyl]-2,2'-diyl)dipyridine (3.2.5):

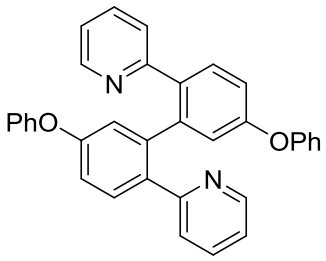

Following the General Procedure A. The product was isolated as a white solid (105 mg, 85% yield). ^{1}H NMR (400 MHz, $CDCl_3$) δ 8.43 (d, J = 4.7 Hz, 2H), 7.58 (d, J = 8.5 Hz, 2H), 7.47 (td, J = 7.7, 1.5 Hz, 2H), 7.34-7.26 (m, 4H), 7.15-7.08 (m, 4H), 7.06 (dd, J = 8.5, 2.5 Hz, 2H), 7.01 (d, J = 7.9 Hz, 2H), 6.96-6.85 (m, 6H). ^{13}C NMR (100 MHz, $CDCl_3$) δ 157.6, 157.0, 156.5, 149.0, 140.9, 135.3, 134.7, 131.7, 129.6(2C), 124.3, 123.3, 121.0, 120.7, 118.7(2C), 118.1. ESI-HRMS (m/z): $[M+H]^+$ Calcd for $C_{34}H_{25}N_2O_2$: 493.1911, Found: 493.1912.

2,2'-Di(isoquinolin-1-yl)-1,1'-biphenyl (3.2.6):

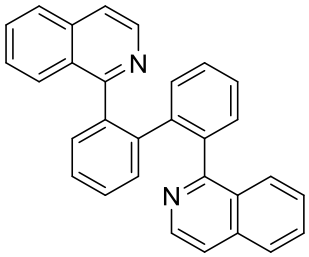

Following the General Procedure A. The product was isolated as a white solid (60 mg, 59% yield). ^{1}H NMR (400 MHz, $CDCl_3$) δ 7.83 (d, J = 8.3 Hz, 2H), 7.76 (d, J = 8.1 Hz, 2H), 7.58 (t, J = 7.0 Hz, 2H), 7.44-7.04 (m, 14H). ^{13}C NMR (100 MHz, $CDCl_3$) δ 160.4, 141.6, 140.6, 136.1, 131.8, 131.1, 129.5, 129.0, 128.1, 127.7, 127.2, 126.5, 126.4, 126.0, 119.7. ESI-HRMS (m/z): $[M+H]^+$ Calcd for $C_{30}H_{21}N_2$: 409.1699, Found: 409.1698.

1,1'-Di(pyridin-2-yl)-2,2'-binaphthalene (3.2.7):

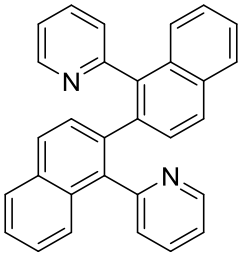

Following the General Procedure A. The product was isolated as a white solid (52 mg, 51% yield). ^{1}H NMR (400 MHz, $CDCl_3$) δ 8.66 (s, 2H), 7.79 (d, J = 7.9 Hz, 2H), 7.75-7.28 (m, 12H), 7.24-7.02 (m, 4H). ^{13}C NMR (100 MHz, $CDCl_3$) δ 158.2, 149.0, 138.1, 136.9, 135.8, 132.4, 132.1, 129.2, 127.8, 127.1, 126.8, 126.3, 126.0, 125.6, 121.6. ESI-HRMS (m/z): $[M+H]^+$ Calcd for $C_{30}H_{21}N_2$: 409.1699, Found: 409.1697.

2,2'-Di(pyridin-2-yl)-3,3'-bithiophene (3.2.8):

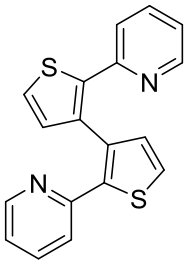

Following the General Procedure A. The product was isolated as a yellow solid (62 mg, 77% yield). ^{1}H NMR (400 MHz, $CDCl_3$) δ 8.48 (d, J = 4.3 Hz, 2H), 7.45 (d, J = 5.1 Hz, 2H), 7.37 (td, J = 7.9, 1.7 Hz, 2H), 7.07-6.99 (m, 4H), 6.97 (d, J = 5.1 Hz, 2H). ^{13}C NMR (100 MHz, $CDCl_3$) δ 152.2, 149.2, 140.9, 136.4, 134.1, 130.8, 127.3, 121.8, 120.1.

2,2'-Di(1*H*-pyrazol-1-yl)-1,1'-biphenyl (3.2.9):

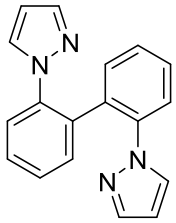

Following the General Procedure A. The product was isolated as a white solid (47 mg, 66% yield). ^{1}H NMR (400 MHz, $CDCl_3$) δ 7.54-7.46 (m, 4H), 7.42 (t, J = 7.7 Hz, 2H), 7.32 (t, J = 7.5 Hz, 2H), 7.25-7.16 (m, 4H), 6.17 (s, 2H). ^{13}C NMR (100 MHz, $CDCl_3$) δ 140.2, 138.8, 133.3, 130.9, 130.2, 128.7, 127.7, 125.5, 106.4.

The experimental data obtained are in accordance with the literature.[110]

2,2'-(4,4'-Bis(trifluoromethyl)-[1,1'-biphenyl]-2,2'-diyl)dipyridine (2.2.4a)

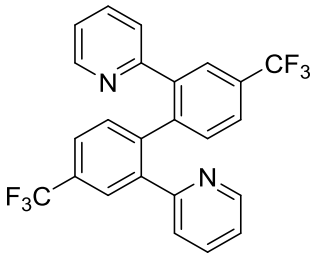

Following the General Procedure A. The product was isolated as a white solid (87 mg, 78% yield). ^{1}H NMR (400 MHz, $CDCl_3$) δ 8.38 (d, J = 4.4 Hz, 2H), 7.83 (s, 2H), 7.65 (d, J = 8.0 Hz, 2H), 7.47-7.37 (m, 4H), 7.10 (dd, J = 6.8, 5.0 Hz, 2H), 6.89 (d, J = 7.9 Hz, 2H). ^{13}C NMR (100 MHz, $CDCl_3$) δ 156.4, 149.4, 142.4, 140.4, 135.8, 131.6, 130.4 (q, $J_{C\text{-}F}$ = 32.8 Hz), 127.2-127.0 (m, 1C), 125.3-125.1 (m, 1C), 124.2, 122.5, 122.0. ^{19}F NMR (376 MHz, $CDCl_3$) δ -62.4 (s).

2,2'-(4,4',5,5'-Tetramethoxy-[1,1'-biphenyl]-2,2'-diyl)dipyridine (3.2.10):

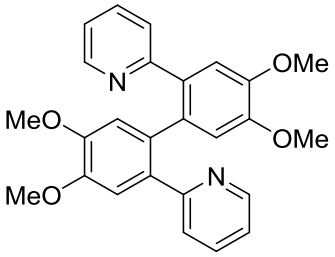

Following the General Procedure A. The product was isolated as a white solid (45 mg, 43% yield). ^{1}H NMR (400 MHz, $CDCl_3$) δ 8.37 (d, J = 4.3 Hz, 2H), 7.33 (td, J = 7.8, 1.6 Hz, 2H), 7.14 (s, 2H), 7.00 (dd, J = 6.7, 5.2 Hz, 2H), 6.83 (d, J = 7.9 Hz, 2H), 6.72 (s, 2H), 3.91 (s, 6H), 3.75 (s, 6H). ^{13}C NMR (100 MHz, $CDCl_3$) δ 157.9, 148.8, 148.7, 148.2, 135.2, 132.4, 131.9, 124.6, 120.9, 114.0, 112.6, 55.8(2C). ESI-HRMS (m/z): $[M+H]^+$ Calcd for $C_{26}H_{25}N_2O_4$: 429.1809, Found: 429.1808.

3,3'-Di(pyridin-2-yl)-2,2'-bithiophene (3.2.11):

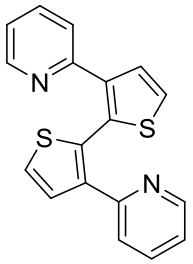

Following the General Procedure A. The product was isolated as a white solid (22 mg, 28% yield). ^{1}H NMR (400 MHz, $CDCl_3$) δ 8.41 (d, J = 4.2 Hz, 2H), 7.56 (d, J = 5.3 Hz, 2H), 7.47-7.35 (m, 4H), 7.06 (d, J = 8.0 Hz, 2H), 7.02-6.92 (m, 2H). ^{13}C NMR (100 MHz, $CDCl_3$) δ 153.5, 149.1, 140.6, 136.0, 131.6, 129.7, 126.4, 122.5, 121.5.

2,2'-(4-Bromo-4'-methoxy-[1,1'-biphenyl]-2,2'-diyl)dipyridine (3.2.14):

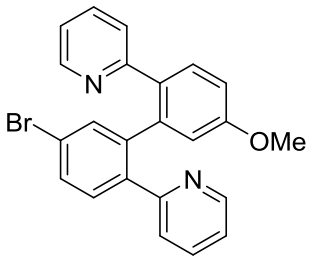

A 80 mL Fischer-Porter glassware was charged with Ru/C (202 mg, 10 mol%), $FeCl_3$ (162 mg, 1 mmol), 2-(4-methoxyphenyl)pyridine (92 mg, 0.5 mmol) and 2-(4-bromophenyl)pyridine (117 mg, 0.5 mmol) under air. The Fischer-Porter glassware was then left under vacuum for 5 min and pressurized with Ar gas. Then toluene (4 mL) was added under argon. The reaction mixture was magnetically stirred at 150 ℃ (sand bath) under Ar during 72 hours. The solution was cooled down to room temperature, then Et_3N (~4mL) was added and stirred at room temperature for 10 min before filtered through silica gel and washed with CH_2Cl_2 (60 mL). Then the filtrate was concentrated under vacuum and the crude product was purified by flash chromatography on silica gel (eluent: cyclohexane/AcOEt = 5/1 – 2/1 – 1/1). The product was isolated as a white solid (63 mg, 30% yield). ^{1}H NMR (400 MHz, $CDCl_3$) δ 8.29 (d, J = 4.3 Hz, 1H), 8.26 (d, J = 4.3 Hz, 1H), 7.60 (d, J = 1.9 Hz, 1H), 7.52 (dd, J = 8.3, 2.0 Hz, 1H), 7.44 (d, J = 8.4 Hz, 1H), 7.39 (d, J = 8.3 Hz, 1H), 7.36-7.28 (m, 2H), 7.05-6.90 (m, 4H), 6.74 (d, J = 7.9 Hz, 1H), 6.67 (d, J = 7.9 Hz, 1H), 3.83 (s, 3H). ^{13}C NMR (100 MHz, $CDCl_3$) δ 159.7, 157.2, 156.7, 148.9, 148.8, 141.6, 139.6, 138.7, 135.3 (2C), 133.6, 132.6, 131.6, 131.5, 130.8, 124.2, 124.1, 122.5, 121.4, 120.8, 116.1, 113.9, 55.4.

2,2'-(4-Fluoro-4'-methoxy-[1,1'-biphenyl]-2,2'-diyl)dipyridine (3.2.16):

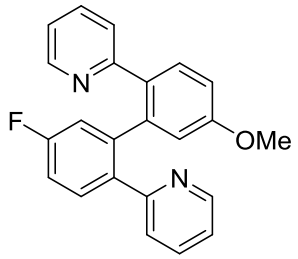

A 80 mL Fischer-Porter glassware was charged with Ru/C (202 mg, 10 mol%), $FeCl_3$ (162 mg, 1 mmol), 2-(4-methoxyphenyl)pyridine (92 mg, 0.5 mmol) and 2-(4-fluorophenyl)pyridine (86 mg, 0.5 mmol) under air. The Fischer-Porter glassware was then left under vacuum for 5 min and pressurized with Ar gas. Then toluene (4 mL) was added under argon. The reaction mixture was magnetically stirred at 150 ℃ (sand bath) under Ar during 72 hours. The solution was cooled down to room temperature, then Et_3N (~4mL) was added and stirred at room temperature for 10 min before filtered through silica gel and washed with CH_2Cl_2 (60 mL). Then the filtrate was concentrated under vacuum and the crude product was purified by flash chromatography on silica gel (eluent: cyclohexane/AcOEt = 5/1 – 2/1 – 1/1). The product was isolated as a white solid (35 mg, 19% yield). ^{1}H NMR (400 MHz, $CDCl_3$) δ 8.36-8.24 (m, 2H), 7.52 (dd, J = 8.3, 6.1 Hz, 1H), 7.47 (d, J = 8.6 Hz, 1H), 7.33 (t, J = 7.7 Hz, 2H), 7.16-7.06 (m, 2H), 7.04-6.93 (m, 3H), 6.90 (d, J = 2.3 Hz, 1H), 6.77 (d, J = 7.9 Hz, 1H), 6.71 (d, J = 7.8 Hz, 1H), 3.82 (s, 3H). ^{13}C NMR (100 MHz, $CDCl_3$) δ 163.8, 161.4, 159.7, 157.4, 157.0, 148.9, 141.9 (d, $J_{C\text{-}F}$ = 7.7 Hz), 139.9, 136.0 (d, $J_{C\text{-}F}$ = 3.1 Hz), 135.2, 132.6, 131.9 (d, $J_{C\text{-}F}$ = 7.7 Hz), 131.5, 124.2, 124.0, 121.2, 120.9, 117.6 (d, $J_{C\text{-}F}$ = 23.0 Hz), 116.0, 114.8, 114.6, 113.9, 55.4. ^{19}F NMR (376 MHz, $CDCl_3$) δ -113.5 (s).

2-(2-(Dimethylboranyl)phenyl)pyridine (3.4.1):

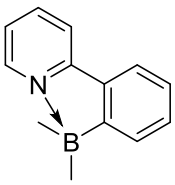

Following the General Procedure B. The product was isolated as a white solid (94 mg, 96% yield). ^{1}H NMR (400 MHz, $CDCl_3$) δ 8.48 (d, J = 5.6 Hz, 1H), 7.99-7.92 (m, 2H), 7.91 (d, J = 7.6 Hz, 1H), 7.78 (d, J = 7.2 Hz, 1H), 7.54 (t, J = 7.2 Hz, 1H), 7.42-7.32 (m, 2H), 0.20 (s, 6H). ^{13}C NMR (100 MHz, $CDCl_3$) δ 167.7, 156.8, 142.1, 139.2, 135.0, 130.2, 129.1, 125.1, 121.5, 121.3, 117.7, 8.9(2C).

The experimental data obtained are in accordance with the literature.[113]

2-(2-(Dimethylboranyl)-4-methylphenyl)pyridine (3.4.2):

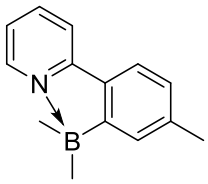

Following the General Procedure B. The product was isolated as a white solid (70 mg, 67% yield). ^{1}H NMR (400 MHz, $CDCl_3$) δ 8.43 (d, J = 5.7 Hz, 1H), 7.94-7.85 (m, 2H), 7.77 (d, J = 7.8 Hz, 1H), 7.54 (s, 1H), 7.29 (td, J = 6.1, 2.1 Hz, 1H), 7.16 (d, J = 7.7 Hz, 1H), 2.51 (s, 3H), 0.13 (s, 6H). ^{13}C NMR (100 MHz, $CDCl_3$) δ 168.3, 156.9, 142.0, 140.4, 139.1, 132.7, 129.7, 126.3, 121.4, 120.8, 117.4, 22.0, 9.1(2C). ESI-HRMS (m/z): $[M+H]^+$ Calcd for $C_{14}H_{17}BN$: 210.1449, Found: 210.1451.

2-(3-(Dimethylboranyl)-[1,1'-biphenyl]-4-yl)pyridine (3.4.3):

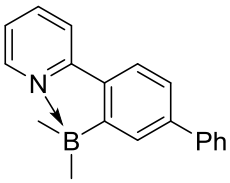

Following the General Procedure B. The product was isolated as a white solid (41 mg, 76% yield starting from 0.2 mmol of the corresponding 2-phenylpyridine). ^{1}H NMR (400 MHz, $CDCl_3$) δ 8.46 (d, J = 5.6 Hz, 1H), 7.99-7.87 (m, 4H), 7.76 (d, J = 7.3 Hz, 2H), 7.57 (dd, J = 7.9, 1.7 Hz, 1H), 7.50 (t, J = 7.6 Hz, 2H), 7.40 (t, J = 7.4 Hz, 1H), 7.34 (td, J = 5.6, 3.0 Hz, 1H), 0.15 (s, 6H). ^{13}C NMR (100 MHz, $CDCl_3$) δ 168.5, 156.6, 142.9, 142.3, 141.9, 139.3, 134.4, 128.6(2C), 127.8, 127.5(2C), 127.3, 124.5, 121.8, 121.2, 117.8, 9.2(2C). ESI-HRMS (m/z): $[M+H]^+$ Calcd for $C_{19}H_{19}BN$: 272.1605, Found: 272.1607.

2-(2-(Dimethylboranyl)-4-fluorophenyl)pyridine (3.4.4):

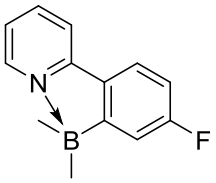

Following the General Procedure B. The product was isolated as a white solid (43 mg, 75% yield starting from 0.27 mmol of the corresponding 2-phenylpyridine). ^{1}H NMR (400 MHz, $CDCl_3$) δ 8.41 (d, J = 5.6 Hz, 1H), 7.94 (t, J = 7.7 Hz, 1H), 7.86 (d, J = 8.0 Hz, 1H), 7.79 (dd, J = 8.3, 4.7 Hz, 1H), 7.36-7.27 (m, 2H), 6.96 (td, J = 8.8, 2.4 Hz, 1H), 0.06 (s, 6H). ^{13}C NMR (100 MHz, $CDCl_3$) δ 171.7, 164.9 (d, $J_{C\text{-}F}$ = 251.7 Hz), 156.0, 142.2, 139.4, 131.0, 123.3 (d, $J_{C\text{-}F}$ = 8.8 Hz), 121.0, 117.5, 115.3 (d, $J_{C\text{-}F}$ = 18.4 Hz), 112.7 (d, $J_{C\text{-}F}$ = 24.5 Hz), 8.8(2C). ^{19}F NMR (376 MHz, $CDCl_3$) δ -110.4 (s). ESI-HRMS (m/z): $[M+H]^+$ Calcd for $C_{13}H_{14}BFN$: 214.1198, Found: 214.1200.

1-(2-(Dimethylboranyl)phenyl)isoquinoline (3.4.5):

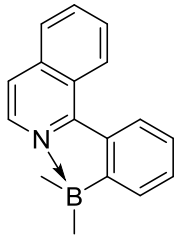

Following the General Procedure B. The product was isolated as a yellow solid (69 mg, 94% yield starting from 0.3 mmol of 1-phenylisoquinoline). ^{1}H NMR (400 MHz, $CDCl_3$) δ 9.13 (d, J = 8.3 Hz, 1H), 8.58 (d, J = 8.0 Hz, 1H), 8.35 (d, J = 6.3 Hz, 1H), 7.97-7.89 (m, 1H), 7.89-7.72 (m, 3H), 7.67 (d, J = 6.3 Hz, 1H), 7.56 (t, J = 7.1 Hz, 1H), 7.51-7.38 (m, 1H), 0.20 (s, 6H). ^{13}C NMR (100 MHz, $CDCl_3$) δ 172.1, 155.6, 137.5, 136.8, 134.0, 131.7, 129.9, 129.1, 128.7, 127.8, 126.2, 125.9, 125.8, 125.4, 120.3, 8.9(2C). ESI-HRMS (m/z): $[M+H]^+$ Calcd for $C_{17}H_{17}BN$: 246.1449, Found: 246.1451.

2,2'-(3,3'-Bis(dimethylboranyl)-[1,1'-biphenyl]-2,2'-diyl)dipyridine (3.4.7):

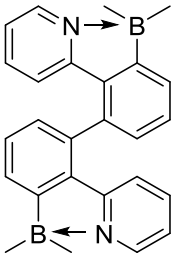

Following the General Procedure B. The product was isolated as a white solid (64 mg, 82% yield starting from 0.2 mmol of **2.2.4**). ^{1}H NMR (400 MHz, $CDCl_3$) δ 8.39 (d, J = 5.4 Hz, 2H), 7.82 (d, J = 7.2 Hz, 2H), 7.60 (t, J = 7.3 Hz, 2H), 7.46 (t, J = 7.8 Hz, 2H), 7.29 (d, J = 7.2 Hz, 2H), 7.18 (t, J = 6.5 Hz, 2H), 6.53 (d, J = 8.3 Hz, 2H), 0.16 (s, 6H), 0.10 (s, 6H). ^{13}C NMR (100 MHz, $CDCl_3$) δ 169.9, 156.4, 142.0, 139.1, 137.7, 132.8, 130.2, 128.5, 126.3, 121.1, 120.7, 10.4, 8.7. ESI-HRMS (m/z): $[M+H]^+$ Calcd for $C_{26}H_{27}B_2N_2$: 389.2355, Found: 389.2360.

2,2'-(3,3'-Bis(dimethylboranyl)-5,5'-dimethyl-[1,1'-biphenyl]-2,2'-diyl)dipyridine (3.4.8):

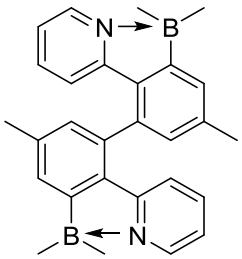

Following the General Procedure B. The product was isolated as a white solid (61 mg, 98% yield starting from 0.15 mmol of **2.3.10**). ^{1}H NMR (400 MHz, $CDCl_3$) δ 8.33 (d, J = 5.5 Hz, 2H), 7.58 (s, 2H), 7.47-7.38 (m, 2H), 7.14-7.08 (m, 2H), 7.07 (s, 2 H), 6.53 (d, J = 8.4 Hz, 2H), 2.52 (s, 6H), 0.11 (s, 6H), 0.06 (s, 6H). ^{13}C NMR (100 MHz, $CDCl_3$) δ 170.0, 156.5, 141.8, 140.5, 139.0, 137.6, 130.4, 129.1, 127.4, 120.6, 120.3, 21.8, 10.3, 8.7. ESI-HRMS (m/z): $[M+H]^+$ Calcd for $C_{28}H_{31}B_2N_2$: 417.2668, Found: 417.2677.

2,2'-(3,3'-Bis(dimethylboranyl)-5,5'-diphenyl-[1,1'-biphenyl]-2,2'-diyl)dipyridine (3.4.9):

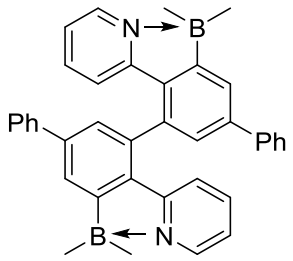

Following the General Procedure B. The product was isolated as a yellow solid (80 mg, 87% yield starting from 0.17 mmol of **3.2.1**). ^{1}H NMR (400 MHz, $CDCl_3$) δ 8.41 (d, J = 5.4 Hz, 2H), 8.09 (s, 2H), 7.85 (d, J = 7.8 Hz, 4H), 7.65 (s, 2H), 7.55-7.45 (m, 6H), 7.40 (t, J = 7.3 Hz, 2H), 7.21-7.15 (m, 2H), 6.73 (d, J = 8.3 Hz, 2H), 0.21 (s, 6H), 0.16 (s, 6H). ^{13}C NMR (100 MHz, $CDCl_3$) δ 170.7, 156.1, 142.5, 142.1, 140.9, 139.2, 137.9, 132.1, 128.8(2C), 127.6, 127.4(2C), 127.0, 125.5, 121.1, 120.7, 10.5, 8.8. ESI-HRMS (m/z): $[M+H]^+$ Calcd for $C_{38}H_{35}B_2N_2$: 541.2981, Found: 541.2996.

2,2'-(3,3'-Bis(dimethylboranyl)-5,5'-difluoro-[1,1'-biphenyl]-2,2'-diyl)dipyridine (3.4.10):

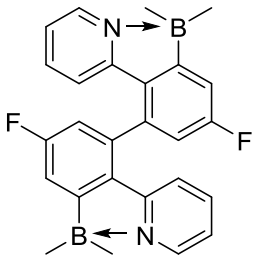

Following the General Procedure B. The product was isolated as a white solid (32 mg, 69% yield starting from 0.11 mmol of **3.2.2**). ^{1}H NMR (400 MHz, $CDCl_3$) δ 8.35 (d, J = 5.5 Hz, 2H), 7.53-7.46 (m, 2H), 7.42 (dd, J = 8.0, 2.4 Hz, 2H), 7.18 (t, J = 6.4 Hz, 2H), 6.95 (dd, J = 9.2, 2.4 Hz, 2H), 6.52 (d, J = 8.4 Hz, 2H), 0.09 (s, 6H), 0.03 (s, 6H). ^{13}C NMR (100 MHz, $CDCl_3$) δ 174.5, 164.3 (d, $J_{C\text{-}F}$ = 254.9 Hz), 155.2, 142.2, 139.4, 138.4 (d, $J_{C\text{-}F}$ = 8.4 Hz), 128.5, 121.1, 120.1, 115.1 (d, $J_{C\text{-}F}$ = 18.1 Hz), 113.7 (d, $J_{C\text{-}F}$ = 24.0 Hz), 10.1, 8.6. ^{19}F NMR (376 MHz, $CDCl_3$) δ -110.2 (s). ESI-HRMS (m/z): $[M+H]^+$ Calcd for $C_{26}H_{25}B_2F_2N_2$: 425.2166, Found: 425.2173.

1,1'-(3,3'-Bis(dimethylboranyl)-[1,1'-biphenyl]-2,2'-diyl)diisoquinoline (3.4.11):

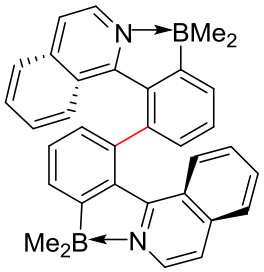

Following the General Procedure B. The product was isolated as a yellow solid (32 mg, 29% yield starting from 0.23 mmol of **3.2.6**). ^{1}H NMR (400 MHz, $CDCl_3$) δ 7.86-7.79 (m, 2H), 7.73 (t, J = 7.2 Hz, 2H), 7.70-7.62 (m, 4H), 7.52 (d, J = 8.0 Hz, 2H), 7.45 (t, J = 7.4 Hz, 2H), 7.28 (d, J = 8.9 Hz, 2H), 7.23 (d, J = 6.3 Hz, 2H), 6.85 (t, J = 7.7 Hz, 2H), -0.29 (s, 6H), -0.51 (s, 6H). ^{13}C NMR (100 MHz, $CDCl_3$) δ 157.1, 141.0, 136.9, 136.0, 132.6, 131.4, 131.0, 129.0, 128.1, 127.4, 127.1, 125.6, 123.8, 120.1. ESI-HRMS (m/z): $[M+H]^+$ Calcd for $C_{34}H_{31}B_2N_2$: 489.2668, Found: 489.2676.

(two carbon signals could not be seen)

Chapter 3 Pd-catalyzed C-H activation intramolecular arylation *via* concerted metalation-deprotonation

1 Introduction and background

The synthesis of biaryl compounds is of great importance in pharmaceuticals, natural products and material science.[118] Traditional transition-metal catalyzed cross-coupling reactions, such as Suzuki coupling, are important and reliable methods to synthesize biaryl compounds (**Scheme 1.1**). However, pre-functionalization of both reagents for Suzuki coupling, namely the aryl (pseudo)halides and organoboron compounds, requires several synthetic steps, which can be a time-consuming and economically inefficient process. In addition, it has led to the formation of large quantities of organic wastes, which can be detrimental to the environment.

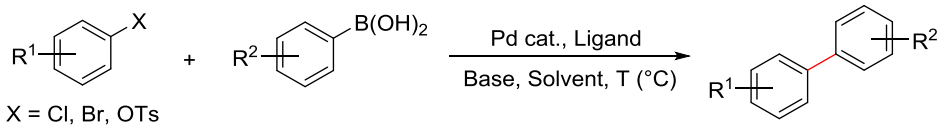

Scheme 1.1 Biaryl synthesis through Suzuki reaction

Regarding the requirements of green chemistry syntheses, a more environmentally friendly and more economically attractive strategy, namely the C-H activation/functionalization strategy, has been developed for the synthesis of biaryl compounds (**Scheme 1.2**).[118b, c] This new strategy requires the pre-synthesis of only one reagent (**Scheme 1.2**, eq. a), or no pre-synthesis of either substrate is needed in the case of cross-dehydrogenative coupling (CDC) (**Scheme 1.2**, eq. b). Obviously, the C-H activation strategy, especially CDC reactions, is preferred for the synthesis of biaryl compounds due to the easier and less expensive access of the substrates. In this context, the development of new C-H activation strategies allowing the versatile synthesis of various biaryl compounds is highly desirable and of great importance.

[118] a) P. E. Fanta, *Chem. Rev.* **1946**, *38*, 139; b) D. Alberico, M. E. Scott, M. Lautens, *Chem. Rev.* **2007**, *107*, 174; c) L. Ackermann, R. Vicente, A. R. Kapdi, *Angew. Chem., Int. Ed.* **2009**, *48*, 9792; d) I. Hussaina, T. Singh, *Adv. Synth. Catal.* **2014**, *356*, 1661; e) I. Hussain, J. Capricho, M. A. Yawer, *Adv. Synth. Catal.* **2016**, *358*, 3320.

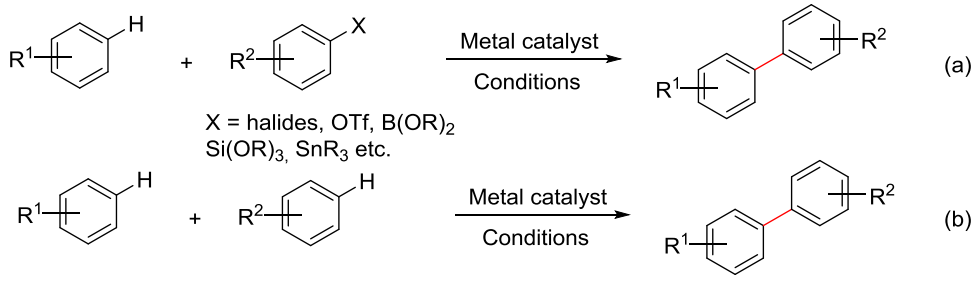

Scheme 1.2 Biaryl synthesis through C-H activation

Among the published methods concerning the biaryl synthesis through C-H activation, Pd-based catalysts are the most studied. Several reaction pathways have been proposed using these Pd-catalysts, like the electrophilic aromatic substitution (S_EAr) mechanism [119] and the concerted metalation-deprotonation (CMD) mechanism. [120] Generally, the S_EAr mechanism is considered when using electron-rich π-nucleophilic (hetero)arenes as substrates for C-H activation, while the CMD pathway is mostly employed when using electron-deficient arenes. The CMD mechanism was initially proposed by S. Winstein and T. G. Traylor for the acetolysis of diphenylmercury in acetic acid in 1955.[121] However, it was K. Fagnou who appointed the name of CMD process, which is now mostly adopted (**Figure 1.1**).[120c, 122] Fagnou's group has made great contributions to the development of C-H activation processes, especially those involving CMD mechanisms. Taking advantage of the CMD processes, Fagnou has developed a series of methods allowing the syntheses of various biaryl compounds, including liner biaryl compounds through intermolecular C-H activation aryl-aryl coupling[123] and polycyclic biaryl compounds through intramolecular C-H functionalization.[124]

---

[119] a) S. Pivsa-Art, T. Satoh, Y. Kawamura, M. Miura, M. Nomura, *Bull. Chem. Soc. Jpn.* **1998**, *71*, 467; b) C.-H. Park, V. Ryabova, I. V. Seregin, A. W. Sromek, V. Gevorgyan, *Org. Lett.* **2004**, *6*, 1159; c) B. S. Lane, M. A. Brown, D. Sames, *J. Am. Chem. Soc.* **2005**, *127*, 8050; d) Y.-X. Jia, J. Zhong, S.-F.Zhu, C.-M. Zhang, Q.-L. Zhou, *Angew. Chem. Int. Ed.* **2007**, *46*, 5565; e) B. Galabov, D. Nalbantova, P. von R. Schleyer, H. F. Schaefer, III, *Acc. Chem. Res.* **2016**, *49*, 1191.

[120] a) D. L. Davies, S. M. A. Donald, S. A. Macgregor, *J. Am. Chem. Soc.* **2005**, *127*, 13754; b) D. Garcia-Cuadrado, A. A. C. Braga, F. Maseras, A. M. Echavarren, *J. Am. Chem. Soc.* **2006**, *128*, 1066; c) M. Lafrance, C. N. Rowley, T. K. Woo, K. Fagnou, *J. Am. Chem. Soc.* **2006**, *128*, 8754; d) D. Garcia-Cuadrado, P. de Mendoza, A. A. C. Braga, F. Maseras, A. M. Echavarren, *J. Am. Chem. Soc.* **2007**, *129*, 6880; e) S. I. Gorelsky, D. Lapointe, K. Fagnou, *J. Am. Chem. Soc.* **2008**, *130*, 10848; f) D. Lapointe, K. Fagnou, *Chem. Lett.* **2010**, *39*, 1118.

[121] S. Winstein, T. G. Traylor, *J. Am. Chem. Soc.* **1955**, *77*, 3747.

[122] D. R. Stuart, K. Fagnou, *Science*, **2007**, *316*, 1172.

[123] See *ref 120c, e*, and *ref 122*, and a) M. Lafrance, D. Shore, K. Fagnou, *Org. Lett.* **2006**, *8*, 5097; b) M. Lafrance, K. Fagnou, *J. Am. Chem. Soc.* **2006**, *128*, 16496; c) L.-C. Campeau, D. J. Schipper, K. Fagnou, *J. Am. Chem. Soc.* **2008**, *130*, 3266; d) L. Caron, L.-C. Campeau, K. Fagnou, *Org. Lett.* **2008**, *10*, 4533; e) D. J. Schipper, L.-C. Campeau, K. Fagnou, *Tetrahedron*, **2009**, *65*, 3155; f) B. Liégault, D. Lapointe, L. Caron, A. Vlassova, K. Fagnou, *J. Org. Chem.* **2009**, *74*, 1826; g) B. Liégault, I. Petrov, S. I. Gorelsky, K. Fagnou, *J. Org. Chem.* **2010**, *75*, 1047; h) O. René, K. Fagnou, *Org. Lett.* **2010**, *12*, 2116; i) O. René, K. Fagnou, *Adv. Synth. Catal.* **2010**, *352*, 2116; j) H.-Y. Sun, S. I. Gorelsky, D. R. Stuart, L.-C. Campeau, K. Fagnou, *J. Org. Chem.* **2010**, *75*, 8180.

[124] a) L.-C. Campeau, M. Parisien, M. Leblanc, K. Fagnou, *J. Am. Chem. Soc.* **2004**, *126*, 9186; b) M. Leblanc, N. Blaquière, K. Fagnou, *Chem. Commun.* **2004**, 2874; c) L.-C. Campeau, P. Thansandote, K. Fagnou, *Org. Lett.* **2005**, *7*, 1857; d) M. Parisien, D. Valette, K. Fagnou, *J. Org. Chem.* **2005**, *70*, 7578; e) L.-C. Campeau, M. Parisien, A. Jean, K. Fagnou, *J. Am. Chem. Soc.* **2006**, *128*, 581; f) J.-P. Leclerc, M. André, K. Fagnou, *J. Org. Chem.* **2006**, *71*, 1711; g) M. Lafrance, D. Lapointe, K. Fagnou, *Tetrahedron*, **2008**, *64*, 6015; h) B. Liégault, D. Lee, M. P. Huestis, D. R. Stuart, K. Fagnou, *J. Org. Chem.* **2008**, *73*, 5022.

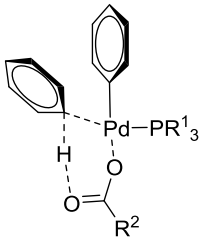

Figure 1.1 Key intermediate in the CMD process proposed by Fagnou[120e]

Polycyclic biaryl compounds commonly exist in various natural compounds and pharmaceuticals (**Figure 1.2**). These compounds have unique pharmacological activities. For example, tricyclic compound **1.1** can inhibit adaptor associated kinase 1 (AAK1), which is a member of the Ark1/Prk1 family of serine/threonine kinases.[125] AAK1 modulates clatherin coated endocytosis, a process that is important in synaptic vesicle recycling and receptor-mediated endocytosis. Colchicine is a microtubule depolymerizing agents, which can help to search for new antitumor agents.[126] However, the high toxicity of such agents has limited their use in the treatment of human neoplasms. Allocolchicine, which is an analogue of colchicine, is less toxic and thus is promising in the search for new antitumor agents. In this context, efficient syntheses of these bioactive compounds are of great importance and challenging.

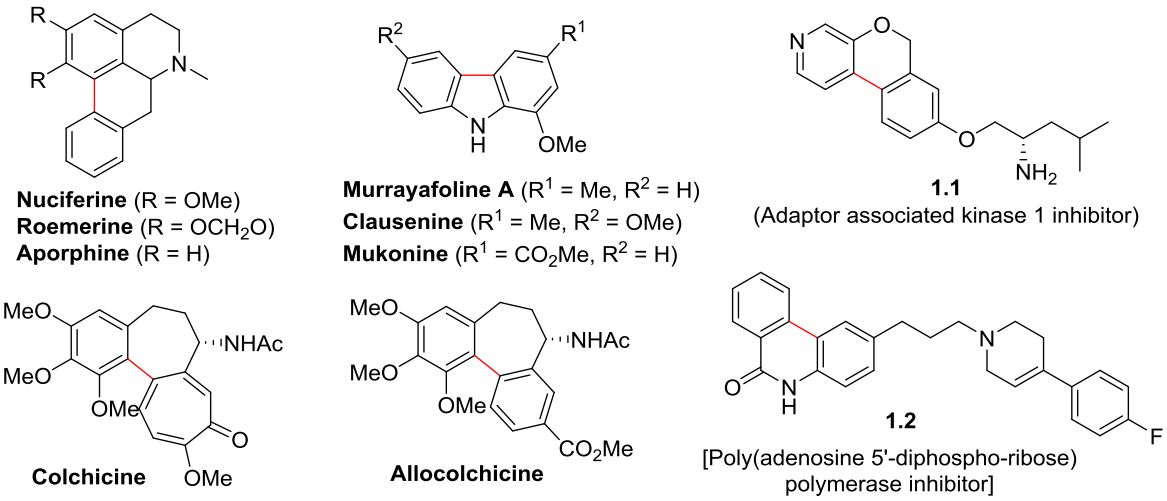

Figure 1.2 Naturally occuring polycyclic biaryl compounds

[125] S. J. Nara, C. D. Dzierba, J. E. Macor, J. J. Bronson, R. Rajamani, T. K. Maishal, M. S. Karatholuvhu, S. Thangavel, K. Thiyagarajan, Int. Pat. Appl. WO 2016164295 A2.

[126] M. Leblanc, K. Fagnou, *Org. Lett.* **2005**, *7*, 2849.

Conventional synthetic methods require multi-step synthesis of these compounds, which are very time and resource consuming.[127] By contrast, synthesis of these compounds through aryl-aryl coupling *via* C-H activation is more convenient, and it provides the possibility to synthesize various analogues using the same method,[124b, 128] which is important in searching new bioactive compounds. In this context, the development of synthetic methods concerning the syntheses of polycyclic biaryl compounds through CMD processes is reviewed herein.

1.1 Synthesis of polycyclic biaryls through intramolecular arylation involving CMD process

In 2004, Fagnou's group reported a method for biaryl synthesis through intramolecular arylation using $Pd(OAc)_2$ as catalyst and compound **1.1.1** as *P*, *N*-bidentate ligand in the presence of K_2CO_3 as base.[124a] Various substrates with electron-rich and electron-deficient groups were coupled under the reaction conditions, and *o*-, *m*-, and *p*-substituted substrates all gave good yields of the coupling products (**Scheme 1.3**, compounds **1.1.2**-**1.1.4**). Notably, the regioselectivity of this method was good, as demonstrated by the synthesis of compound **1.1.2**. Besides, the catalyst loading could be lowered down to 0.1 mol%, although a higher reaction temperature should be used with such low catalyst loading. Interestingly, chloro substituent was tolerated under the reaction conditions, as shown for the synthesis of compound **1.1.5**. Moreover, the syntheses of compounds **1.1.6** and **1.1.7** were achieved, which extended the substrate scope of the reaction, although the catalyst loading should be increased in order to achieve high conversion of these compounds. The authors also succeeded to apply their method to the synthesis of compounds with larger ring sizes through modifying the ligand. Thus, using the electron-deficient ligand **1.1.9**, the authors synthesized compound **1.1.8** with a high yield of 92%. This result represented a rare example of using electron-deficient ligand in the C-H activation process that gave good yields of the products, since electron-rich ligands were used in such reactions more usually.[129] Applications of this method to the syntheses of aporphine alkaloids[124b] and formal enantioselective synthesis allocolchicine[126] were also achieved by the same group with optimized reaction conditions (**Figure 1.3**), demonstrating the usefulness of this method. Notably, an intramolecular k_H/k_D value of 3.5 was observed for this reaction, indicating a CMD mechanism for this transformation.

[127] A. V. Vorogushin, A. V. Predeus, W. D. Wulff, H. J. Hansen, *J. Org. Chem.* **2003**, *68*, 5826.

[128] M. Lafrance, N. Blaquière, K. Fagnou, *Eur. J. Org. Chem.* **2007**, 811.

[129] M. Miura, *Angew. Chem. Int. Ed.* **2004**, *43*, 2201.

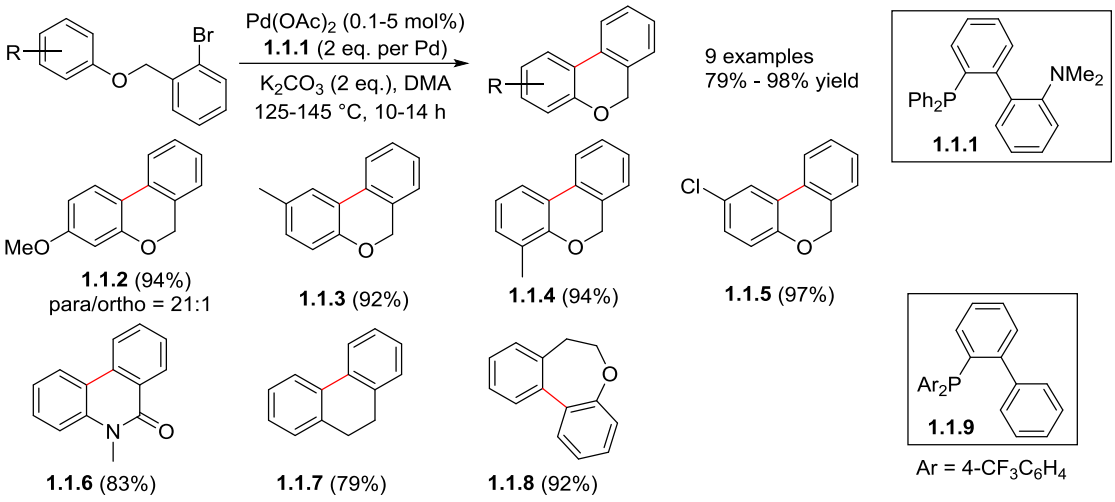

Scheme 1.3 Pd-catalyzed intramolecular arylation

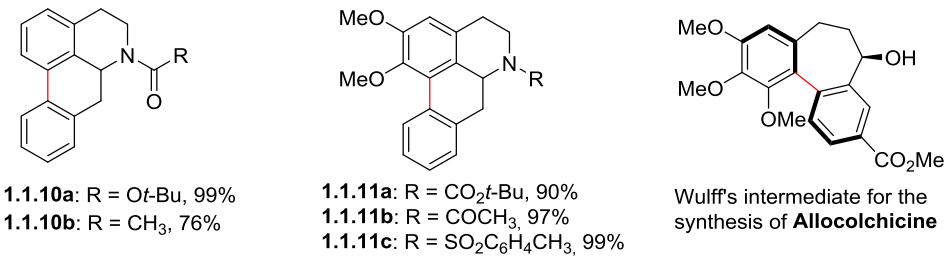

Figure 1.3 Synthesized aporphine alkaloids using Fagnou's method

In 2005, Fagnou's group realized a similar transformation by using aryl chlorides as substrates and a *N*-heterocyclic carbene (NHC) palladium complex **1.1.12** as catalyst (**Scheme 1.4**).[124c] Since aryl chlorides were rarely employed in the intramolecular C-H arylation,[130] this method provided a general way to achieve polycyclic biaryl compounds using aryl chlorides as substrates. The use of NHC hydrochloride salt **1.1.13** as additive significantly increased the turn-over number (TON) of the reaction, because excess **1.1.13** could reactivate the catalyst once catalyst decomposition took place. This effect was also observed in the Stille coupling using the same catalyst, indicating that the addition of imidazolium salt might generally increase the TON of palladium-NHC catalysts. Moreover, this method was applicable to the formation of not only substrates with six-membered rings, but also substrates with five-membered rings (**Scheme 1.4**, compounds **1.1.14-1.1.17**). Notably, a protecting group at the nitrogen atom was not necessary for the syntheses of carbazoles, which was practical in carbazole synthesis. A limitation of this method was that the Pd-NHC catalyst was not effective for the intramolecular C-H arylation of more sterically encumbered substrates.[126]

[130] For an example, see: R. B. Bedford, C. S. J. Cazin, *Chem. Commun.* **2002**, 2310.

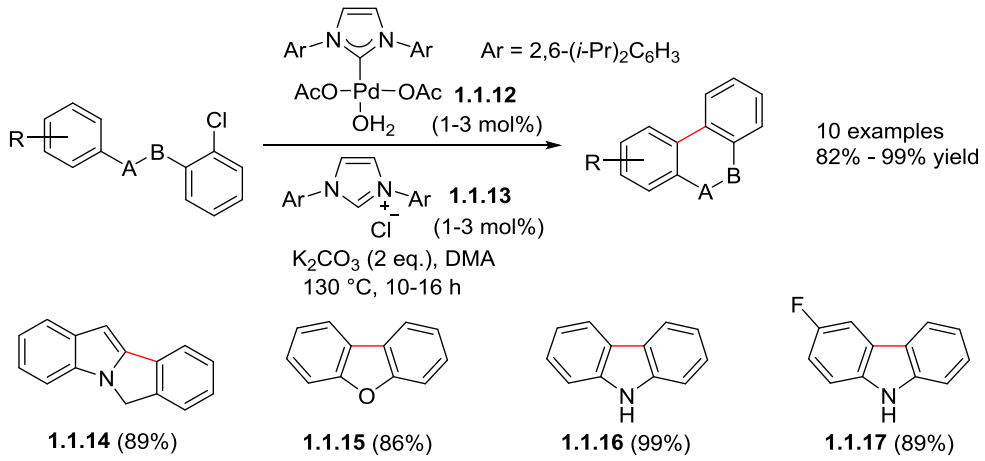

Scheme 1.4 Pd-NHC catalyzed intramolecular arylation

Besides $Pd(OAc)_2$ and Pd-NHC complex, Fagnou's group discovered that the Pearlman's catalyst [$Pd(OH)_2/C$] could also catalyze the intramolecular C-H arylation reactions of aryl iodides and bromides (**Scheme 1.5**).[124d] Under this reaction conditions, no ligands were required, which represented one of the advantages of this method. The reaction had a broad substrate scope, and it exhibited excellent selectivity for arylation over hydrodehalogenation (sulfide palladium on carbon also gave similar yields of the cyclization products, but the ratio of hydrodehalogenation products was higher using this catalyst). Generally, aryl bromides required longer reaction times than aryl iodides, and lower yields were obtained when employing deactivated aryl bromides as substrates (compound **1.1.20**). An unprotected phenol group didn't affect the arylation reaction, as illustrated by the synthesis of compound **1.1.18c**. Besides, substrates with a substituent present within the tether also proceeded efficiently, as indicated by the synthesis of compound **1.1.19**.

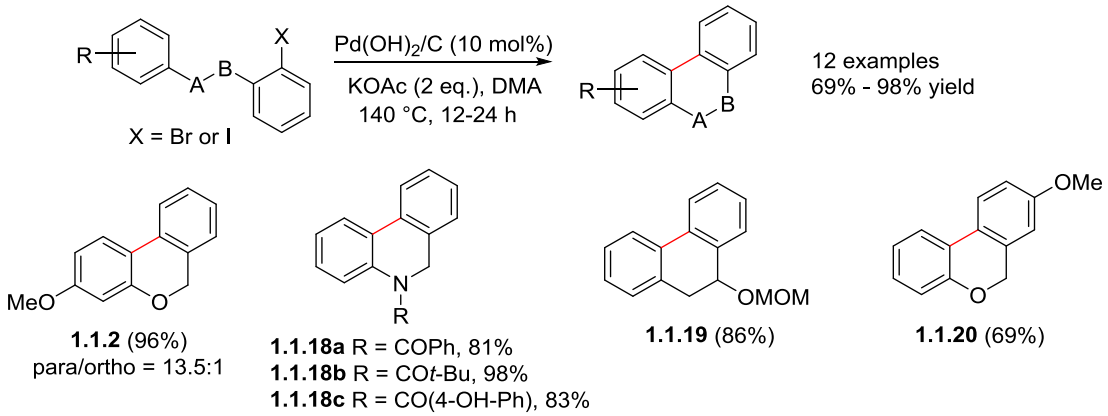

Scheme 1.5 Intramolecular C-H arylation catalyzed by Pearlman's catalyst

To identify the active catalytic species, two three-phase tests were conducted by the authors (**Scheme 1.6**). In the first experiment, the substrate was anchored to a Wang resin through an amide linker (compound **1.1.21**),[131] which should not react with a heterogeneous catalyst. Conducting the arylation reaction with compound **1.1.21** under the standard reaction conditions resulted in full conversion of the arylated product **1.1.18c** after cleavage of the product from the resin, which suggested a homogeneous active catalytic species. In another experiment, substrate **1.1.22** reacted under standard conditions in the presence of a silica-supported thiol-based scavenger resin, which could sequester the homogeneous catalyst after its formation. As a result, less than 5% of the desired product was formed in this case, suggesting that the heterogeneous catalyst had little contribution to the arylation reactions or the trapping of the homogeneous catalyst was not total. These two experiments indicated that the active catalytic species of the intramolecular C-H arylation reactions were homogeneous Pd-species generated *in situ* from the Pearlman's catalyst.

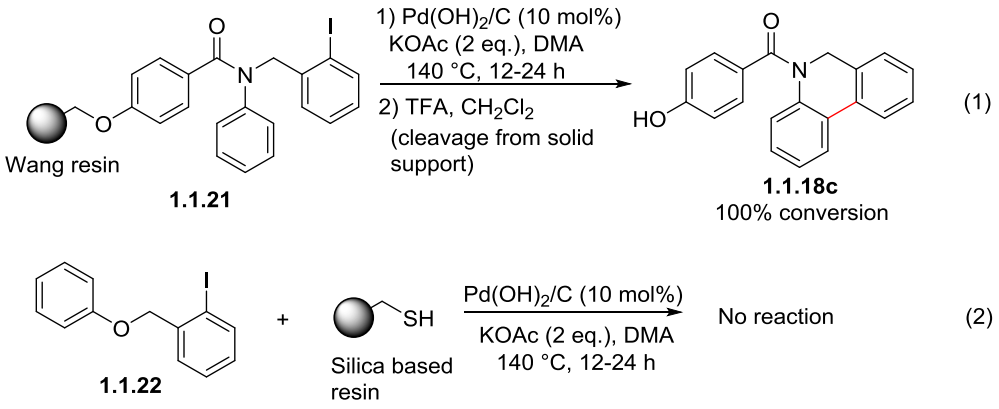

Scheme 1.6 Tests for the determination of active catalytic species

Although the methods described previously had already allowed the C-H arylation of aryl chlorides, bromides and iodides, different reaction conditions should be employed for each type of substrates. In this context, Fagnou's group developed a new catalytic system allowing the C-H arylation of all kinds of substrates described (**Scheme 1.7**).[124e] Using $Pd(OAc)_2$ as catalyst, the authors screened a series of phosphine ligands, finding that trialkylphosphines were better ligands than triarylphosphines and *o*-biarylphosphines, among which tricyclohexylphosphine (PCy_3, added as the air-stable HBF_4 salts) gave the best results of the arylation reactions. The authors also discovered that the nature of the base and its counterion had a significant impact on catalyst reactivity and selectivity, and potassium bases generally gave better results than sodium bases (the use of K_2CO_3 as base gave 100% conversion and >99:1 ratio of desired product, while the use of Na_2CO_3 as base gave only 11% conversion and 20:1 ratio of desired product).

[131] A. Bianco, J. Furrer, D. Limal, G. Guichard, K. Elbayed, J. Raya, M. Piotto, J.-P. Briand, *J. Comb. Chem.* **2000**, *2*, 681.

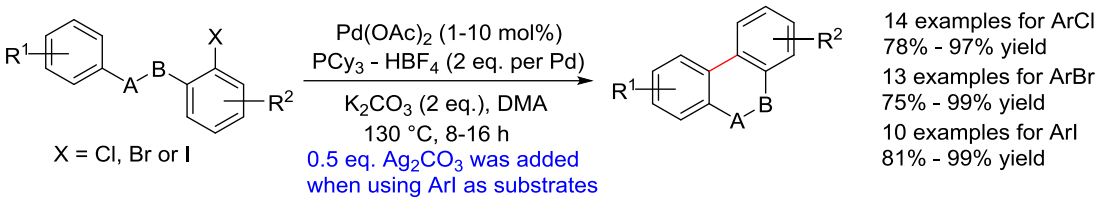

Scheme 1.7 New catalytic system for intramolecular C-H arylation

Using this new catalytic system, the syntheses of sterically hindered biaryls from aryl chlorides were achieved (**Figure 1.4**, compounds **1.1.23** and **1.1.24**), which was an improvement of the previous method.[124c] The arylation of *N*-alkyl indoles preferentially occurred at the C-2 position, while C-8 arylation occurred if C-2 position was blocked (**Figure 1.4**, compounds **1.1.14** and **1.1.25**). The use of heterocycles such as furan were also permitted under the reaction conditions (compound **1.1.26**), and *N*-unprotected product **1.1.27** with seven-membered ring was also efficiently formed with high yield. This method was applied in the synthesis of mukonine, a natural carbazole alkaloid, in three steps with a 75% overall yield.

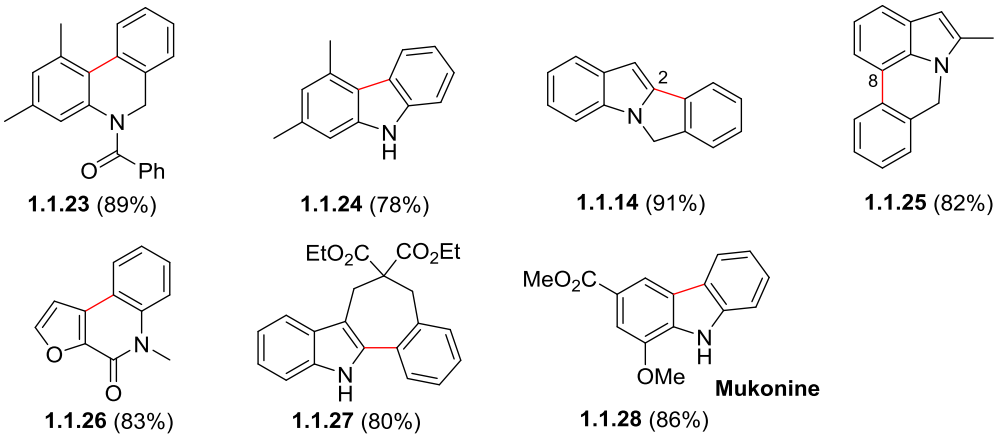

Figure 1.4 Biaryl synthesis using aryl chlorides as substrates

The use of aryl bromides as substrates allowed the presence of a chloride substituent, as already been observed previously in the synthesis of compound **1.1.5**,[124a] which demonstrated the good selectivity of the catalytic system. Moreover, the convenient syntheses of sterically hindered tri- and tetra-*o*-substituted biaryls were one of the advantages of this method (**Figure 1.5**, compounds **1.1.29**-**1.1.32**). These cyclic biaryls could be readily converted into acyclic biaryls by treating them with BBr_3 in CH_2Cl_2 at room temperature followed by trapping with acetic anhydride, which offered an alternative access of the sterically hindered biaryls to conventional cross-coupling protocols.

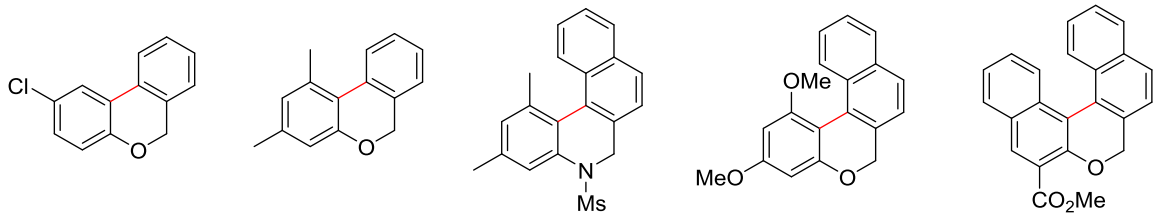

1.1.5 (90%) **1.1.29** (86%) **1.1.30** (97%) **1.1.31** (90%) **1.1.32** (85%)

Figure 1.5 Biaryl synthesis using aryl bromides as substrates

When using aryl iodides as substrates, the addition of 0.5 equivalent of Ag_2CO_3 was essential to achieve high conversions of the reactions. This was due to the poisoning of the catalyst by iodide, and the addition of silver salt could remove the iodide ion through precipitation. Moreover, the addition of Ag_2CO_3 accelerated the reaction time and allowed the use of a lower reaction temperature (80 ℃). A nitrogen atom present within the tether should be transformed into amide group before conducting the arylation reaction (**Figure 1.6**, compound **1.1.33**). The use of heterocycles such as furan and thiophene were tolerated under the reaction conditions, giving high yields of the arylated products (**Figure 1.6**, compounds **1.1.34** and **1.1.35**). This method was also applicable to the synthesis of dibenzo[*b*,*d*]furan, carbazole and fluorene (**Figure 1.6**, compounds **1.1.15**, **1.1.16** and **1.1.36**), demonstrating the broad substrate scope of the reaction.

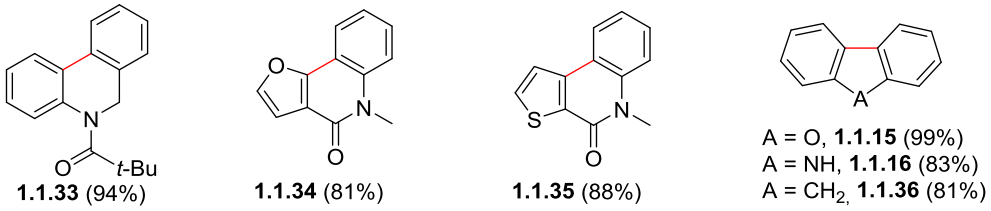

1.1.33 (94%) **1.1.34** (81%) **1.1.35** (88%)

Figure 1.6 Biaryl synthesis using aryl iodides as substrates

A study about the influence of steric and electronic effects on the regioselectivity of arylation reactions was conducted by the authors, revealing that the preferential arylation site was the most sterically accessible one in general (**Scheme 1.8**, compound **A**). However, halide substituents gave poor regioselectivity of the reaction, and the employment of a fluorine atom resulted in a reversed selectivity, giving compound **B** as the major product. This type of effect with fluorine had also been observed in other cases,[132] which might be due to the influence of the acidity of the C-H bond on both site selectivity and reactivity[124g] or the lone pair electrons of fluorine directed the metal to the adjacent position.[132b]

[132] a) G. A. Chotana, M. A. Rak, M. R. Smith III, *J. Am. Chem. Soc.* **2005**, *127*, 10539; b) M. Sonoda, F. Kakiuchi, N. Chatani, S. Murai, *Bull. Chem. Soc. Jpn.* **1997**, *70*, 3117.

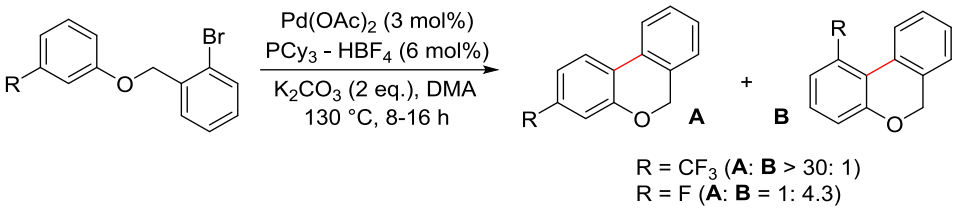

Scheme 1.8 Influence of steric and electronic effects on the regioselectivity of arylation

Several experiments were conducted to ascertain the reaction mechanism. Intramolecular competition reactions showed a small electronic bias towards the more electron-rich ring. The intramolecular C-H arylation of naphthyl substrate also resulted in low preference at the 1-position, which was the most electron-rich site. A primary intramolecular kinetic isotope effect (KIE) of 4.25 was observed using mono-deuterated compound **1.1.37** as substrate (**Scheme 1.9**). These experiments did not support an electrophilic aromatic substitution (S_EAr) mechanism, which normally showed large electronic bias and did not exhibit KIEs.[133] The small electronic bias might point to a lack of cationic areneium character at the rate-determining step, while the presence of primary kinetic isotope effects indicated that the C-H bond cleavage was a kinetically significant step in the catalytic cycle. Thus, a concerted metalation-deprotonation (CMD) process was more reasonable to explain the observations.

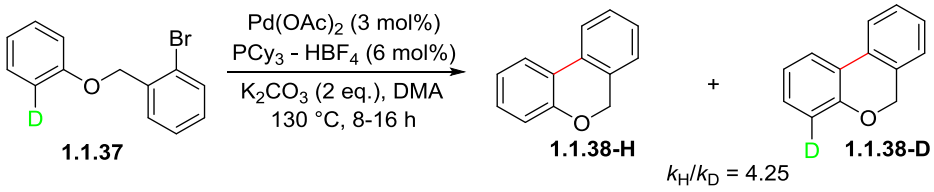

Scheme 1.9 KIE study of intramolecular C-H arylation

Almost at the same time, Fagnou's group discovered that the addition of a catalytic amount of pivalic acid (30 mol %) significantly promoted the benzene arylation reactions.[123b] Based on this observation, the group developed milder reaction conditions for the intramolecular C-H arylation reactions thanks to the screening of the phosphine ligands, which allowed the reactions to occur at low temperatures such as 50 ℃.[124g] The effect of the nature of phosphine ligands was carefully studied by the authors, revealing that the electron-deficient ligand tri(4-fluorophenyl)phosphine was the best one for arylation reactions, while the electron-neutral ligand triphenylphosphine also gave good results. Various electron-rich, electron-deficient and sterically encumbered substrates were used under the optimized reaction conditions, giving the biaryls with good yields. Notably, a KIE of 5.4 was observed using

[133] B. Martín-Matute, C. Mateo, D. J. Cárdenas, A. M. Echavarren, *Chem. Eur. J.* **2001**, *7*, 2341.

compound **1.1.37** as substrate under the reaction conditions, suggesting that the cleavage of C-H bond was the rate-determining step of the arylation reaction.

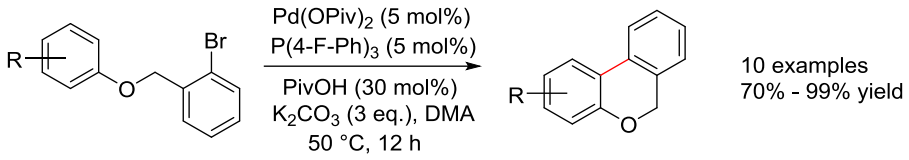

Scheme 1.10 Optimized reaction conditions for intramolecular C-H arylation

Based on the results, especially the observation of KIEs of the reaction, a mechanism based on CMD process was proposed by the authors (**Scheme 1.11**). First of all, oxidative insertion of palladium into the C-Br bond gave intermediate **M1**, which might be followed by two different pathways. In the first pathway, the bromide ligand was exchanged with a pivalate to give **M2**, which underwent a concerted palladation-deprotonation to give the biarylpalladium(II) intermediate **M4** *via* transition state **M3**. Reductive elimination of **M4** gave the desired product and closed the catalytic cycle. Alternatively, the pivalate might act as an external base in the concerted palladation-deprotonation step, which gave biaryl-palladium(II) intermediate **M4** *via* transition state **M5**. During the proposed catalytic cycle, the concerted palladation-deprotonation was the rate determining step, which was in accordance with the observed results.

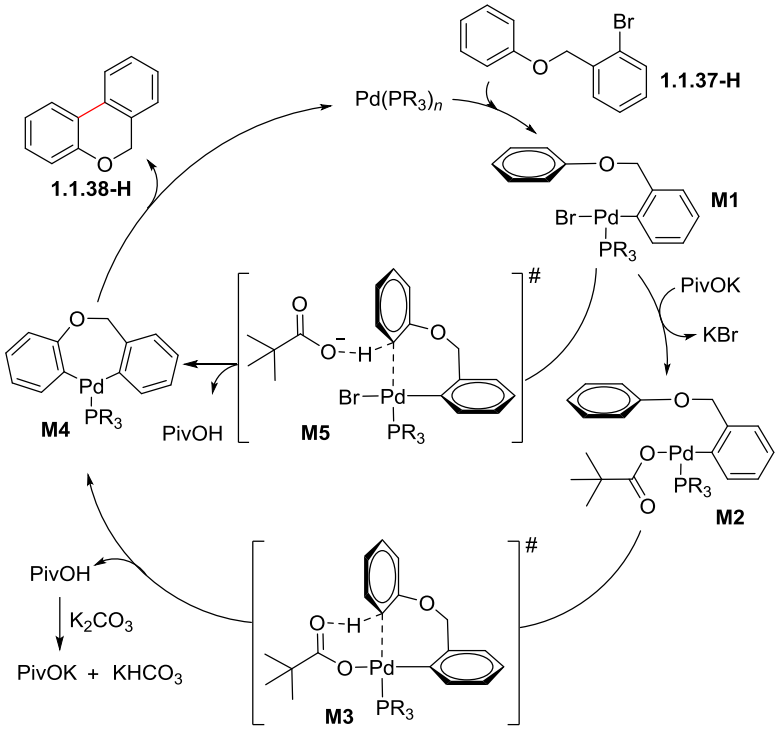

Scheme 1.11 Proposed mechanism for intramolecular C-H arylation

In 2015, T. Korenaga's group reported their experimental and theoretical studies of the ligand acceleration effect (LAE) on intramolecular C-H arylation reactions using compound **1.1.37-H** as substrate (**Scheme 1.12**).[134] The Pd-catalyst and the ligand were stirred in DMA for 10 min at room temperature before adding the substrate to ensure the coordination of the ligand to the catalyst. By doing this, the conversion of the reaction was improved significantly from 65% to 96% using electron-deficient ligand **1.1.39**. The order of LAE was shown in **Scheme 1.12**. According to the authors, the conversion of the arylation reaction tended to decrease with the increase of electron-donating ability of the ligand, except the results obtained using tricyclohexylphosphine (PCy_3) and tris(pentafluorophenyl)phosphine (compound **1.1.43**) as ligands. Thus, the best ligand for this reaction was compound **1.1.39**. The poor LAE of compound **1.1.43** could be attributed to its poor coordination ability towards Pd, which was due to its weak electron-donating nature and large cone angle (184 °).[135] ^{13}P NMR analysis showed no ligated palladium species when using compound **1.1.43** as ligand, proving its poor coordination ability towards Pd. To explain the good LAE of PCy_3, DFT calculations were conducted. As a result, evaluation of natural bond orbitals (NBO) deletion energy showed that ligand **1.1.39** stabilized the C^{Ar}→Pd interaction (in the C^{Ar}···Pd bond formation process) and PCy_3 stabilized the O→H···C^{Ar} interaction (in the C···H bond breaking process) in the transition state in the CMD process. Thus, the good LAE of PCy_3 could be attributed to its good stabilizing ability for the transition state of the reaction. The information obtained in this study is helpful in future studies on C-H arylation reactions through the CMD process.

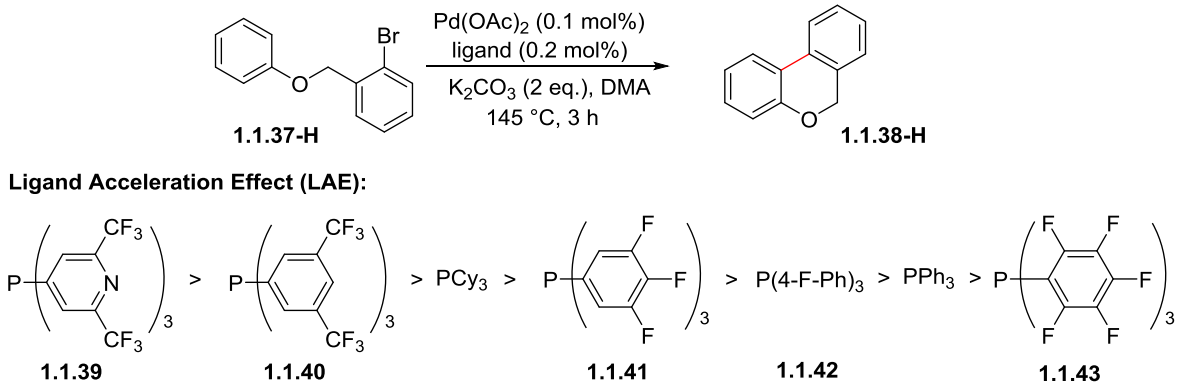

Scheme 1.12 Ligand effect on intramolecular C-H arylation reactions

[134] T. Korenaga, N. Suzuki, M. Sueda, K. Shimada, *J. Organomet. Chem.* **2015**, *780*, 63.

[135] T. Korenaga, A. Ko, K. Uotani, Y. Tanaka, T. Sakai, *Angew. Chem. Int. Ed.* **2011**, *50*, 10703.

1.2 Synthesis of polycyclic biaryls through intramolecular arylation involving pyridine derivatives

Pyridine derivatives are an important class of natural products that have a number of biological activities, including anti-tumor,[136] anti-viral,[137] anti-microbial,[138] anti-diabetic,[139] anti-leishmanial[140] and anti-oxidant.[141] Besides, compounds with biaryl moieties bearing a pyridine ring are also reported to have unique biological activities (**Figure 1.7**).[125, 142] For example, compound **1.2.3** was reported to be a diacylglycerol acyltransferase enzyme (DGAT1) inhibitor, which exhibited an *in vitro* half maximal inhibitory concentration (IC_{50}) of 17 nM.[142a] Compound **1.2.4** was reported to be a potent lysine specific demethylase 1 (LSD1) inhibitors with an inhibition constant (K_i) value as low as 29 nM. However, despite their broad occurrences and significant biological activities, there are only a few methods that have been developed for their synthesis. Moreover, most of them existed as a special case study, and no general method has been developed for the synthesis of such compounds.

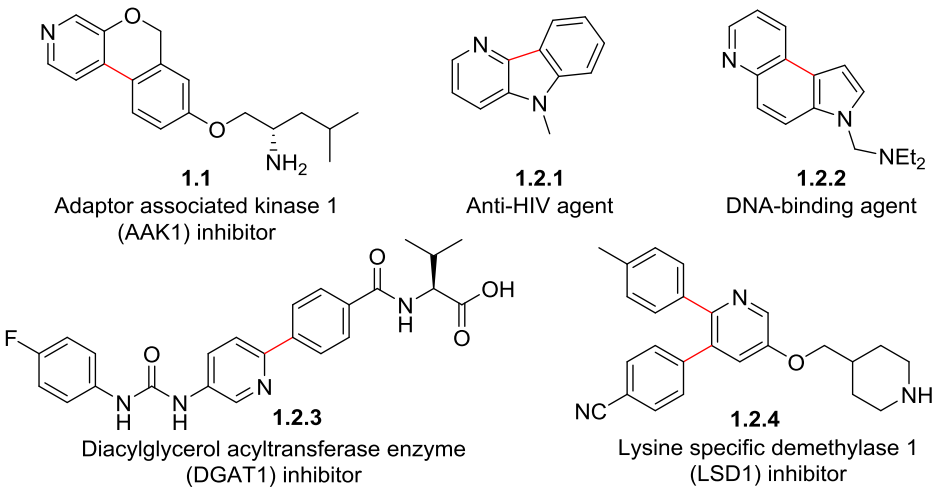

Figure 1.7 Selected examples of biologically active biaryls bearing a pyridine ring

---

[136] a) K. C. Nicolaou, R. Scarpelli, B. Bollbuck, B. Werschkun, M. M. A. Pereira, M. Wartmann, K.-H. Altmann, D. Zaharevitz, R. Gussio, P. Giannakakou, *Chem. Biol.* **2000**, *7*, 593; b) J.-P. Liou, K.-S. Hsu, C.-C. Kuo, C.-Y. Chang, J.-Y. Chang, *J. Pharmacol. Exp. Ther.* **2007**, *323*, 398.

[137] a) A. M. R. Bernardino, L. C. da Silva Pinheiro, C. R. Rodrigues, N. I. Loureiro, H. C. Castro, A. Lanfredi-Rangel, J. Sabatini-Lopes, J. C. Borges, J. M. Carvalho, G. A. Romeiro, V. F. Ferreira, I. C. P. P. Frugulhetti, M. A. Vannier-Santos, *Bioorg. Med. Chem.* **2006**, *14*, 5765; b) A. M. Attla, H. A. Mansour, A. A. Almehdi, M. M. Abbasi, *Nucleosides Nucleotides* **1999**, *18*, 2301; c) J.-M. Chezal, J. Paeshuyse, V. Gaumet, D. Canitrot, A. Maisonial, C. Lartigue, A. Gueiffier, E. Moreau, J.-C. Teulade, O. Chavignon, J. Neyts, *Eur. J. Med. Chem.* **2010**, *45*, 2044.

[138] a) F. E. Goda, A. A.-M. Abdel-Aziz, O. A. Attef, *Bioorg. Med. Chem.* **2004**, *12*, 1845; b) S. Bondock, R. Rabie, H. A. Etman, A. A. Fadda, *Eur. J. Med. Chem.* **2008**, *43*, 2122.

[139] R. H. Bahekar, M. R. Jain, P. A. Jadav, V. M. Prajapati, D. N. Patel, A. A. Gupta, A. Sharma, R. Tom, D. Bandyopadhya, H. Modi, P. R. Patel, *Bioorg. Med. Chem.* **2007**, *15*, 6782.

[140] E. V. Costa, M. L. B. Pinheiro, C. M. Xavier, J. R. A. Silva, A. C. F. Amaral, A. D. L. Souza, A. Barison, F.R. Campos, A. G. Ferreira, G. M. C. Machado, L. L. P. Leon, *J. Nat. Prod.* **2006**, *69*, 292.

[141] F. Shi, C. Li, M. Xia, K. Miao, Y. Zhao, S. Tu, W. Zheng, G. Zhang, N. Ma, *Bioorg. Med. Chem. Lett.* **2009**, *19*, 5565.

[142] a) H. Motiwala, S. Kandre, V. Birar, K. S. Kadam, A. Rodge, R. D. Jadhav, M. M. K. Reddy, M. K. Brahma, N. J. Deshmukh, A. Dixit, L. Doshi, A. Gupte, A. K. Gangopadhyay, R. A. Vishwakarma, S. Srinivasan, M. Sharm, K. V. S. Nemmani, R. Sharma, *Bioorg. Med. Chem. Lett.* **2011**, *21*, 5812; b) F. Wu, C. Zhou, Y. Yao, L. Wei, Z. Feng, L. Deng, Y. Song, *J. Med. Chem.* **2016**, *59*, 253; c) Y. Lin, X. Yang, W. Pan, Y. Rao, *Org. Lett.* **2016**, *18*, 2304.

In 1994, B. H. Lipshutz reported a method for the synthesis of polycyclic biaryl compounds *via* diarylcyanocuprate intermediates.[143] This method could be used for the synthesis of pyridine-containing polycyclic biaryl compounds with moderate yields (**Scheme 1.13**, compounds **1.2.6a** and **1.2.6b**). However, the harsh reaction conditions and narrow substrate scope limited the application of this method.

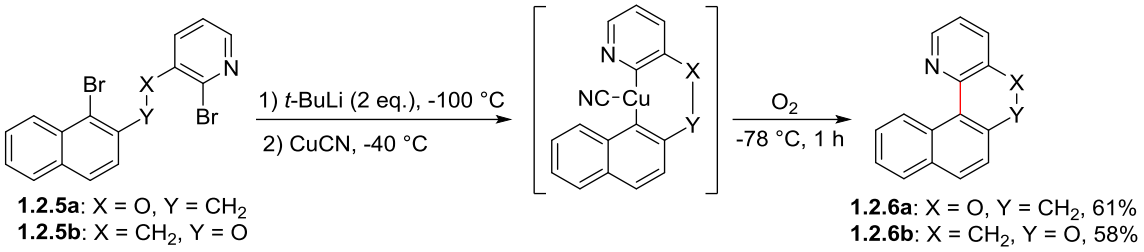

Scheme 1.13 Synthesis of pyridine-containing polycyclic biaryl compounds-(1)

W. B. Motherwell reported a radical cyclization method for the synthesis of biaryl compounds.[144] Through the combined use of *n*-Bu_3SnH and azobisisobutyronitrile (AIBN), various substituted biphenyl derivatives could be synthesized. Besides, this method was applied in the synthesis of two pyridine-containing polycyclic biaryl compounds **1.2.8a** and **1.2.8b** (**Scheme 1.14**).[144a] The formation of compound **1.2.9a** when using **1.2.7a** as substrate was due to the intramolecular free radical *ipso*-substitution and the subsequent elimination of sulfur dioxide. The same method was also applicable to the synthesis of biaryl compound **1.2.11**, which had a seven-membered ring.[144b, c] Interestingly, the C-4 arylation product **1.2.12** was obtained as 1,4-dihydropyridine form together with compound **1.2.11**.

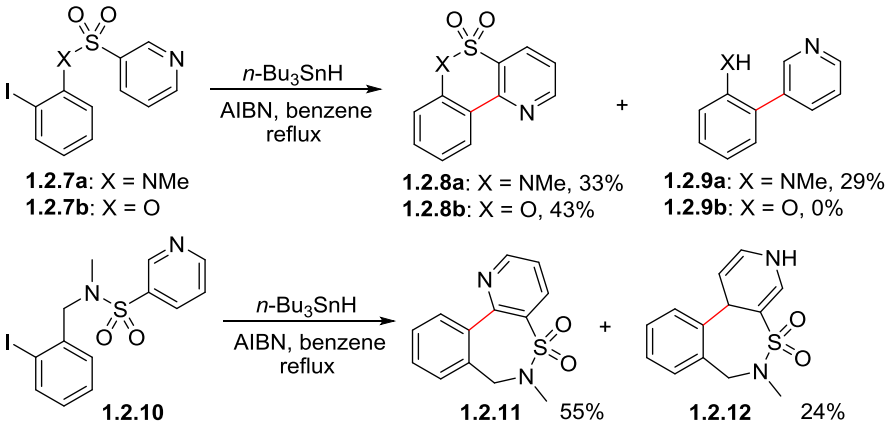

Scheme 1.14 Synthesis of pyridine-containing polycyclic biaryl compounds-(2)

[143] B. H. Lipshutz, F. Kayser, N. Maullin, *Tetrahedron Lett.* **1994**, *35*, 815.

[144] a) M. L. E. N. de Mata, W. B. Motherwell, F. Ujjainwalla, *Tetrahedron Lett.* **1997**, *38*, 137; b) M. L. E. N. de Mata, W. B. Motherwell, F. Ujjainwalla, *Tetrahedron Lett.* **1997**, *38*, 141; c) F. Ujjainwalla, M. L. E. N. da Mata, A. M. K. Pennell, C. Escolano, W. B. Motherwell, S. Vázquez, *Tetrahedron* **2015**, *71*, 6701.

D. C. Harrowven's group also reported a series of works for the synthesis of toddaquinoline, an alkaloid from the root bark of Formosan *Toddalia asiatica*,[145] and its analogues based on radical cyclization.[146] In 1998, Harrowven's group reported for the first time the synthesis of toddaquinoline methyl ether **1.1.19** and its regioisomer **1.2.18** (**Scheme 1.15**).[146a] The four-step synthetic sequence resulted in a 1:1 mixture of *C4*-arylated product **1.2.18** and *C6*-arylated product **1.2.19** with a global yield of 19%. Notably, compound **1.2.16** used in the Wittig reaction was synthesized in two steps with a combined yield of 52%. Thus, the low regioselectivity of the arylation reaction and the multi-step synthetic procedure limited the application of this method.

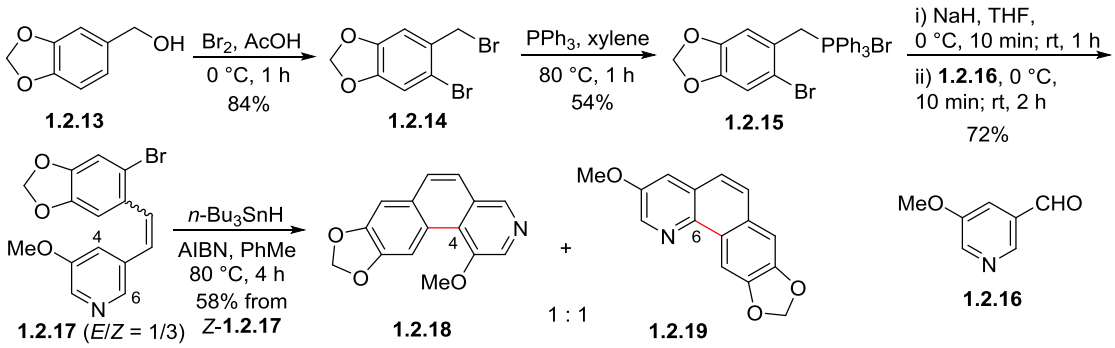

Scheme 1.15 Synthesis of toddaquinoline methyl ether **1.1.21**

Later, the same group improved the regioselectivity of arylation by using a Co^{I}-complex **1.2.20** as photocatalyst (**Scheme 1.16**).[146b, d] Using this catalyst, the authors were able to obtain the *C6*-arylated products **1.2.19** and **1.2.22** exclusively. The mechanism of regioselective arylation was shown in **Scheme 1.16**. The coordination of pyridine to cobalt center followed by single electron transfer from the catalyst to the substrate gave intermediate **M1**, which gave aryl radical species **M2** after elimination of a molecule of NaBr. The formation of **M2** increased the electrophilicity at C-6 in the pyridine, thus accelerating the addition of the nucleophilic aryl radical to C-6 relative to C-4, giving Co^{III}-species **M3**. Aromatization of **M3** and elimination of the Co-catalyst gave the desired product. Notably, the authors also tested the radical cyclization reaction under photochemical conditions. Thus, irradiation of a cyclohexane solution of compound **1.2.23** with a medium pressure mercury lamp led to

[145] I.-S. Chen, I.-L. Tsai, S.-J. Wu, W.-S. Sheen, T. Ishikawa, H. Ishii, *Phytochem,* **1993**, *34*, 1449.

[146] a) D. C. Harrowven, M. I. T. Nunn, *Tetrahedron Lett.* **1998**, *39*, 5875; b) D. C. Harrowven, M. I. T. Nunn, N. J. Blumire, D. R. Fenwick, *Tetrahedron Lett.* **2000**, *41*, 6681; c) D. C. Harrowven, B. J. Sutton, S. Coulton, *Tetrahedron Lett.* **2001**, *42*, 2907; d) D. C. Harrowven, M. I. T. Nunn, N. J. Blumire, D. R. Fenwick, *Tetrahedron* **2001**, *57*, 4447; e) D. C. Harrowven, B. J. Sutton, S. Coulton, *Tetrahedron* **2002**, *58*, 3387.

a readily separable 5:2 mixture of **1.2.18** and **1.2.19** (**Scheme 1.17**). The formation of compound **1.2.18** as the main product could be rationalized by favorable molecular orbital interactions.[147]

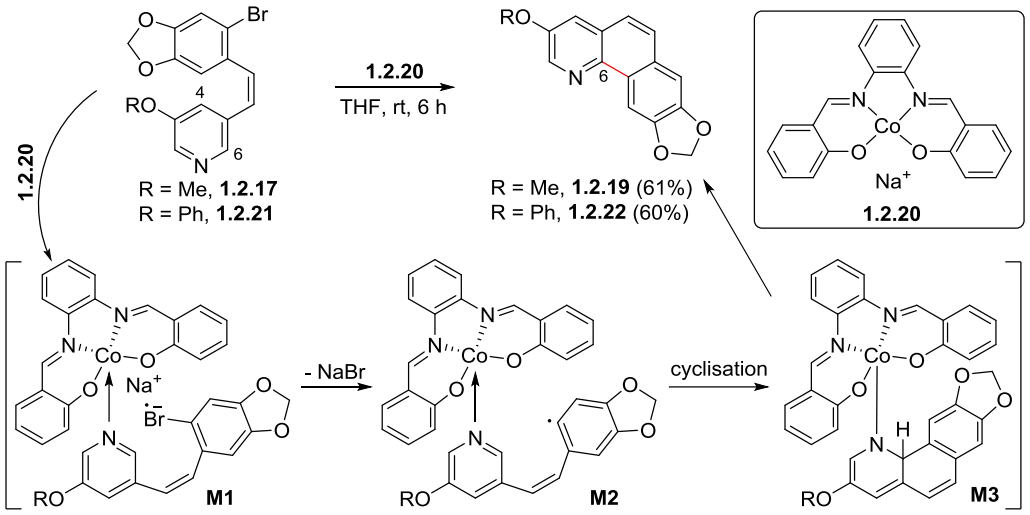

Scheme 1.16 Regioselective arylation catalyzed by Co^{I}-complex **1.2.20**

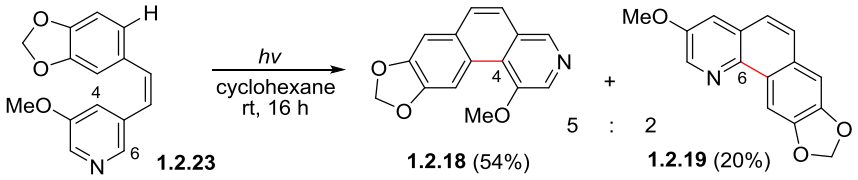

Scheme 1.17 Synthesis of toddaquinoline methyl ether by photocyclization

The synthesis of toddaquinoline was problematic when using methyl ether **1.2.19** as substrate, obtaining either low yield of the product or only the starting compound using various deprotection methods. By contrast, using the benzyl ether **1.2.22** as substrate gave toddaquinoline smoothly with a yield of 86% (**Scheme 1.18**).

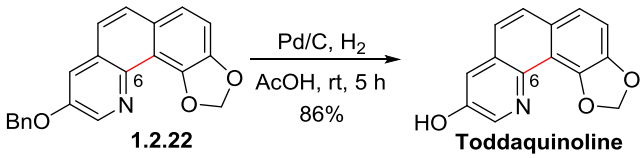

Scheme 1.18 Synthesis of toddaquinoline

[147] F. B. Mallory, C. W. Mallory, *Org. React.* **1984**, *30*, 1.

Harrowven's group also applied the radical cyclization method to the synthesis of various quinoline derivatives (**Figure 1.8**).[146c, e] These compounds were synthesized using the *n*-BuSnH/AIBN system, and the yields shown in **Figure 1.8** referred to the cyclization step using the corresponding aryl iodides as substrates. The use of aryl bromides as substrates gave either no reaction or lower yields. An attempt to synthesize compounds with a five-membered ring failed, showing the limits of this method.

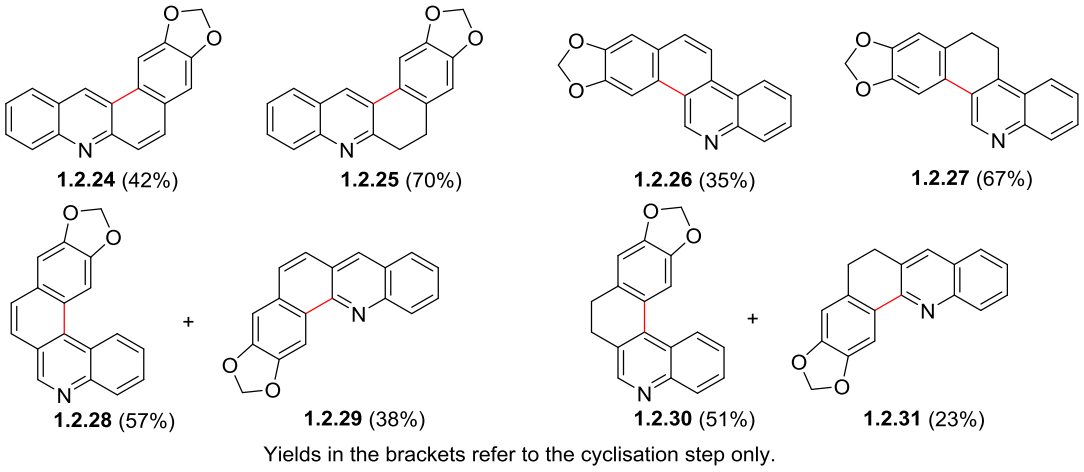

Figure 1.8 Quinoline derivatives obtained from intramolecular radical cyclization

In 2008, V. Mamane's group reported a method for the synthesis of substituted benzo-(*iso*)quinoline derivatives.[148] This method was based on a Suzuki or Negishi cross-coupling followed by a *t*-BuOK promoted cyclization to form the core structure of benzo-(*iso*)quinoline derivatives (**Scheme 1.19**). Using this method, the authors synthesized the four isomers of benzo-(*iso*)quinoline (compounds **1.2.35-1.2.37** and compound **1.2.40b**).

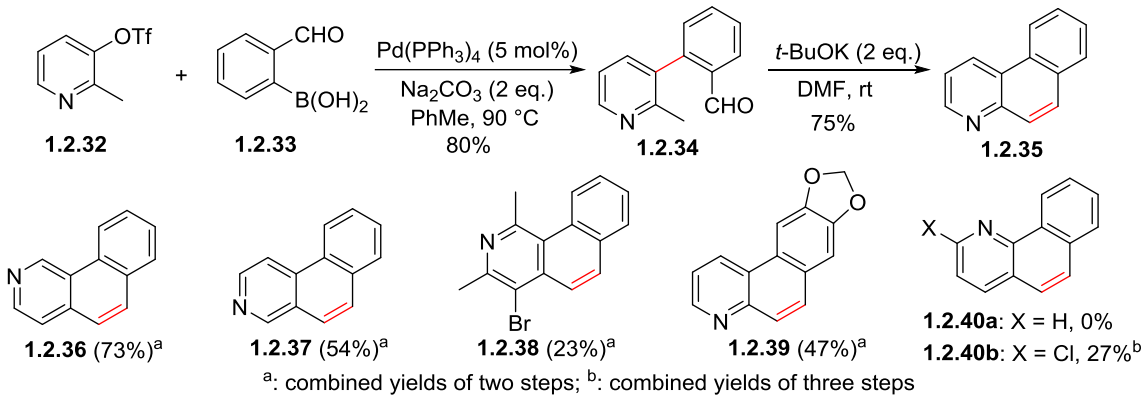

Scheme 1.19 Synthesis of substituted benzo-(*iso*)quinoline derivatives

[148] V. Mamane, F. Louërat, J. Iehl, M. Abboud, Y. Fort, *Tetrahedron* **2008**, *64*, 10699.

The synthesis of compound **1.2.40a** failed due to the formation of lactam **1.2.43** after the Suzuki coupling (**Scheme 1.20**). The introduction of a chloride substituent at the α-position of the nitrogen atom decreased the nucleophilicity of the pyridine, thus increasing the stability of compound **1.2.47** and allowing the synthesis of compound **1.2.40b** (**Scheme 1.21**). Notably, the chloride substituent in compound **1.2.40b** also allowed further functionalization of this molecule by Suzuki coupling.

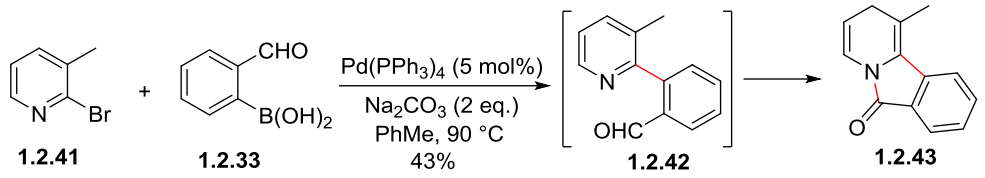

Scheme 1.20 Formation of lactam **1.2.43**

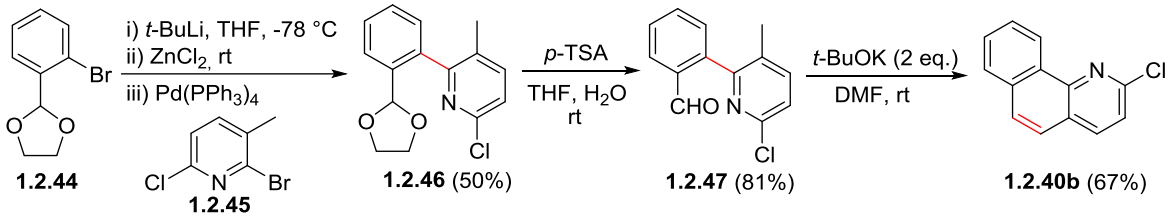

Scheme 1.21 Synthesis of compound **1.2.40b** through Negishi coupling

In 2009, K. C. Majumdar's group reported a palladium-catalyzed intramolecular biaryl coupling for the synthesis of various polycyclic biaryl quinoline derivatives (**Scheme 1.22**).[149] The coupling reactions proceeded smoothly under ligand-free conditions, which was one of the advantages of this method. The use of tetrabutylammonium bromide (TBAB) was indispensable for the arylation reactions, since debrominated product was obtained as main product without using it. However, all the arylation reactions occurred on the benzene ring of quinoline, not on the pyridine ring, which made it less interesting for our investigations. The authors also succeeded to synthesize compound **1.2.53** using optimized reaction conditions. However, this was the only case for this type of molecules.

[149] K. C. Majumdar, A. Taher, P. Debnath, *Synthesis* **2009**, 793.

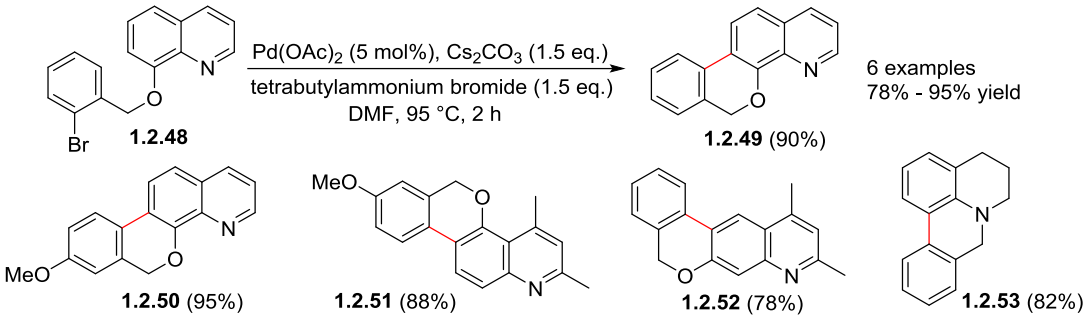

Scheme 1.22 Palladium-catalyzed synthesis of polycyclic biaryl quinoline derivatives

In 2013, A. Bisai's group reported a DDQ-mediated intramolecular-dehydrogenative-coupling (IDC) method for the synthesis of 2-oxindoles bearing an all-carbon quaternary center at the pseudobenzylic position.[150] Among the substrates tested, a pyridine derivative was employed (**Scheme 1.23**, compound **1.2.56**), which was formed by alkylation and subsequent intramolecular-dehydrogenative-coupling in one-pot. An all-carbon quaternary center was formed by this one-pot reaction, although it was obtained in a racemic form. Pd-catalyzed intramolecular C-H arylation of compound **1.2.56** gave pyridine-containing biaryl compound **1.2.57** with 85% yield.

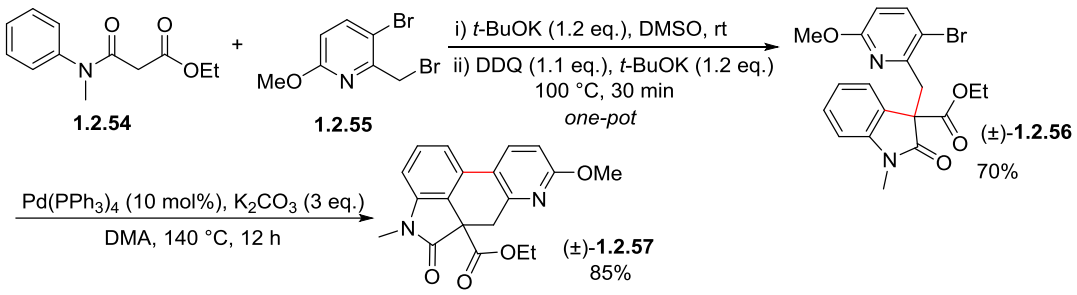

Scheme 1.23 Synthesis of pyridine-containing biaryl compound **1.2.57**

Recently, S. Samanta and co-workers reported a method for the synthesis of biaryl compounds bearing a pyrrole or pyridine moiety (**Scheme 1.24**).[151] Different from all the works described above, this work synthesized biaryl compounds through the construction of the heterocyclic ring rather than coupling the existed rings. Thus, it offered a novel pathway for the synthesis of biaryl compounds bearing heterocycles. However, the use of highly toxic NaN_3 as reagent left potential safety risk of the method.

[150] S. Bhunia, S. Ghosh, D. Dey, A. Bisai, *Org. Lett.* **2013**, *15*, 2426.

[151] A. Jana, S. K. Manna, S. K. Mondal, A. Mandal, S. K. Manna, A. Jana, B. K. Senapati, M. Jana, S. Samanta, *Tetrahedron Lett.* **2016**, *57*, 3722.

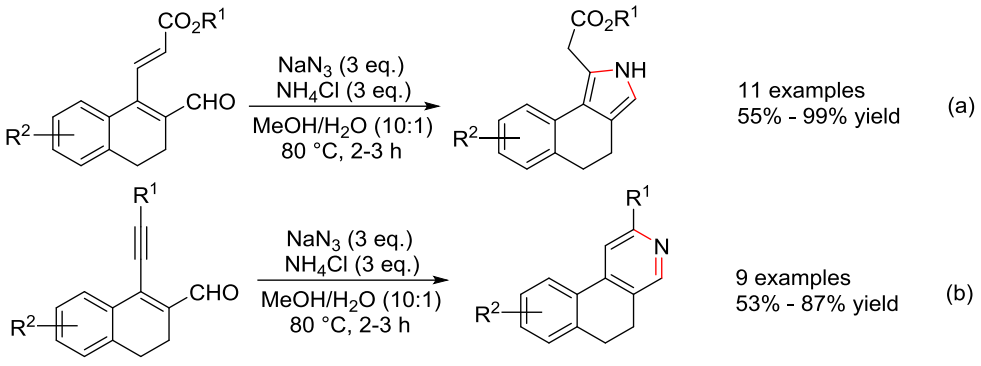

Scheme 1.24 Synthesis of biaryl compounds bearing a pyrrole or pyridine moiety

In summary, the synthesis of biaryl compounds bearing a pyridine moiety remains a challenging task for organic chemists. The existing methods suffer from the drawbacks of harsh reaction conditions, poor regioselectivity and narrow substrate scope. Radical cyclization represents an efficient method for the synthesis of pyridine-containing biaryls. However, the poor regioselectivity and the use of stoichiometric amount of highly toxic *n*-Bu_3SnH limit the applications of this method. Thus, the development of novel method allowing the synthesis of various pyridine-containing biaryls with good regioselectivity and broad substrate scope is highly desired and of great importance.

2 Results and discussions

As part of our efforts to develop new C-H activation reactions, we have designed a series of substrates to investigate their reactivity using various transition metal catalysts (see chapter 2). During this process, we discovered that the use of compound **2.1** as substrate under the reaction conditions shown in **Scheme 2.1** gave the arylated product in trace amount. Since no study has been reported for the cyclization of such substrates, and molecules with a core structure of compound **2.2** were reported to be kinase inhibitors (**Figure 1.2**, compound **1.1**), we decided to optimize the reaction conditions to achieve better conversion of the reaction.

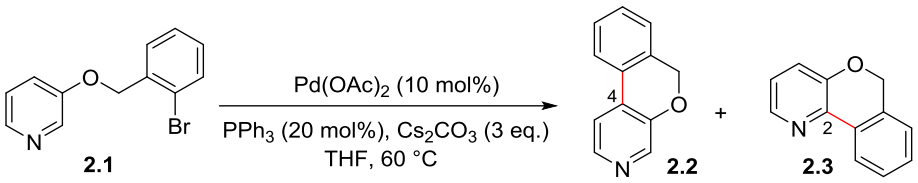

Scheme 2.1 Pd-catalyzed intramolecular C-H arylation

As shown in **Table 2.1**, various reaction conditions using different catalysts, ligands, additives, bases, solvents and reaction temperatures were investigated. Conducting the reaction using $Pd(OAc)_2$ in dioxane at 100 ℃ gave no significant improvement of the conversion with or without an additive (**Table 2.1**, Entries 2 and 3). The use of toluene as solvent was found to be beneficial for the arylation reaction. Using K_3PO_4 as base and reacting at 120 ℃ in toluene overnight, the desired *C4*-arylated product **2.2** was isolated with a yield of 44% (**Table 2.1**, Entry 4). Interestingly, the *C2*-arylated compound **2.3** was not observed in the crude mixture, indicating that the arylation reaction might occur in a regioselective way. The yield of arylated product **2.2** was significantly improved with a prolonged reaction time, giving a yield of 80% for compound **2.2** after reacting for 3 days (**Table 2.1**, Entry 5). Again, no *C2*-arylated compound **2.3** was observed under the reaction conditions. Replacing K_3PO_4 with K_2CO_3 as base slightly improved the yield of compound **2.2**, and the regioselectivity was retained (**Table 2.1**, Entry 6). Electron-deficient ligand $P(4\text{-F-Ph})_3$ was also effective for the arylation reaction, which resulted in 75% isolated yield of compound **2.2** (**Table 2.1**, Entry 7). Since DMA was successfully used as solvent for intramolecular C-H arylation by Fagnou's group, we also employed it in our reaction. However, poor yield of the arylated product was obtained in our case, and the main product was the corresponding debrominated compound (62%) (**Table 2.1**, Entry 8). Furthermore, the reaction could be conducted under an air atmosphere with a lower but synthetically useful yield, demonstrating the robustness of the catalytic system (**Table 2.1**, Entry 9). Thus, the best reaction conditions for the intramolecular C-H arylation reactions were as following: 10 mol% $Pd(OAc)_2$ as

catalyst, 20 mol% PPh_3 as ligand and 3 equivalents of K_2CO_3 as base, reacting in toluene for 3 days at 120 ℃ under a nitrogen atmosphere.

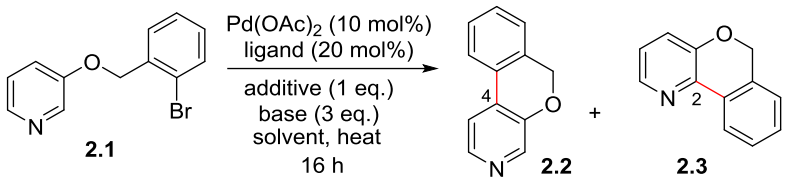

Entry	Ligand	Additive	Base	Solvent	T / ℃	Yield
1	PPh_3	-	Cs_2CO_3	THF	60	trace
2	PPh_3	-	Cs_2CO_3	dioxane	100	trace
3	PPh_3	Ag_2O	Cs_2CO_3	dioxane	100	trace
4	PPh_3	-	K_3PO_4	PhMe	120	44% (**2.2**)
5[a]	PPh_3	-	K_3PO_4	PhMe	120	80% (**2.2**)
6[a]	PPh_3	-	K_2CO_3	PhMe	120	84% (**2.2**)
7[a]	P(4-F-Ph)$_3$	-	K_2CO_3	PhMe	120	75% (**2.2**)
8[a]	PPh_3	-	K_2CO_3	DMA	120	24% (**2.2**) [b]
9[a, c]	PPh_3	-	K_2CO_3	PhMe	120	69% (**2.2**)

Table 2.1 Optimization of reaction conditions for intramolecular arylation reaction

[a]: Reaction run for 3 days; [b]: Debrominated product was obtained as side-product with a yield of 62%; [c]:Reaction run under air.

Having the best reaction conditions in hand, we started to investigate the substrate scope of the intramolecular C-H arylation reaction. However, we encountered a problem during the synthesis of the substrates: the alkylation yields were generally low. In order to obtain good yields of the substrates, various alkylation conditions were tested (**Table 2.2**). However, although we observed full conversion of compound **2.4** in all cases by LC-MS, the yield of desired *O*-alkylated product was always low. Notably, we observed one peak that corresponded to the mass of dialkylated product together with the desired peak of the product from LC-MS analysis of the crude product (**Figure 2.1**). It indicated that the alkylation occurred at both oxygen and nitrogen atoms, which explained the low yield of the desired *O*-alkylated product. In this context, we decided to use the conditions in **Table 2.2**, Entry 1 directly for the synthesis of substrates derived from 3-hydroxypyridine **2.4**.

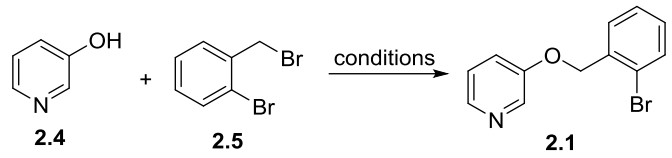

Entry	Reaction conditions	Yield
1	Cs_2CO_3 (1 eq.), DMF, rt	37%
2	NaH (1.1 eq.), THF, rt	3%
3	K_2CO_3 (3 eq.), acetone, reflux	13%
4	K_2CO_3 (3 eq.), acetone, rt	11%
5	Ag_2O (1.2 eq.), EtOAc, rt	11%
6[a]	DIAD (1.1 eq.), PPh_3 (1.1 eq.), CH_2Cl_2, rt	Not determined [b]

Table 2.2 Optimizing the reaction conditions for alkylation of 3-hydroxypyridine

[a]: Using compound **2.4** and 3-bromobenzyl alcohol as substrates; [b]: The product was mixed with the residues of DIAD and could not be separated.

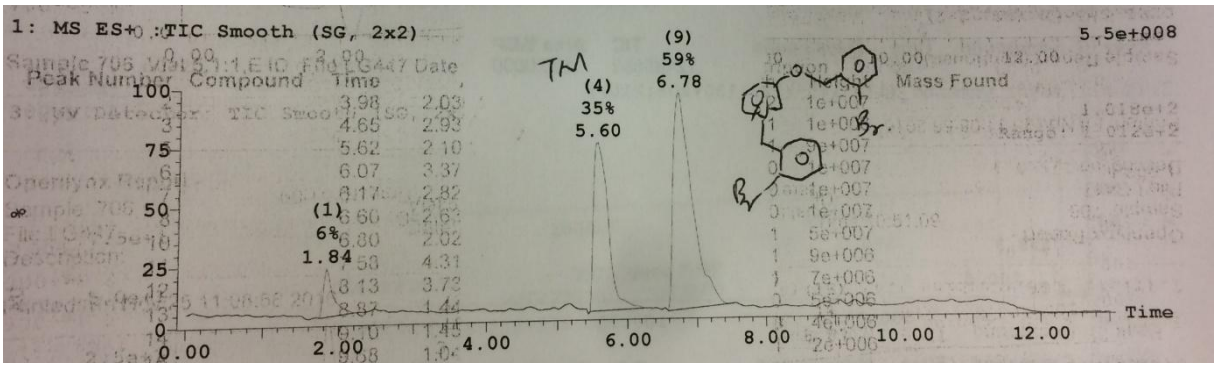

Figure 2.1 LC-MS analysis of crude product of alkylation (TM: target molecule, monoalkylation)

As shown in **Scheme 2.2**, various intramolecular C-H arylation substrates with electron-rich (compounds **2.8** and **2.9**) and electron-deficient (compounds **2.11** to **2.16**) substituents as well as sterically hindered substrates (compounds **2.10** and **2.18**) and heterocycles such as thiophene (compound **2.17**) were synthesized successfully. Besides, aryl chloride **2.6** and aryl iodide **2.7** were also synthesized to investigate the effect of the nature of the halide on the intramolecular C-H arylation reactions. Moreover, other types of substrates with different tethers such as alkene, ether, ester and amide were also synthesized, listed in **Figure 2.2**. These substrates were generally obtained with good yields because the *N*-alkylation reaction could not occur. Imide **2.31** was obtained as a side-

product in the synthesis of amide **2.30**. However, it is interesting to see if a double intramolecular C-H arylation or a regioselective C-H arylation will occur on this substrate.

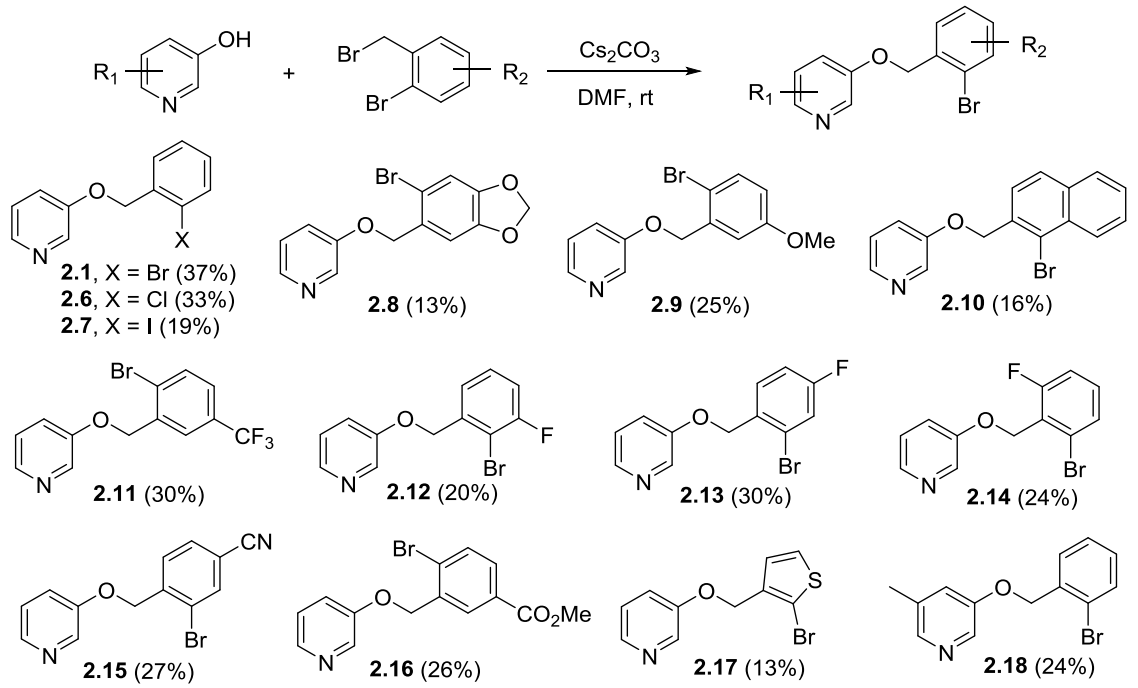

Scheme 2.2 Synthesis of various substrates for intramolecular C-H arylation

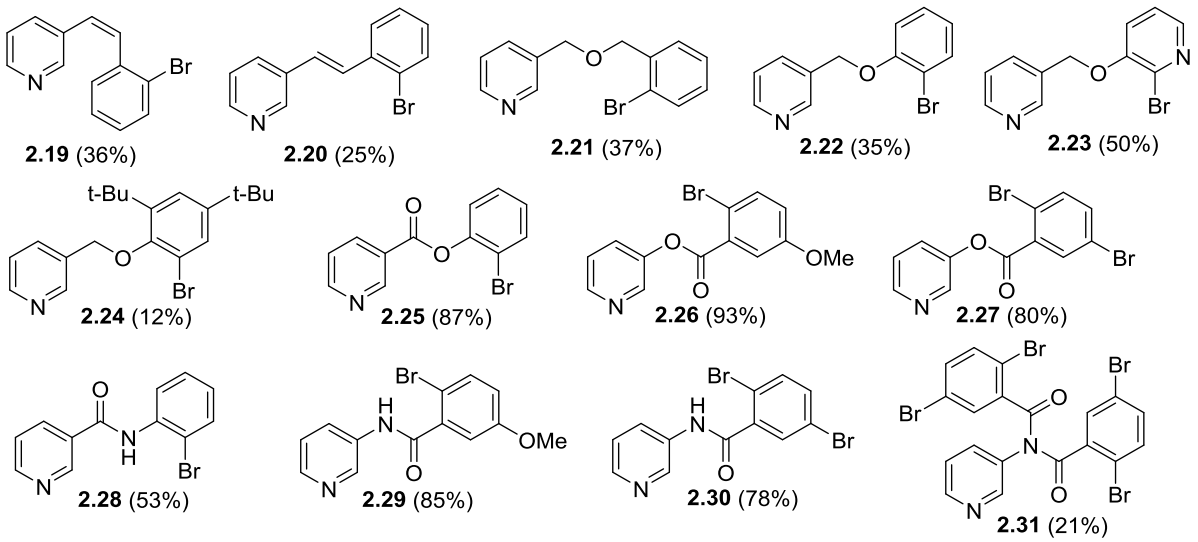

Figure 2.2 Substrates for intramolecular C-H arylation

After the obtention of starting material, we started to explore the substrate scope of the intramolecular C-H arylation reactions using the optimized reaction conditions. We first employed compound **2.13** as

substrate. The *C4*-arylated product **2.32** was obtained with a yield of 62% using PPh_3 as ligand without the observation of compound **2.33**. Interestingly, the use of $P(4\text{-F-Ph})_3$ as ligand significantly increased the conversion, giving *C4*-arylated product **2.32** with a yield of 82% together with *C2*-arylated product **2.33** with a yield of 15% (**Scheme 2.3**). The structure of *C4*-arylated product was determined by its COSY NMR spectrum. As shown in **Figure 2.3**, the proton at C-5 position (H-3) of the pyridine ring correlated with only one proton (H-2), indicating that this product had no proton at C-4 position of the pyridine ring, thus confirming the structure of compound **2.32**.

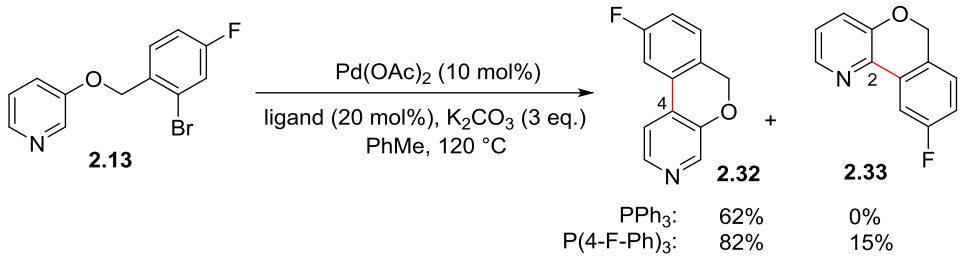

Scheme 2.3 Pd-catalyzed intramolecular C-H arylation of compound **2.13**

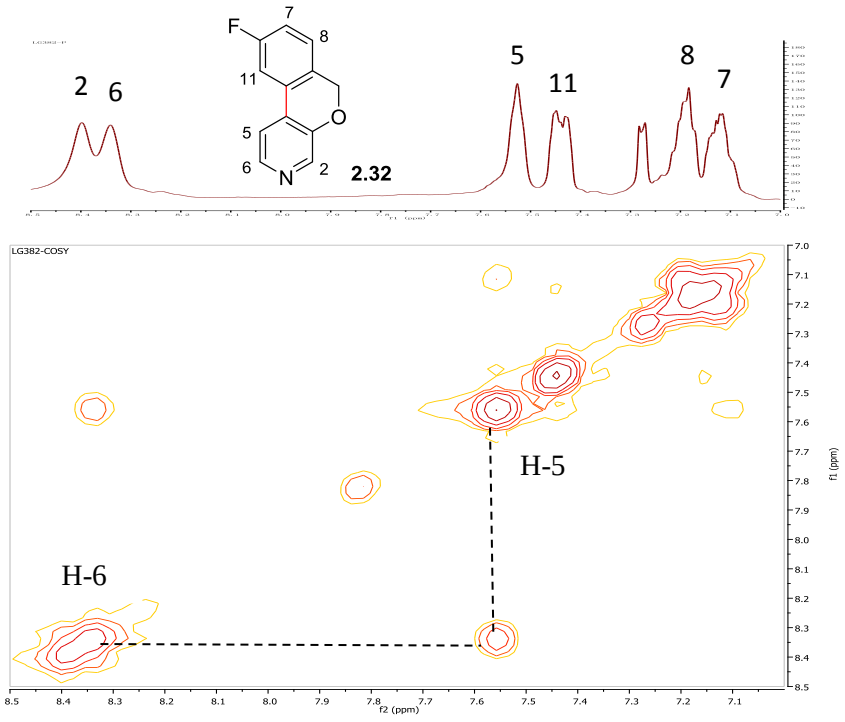

Figure 2.3 COSY NMR spectrum of compound **2.32**

Similar results were obtained using compound **2.11** as substrate (**Scheme 2.4**). The use of PPh_3 as ligand resulted in regioselective arylation at C-4 position of the pyridine ring, giving compound **2.34** as sole product with a yield of 53%. By contrast, using $P(4\text{-F-Ph})_3$ as ligand gave two regioisomers

with a combined yield of 55% favoring the C-4 arylated product. The structure of compound **2.34** was also determined by its COSY NMR spectrum (**Figure 2.4**).

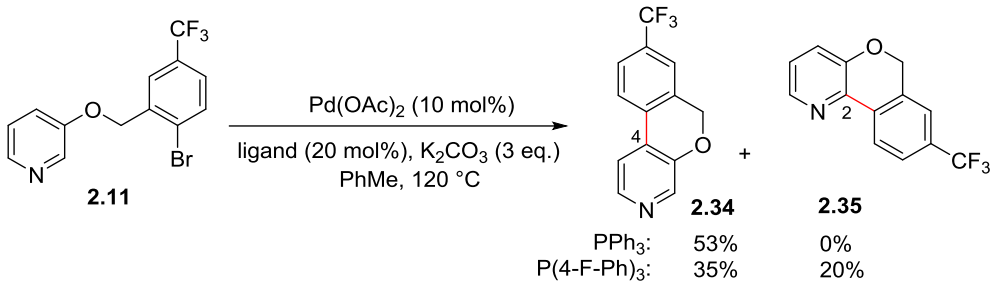

Scheme 2.4 Pd-catalyzed intramolecular C-H arylation of compound **2.11**

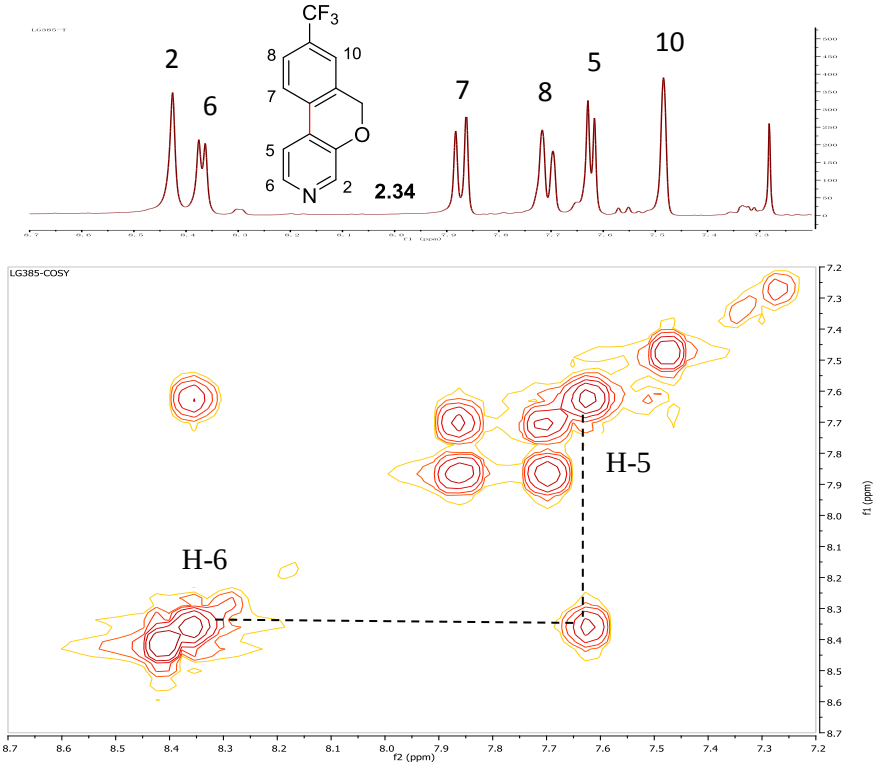

Figure 2.4 COSY NMR spectrum of compound **2.34**

Encouraged by these results, more substrates were tested under the reaction conditions, and the results were shown in **Table 2.3**. Substrate **2.19** with an alkene tether gave two regioisomers **1.2.37** and **1.2.40a** with a total yield of 31% and a ratio of 2:1 favoring *C4*-arylated product under standard reaction conditions (**Table 2.3**, Entry 1). *C5*-methyl substituted substrate **2.18** also gave a similar ratio of regioisomers, but with a higher conversion (**Table 2.3**, Entry 2).

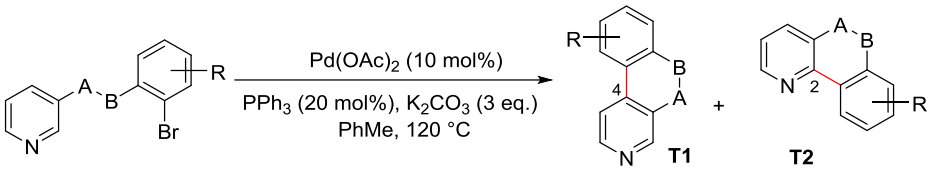

Entry	Substrate	T1	T2	Entry	Substrate	T1	T2
1	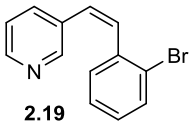 2.19	**1.2.37** (20%)	**1.2.40a** (11%)	6	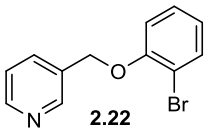 2.22	0%	0%
2	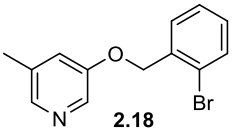 2.18	**2.36** (40%)	**2.37** (22%)	7	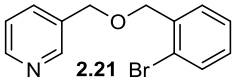 2.21	0% [b]	0% [b]
3	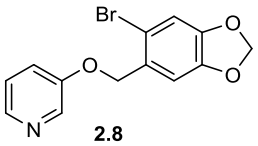 2.8	0% [b]	0% [b]	8	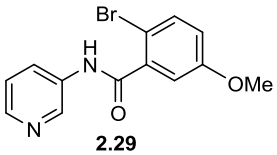 2.29	0%	0%
4	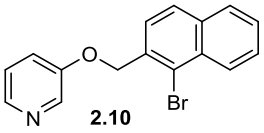 2.10	0% [b]	0% [b]	9	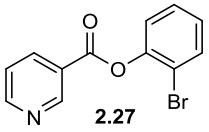 2.27	0%	0%
5	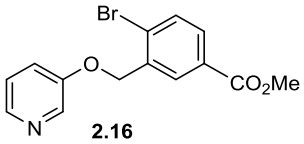 2.16	0%	0%				

Table 2.3 Substrate scope of Pd-catalyzed intramolecular C-H arylation

[a]: Trace amount of product was detected by LC-MS.

Electron-rich substrate **2.8** had difficulty to undergo intramolecular C-H arylation (**Table 2.3**, Entry 3), perhaps due to the deactivation of the substituent. Same results were obtained with sterically hindered substrate **2.10** (**Table 2.3**, Entry 4), which might be due to steric effects which prevented the coupling of the two aryl rings. Trace amounts of products were detected in these two cases, but they could not be isolated. Interestingly, substrate **2.16** with an ester substituent on the phenyl ring did not react at all (**Table 2.3**, Entry 5), which might be due to the interaction between the palladium catalyst and the ester group. Substrate **2.22**, which differed from compound **2.1** only by the position of the oxygen atom in the tether, did not react under the standard reaction conditions (**Table 2.3**, Entry 6). This result supported a CMD mechanism of the reaction, because the deprotonation of compound **2.1** was easier than compound **2.22**, and the C-H insertion of palladium into the C-Br bond of compound **2.22** was more difficult than the one of compound **2.1**. An attempt to synthesize biaryl compound with a seven-

membered ring failed (**Table 2.3**, Entry 7), perhaps due to the difficulty to form a seven-membered ring and/or the difficulty of deprotonation of this substrate. Substrates with an amide or ester tether did not react under the reaction conditions (**Table 2.3**, Entries 8 and 9), perhaps due to the interactions between the catalyst and the functional groups.

The excellent regioselectivity obtained from the arylation of compounds **2.1**, **2.11** and **2.13** using PPh_3 as ligand indicated a unique mechanism of the reaction, which might be a CMD process due to the slightly lower pK_a value of the C-H bond at C-4 position relative to the one at C-2 position.[152] A plausible reaction mechanism was proposed according to the results of preliminary experiments (**Scheme 2.5**). Oxidative addition of $Pd(OAc)_2$ into the C-Br bond of the substrate **2.1** gave intermediate **M1**, which underwent ligand exchange to give **M2**. Two possible ways could be followed starting from **M2**: the C-4 deprotonation assisted by carbonate gave diarylpalladium species **M4** *via* transition state **M3**, which underwent reductive elimination to give *C4*-arylated product **2.2**; alternatively, the C-2 deprotonation assisted by carbonate might occur if the *C5*-position of the pyridine ring was substituted, giving diarylpalladium species **M6** *via* transition state **M5**, which underwent reductive elimination to give *C2*-arylated product **2.3**. The deprotonation step was the rate-determining step, thus the arylation of substrates without oxygen atom attached to the pyridine ring (such as compound **2.22**) was difficult due to the high pK_a of C-H bonds in these substrates.

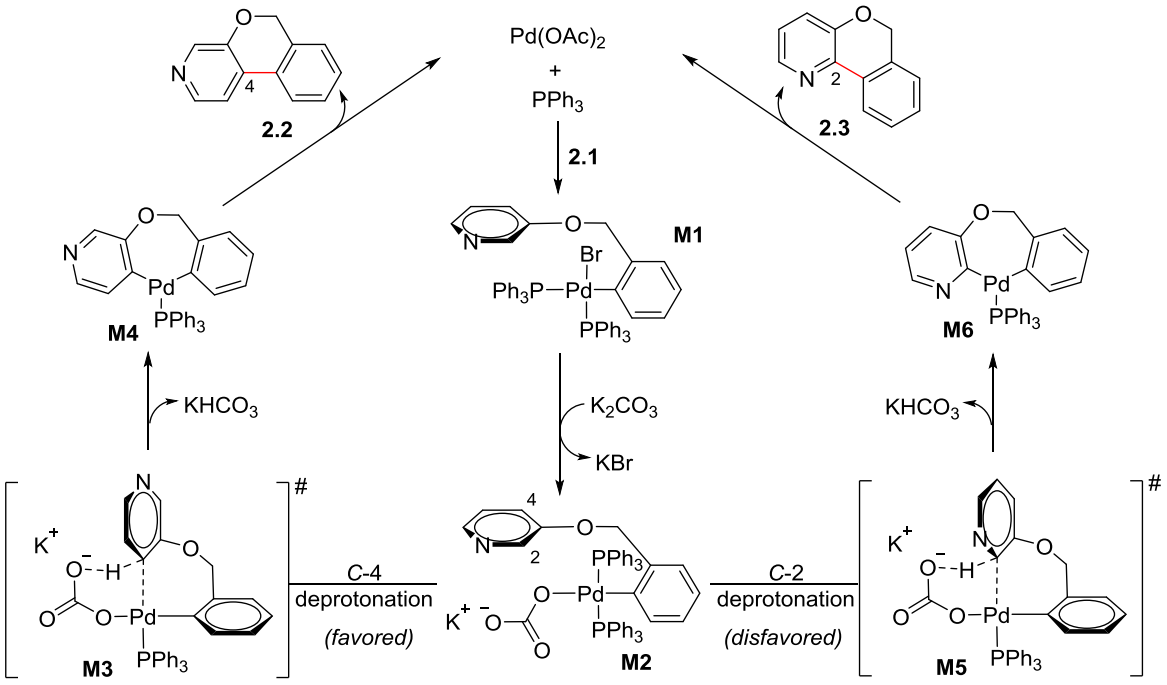

Scheme 2.5 Proposed mechanism for the Pd-catalyzed intramolecular C-H arylation

[152] K. Shen, Y. Fu, J.-N. Li, L. Liu, Q.-X. Guo, *Tetrahedron* **2007**, *63*, 1568.

Due to time limitations, we don’t have further results on the intramolecular C-H arylation reactions. To the best of our knowledge, there is no method describing the intramolecular arylation involving pyridine derivatives with a CMD mechanism. The preliminary experiments showed some encouraging results, but it still needs to be improved due to the low conversions of some substrates and the lack of reactivity for the substrates with ester and amide functional groups. Thus, the investigation will be continued in the future. For example, we could select a proper ligand to conduct the reaction, or an additive such as pivalate acid could also be considered to promote the reaction. Further substrate extension and mechanism investigations will be conducted in the future.

3 Experimental section

3.1 Reagents and General Procedures

All intramolecular C-H arylation reactions were carried out in a Schlenk tube. Commercially substrates were used without any further purification. All work-up and purification procedures were carried out with reagent-grade solvents. Flash column chromatography was performed using Merck silica gel 60 (0.040-0.063 mm). ^{1}H NMR (400 MHz), ^{13}C NMR (100 MHz) spectra were recorded on a Bruker Avance 400 MHz spectrometer. Chemical shifts are reported in parts per million (ppm) downfield from residual solvent peaks and coupling constants are reported in Hertz (Hz). Splitting patterns are designated as singlet (s), doublet (d), triplet (t). Splitting patterns that could not be interpreted or easily visualized are designated as multiplet (m). Electrospray mass spectra were recorded using an ESI/TOF Mariner Mass Spectrometer.

General Procedure A: synthesis of compounds **2.1**-**2.18**:

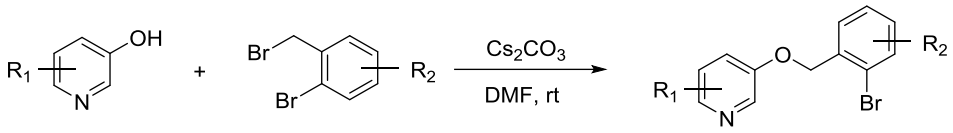

A 50 mL round-bottom flask was charged with 3-hydroxypyridine **2.4** (475 mg, 5 mmol) and Cs_2CO_3 (1630 mg, 5 mmol) with a magnetic stirring bar under air, then *N*,*N*-dimethylformamide (DMF) (25 mL) was added and the resulting mixture was magnetically stirred at room temperature under air. 2-Bromo-benzyl bromide **2.5** (1250 mg, 5 mmol) was then added slowly, and the reaction mixture was magnetically stirred at room temperature under air overnight. After the completion of reaction, ethyl acetate (60 mL) and water (15 mL) were added. The resulting mixture was extracted with ethyl acetate (30 mL ×4), and the combined organic layers were washed with brine, dried over $MgSO_4$ and concentrated under vacuum. The crude product was purified by flash chromatography on silica gel (eluent: cyclohexane/AcOEt = 2/1) to give compound **2.1** (486 mg, 37%) as an orange oil.

General Procedure B: synthesis of compounds **2.22-2.24**:

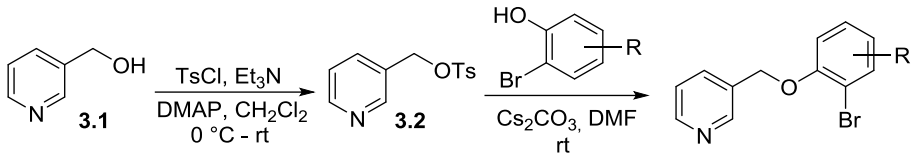

A 25 mL round-bottom flask was charged with 4-dimethylaminopyridine (DMAP) (12 mg, 0.1 mmol) with a magnetic stirring bar under air, then the flask was put under vacuum and filled with N_2. After adding compound **3.1** (109 mg, 1 mmol), triethylamine (0.28 mL, 2 mmol) and CH_2Cl_2 (3 mL) under N_2, the solution was cooled to 0 ℃ using an ice-bath. A solution of 4-toluenesulfonyl chloride (TsCl) (286 mg, 1.5 mmol) in CH_2Cl_2 (2 mL) was added dropwise into the cooled reaction mixture at 0 ℃ and the resulting mixture was magnetically stirred at 0 ℃ for additional 30 min. Then the reaction was allowed to stir at room temperature overnight. After the completion of reaction, the reaction was quenched by adding saturated aqueous $NaHCO_3$. The resulting mixture was extracted with CH_2Cl_2 (10 mL ×3), and the combined organic layers were washed with brine, dried over $MgSO_4$ and concentrated under vacuum. The crude product **3.2** was used in the next step without further purification.

A 25 mL round-bottom flask was charged with the crude product **3.2** (80 mg, 0.3 mmol) and Cs_2CO_3 (149 mg, 0.45 mmol) with a magnetic stirring bar under air, then the flask was put under vacuum and filled with N_2. Then DMF (8 mL) and 2-bromophenol (35 μL, 0.3 mmol) were added at room temperature and magnetically stirred overnight. After the completion of reaction, water (10 mL) was added. The resulting mixture was extracted with ethyl acetate (10 mL ×4), and the combined organic layers were washed with brine, dried over $MgSO_4$ and concentrated under vacuum. The crude product was purified by flash chromatography on silica gel (eluent: cyclohexane/AcOEt = 2/1) to give compound **2.22** (28 mg, 35%) as a colorless oil.

General Procedure C: synthesis of compounds **2.25-2.31**:

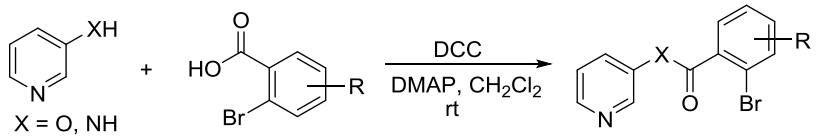

A 50 mL round-bottom flask was charged with 3-hydroxypyridine **2.4** (190 mg, 2 mmol), 2-bromo-5-methoxybenzoic acid (462 mg, 2 mmol) and DMAP (24 mg, 0.2 mmol) with a magnetic stirring bar under air. Then the flask was put under vacuum and filled with N_2. After adding CH_2Cl_2 (16 mL) under N_2, the solution was cooled to 0 ℃ with an ice-bath. A solution of *N*,*N'*-dicyclohexyl-

carbodiimide (DCC) (453 mg, 2.2 mmol) in CH_2Cl_2 (4 mL) was added dropwise into the cooled reaction mixture at 0 ℃ and the resulting mixture was magnetically stirred at 0 ℃ for additional 30 min. The reaction mixture was magnetically stirred at room temperature overnight. After the completion of reaction, the reaction mixture was extracted with CH_2Cl_2 (20 mL×3), and the combined organic layers were washed with brine, dried over $MgSO_4$ and concentrated under vacuum. The crude product was purified by flash chromatography on silica gel (eluent: cyclohexane/AcOEt = 1/1) to give compound **2.26** (576 mg, 93%) as a white solid.

General Procedure D: Pd-catalyzed intramolecular C-H arylation:

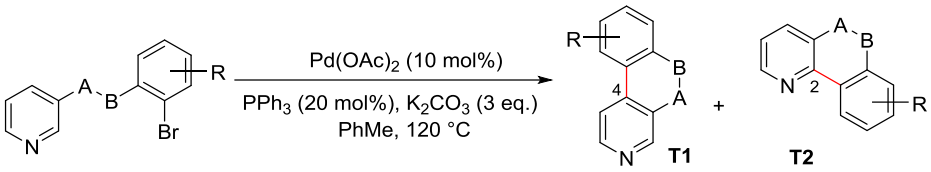

A 80 mL Schlenk tube was charged with aryl bromide (0.1 mmol), $Pd(OAc)_2$ (2.3 mg, 0.01 mmol), PPh_3 (5.2 mg, 0.02 mmol) and K_2CO_3 (41 mg, 0.3 mmol) with a magnetic stirring bar under air, then the Schlenk tube was put under vacuum and filled with N_2. After adding toluene into the reaction mixture, the Schlenk tube was magnetically stirred at 120 ℃ (sand bath) for 3 days. After the completion, the reaction mixture was cooled down to room temperature and concentrated under vacuum. The crude product was purified by flash chromatography on silica gel (eluent: cyclohexane/AcOEt = 1/1) to give biaryl compound **T1** (and **T2**).

3.2 Experimental details and characterization for synthesized compounds

3-((2-Bromobenzyl)oxy)pyridine (2.1):

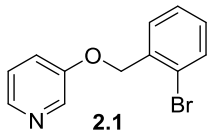

2.1

Following the General Procedure A. The product was isolated as an orange oil (486 mg, 37%) starting from 3-hydroxypyridine **2.4** (475 mg, 5 mmol) and 2-bromo-benzyl bromide **2.5** (1250 mg, 5 mmol). ^{1}H NMR (400 MHz, $CDCl_3$) δ 8.43 (d, J = 2.6 Hz, 1H), 8.27 (d, J = 3.5 Hz, 1H), 7.62 (d, J = 7.9 Hz, 1H), 7.55 (d, J = 7.5 Hz, 1H), 7.36 (t, J = 7.5 Hz, 1H), 7.32-7.19 (m, 3H), 5.20 (s, 2H). ^{13}C NMR (100 MHz, $CDCl_3$) δ 154.6, 142.5, 138.4, 135.4, 132.7, 129.5, 128.9, 127.6, 123.9, 122.4, 121.4, 69.6.

3-((2-Chlorobenzyl)oxy)pyridine (2.6):

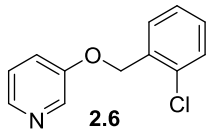

2.6

Following the General Procedure A. The product was isolated as a brown oil (217 mg, 33%) starting from 3-hydroxypyridine **2.4** (285 mg, 3 mmol) and 2-chloro-benzyl bromide (0.47 mL, 3.6 mmol). ^{1}H NMR (400 MHz, $CDCl_3$) δ 8.41 (s, 1H), 8.24 (d, J = 3.4 Hz, 1H), 7.55-7.47 (m, 1H), 7.43-7.35 (m, 1H), 7.31-7.16 (m, 4H), 5.17 (s, 2H). ^{13}C NMR (100 MHz, $CDCl_3$) δ 154.4, 142.4, 138.3, 133.6, 132.5, 129.3, 129.2, 128.6, 126.9, 123.7, 121.1, 67.2.

3-((2-Iodobenzyl)oxy)pyridine (2.7):

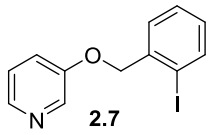

2.7

Following the General Procedure A. The product was isolated as a brown oil (173 mg, 19%) starting from 3-hydroxypyridine **2.4** (285 mg, 3 mmol) and 2-iodo-benzyl bromide (285 mg, 3.6 mmol). ^{1}H NMR (400 MHz, $CDCl_3$) δ 8.40 (s, 1H), 8.24 (s, 1H), 7.84 (d, J = 7.7 Hz, 1H), 7.46 (d, J = 7.3 Hz,

1H), 7.34 (t, *J* = 7.3 Hz, 1H), 7.26-7.16 (m, 2H), 7.01 (td, *J* = 7.8, 1.3 Hz, 1H), 5.05 (s, 2H). ^{13}C NMR (100 MHz, $CDCl_3$) δ 154.4, 142.4, 139.2, 138.3, 138.1, 129.7, 128.5, 128.3, 123.8, 121.3, 97.2, 73.9.

3-((6-Bromobenzo[*d*][1,3]dioxol-5-yl)methoxy)pyridine (2.8):

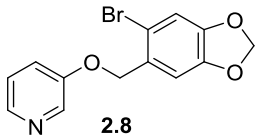

2.8

Following the General Procedure A. The product was isolated as a yellow oil (81 mg, 13%) starting from 3-hydroxypyridine **2.4** (190 mg, 2 mmol) and 5-bromo-6-(bromomethyl)benzo[*d*][1,3]dioxole (706 mg, 2.4 mmol). ^{1}H NMR (400 MHz, $CDCl_3$) δ 8.36 (s, 1H), 8.22 (s, 1H), 7.25-7.16 (m, 2H), 7.00 (s, 1H), 6.96 (s, 1H), 5.95 (s, 2H), 5.03 (s, 2H). ^{13}C NMR (100 MHz, $CDCl_3$) δ 154.4, 148.1, 147.5, 142.4, 138.2, 128.4, 123.8, 121.4, 113.0, 112.6, 108.8, 101.8, 69.5.

3-((2-Bromo-5-methoxybenzyl)oxy)pyridine (2.9):

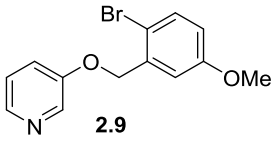

2.9

Following the General Procedure A. The product was isolated as a yellow oil (147 mg, 25%) starting from 3-hydroxypyridine **2.4** (190 mg, 2 mmol) and 1-bromo-2-(bromomethyl)-4-methoxybenzene (560 mg, 2 mmol). ^{1}H NMR (400 MHz, $CDCl_3$) δ 8.37 (s, 1H), 8.21 (d, *J* = 3.3 Hz, 1H), 7.41 (d, *J* = 8.8 Hz, 1H), 7.24-7.14 (m, 2H), 7.04 (d, *J* = 3.0 Hz, 1H), 6.70 (dd, *J* = 8.8, 3.0 Hz, 1H), 5.06 (s, 2H), 3.72 (s, 3H). ^{13}C NMR (100 MHz, $CDCl_3$) δ 159.0, 154.3, 142.4, 138.3, 136.2, 133.1, 123.7, 121.1, 114.8, 114.3, 112.2, 69.4, 55.3.

3-((1-Bromonaphthalen-2-yl)methoxy)pyridine (2.10):

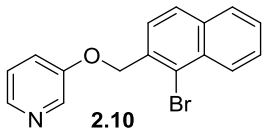

2.10

Following the General Procedure A. The product was isolated as a yellow oil (50 mg, 16%) starting from 3-hydroxypyridine **2.4** (95 mg, 1 mmol) and 1-bromo-2-(bromomethyl)naphthalene (330 mg, 1.1 mmol). ^{1}H NMR (400 MHz, $CDCl_3$) δ 8.46 (d, J = 2.3 Hz, 1H), 8.34 (d, J = 8.5 Hz, 1H), 8.26 (d, J = 4.2 Hz, 1H), 7.84 (d, J = 8.4 Hz, 2H), 7.66-7.60 (m, 2H), 7.55 (t, J = 7.1 Hz, 1H), 7.33-7.27 (m, 1H), 7.23 (dd, J = 8.4, 4.6 Hz, 1H), 5.43 (s, 2H). ^{13}C NMR (100 MHz, $CDCl_3$) δ 154.7, 142.3, 138.3, 134.1, 133.5, 132.1, 128.2, 128.1, 127.7, 127.0, 126.9, 125.3, 124.0, 122.5, 121.6, 70.4.

3-((2-Bromo-5-(trifluoromethyl)benzyl)oxy)pyridine (2.11) :

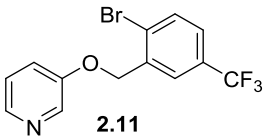

2.11

Following the General Procedure A. The product was isolated as a yellow solid (98 mg, 30%) starting from 3-hydroxypyridine **2.4** (104 mg, 1.1 mmol) and 1-bromo-2-(bromomethyl)-4-(trifluoromethyl)-benzene (318 mg, 1 mmol). ^{1}H NMR (400 MHz, $CDCl_3$) δ 8.45 (s, 1H), 8.31 (d, J = 3.9 Hz, 1H), 7.85 (s, 1H), 7.74 (d, J = 8.3 Hz, 1H), 7.48 (d, J = 8.3 Hz, 1H), 7.35-7.30 (m, 1H), 7.28 (dd, J = 8.1, 4.8 Hz, 1H), 5.19 (s, 2H). ^{13}C NMR (100 MHz, $CDCl_3$) δ 154.3, 142.9, 138.0, 136.7, 133.2, 130.2 (q, $J_{C\text{-}F}$ = 33.1 Hz), 126.1 (q, $J_{C\text{-}F}$ = 3.7 Hz), 125.9, 125.4 (q, $J_{C\text{-}F}$ = 3.7 Hz), 124.0, 123.6 (d, $J_{C\text{-}F}$ = 273.0 Hz), 121.7, 69.1. ^{19}F NMR (376 MHz, $CDCl_3$) δ -62.7 (s).

3-((2-Bromo-3-fluorobenzyl)oxy)pyridine (2.12):

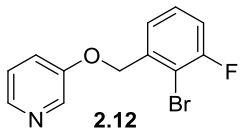

2.12

Following the General Procedure A. The product was isolated as a yellow solid (115 mg, 20%) starting from 3-hydroxypyridine **2.4** (190 mg, 2 mmol) and 2-bromo-1-(bromomethyl)-3-fluorobenzene (536 mg, 2 mmol). ^{1}H NMR (400 MHz, $CDCl_3$) δ ^{1}H NMR (400 MHz, $CDCl_3$) δ 8.40 (s, 1H), 8.26 (d, J = 2.6 Hz, 1H), 7.36-7.28 (m, 2H), 7.27-7.19 (m, 2H), 7.14-7.05 (m, 1H), 5.16 (s, 2H). ^{13}C NMR (100 MHz, $CDCl_3$) δ 158.9 (d, J_{C-F} = 247.3 Hz), 154.3, 142.6, 138.3, 137.7, 128.6 (d, J_{C-F} = 8.1 Hz), 123.9 (d, J_{C-F} = 3.2 Hz), 123.8, 121.2, 115.7 (d, J_{C-F} = 22.6 Hz), 109.1 (d, J_{C-F} = 21.6 Hz), 69.1 (d, J_{C-F} = 3.3 Hz). ^{19}F NMR (376 MHz, $CDCl_3$) δ -105.6 (s).

3-((2-Bromo-4-fluorobenzyl)oxy)pyridine (2.13):

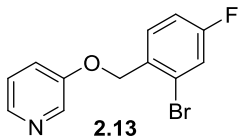

2.13

Following the General Procedure A. The product was isolated as a light yellow solid (168 mg, 30%) starting from 3-hydroxypyridine **2.4** (190 mg, 2 mmol) and 2-bromo-1-(bromomethyl)-4-fluorobenzene (536 mg, 2 mmol). ^{1}H NMR (400 MHz, $CDCl_3$) δ 8.43 (s, 1H), 8.29 (s, 1H), 7.52 (dd, J = 8.5, 6.0 Hz, 1H), 7.37 (dd, J = 8.1, 2.5 Hz, 1H), 7.27 (s, 2H), 7.08 (td, J = 8.3, 2.5 Hz, 1H), 5.14 (s, 2H). ^{13}C NMR (100 MHz, $CDCl_3$) δ 162.0 (d, J_{C-F} = 251.5 Hz), 142.6, 138.2, 131.4 (d, J_{C-F} = 3.4 Hz), 130.2 (d, J_{C-F} = 8.6 Hz), 122.6 (d, J_{C-F} = 9.5 Hz), 121.5, 120.2, 120.0, 114.9, 114.7, 69.1. ^{19}F NMR (376 MHz, $CDCl_3$) δ -111.5 (s).

3-((2-Bromo-6-fluorobenzyl)oxy)pyridine (2.14):

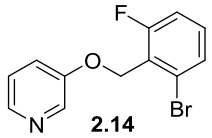

2.14

Following the General Procedure A. The product was isolated as a yellow oil (138 mg, 24%) starting from 3-hydroxypyridine **2.4** (190 mg, 2 mmol) and 1-bromo-2-(bromomethyl)-3-fluorobenzene (536 mg, 2 mmol). ^{1}H NMR (400 MHz, $CDCl_3$) δ 8.41 (d, J = 2.8 Hz, 1H), 8.28-8.22 (m, 1H), 7.41 (d, J = 8.0 Hz, 1H), 7.34-7.27 (m, 1H), 7.25-7.18 (m, 2H), 7.06 (t, J = 8.7 Hz, 1H), 5.20 (d, J = 1.8 Hz, 2H). ^{13}C NMR (100 MHz, $CDCl_3$) δ 161.6 (d, $J_{C\text{-}F}$ = 252.8 Hz), 154.6, 142.6, 138.3, 131.3 (d, $J_{C\text{-}F}$ = 9.4 Hz), 128.7 (d, $J_{C\text{-}F}$ = 3.6 Hz), 126.2 (d, $J_{C\text{-}F}$ = 3.9 Hz), 123.7, 123.2 (d, $J_{C\text{-}F}$ = 16.8 Hz), 121.5, 114.8 (d, $J_{C\text{-}F}$ = 22.8 Hz), 63.6 (d, $J_{C\text{-}F}$ = 4.0 Hz). ^{19}F NMR (376 MHz, $CDCl_3$) δ -112.2 (s).

3-Bromo-4-((pyridin-3-yloxy)methyl)benzonitrile (2.15):

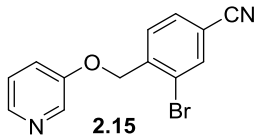

2.15

Following the General Procedure A. The product was isolated as an orange solid (158 mg, 27%) starting from 3-hydroxypyridine **2.4** (190 mg, 2 mmol) and 3-bromo-4-(bromomethyl)benzonitrile (550 mg, 2 mmol). ^{1}H NMR (400 MHz, $CDCl_3$) δ 8.41 (s, 1H), 8.29 (s, 1H), 7.88 (s, 1H), 7.71 (d, J = 8.0 Hz, 1H), 7.66 (d, J = 8.0 Hz, 1H), 7.32-7.23 (m, 2H), 5.19 (s, 2H). ^{13}C NMR (100 MHz, $CDCl_3$) δ 154.0, 143.1, 141.1, 138.2, 135.6, 131.2, 128.7, 123.9, 122.0, 121.3, 117.0, 113.2, 68.9.

Methyl 4-bromo-3-((pyridin-3-yloxy)methyl)benzoate (2.16):

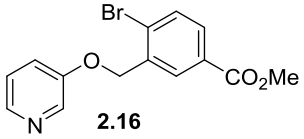

2.16

Following the General Procedure A. The product was isolated as a white solid (165 mg, 26%) starting from 3-hydroxypyridine **2.4** (190 mg, 2 mmol) and methyl 4-bromo-3-(bromomethyl)benzoate (739

mg, 2.4 mmol). ^{1}H NMR (400 MHz, $CDCl_3$) δ 8.42 (d, J = 2.5 Hz, 1H), 8.26 (d, J = 4.4 Hz, 1H), 8.18 (s, 1H), 7.84 (d, J = 8.3 Hz, 1H), 7.66 (d, J = 8.3 Hz, 1H), 7.31-7.26 (m, 1H), 7.23 (dd, J = 8.3, 4.5 Hz, 1H), 5.15 (s, 2H), 3.90 (s, 3H). ^{13}C NMR (100 MHz, $CDCl_3$) δ 166.0, 154.3, 142.7, 138.2, 135.9, 132.9, 130.3, 129.7, 129.6, 127.6, 123.8, 121.4, 69.2, 52.3.

3-((2-Bromothiophen-3-yl)methoxy)pyridine (2.17):

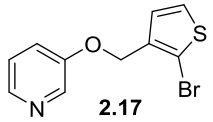

2.17

Following the General Procedure A. The product was isolated as a brown oil (71 mg, 13%) starting from 3-hydroxypyridine **2.4** (190 mg, 2 mmol) and 2-bromo-3-(bromomethyl)thiophene (512 mg, 2 mmol). ^{1}H NMR (400 MHz, $CDCl_3$) δ 8.38 (d, J = 2.4 Hz, 1H), 8.28-8.20 (m, 1H), 7.29 (d, J = 5.6 Hz, 1H), 7.27-7.19 (m, 2H), 7.04 (d, J = 5.6 Hz, 1H), 5.04 (s, 2H). ^{13}C NMR (100 MHz, $CDCl_3$) δ 154.4, 142.5, 138.3, 136.0, 127.7, 126.5, 123.8, 121.3, 111.6, 64.7.

3-((2-Bromobenzyl)oxy)-5-methylpyridine (2.18):

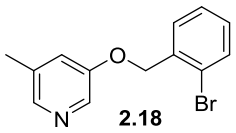

2.18

Following the General Procedure A. The product was isolated as a brown oil (134 mg, 24%) starting from 5-methylpyridin-3-ol (218 mg, 2 mmol) and 2-bromo-benzyl bromide **2.5** (600 mg, 2.4 mmol). ^{1}H NMR (400 MHz, $CDCl_3$) δ 8.20 (d, J = 2.2 Hz, 1H), 8.07 (s, 1H), 7.56 (d, J = 7.9 Hz, 1H), 7.50 (d, J = 7.4 Hz, 1H), 7.31 (t, J = 7.2 Hz, 1H), 7.17 (td, J = 7.8, 1.3 Hz, 1H), 7.07 (s, 1H), 5.12 (s, 2H), 2.30 (s, 3H). ^{13}C NMR (100 MHz, $CDCl_3$) δ 154.3, 143.0, 135.4, 135.2, 133.9, 132.6, 129.4, 128.8, 127.5, 122.3, 122.2, 69.5, 18.2.

(*Z*)-3-(2-bromostyryl)pyridine (2.19) and (*E*)-3-(2-bromostyryl)pyridine (2.20):

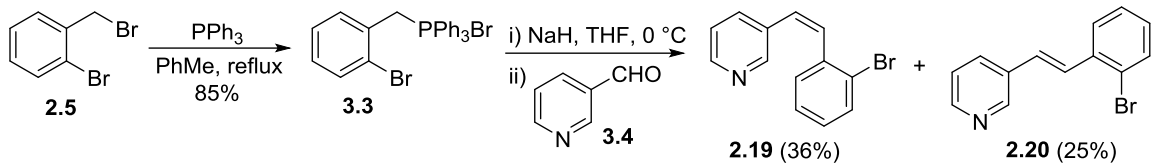

A 25 mL two-neck round-bottom flask was charged with PPh_3 (524 mg, 2 mmol) and equipped with a reflux condenser and a magnetic stirring bar under air, then the flask was put under vacuum and filled with N_2. After adding compound **2.5** (500 mg, 2 mmol) and toluene (10 mL) into the flask, the reaction mixture was magnetically stirred at 125 ℃ for 5 hours. After the completion of reaction, the reaction mixture was cooled down to room temperature. The resulting mixture was filtered, and the solid was washed with toluene (10 mL×3) and hexane (10 mL) to give compound **3.3** (872 mg, 85%) as a white solid.

A 25 mL round-bottom flask was charged with 60% NaH (74 mg, 1.8 mmol) under air, then the flask was put under vacuum and filled with N_2. After adding THF (10 mL) under N_2, the solution was cooled to 0 ℃ with an ice-bath. Compound **3.3** (872 mg, 1.7 mmol) was then added quickly into the cooled reaction mixture at 0 ℃ and the resulting mixture was magnetically stirred at 0 ℃ for additional 2 hours before adding aldehyde **3.4** (0.13 mL, 1.4 mmol). The reaction mixture was magnetically stirred at 0 ℃ for 2 hours, and then it was quenched by adding water (5 mL). The reaction mixture was extracted with diethyl ether (20 mL×3), and the combined organic layers were washed with brine, dried over $MgSO_4$ and concentrated under vacuum. The crude product was purified by flash chromatography on silica gel (eluent: cyclohexane/AcOEt = 3/1) to give compound **2.19** (132 mg, 36%) as a colorless oil and compound **2.20** (94 mg, 25%) as a colorless oil.

2.19: ^{1}H NMR (400 MHz, $CDCl_3$) δ 8.43-8.33 (m, 2H), 7.62-7.54 (m, 1H), 7.36 (d, J = 7.9 Hz, 1H), 7.12-7.02 (m, 4H), 6.74 (d, J = 12.1 Hz, 1H), 6.62 (d, J = 12.1 Hz, 1H). ^{13}C NMR (100 MHz, $CDCl_3$) δ 150.0, 148.1, 137.1, 135.6, 132.8, 132.0, 131.8, 130.3, 129.0, 127.6, 127.2, 123.6, 122.8.

2.20: ^{1}H NMR (400 MHz, $CDCl_3$) δ 8.73 (s, 1H), 8.51 (d, J = 4.3 Hz, 1H), 7.86 (d, J = 7.9 Hz, 1H), 7.65 (d, J = 7.8 Hz, 1H), 7.58 (d, J = 8.0 Hz, 1H), 7.51 (d, J = 16.3 Hz, 1H), 7.35-7.25 (m, 2H), 7.13 (t, J = 7.8 Hz, 1H), 6.98 (d, J = 16.3 Hz, 1H). ^{13}C NMR (100 MHz, $CDCl_3$) δ 148.8, 148.6, 136.3, 133.0, 132.8, 132.5, 129.4, 129.2, 127.5, 127.4, 126.6, 124.1, 123.5.

The experimental data obtained for compound **2.20** are in accordance with the literature.[153]

[153] D. C. Hamm, L. A. Braun, A. N. Burazin, A. M. Gauthier, K. O. Ness, C. E. Biebel, J. S. Sauer, R. Tanke, B. C. Noll, E. Bosch, N. P. Bowling, *Dalton Trans.* **2013**, *42*, 948.

3-(((2-Bromobenzyl)oxy)methyl)pyridine (2.21):

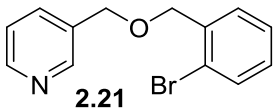

2.21

A 25 mL round-bottom flask was charged with compound **3.1** (218 mg, 2 mmol) with a magnetic stirring bar under air, then the flask was put under vacuum and filled with N_2. After adding THF (10 mL) under N_2, 60% NaH (96 mg, 2.4 mmol) was added into the reaction mixture in one portion and magnetically stirred at room temperature for 30 min. 2-Bromo-benzyl bromide **2.5** (600 mg, 2.4 mmol) was then added slowly, and the reaction mixture was magnetically stirred at room temperature overnight. After the completion of reaction, water (10 mL) was added and the resulting mixture was extracted with ethyl acetate (15 mL×3). The combined organic layers were washed with brine, dried over $MgSO_4$ and concentrated under vacuum. The crude product was purified by flash chromatography on silica gel (eluent: cyclohexane/AcOEt = 3/1) to give compound **2.21** (208 mg, 37%) as a yellow oil.

^{1}H NMR (400 MHz, $CDCl_3$) δ 8.63 (s, 1H), 8.56 (d, J = 3.8 Hz, 1H), 7.76 (d, J = 7.8 Hz, 1H), 7.55 (d, J = 8.0 Hz, 1H), 7.49 (d, J = 7.5 Hz, 1H), 7.36-7.28 (m, 2H), 7.16 (t, J = 7.4 Hz, 1H), 4.65 (s, 4H). ^{13}C NMR (100 MHz, $CDCl_3$) δ 148.92, 148.90, 137.0, 135.7, 133.6, 132.6, 129.23, 129.16, 127.4, 123.5, 122.9, 71.9, 70.1.

3-((2-Bromophenoxy)methyl)pyridine (2.22):

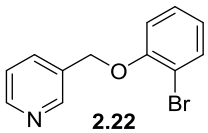

2.22

Following the General Procedure B. The product was isolated as a colorless oil (28 mg, 35%) starting from compound **3.1** (109 mg, 1 mmol). After obtaining the crude product of **3.2**, it was mixed (80 mg, 0.3 mmol) immediately with 2-bromophenol (53 mg, 0.3 mmol). ^{1}H NMR (400 MHz, $CDCl_3$) δ 8.74 (s, 1H), 8.61 (d, J = 2.8 Hz, 1H), 7.89 (d, J = 7.8 Hz, 1H), 7.58 (dd, J = 7.9, 1.5 Hz, 1H), 7.37 (dd, J = 7.7, 4.9 Hz, 1H), 7.32-7.24 (m, 1H), 6.97 (dd, J = 8.2, 1.0 Hz, 1H), 6.90 (td, J = 7.8, 1.2 Hz, 1H), 5.17 (s, 2H). ^{13}C NMR (100 MHz, $CDCl_3$) δ 154.6, 149.2, 148.4, 135.1, 133.5, 132.2, 128.5, 123.6, 122.6, 113.8, 112.6, 68.4.

2-Bromo-3-(pyridin-3-ylmethoxy)pyridine (2.23):

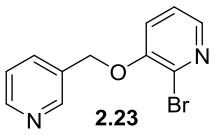

2.23

Following the General Procedure B. The product was isolated as a colorless oil (54 mg, 50%) starting from compound **3.1** (109 mg, 1 mmol). After obtaining the crude product of **3.2**, it was mixed (132 mg, 0.5 mmol) immediately with 2-bromopyridin-3-ol (70 mg, 0.4 mmol). ^{1}H NMR (400 MHz, $CDCl_3$) δ 8.68 (s, 1H), 8.57 (d, J = 3.7 Hz, 1H), 7.98 (t, J = 3.1 Hz, 1H), 7.82 (d, J = 7.8 Hz, 1H), 7.33 (dd, J = 7.7, 4.9 Hz, 1H), 7.18 (d, J = 3.1 Hz, 2H), 5.14 (s, 2H). ^{13}C NMR (100 MHz, $CDCl_3$) δ 151.5, 149.5, 148.3, 141.9, 135.1, 133.2, 131.2, 123.6, 123.3, 120.3, 68.4.

3-((2-Bromo-4,6-di-*tert*-butylphenoxy)methyl)pyridine (2.24):

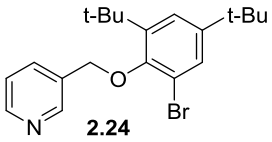

2.24

Following the General Procedure B. The product was isolated as a light yellow oil (96 mg, 12%) starting from compound **3.1** (218 mg, 2 mmol). After obtaining the crude product of **3.2**, it was mixed immediately with 2-bromo-4,6-di-*tert*-butylphenol (570 mg, 2 mmol). ^{1}H NMR (400 MHz, $CDCl_3$) δ 8.77 (s, 1H), 8.59 (s, 1H), 7.94 (d, J = 7.8 Hz, 1H), 7.45 (d, J = 2.3 Hz, 1H), 7.37-7.29 (m, 2H), 5.14 (s, 2H), 1.40 (s, 9H), 1.30 (s, 9H). ^{13}C NMR (100 MHz, $CDCl_3$) δ 151.9, 149.0, 148.6, 147.8, 144.2, 135.1, 133.0, 129.0, 123.9, 123.4, 117.8, 71.5, 35.8, 34.6, 31.3(3C), 31.0(3C).

2-Bromophenyl nicotinate (2.25):

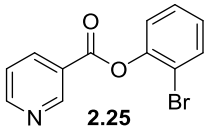

2.25

Following the General Procedure C. The product was isolated as a white solid (482 mg, 87%) starting from nicotinic acid (246 mg, 2 mmol) and 2-bromophenol (346 mg, 2 mmol). ^{1}H NMR (400 MHz,

$CDCl_3$) δ 9.44 (s, 1H), 8.87 (d, J = 3.9 Hz, 1H), 8.49 (dt, J = 6.2, 1.6 Hz, 1H), 7.66 (dd, J = 8.0, 1.1 Hz, 1H), 7.48 (dd, J = 7.9, 4.9 Hz, 1H), 7.43-7.35 (m, 1H), 7.29 (dd, J = 8.0, 1.2 Hz, 1H), 7.18 (td, J = 8.0, 1.3 Hz, 1H). ^{13}C NMR (100 MHz, $CDCl_3$) δ 162.9, 154.0, 151.4, 147.9, 137.8, 133.4, 128.6, 127.7, 125.1, 123.7, 123.5, 116.0.

Pyridin-3-yl 2-bromo-5-methoxybenzoate (2.26):

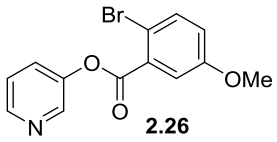

2.26

Following the General Procedure C. The product was isolated as a white solid (576 mg, 93%) starting from 3-hydroxypyridine **2.4** (190 mg, 2 mmol) and 2-bromo-5-methoxybenzoic acid (462 mg, 2 mmol). ^{1}H NMR (400 MHz, $CDCl_3$) δ 8.55 (d, J = 2.1 Hz, 1H), 8.48 (d, J = 4.5 Hz, 1H), 7.63-7.57 (m, 1H), 7.54 (d, J = 8.8 Hz, 1H), 7.48 (d, J = 3.0 Hz, 1H), 7.33 (dd, J = 8.3, 4.7 Hz, 1H), 6.92 (dd, J = 8.8, 3.0 Hz, 1H), 3.79 (s, 3H). ^{13}C NMR (100 MHz, $CDCl_3$) δ 173.3, 158.6, 157.2, 138.8, 134.0, 133.2, 132.4, 129.6, 126.2, 117.2, 114.4, 110.0, 55.5.

Pyridin-3-yl 2,5-dibromobenzoate (2.27):

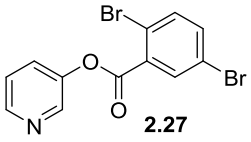

2.27

Following the General Procedure C. The product was isolated as a white solid (571 mg, 80%) starting from 3-hydroxypyridine **2.4** (190 mg, 2 mmol) and 2,5-dibromobenzoic acid (560 mg, 2 mmol). ^{1}H NMR (400 MHz, $CDCl_3$) δ 8.59 (d, J = 2.4 Hz, 1H), 8.56 (d, J = 4.2 Hz, 1H), 8.16 (d, J = 2.3 Hz, 1H), 7.65 (ddd, J = 8.3, 2.4, 1.2 Hz, 1H), 7.61 (d, J = 8.5 Hz, 1H), 7.55 (dd, J = 8.5, 2.3 Hz, 1H), 7.41 (dd, J = 8.3, 4.8 Hz, 1H). ^{13}C NMR (100 MHz, $CDCl_3$) δ 162.6, 147.3, 147.2, 143.1, 136.5, 136.1, 134.7, 131.8, 129.3, 124.0, 121.23, 121.22.

***N*-(2-Bromophenyl)nicotinamide (2.28):**

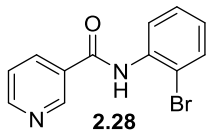

2.28

Following the General Procedure C. The product was isolated as a white solid (148 mg, 53%) starting from nicotinic acid (123 mg, 1 mmol) and 2-bromoaniline (172 mg, 1 mmol). ^{1}H NMR (400 MHz, $CDCl_3$) δ 9.24 (s, 1H), 8.83 (s, 1H), 8.55 (s, 1H), 8.47 (d, J = 8.2 Hz, 1H), 8.32 (d, J = 7.9 Hz, 1H), 7.61 (d, J = 8.0 Hz, 1H), 7.54 (dd, J = 7.3, 5.2 Hz, 1H), 7.40 (t, J = 7.8 Hz, 1H), 7.07 (t, J = 7.7 Hz, 1H). ^{13}C NMR (100 MHz, $CDCl_3$) δ 163.4, 152.8, 148.0, 135.2, 135.1, 132.3, 130.2, 128.5, 125.8, 123.7, 122.0, 114.0.

The experimental data obtained are in accordance with the literature.[154]

2-Bromo-5-methoxy-*N*-(pyridin-3-yl)benzamide (2.29):

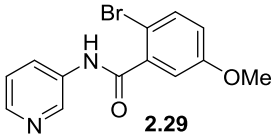

2.29

Following the General Procedure C. The product was isolated as a white solid (522 mg, 85%) starting from pyridin-3-amine (188 mg, 2 mmol) and 2-bromo-5-methoxybenzoic acid (462 mg, 2 mmol). ^{1}H NMR (400 MHz, $CDCl_3$) δ 9.70 (s, 1H), 8.58 (s, 1H), 8.21 (d, J = 8.2 Hz, 1H), 8.08 (d, J = 4.6 Hz, 1H), 7.33 (d, J = 8.8 Hz, 1H), 7.20 (dd, J = 8.1, 4.8 Hz, 1H), 6.98 (d, J = 2.5 Hz, 1H), 6.74 (dd, J = 8.8, 2.6 Hz, 1H), 3.70 (s, 3H). ^{13}C NMR (100 MHz, $CDCl_3$) δ 166.4, 158.7, 144.8, 140.9, 138.0, 135.0, 134.0, 127.6, 123.7, 117.8, 114.3, 109.4, 55.5.

[154] Y.-T. Park, C.-H. Jung, K.-W. Kim, *J. Org. Chem.* **1999,** *64,* 8546.

2,5-Dibromo-*N*-(pyridin-3-yl)benzamide (2.30) and 2,5-dibromo-*N*-(2,5-dibromobenzoyl)-*N*-(pyridin-3-yl)benzamide (2.31):

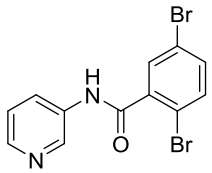

2.30

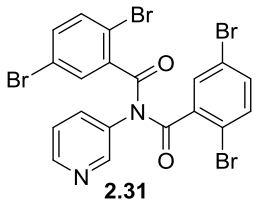

2.31

Following the General Procedure C. Compound **2.30** was isolated as a white solid (558 mg, 78%) and compound **2.31** was isolated as a white solid (128 mg, 21%) starting from pyridin-3-amine (188 mg, 2 mmol) and 2,5-dibromobenzoic acid (560 mg, 2 mmol).

2.30: ^{1}H NMR (400 MHz, $CDCl_3$) δ 9.66 (s, 1H), 8.64 (s, 1H), 8.27 (d, J = 8.2 Hz, 1H), 8.20 (d, J = 4.5 Hz, 1H), 7.63 (s, 1H), 7.44-7.33 (m, 2H), 7.33-7.24 (m, 1H). ^{13}C NMR (100 MHz, $CDCl_3$) δ 164.9, 156.7, 145.4, 141.2, 138.9, 134.8, 134.5, 132.2, 127.8, 123.9, 121.5, 118.1.

2.31: ^{1}H NMR (400 MHz, $CDCl_3$) δ 8.71 (s, 1H), 8.61 (s, 1H), 7.82 (d, J = 8.0 Hz, 1H), 7.49 (d, J = 2.1 Hz, 2H), 7.40 (dd, J = 7.7, 4.8 Hz, 1H), 7.35 (d, J = 8.5 Hz, 2H), 7.30 (dd, J = 8.5, 2.2 Hz, 2H). ^{13}C NMR (100 MHz, $CDCl_3$) δ 168.0(2C), 149.8, 149.0, 138.2(2C), 136.1(2C), 134.8(2C), 134.3(2C), 131.8(2C), 124.0, 121.4(2C), 117.8(2C).

6*H*-Isochromeno[3,4-*c*]pyridine (2.2):

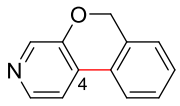

2.2

Following the General Procedure D. The product was isolated as a colorless oil (15 mg, 84%) starting from compound **2.1** (26 mg, 0.1 mmol). ^{1}H NMR (400 MHz, $CDCl_3$) δ 8.35 (s, 1H), 8.30 (s, 1H), 7.77-7.68 (m, 1H), 7.56 (d, J = 4.9 Hz, 1H), 7.47-7.35 (m, 2H), 7.18 (d, J = 6.6 Hz, 1H), 5.19 (s, 2H). ^{13}C NMR (100 MHz, $CDCl_3$) δ 150.6, 143.2, 139.9, 132.2, 129.9, 129.5, 128.7, 127.4, 125.0, 122.7, 116.6, 68.2.

9-Fluoro-6*H*-isochromeno[3,4-*c*]pyridine (2.32) and 9-fluoro-6*H*-isochromeno[4,3-*b*]pyridine (2.33):

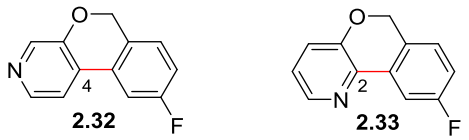

Following the General Procedure D. Compound **2.32** was isolated as a yellow solid (16 mg, 62%) starting from compound **2.13** (37 mg, 0.13 mmol). When using P(4-F-Ph)$_3$ as ligand, compound **2.32** was obtained as a yellow solid (21 mg, 82%) and compound **2.33** was obtained as a yellow solid (4 mg, 15%) starting from compound **2.13** (36 mg, 0.13 mmol).

2.32: ^{1}H NMR (400 MHz, $CDCl_3$) δ 8.37 (s, 1H), 8.31 (d, J = 4.6 Hz, 1H), 7.48 (d, J = 5.0 Hz, 1H), 7.41 (dd, J = 9.3, 2.4 Hz, 1H), 7.20-7.14 (m, 1H), 7.09 (td, J = 8.4, 2.4 Hz, 1H), 5.16 (s, 2H). ^{13}C NMR (100 MHz, $CDCl_3$) δ 163.0 (d, $J_{C\text{-}F}$ = 247.1 Hz), 142.5, 139.3, 129.4 (d, $J_{C\text{-}F}$ = 2.0 Hz), 129.2 (d, $J_{C\text{-}F}$ = 8.1 Hz), 127.9 (d, $J_{C\text{-}F}$ = 3.1 Hz), 126.8 (d, $J_{C\text{-}F}$ = 8.4 Hz), 117.2, 117.0, 110.1, 109.9, 67.9. ^{19}F NMR (376 MHz, $CDCl_3$) δ -112.3 (s).

2.33: ^{1}H NMR (400 MHz, $CDCl_3$) δ 8.30 (dd, J = 4.5, 1.3 Hz, 1H), 7.90 (dd, J = 9.5, 2.5 Hz, 1H), 7.28-7.23 (m, 1H), 7.18 (dd, J = 8.2, 4.6 Hz, 1H), 7.12 (dd, J = 8.2, 5.4 Hz, 1H), 7.06 (td, J = 8.4, 2.6 Hz, 1H), 5.20 (s, 2H). ^{19}F NMR (376 MHz, $CDCl_3$) δ -111.7 (s).

8-(Trifluoromethyl)-6*H*-isochromeno[3,4-*c*]pyridine (2.34) and 8-(trifluoromethyl)-6*H*-isochromeno[4,3-*b*]pyridine (2.35):

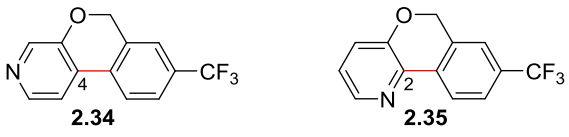

Following the General Procedure D. Compound **2.34** was isolated as a yellow solid (17 mg, 53%) starting from compound **2.11** (45 mg, 0.14 mmol). When using P(4-F-Ph)$_3$ as ligand, compound **2.34** was obtained as a yellow solid (12 mg, 35%) and compound **2.35** was obtained as a yellow solid (7 mg, 20%) starting from compound **2.11** (44 mg, 0.13 mmol).

2.34: ^{1}H NMR (400 MHz, $CDCl_3$) δ 8.40 (s, 1H), 8.35 (d, J = 4.9 Hz, 1H), 7.85 (d, J = 8.1 Hz, 1H), 7.68 (d, J = 8.2 Hz, 1H), 7.60 (d, J = 5.1 Hz, 1H), 7.46 (s, 1H), 5.25 (s, 2H). ^{13}C NMR (100 MHz, $CDCl_3$) δ 150.8, 143.3, 140.2, 132.8, 131.7 (q, $J_{C\text{-}F}$ = 32.9 Hz), 130.9, 128.2, 125.7 (q, $J_{C\text{-}F}$ = 3.7 Hz),

123.6 (d, $J_{C\text{-}F}$ = 273.0 Hz), 123.2, 122.1 (q, $J_{C\text{-}F}$ = 3.7 Hz), 116.9, 67.9. ^{19}F NMR (376 MHz, $CDCl_3$) δ -62.9 (s).

2.35: ^{1}H NMR (400 MHz, $CDCl_3$) δ 8.39-8.27 (m, 2H), 7.69 (d, J = 8.0 Hz, 1H), 7.41 (s, 1H), 7.31-7.27 (m, 1H), 7.25-7.20 (m, 1H), 5.28 (s, 2H). ^{13}C NMR (100 MHz, $CDCl_3$) δ 158.6, 143.4, 140.4, 132.3, 129.0, 128.2, 125.6 (d, $J_{C\text{-}F}$ = 4.0 Hz), 125.3, 125.1, 124.7, 123.5, 121.3 (d, $J_{C\text{-}F}$ = 3.7 Hz), 67.9. ^{19}F NMR (376 MHz, $CDCl_3$) δ -62.7 (s).

Benzo[*f*]isoquinoline (1.2.37) and benzo[*h*]quinolone (1.2.40a):

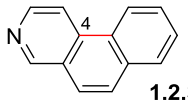

1.2.37

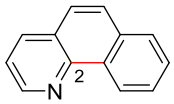

1.2.40a

Following the General Procedure D. Compound **1.2.37** was isolated as a white solid (5 mg, 20%) and compound **1.2.40a** was isolated as a white solid (2 mg, 11%) starting from compound **2.19** (33 mg, 0.13 mmol).

1.2.37: ^{1}H NMR (400 MHz, $CDCl_3$) δ ^{1}H NMR (400 MHz, $CDCl_3$) δ 9.28 (s, 1H), 8.77 (s, 1H), 8.73-8.66 (m, 1H), 8.48 (d, J = 5.6 Hz, 1H), 8.00-7.93 (m, 1H), 7.89 (d, J = 8.9 Hz, 1H), 7.84 (d, J = 8.9 Hz, 1H), 7.79-7.72 (m, 2H).

1.2.40a: ^{1}H NMR (400 MHz, $CDCl_3$) δ 9.31 (d, J = 8.0 Hz, 1H), 9.01 (dd, J = 4.3, 1.6 Hz, 1H), 8.17 (dd, J = 8.0, 1.6 Hz, 1H), 7.95-7.89 (m, 1H), 7.81 (d, J = 8.8 Hz, 1H), 7.79-7.64 (m, 3H), 7.52 (dd, J = 8.0, 4.4 Hz, 1H).

The experimental data obtained for compound **1.2.37** are in accordance with the literature.[155]

The experimental data obtained for compound **1.2.40a** are in accordance with the literature.[156]

[155] I. Dix, C. Doll, H. Hopf, P. G. Jones, *Eur. J. Org. Chem.* **2002**, 2547.
[156] X.-T. Sun, J. Zhu, Y.-T. Xia, L. Wu, *ChemCatChem* **2017**, *9*, 2463.

1-Methyl-6*H*-isochromeno[3,4-*c*]pyridine (2.36) and 3-methyl-6*H*-isochromeno[4,3-*b*]pyridine (2.37):

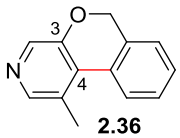

2.36

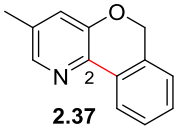

2.37

Following the General Procedure D. Compound **2.36** was isolated as a white solid (9 mg, 40%) and compound **2.37** was isolated as a white solid (5 mg, 22%) starting from compound **2.18** (31 mg, 0.11 mmol). Notably, compound **2.36** contained an unknown impurity after flash column chromatography. In order to obtain data from pure product, partial product was further purified by preparative HPLC to give 3 mg of compound **2.36**.

2.36: ^{1}H NMR (400 MHz, $CDCl_3$) δ 8.42-8.04 (m, 2H), 7.85 (d, J = 7.2 Hz, 1H), 7.49-7.38 (m, 2H), 7.27 (d, J = 6.8 Hz, 1H), 5.05 (s, 2H), 2.68 (s, 3H). ^{13}C NMR (100 MHz, $CDCl_3$) δ 144.9, 138.1, 136.9, 134.4, 130.6, 129.3, 128.4, 128.1, 126.7, 125.3, 68.9, 19.5. (The carbon signal at C-3 position could not be identified from ^{13}C NMR.)

2.37: ^{1}H NMR (400 MHz, $CDCl_3$) δ 8.19 (d, J = 7.7 Hz, 1H), 8.14 (s, 1H), 7.43 (t, J = 7.5 Hz, 1H), 7.35 (t, J = 7.4 Hz, 1H), 7.13 (d, J = 7.4 Hz, 1H), 7.08 (s, 1H), 5.21 (s, 2H), 2.34 (s, 3H). ^{13}C NMR (100 MHz, $CDCl_3$) δ 150.8, 143.1, 138.9, 134.4, 131.7, 130.0, 129.2, 128.8, 125.0, 124.1, 122.9, 68.4, 18.3.

ÉCOLE DOCTORALE
Sciences chimiques : molécules, matériaux, instrumentation et biosystèmes

Titre: Activation de liaisons C-H catalysée par des nanoparticules de Ruthénium

Mots clés: marquage isotopique, C-H activation, deutériation, Ruthénium, nanoparticules

Résumé: Les molécules marquées par des isotopes de l'hydrogène possèdent de nombreuses applications dans divers domaines tels que la chimie, la biologie ou en science des matériaux. Dans le domaine de la recherche de nouveaux médicaments, les études liées à la pharmacocinétique nécessitent un accès rapide à des molécules marquées afin de ne pas impacter les coûts et les délais de développement. Le développement de la métabolomique a aussi entrainé une augmentation du besoin en molécules marquées isotopiquement. En effet, les molécules deuterées peuvent être utilisées en tant qu'étalons internes pout la quantification rapide des métabolites présents dans des tissus ou des fluides biologiques. La première partie de cette thèse concerne le développement d'une méthode générale de marquage de motifs de type thioéther dans des molécules complexes à l'aide d'une nouvelle réaction d'échange isotopique (catalysée par des nanoparticules de Ruthénium). D'un point de vue fondamental cette transformation représente le premier exemple de (Csp^3)-H activation dirigée par un atome de soufre. En termes d'application, cette nouvelle réaction permet la synthèse rapide d'étalons internes pour la quantification LC-MS/MS et le marquage tritium de molécules complexes. La seconde partie de cette thèse relate le développement d'une nouvelle méthode d'homocouplage de phénylpyridines catalysée par Ru/C. Différents substrats comportant des substituants riches et pauvres en électron ont été couplés avec de bons rendements. Ces dimères ont ensuite été utilisés pour synthétiser de nouveaux complexes de bore dont les propriétés photophysiques ont été étudiées. Dans une troisième partie, la mise au point d'une réaction palladocatalysée permettant d'obtenir des molécules polycycliques contenant un motif de type pyridine est développée.

Title: C-H bond activation catalyzed by Ruthenium nanoparticles

Keywords: isotopic labeling, C-H activation, deuteration, Ruthenium, nanoparticles

Abstract: Deuterated and tritiated compounds are widely used in numerous applications in chemistry, biology and material science. In the drug discovery and development process, ADME studies require quick access to labelled molecules, otherwise the drug development costs and timeline are significantly impacted. The rapid development of metabolomics has also increased the need for isotopically labelled compounds. In particular, deuterated molecules are used as internal standards for quantitative LC-MS/MS analysis of metabolites in biological fluids and tissues. In this context, a general method allowing the deuterium and tritium labelling of bioactive thioethers using a HIE reaction is described in the first chapter. From a fundamental point of view, this transformation is the first example of (Csp^3)-H activation directed by a sulfur atom. In terms of application, this new reaction has been proved to be useful for the preparation of deuterated LC-MS/MS reference materials and tritiated pharmaceuticals owning high specific activity.
In the second chapter of this manuscript, the development of a method allowing the cross-dehydrogenative homocoupling of 2-arylpyridines catalyzed by Ru/C is developed. Various substrates with different substituents were efficiently coupled to give the desired dimers in good yield. In terms of application, a series of pyridine-boron complexes derived from the phenyl pyridine dimers were also synthesized and their photophysical properties were studied.
In the third chapter, a regioselective palladium catalyzed intramolecular arylation reaction allowing the synthesis of pyridine containing polycyclic compounds is described.

Université Paris-Saclay
Espace Technologique / Immeuble Discovery
Route de l'Orme aux Merisiers RD 128 / 91190 Saint-Aubin, France